frontiers | Research Topics

Perspectives in avian skeletal systems and skeletal abnormalities

Edited by
Chongxiao Chen, Anthony Pokoo-Aikins, Prafulla Regmi, Shu-cheng Huang and Mujeeb Ur Rehman

Published in
Frontiers in Physiology

ISSN 1664-8714
ISBN 978-2-8325-2835-8
DOI 10.3389/978-2-8325-2835-8

About Frontiers

Frontiers is more than just an open access publisher of scholarly articles: it is a pioneering approach to the world of academia, radically improving the way scholarly research is managed. The grand vision of Frontiers is a world where all people have an equal opportunity to seek, share and generate knowledge. Frontiers provides immediate and permanent online open access to all its publications, but this alone is not enough to realize our grand goals.

Frontiers journal series

The Frontiers journal series is a multi-tier and interdisciplinary set of open-access, online journals, promising a paradigm shift from the current review, selection and dissemination processes in academic publishing. All Frontiers journals are driven by researchers for researchers; therefore, they constitute a service to the scholarly community. At the same time, the *Frontiers journal series* operates on a revolutionary invention, the tiered publishing system, initially addressing specific communities of scholars, and gradually climbing up to broader public understanding, thus serving the interests of the lay society, too.

Dedication to quality

Each Frontiers article is a landmark of the highest quality, thanks to genuinely collaborative interactions between authors and review editors, who include some of the world's best academicians. Research must be certified by peers before entering a stream of knowledge that may eventually reach the public - and shape society; therefore, Frontiers only applies the most rigorous and unbiased reviews. Frontiers revolutionizes research publishing by freely delivering the most outstanding research, evaluated with no bias from both the academic and social point of view. By applying the most advanced information technologies, Frontiers is catapulting scholarly publishing into a new generation.

What are Frontiers Research Topics?

Frontiers Research Topics are very popular trademarks of the *Frontiers journals series*: they are collections of at least ten articles, all centered on a particular subject. With their unique mix of varied contributions from Original Research to Review Articles, Frontiers Research Topics unify the most influential researchers, the latest key findings and historical advances in a hot research area.

Find out more on how to host your own Frontiers Research Topic or contribute to one as an author by contacting the Frontiers editorial office: frontiersin.org/about/contact

Perspectives in avian skeletal systems and skeletal abnormalities

Topic editors

Chongxiao Chen — University of Georgia, United States

Anthony Pokoo-Aikins — Toxicology and Mycotoxin Research Unit, U.S. National Poultry Research Center, Agricultural Research Service (USDA), United States

Prafulla Regmi — University of Georgia, United States

Shu-cheng Huang — Henan Agricultural University, China

Mujeeb Ur Rehman — Directorate Planning and Development, Livestock & Dairy Development Department, Pakistan

Citation

Chen, C., Pokoo-Aikins, A., Regmi, P., Huang, S.-c., Ur Rehman, M., eds. (2023). *Perspectives in avian skeletal systems and skeletal abnormalities*. Lausanne: Frontiers Media SA. doi: 10.3389/978-2-8325-2835-8

Table of contents

frontiers | Frontiers in Physiology

TYPE Editorial
PUBLISHED 13 June 2023
DOI 10.3389/fphys.2023.1229943

OPEN ACCESS

EDITED AND REVIEWED BY
Sandra G. Velleman,
The Ohio State University, United States

*CORRESPONDENCE
Chongxiao Chen,
sean.chen@uga.edu

RECEIVED 27 May 2023
ACCEPTED 31 May 2023
PUBLISHED 13 June 2023

CITATION
Chen C, Pokoo-Aikins A, Huang S-C, Regmi P and Ur Rehman M (2023), Editorial: Perspectives in avian skeletal systems and skeletal abnormalities. *Front. Physiol.* 14:1229943. doi: 10.3389/fphys.2023.1229943

Editorial: Perspectives in avian skeletal systems and skeletal abnormalities

Chongxiao Chen[1]*, Anthony Pokoo-Aikins[2], Shu-Cheng Huang[3], Prafulla Regmi[1] and Mujeeb Ur Rehman[4,5]

[1]Department of Poultry Science, University of Georgia, Athens, GA, United States, [2]Toxicology and Mycotoxin Research Unit, U.S. National Poultry Research Center, Agricultural Research Service (USDA), Athens, GA, United States, [3]College of Veterinary Medicine, Henan Agricultural University, Zhengzhou, China, [4]State Key Laboratory of Marine Resource Utilization in South China Sea, College of Oceanology, Hainan University, Haikou, Hainan, China, [5]Directorate Planning and Development, Livestock and Dairy Development Department, Quetta, Balochistan, Pakistan

KEYWORDS

bone health, abnormalities, oxidative stress, mineral homeostasis, poultry

Editorial on the Research Topic
Perspectives in avian skeletal systems and skeletal abnormalities

Introduction

The avian skeletal system is gaining increasing attention from researchers as a unique research model for studying bone metabolism, pathologies, and the significance of bone health in relation to animal productivity and welfare. The avian skeleton is a delicate system providing structural support, minerals for eggshell formation, and even acting as an immune organ. Skeletal abnormalities in avian species can have significant implications for poultry farming. Conditions such as osteomyelitis, rickets, and chondrodystrophy, can lead to changes in gait patterns, mobility, and pathophysiologies resulting in detrimental effects on growth performance, health, and economic losses. The current Research Topic entitled "*Perspectives in avian skeletal system and skeletal abnormalities*" collected ten original research publications, including topics in bone health in meat birds (four articles), bone health in laying hens (four articles), oxidative stress and bone health (two articles). The compilation provides insights into the impact of nutrition and environmental management on bone health, the relationship between physiological parameters and bone quality, dedicated research into the mechanism of bone remodeling, and the oxidative stresses affecting bone development.

Bone health in meat birds

The increased emphasis on genetic selection for meat production has led to birds being required to carry more muscle mass than ever, which poses significant challenges to bone health. Lameness is the most common bone issue, impacting not only birds' performance but also animal welfare. The common causes of lameness in broilers include femoral head

necrosis (FHC, or bacterial chondronecrosis with osteomyelitis, BCO) and tibial dyschondroplasia (TD).

FHC is associated with microfractures followed by opportunistic bacterial infection. According to the research from Fan et al., FHN is also linked to dyslipidemia where high lipids levels could increase the blood viscosity, leading to tissue hypoxia, elevated intraosseous pressure, and impaired nutrient transportation. These factors contribute to the development of FHN. Fan et al. investigated the lipid metabolism and bone-related parameters in healthy and spontaneous FHN broilers at 3–5 weeks of age. The results indicated a lipid metabolism disorder in FHN birds, characterized by higher total cholesterol (TC), triglycerides (TG), and low-density lipoprotein cholesterol (LDL-C) compared to healthy birds. Furthermore, metabolism-related markers provided evidence of increased fat synthesis and decomposition in the FHN group.

Femoral head separation (FHS) is characterized by the detachment of growth plate (GP) and articular cartilage. This condition predisposes the birds to FHN. The causes of FHS are still unclear, but in recent research conducted by Ibelli et al. found differential expression of 34 genes, including downregulation of chondrogenesis and bone differentiation in FHS-affected birds when compared to healthy birds. Moreover, twelve single-nucleotide polymorphisms (SNPs) associated with FHS were identified. This research project provides fundamental information to enhance our understanding of the causes of FHS.

Another common cause of lameness in broilers is tibial dyschondroplasia (TD), characterized by an abnormality in the bone growth plate where excess cartilage template remains without being replaced by bone. The diagnosis of TD typically involves invasive methods, such as exposing the tibial head to observe morphological changes in the growth plate. However, Huang et al. revealed a potential non-invasive biomarker, 4-hydroxybenzaldehyde, which can be obtained from fecal samples and used to distinguish TD broilers from normal ones. This potential marker could become a powerful tool for TD diagnosis in the field. In another research project by Lee et al., the researchers explored a different trait affecting bone quality and discovered that Japanese quails with mutated myostatin (MSTN) exhibited higher tibia bone mass and better structural quality. This finding highlights the potential application of MSTN in improving meat yield and bone quality in meat-producing birds.

Bone health in laying hens

Laying hen bones exhibit unique structures compared to mammalian bones due to the eggshell formation process. Due the need of eggshell formation, unique woven-like medullary bones are developed during sexual maturation to provide a calcium source for eggshell. Genetic selection has led to high egg production, which constantly pressures bone renewal. As the birds age, bone quality issues become significant. Despite numerous papers published in this area, finding an effective solution to reduce this problem remains elusive. Several factors contribute to laying hen bone health, including environmental management, dietary factors, and diseases.

Regarding management, the transition to cage-free systems is a growing trend driven by animal welfare concerns and consumer preferences. A study conducted by Fu et al. demonstrated improvement in eggshell quality and bone quality in aviary systems compared to conventional cages. Notably, the femur showed increased bone resorption activity, possibly related to the enhanced eggshell quality observed. Nevertheless, it is important to note that adopting cage-free production systems can result in increased environmental impacts, a higher incidence of keel bone fractures, and increased gut health challenges. Further research is needed to assess animal welfare in cage-free systems comprehensively, determine the nutrition requirements, and develop strategies to mitigate gut health issues.

Nutrition plays an essential role in bone health and laying performance. Extensive research has been conducted to improve laying performance and bone health via nutritional interventions. Previous studies have highlighted the significance of pullet bone quality and its long-term impact on bone health and laying performance during the late laying period (Sinclair-Black et al.). Notably, White et al. conducted an interesting study demonstrating that combining 25-hydroxyvitamin D3 with optimized calcium/phosphorus levels improved pullet bone quality, as evidenced by enhanced cortical and trabecular bone 3D structures. In contrast, the research presented by Xin et al. showed that protein level (15% vs. 16.5%) and energy level (2,700 vs. 2,800 kcal/kg) during the prelay period (15–20 weeks) did not impact laying performance. Only slight improvements in egg shape index and eggshell thickness were observed in the high protein treatment group. Molecular parameters indicated that protein and energy levels influenced the expression of HPG axis-related genes of hens towards the end of the laying cycle without altering the circulating sex hormone profile.

A review by Sinclair-Black et al. summarized physiological regulations of vitamin D3, calcium, and phosphorus and provided an overview of calcium and phosphorus homeostasis during eggshell mineralization in laying hens. The review also identified several research gaps, such as FGF23 expression which is important for calcium and phosphorus homeostasis. Additionally, the lack of tools for studying avian species' vitamin D3 metabolism and shell gland calcium transportation was highlighted. The review emphasized the limitations of applying mammalian research models to birds, given the unique characteristics of medullary bone and eggshell calcification in avian species. Therefore, additional tools, such as *in vitro* models, are needed to advance research in this area (Sinclair-Black et al.).

Oxidative stress and bone health

Bone health issues are usually linked to nutritional imbalance, diseases, and management factors. However, research presented by Tompkins et al. has shown that coccidiosis, a protozoal disease, may contribute to bone loss by altering redox balance and impairing antioxidant status induced by *coccidia* infection caused by *Eimeria* infection. The authors of this study also mentioned that immune status could be a critical factor in the pathogenesis of bone abnormalities during intestinal parasite infections, warranting further research. This finding highlights that bones are not only

structural support for birds but also vital immune organs. In another study conducted by Tompkins et al., mesenchymal stem cells (MSCs) were used as a research model to investigate the effects of oxidative stress on cell fate. The study demonstrated that long-term treatment of chicken MSCs with H_2O_2 impaired osteogenic differentiation. This research further emphasizes the impact of oxidative stress on bone-related cellular processes.

Perspectives

The avian skeletal system is not only a fascinating research model for bone health but also holds great significance in enhancing food production and animal welfare. This Research Topic should inspire future projects to advance our knowledge of avian bone physiology and health. Future research in this field could focus on developing novel tools to evaluate bone quality, uncovering avian osteoimmunology, and exploring the immune functions of bones under various challenges. Furthermore, research is still needed to improve skeletal health through advancements in nutrition, environmental management, breeding strategies, and other relevant areas.

Author contributions

All authors listed have made a substantial, direct, and intellectual contribution to the work and approved it for publication.

Conflict of interest

The authors declare that the research was conducted in the absence of any commercial or financial relationships that could be construed as a potential conflict of interest.

Publisher's note

frontiers in Physiology

ORIGINAL RESEARCH
published: 14 June 2021
doi: 10.3389/fphys.2021.685968

Abnormal Lipid Profile in Fast-Growing Broilers With Spontaneous Femoral Head Necrosis

*Rubin Fan, Kangping Liu and Zhenlei Zhou**

Department of Veterinary Clinical Science, College of Veterinary Medicine, Nanjing Agricultural University, Nanjing, China

This study investigated lipid metabolism in broilers with spontaneous femoral head necrosis (FHN) by determining the levels of markers of the blood biochemistry and bone metabolism. The birds were divided into a normal group and FHN group according to the femoral head scores of 3-, 4-, and 5-week-old chickens with FHN, and a comparative study was conducted. The study showed that spontaneous FHN broilers had a lipid metabolism disorder, hyperlipidemia, and an accumulation of lipid droplets in the femur. In addition, there were significant changes in the bone parameters and blood bone biochemistry markers, and the expression of genes related to lipid metabolism in the femoral head was also significantly increased. Therefore, FHN may result from dyslipidemia, which affects the bone growth and development of broilers.

Keywords: femoral head necrosis, bone metabolism, broiler, hyperlipidemia, lipid metabolism disorder

OPEN ACCESS

Edited by:
Shu-cheng Huang,
Henan Agricultural University, China

Reviewed by:
Wenting Li,
Henan Agricultural University, China
Ali Raza Jahejo,
Shanxi Agricultural University, China
Hui Zhang,
Huazhong Agricultural University, China

***Correspondence:**
Zhenlei Zhou
zhouzl@njau.edu.cn

Specialty section:
This article was submitted to Avian Physiology, a section of the journal Frontiers in Physiology

Received: *26 March 2021*
Accepted: *26 April 2021*
Published: *14 June 2021*

Citation:
Fan R, Liu K and Zhou Z (2021) Abnormal Lipid Profile in Fast-Growing Broilers With Spontaneous Femoral Head Necrosis. Front. Physiol. 12:685968. doi: 10.3389/fphys.2021.685968

INTRODUCTION

In the past few decades, substantial progress has been made in improving the feed efficiency and growth rate in fast-growing broilers, and the growth rate and body weight at market age have increased almost threefold (Havenstein et al., 2003). However, the heavier body weight also exerts negative effects on body health, and metabolic problems are promoted, such as pulmonary hypertension, fatty liver syndrome, lameness, and skeletal problems (Packialakshmi et al., 2015b). Femoral head necrosis (FHN) is one of the most common leg problems, and it leads to lameness and affects the growth and development of broilers. According to investigations and studies, at a high stock density, the incidence of leg problems is about 2%, and the detection rate of FHN is as high as 13.33% (Applegate and Lilburn, 2002; Li et al., 2015), which often affects broilers at 5 to 6 weeks of age. FHN is often characterized by the squatting position and rarely standing and walking, and severely affected broilers even limp. Due to the limited access to feed, FHN not only drastically reduces the production performance of broiler chickens, giving rise to a poor bird welfare, but also causes considerable economic losses (Julian, 2005).

A disorder of lipid metabolism is considered to be one of the main factors in FHN-affected broilers (Brewer et al., 1972; Yamamoto et al., 1997). The pathogenesis of FHN is often accompanied by the occurrence of hyperlipidemia (Yu et al., 2016; Liu et al., 2021). However, the influences of lipid metabolism disorder are not clearly understood in FHN broilers. It is believed that if blood lipids are abnormal, the levels of, for example, triglycerides (TG), lipoprotein (LDL), and total cholesterol (TC) increase significantly, the high blood viscosity lowers the blood flow, and, as a result, fat emboli in blood vessels develop (Durairaj et al., 2009; Packialakshmi et al., 2015a; Wang et al., 2018; Guo et al., 2019). Then, the intramedullary microcirculation problem causes tissue hypoxia, high intraosseous pressure, and deficient nutrient transport, which ultimately promotes

bone cell necrosis (Lee et al., 2006). In addition, neutral fatty acids can result in capillary intima falling off, vascular wall edema, intravascular congestion, and the aggravation of the femoral head ischemia (Teitelbaum, 2000).

Bone is a dynamic endocrine organ that regulates its own and even the whole body's steady-state balance (Alekos et al., 2020). Bone modeling and remodeling are strictly controlled by many factors, including lipids. The lipids in bones are generally considered to exist only in the bone marrow, and the mineralized bone tissue itself contains a small amount of lipids, which may play an important role in bone physiology. Among the total fatty acids, for chicken, the bones mainly contain oleic acid (18:1n-9) (35–45%) and palmitic acid (16:0) (25%) [% of the total fatty acids (Wolinsky and Guggenheim, 1970)], which is similar to the distribution of fatty acids in human bones (Dirksen and Marinetti, 1970). Among the bone components, chicken cortical bone contains a higher fatty acid content than cancellous bone, which allows the intensity of metabolic activity to be maintained (Dolegowska et al., 2006; Liu et al., 2021). In addition, the utilization of fatty acids in bone is comparable to that in tissues with more a classic fatty acid metabolism (Alekos et al., 2020). Increasing evidence shows that there is a close correlation between bone fat and many bone diseases (Bermeo et al., 2014). In patients with osteoporosis, abnormal blood lipid levels are associated with a decreased bone density and bone loss (Nuzzo et al., 2009; Chen et al., 2016; Saoji et al., 2018; Chi et al., 2019). In addition to hyperlipidemia, mice receiving a high-fat diet treatment also showed trabecular bone destruction and a decreased bone strength (Chen et al., 2016).

Despite extensive research, the biological mechanisms underlying the relationship between FHN and lipid metabolism disorders in broilers and other animals is an issue that is worth investigating. The aim of this study was to determine how spontaneous FHN is influenced by lipid metabolism disorders in broilers by analyzing blood lipid metabolism markers and the expression of related genes in the femoral head and bone parameters.

MATERIALS AND METHODS

Sample Collection

The broilers (Gallus gallus, AA broilers) of both sexes were sampled from a chicken farm in Jiangsu province. The birds were fed a two-phase commercial diet *ad libitum*: a starter ration (21.00% crude protein, 1.00% Ca, 0.52% total P, and 0.45% methionine) from 0 to 21 days and a grower ratio (19.00% crude protein, 0.95% Ca, 0.47% total P, 0.38% methionine) from 22 to 35 days. At the ages of 3, 4, and 5 weeks, eight normal broilers and eight FHN-affected broilers were selected for the collection of serum, plasma, and tissue samples. After the body weight was recorded, blood samples were collected from the wing vein and centrifuged at 4,000 *g* for 15 min. The serum and plasma were collected and then stored at −20°C for analysis. The liver samples from the broilers at the age of 5 weeks were collected immediately, rinsed with normal saline, and fixed in 4% formaldehyde. Both sides of the femur and tibia from the normal and FHN-affected birds were harvested and maintained at −20°C for the determination of the bone density and biomechanics. The femoral head was cut along the sagittal plane and rinsed with normal saline. One half was cleaned with PBS and fixed in 4% paraformaldehyde at 4°C, and the other half was subjected to DEPC and then stored in liquid nitrogen. According to the FHN diagnosis standard, the broilers were divided into two groups: a normal group and FHN-affected group.

Biochemistry

The levels of serum alkaline phosphatase(ALP), Ca, P, triglycerides (TG), total cholesterol (TC), high-density lipoproteins (HDL), and low-density lipoproteins (LDL) were detected using a BS-300 automatic biochemical detector (Mindray Biomedical Electronics Co., Ltd.). Each sample was measured in triplicate.

ELISA Assay

Two kinds of indicants in the plasma were measured using a chicken-specific ELISA kit. Seven indicators related to lipid metabolism were determined, including acetyl-CoA carboxylase (ACC), fatty acid synthase (FAS), lipoprotein lipase (LPL), adipose triglyceride lipase (ATGL), hormone-sensitive lipase (HSL), peroxisome proliferator-activated receptor (PPARγ), and free fatty acid (FFA). Two indicators of bone metabolism were analyzed, including bone alkaline phosphatase (BALP) and tartrate resistant acid phosphatase(TRACP-5b. Each sample was measured in triplicate.

HE Staining

The femoral head was fixed in 4% PFA, rinsed overnight with tap water, and decalcified with 10% EDTA for 2 weeks. After the treatment, the bone tissue and the PFA-fixed liver tissue were dehydrated with ethanol, cleared with xylene, and embedded in paraffin. Hematoxylin-eosin (HE) staining was performed to observe the degree of lesion changes. The area of lipid droplets in

TABLE 1 | Sequences of primers used to express specific mRNAs by RT q-PCR.

Target gene	Primer sequence (5′-3′)
ACSL1	F:TGGAACGTGGCAAGAAGTGT
	R: CCCTTGGGGTTTCCTGTTGT
ACC	F: GCTTCCCATTTGCCGTCCTA
	R:GCCATTCTCACCACCTGATTACTG
FAS	F: TTTGGTGGTTCGAGGTGGTA
	R: CAAAGGTTGTATTTCGGGAGC
CPT1	F: TAGAGGGCGTGGACCAATAA
	R: TGGGATGCGGGAGGTATT
ATGL	F: TCCTAGGGGCCTACCACATC
	R: CCAGGAACCTCTTTCGTGCT
PPARγ	F: GTGCAATCAAAATGGAGCC
	R: CTTACAACCTTCACATGCAT
LRP1	F: CTCTGTGGATTGGGTTTCC
	R: ACCAGGCAGTGGGGTTTA
GAPDH	F: GAACATCATCCCAGCGTCCA
	R: CGGCAGGTCAGGTCAACAAC
APOB	F: GCAGCCTATGGAACAGA
	R: TAGTGGAACGCAGAGCA

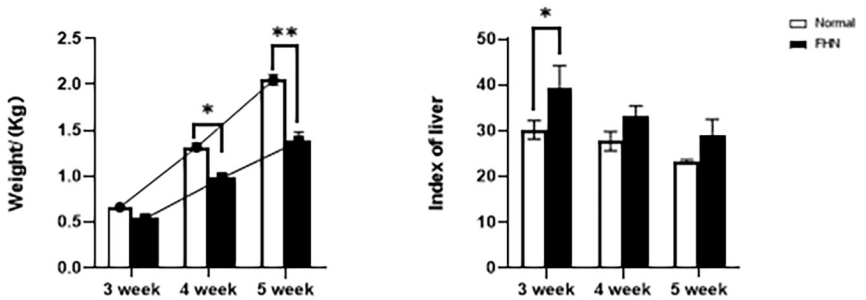

FIGURE 1 | The weight and liver coefficient changes for 3∼5 weeks of FHN. *indicates a significant difference ($P < 0.05$). **indicates an extremely significant difference ($P < 0.01$).

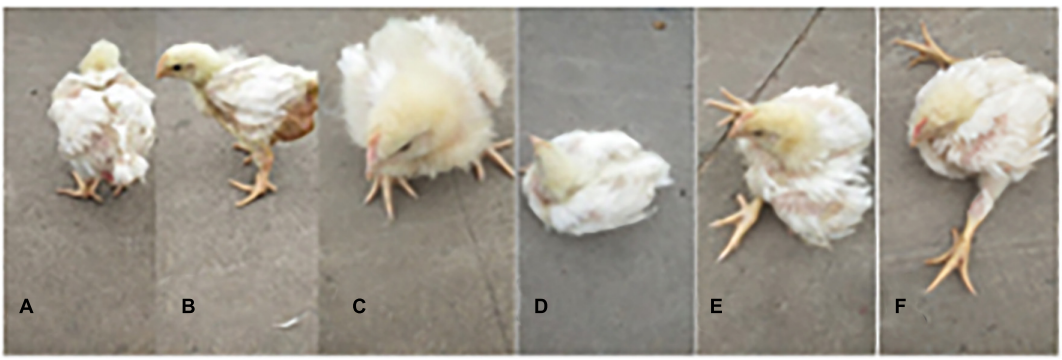

FIGURE 2 | The varying degrees of gait changes in broilers with FHN. Gait score of 0 **(A)** The bird walked normally, with no detectable abnormality; Gait score of 1 **(B)** The bird had a slight defect, which was difficult to define precisely; Gait score of 2 **(C)** The bird had a definite and identifiable defect in its gait; Gait score of 3 **(D)** The bird had an obvious gait defect, which affected its ability to move about; Gait score of 4 **(E)** The bird had a severe gait defect; Gait score of 5 **(F)** The bird was incapable of sustained walking on its feet.

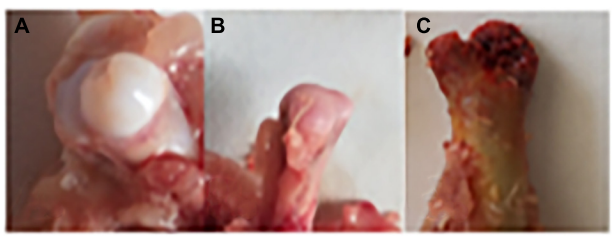

FIGURE 3 | Clinical and anatomical manifestations of FHN broilers. **(A)** Normal broilers; **(B,C)** FHN-affected broilers. Panel **(B)** shows a cartilage loss, and the subchondral bone had ivory-like changes; Panel **(C)** indicates a cartilage separation, and the epiphysis is broken.

the liver and femoral head were analyzed using ImageJ (Huang et al., 2018; Jahejo et al., 2020).

Bone Parameters

The bone mineral density (BMD) of the tibia and femur were measured using a dual energy X-ray bone densitometer (MEDIKORS, Gyeonggi, South Korea). The test mode was set with a high energy parameter of 80 kVp/1.0 mA and a low energy parameter of 55 kVp/1.25 mA. The InAlyzer 1.0 image processing system was used to analyze and process the captured pictures and measure and record the length of the femur and tibia and the density of the midsection (Li et al., 2015).

The strength of the tibia and femur was determined using a three-point bending test. The tibia and femur were placed on the working platform of a universal material testing machine (LR10K Plus, Lloyd Instruments Ltd., United Kingdom), with a known span. The following parameters were set: preload: 5 N; preload speed: 15 mm/min; and the test was stopped when the bone was fractured. The bone strength curve was obtained by NEXYGEN Plus software. The highest point of the curve was the bone strength value (N).

Total RNA Extraction and RT q-PCR

The femoral head samples in broilers at the age of 5 weeks were pulverized in a low-temperature environment and treated with trizol (Nanjing Angel Gene Biotechnology Co., Ltd., Nanjing) to extract the total RNA. The use of HiScript II QRT SuperMix for qPCR (+ gDNA wiper; Zazyme, Nanjing, China) resulted in reverse transcriptional synthesis of complementary DNA. Using the ABI PRISM 7300 HT sequence detection system (Application Biossystems, Inc., Foster City, CA, United States), SYBR Green PCR technology was used to detect the expression of lipid metabolism-related genes. All PCR operations were performed

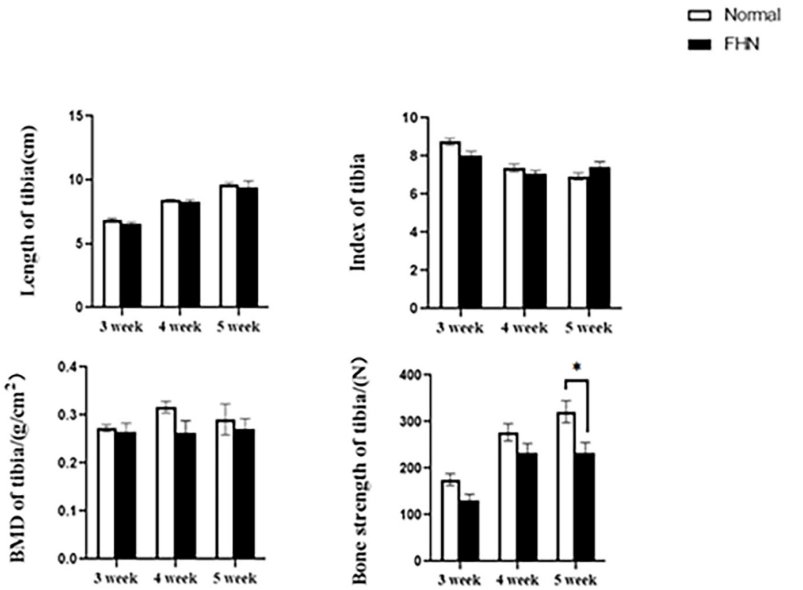

FIGURE 4 | Tibia parameters in broilers. *indicates a significant difference ($P < 0.05$).

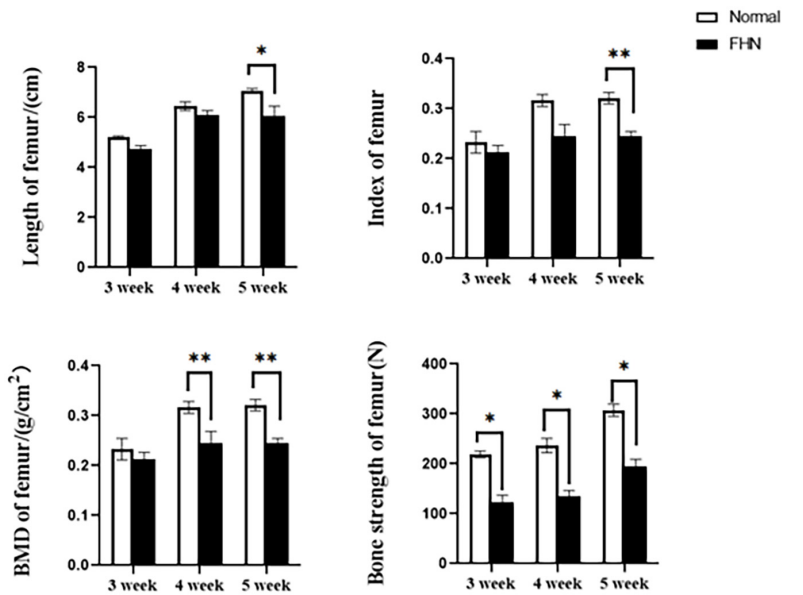

FIGURE 5 | Femur parameters in broilers. *indicates a significant difference ($P < 0.05$). **indicates an extremely significant difference ($P < 0.01$).

in triplicate. The selected genes and the primer sequences for the corresponding genes are shown in **Table 1**. Housekeeper GAPDH was used as an internal standard for the quantity and quality of cDNA.

Statistical Analysis

The statistical analysis was conducted using SPSS 17.0 for windows. The data were expressed as the mean ± SEM, and the differences between groups were determined using one-way analysis of variance (ANOVA, SNK). Significant differences were accepted at two levels: P<0.05 (significant) and P<0.01 (extremely significant).

RESULTS

FHN Affected the Bone Growth in Broilers, Especially That of the Femur

The chicken farm has a total of 252,000 chickens, with a mortality rate of 3.80% and a culling rate of 1.15%. Of the 80 lame chickens

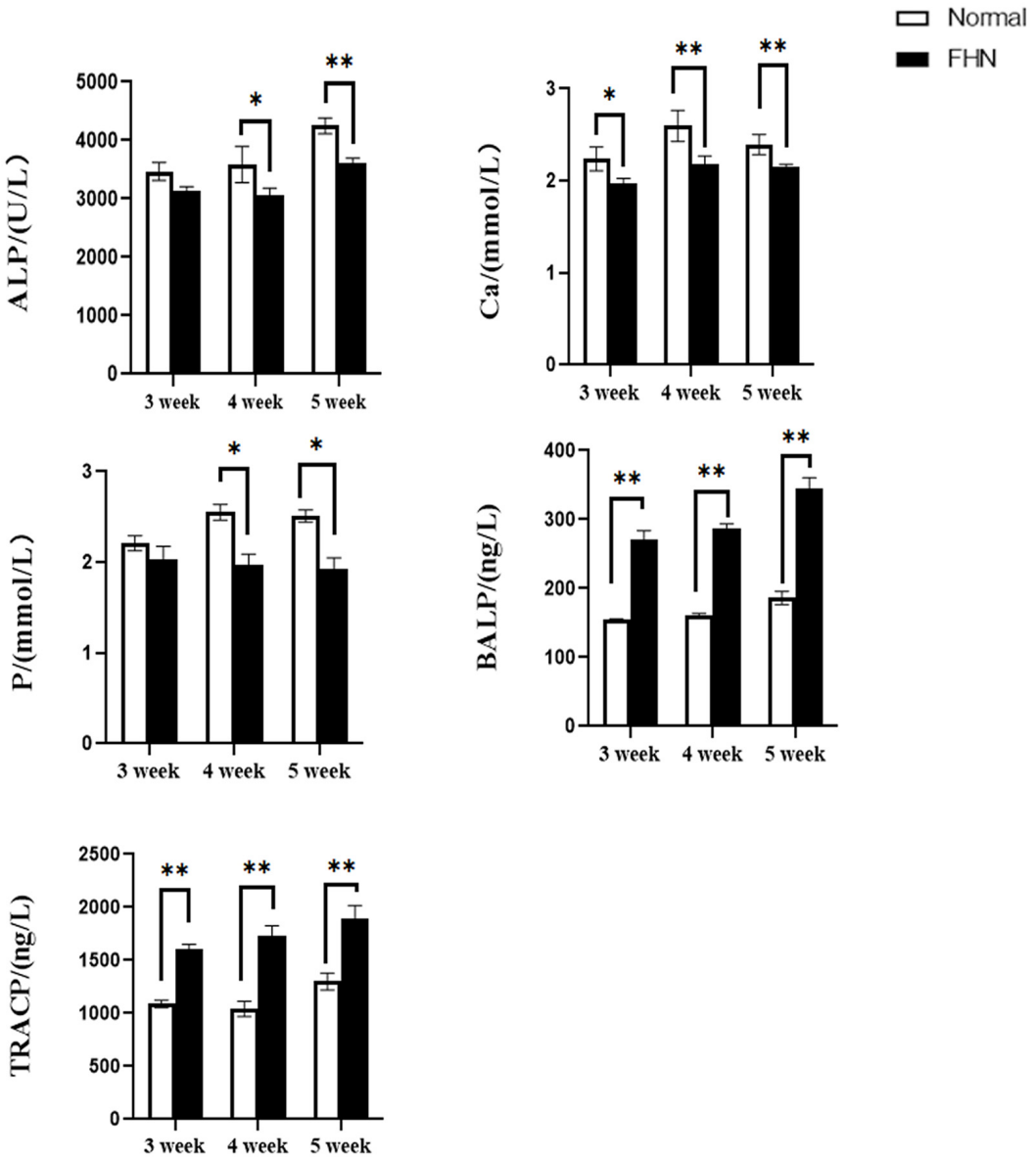

FIGURE 6 | The changes of serum biochemical indicators and bone metabolism. *indicates a significant difference ($P < 0.05$). **indicates an extremely significant difference ($P < 0.01$).

examined, 48 had FHN, and their gait scores (Kestin et al., 1992) were point 4. 8 for normal broilers and 8 for FHN-affected chickens when analyzed at 3, 4, and 5 weeks. The body weight of the normal broiler chickens increased from the 3th to the 5th weeks, but the body weight of the chickens with FHN decreased significantly in the 4th and 5th weeks ($P < 0.05$). The body weight of the FHN birds (1.227 ± 0.103 kg) was significantly lighter than that of the normal ones (2.050 ± 0.053 kg) ($P < 0.01$) in the 5th week (**Figure 1**). In addition, most broilers suffering from FHN showed an abnormal gait. The varying degrees of gait changes in the broilers with FHN are shown in **Figure 2**. FHN in broilers was defined as a separation of the femoral head cartilage from the underlying growth plate, damage to the growth plate, or even a breakage of the epiphysis. **Figure 3** shows the apparent changes of the FHN-affected broilers.

The bone length, bone index, bone strength, and bone density of the tibia did not differ significantly between the normal and the FHN-affected group, except for the tibia bone strength in the 5th week, and the difference in the performance of the bone index on the femur was very obvious. The length and bone index of the femur in the FHN group in the 5th week were significantly lower than those in the normal group ($P < 0.05$). The bone density of the femur was also significantly decreased in the 4th and 5th weeks in the FHN group. At the same time, the bone strength in the FHN group decreased significantly in 3∼5 weeks ($P < 0.05$). The results show that FHN affected the bone density

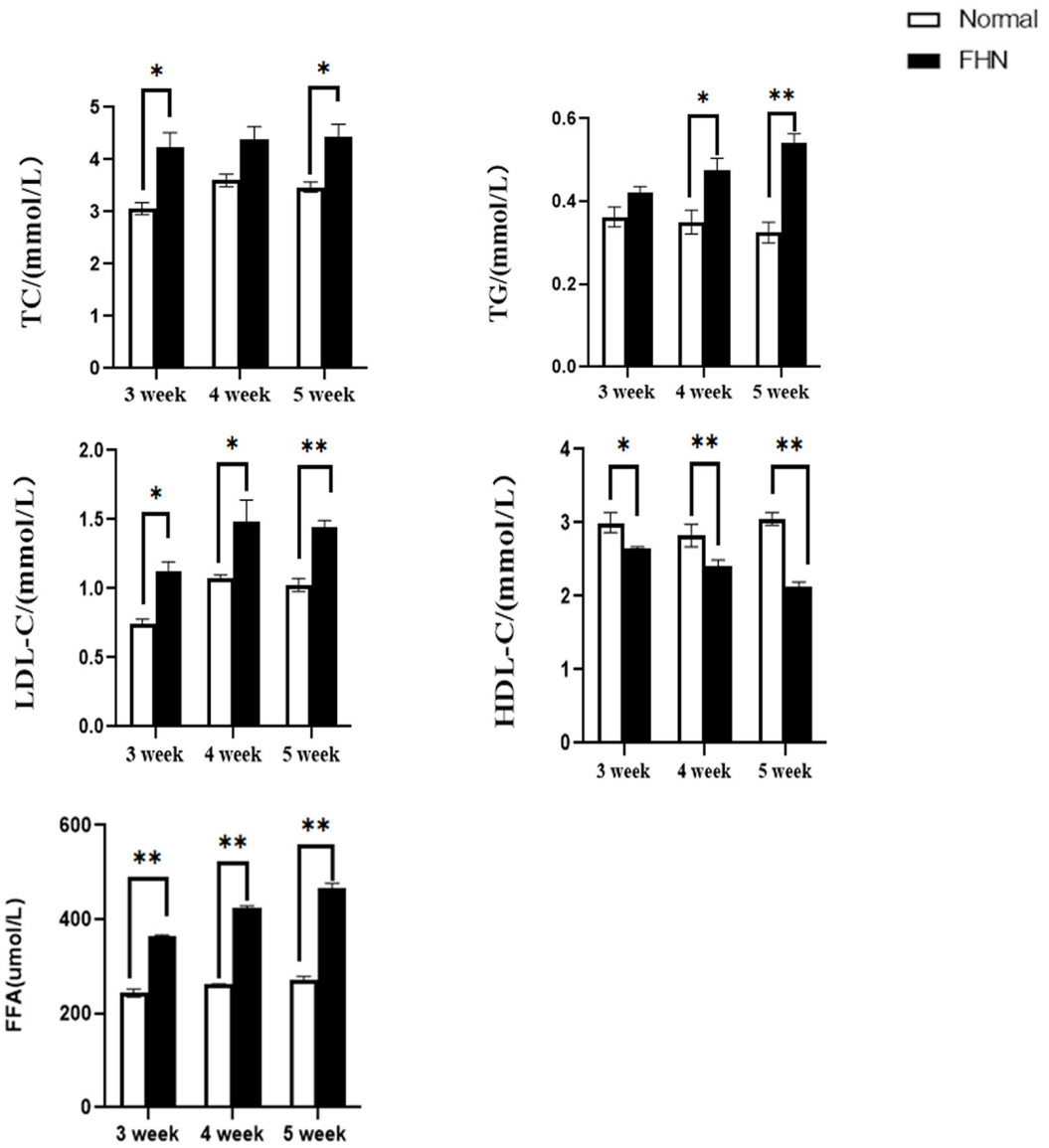

FIGURE 7 | The changes in serum biochemical indicators regarding lipid metabolism. *indicates a significant difference ($P < 0.05$). **indicates an extremely significant difference ($P < 0.01$).

and strength of long bones, especially the femur (**Figures 4**, **5**). The levels of ALP, Ca, and P in the FHN group were lower than those in the normal group in the 4th and 5th weeks ($P < 0.05$). In addition, the BALP and TRACP activities in the FHN group were elevated ($P < 0.05$), indicating that the bone formation and bone resorption activities were enhanced in the pathogenesis of FHN (**Figure 6**).

Lipid Metabolism Disorder Appeared in FHN

Compared with normal broilers, a higher TC, TG, and LDL-C were detected in the FHN broilers, and the HDL-C was lower, leading to an elevated FFA (**Figure 7**).

Lipid metabolism-related enzymes and markers were detected using an ELISA. Two key rate-limiting enzymes affecting FAS and ACC were significantly increased in the FHN group, and the two enzymes involved in ATGL and HSL were significantly decreased. Compared with the normal group, the fat synthesis and decomposition of the FHN group were increased, which also caused an accumulation of fat. The increase in LPL and PPARγ in the FHN group also indicated this trend, as shown in **Figure 8**.

HE staining (**Figure 9**) showed that the liver cells in the control broilers at the age of 5 weeks had a normal morphology and complete structure, while in the broilers affected by FHN, round cavities of different sizes appeared, indicating that the liver structure in the FHN birds was damaged to varying degrees. The liver of the FHN-affected broilers was likely to

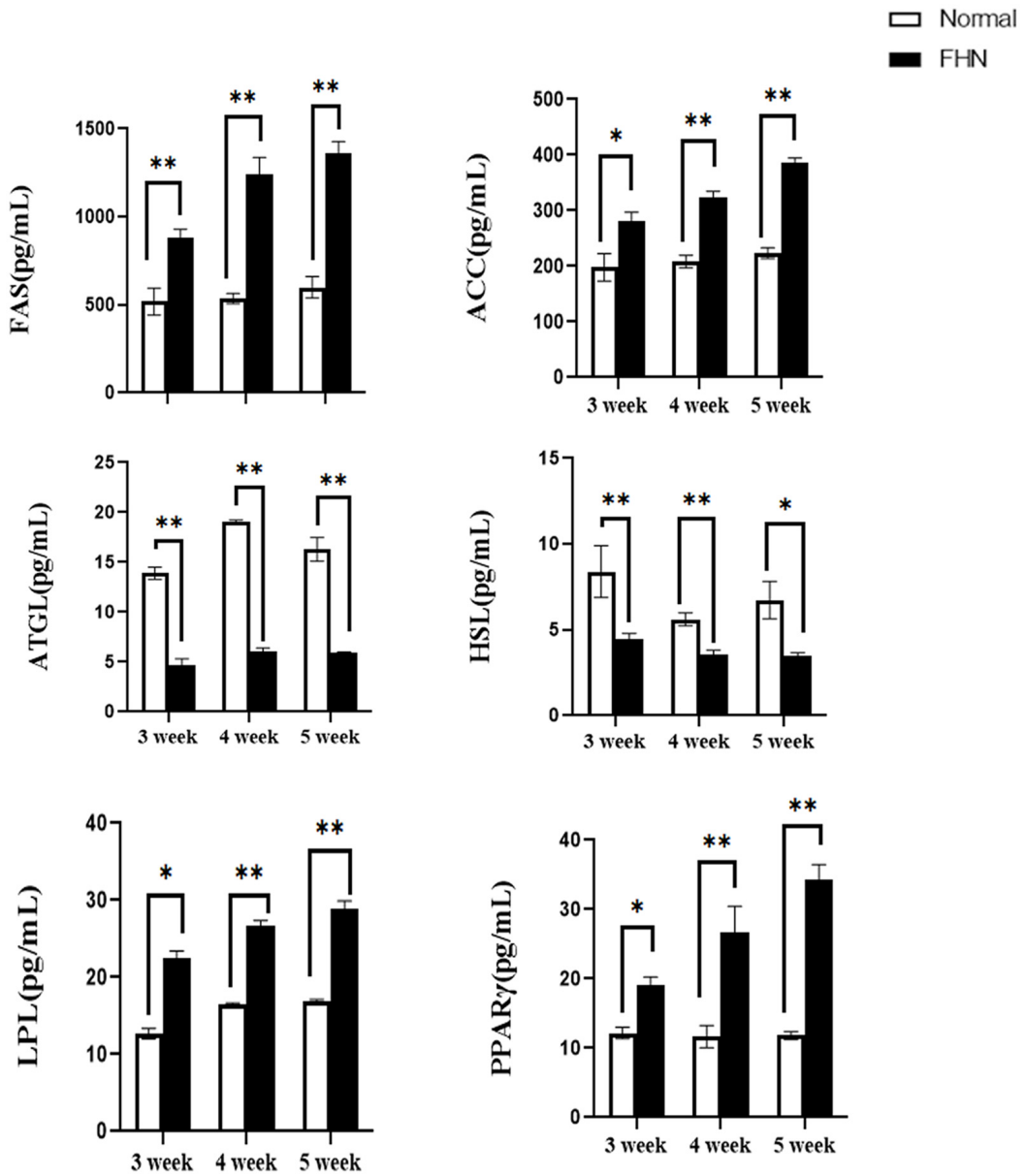

FIGURE 8 | The changes in serum lipid metabolism-related enzymes and markers. *indicates a significant difference ($P < 0.05$). **indicates an extremely significant difference ($P < 0.01$).

have steatosis. In addition, HE staining (**Figure 10**) reflected the presence of lipid droplets of different sizes in the subchondral bone in the FHN birds, indicating that the femoral head was infiltrated with fat when necrosis occurred. In addition, the gene expression related to the fatty acid synthesis pathway in the liver was detected, including an increase in ACC and FAS and a decrease in PPARγ, which resulted in lipid deposition during liver metabolism (**Figure 11A**).

Expression of Lipid-Related Genes

Figure 11B shows the mRNA expression of some genes related to lipid metabolism in the subchondral bone of the femoral head in the broilers at the age of 5 weeks. Compared with the normal group, the fat mobilization genes, including CPT1, ACSL, and ATGL, were significantly promoted in the FHN birds, and the genes related to fat synthesis were also significantly increased, including FAS, PPARγ, and LRP1.

DISCUSSION

Recent studies have shown that with the deepening of lipid metabolism disorders, abnormal bone metabolism, osteoarthritis, osteoporosis, bone loss, and other diseases may occur, and

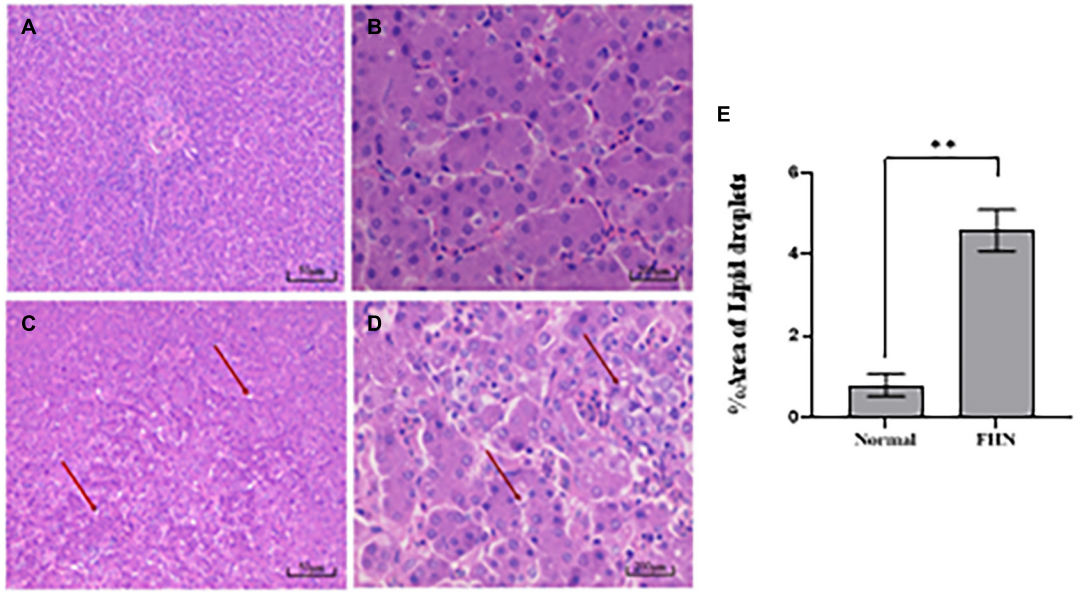

FIGURE 9 | HE staining of the liver in broilers at the age of 5 weeks. Normal broilers: **(A,B)**; FHN broilers: **(C,D)**; analysis of the area of lipid droplets in the liver **(E)**. The red arrow points to the site where vacuolar degeneration occurred. **indicates an extremely significant difference ($P < 0.01$).

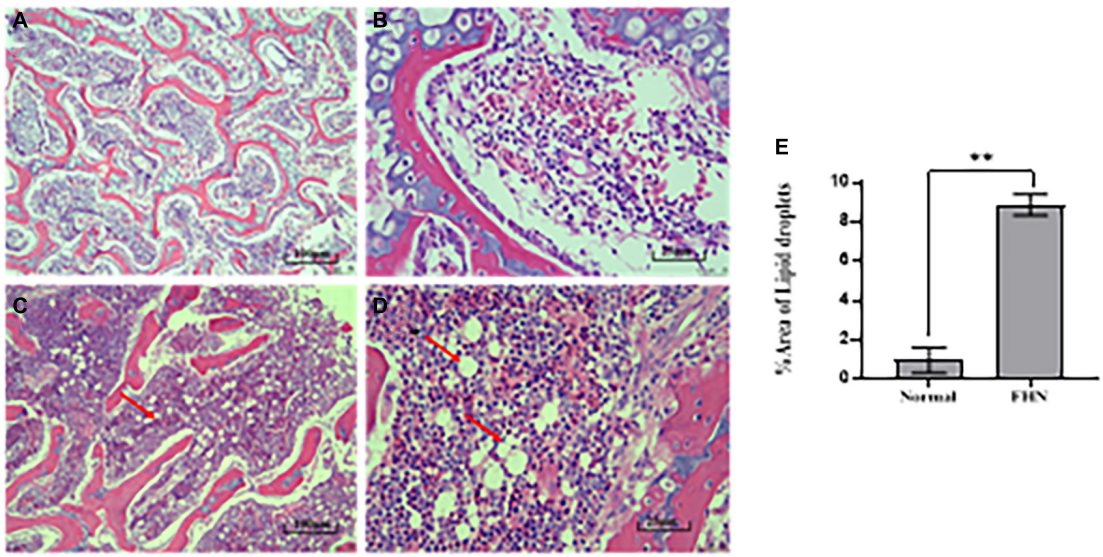

FIGURE 10 | HE staining of the femoral head in the broilers at the age of 5 weeks. Normal broilers: **(A,B)**; FHN broilers: **(C,D)**; analysis of the area of lipid droplets in the femoral head **(E)**. The red arrow points to the site where vacuolar degeneration occurred. **indicates an extremely significant difference ($P < 0.01$).

the risk of fractures increases. Gu et al. (2019), Yang et al. (2019) found that there is a negative relationship between fat intake and bone density. Mice fed a high-fat for a long time show a decrease in the amount of osteoid, cancellous bone, and type I collagen. Osteoporosis is also closely related to hyperlipidemia (During, 2020). As the plasma TC concentration increases, the bone density decreases. Clinically, statins are used to antagonize osteoporosis (Chamani et al., 2021). In addition, the inflammatory microenvironment caused by fat has a stimulating effect on the formation of bone cells, releasing a large number of inflammatory factors, aggravating the destruction of cartilage damage and synovial inflammation, and increasing the incidence of arthritis (Pousinis et al., 2020).

Lipid metabolism disorder has been recognized as one of the factors of femoral head necrosis, particularly hormonal femoral head necrosis, which is mainly attributed to hyperlipidemia. Hormonal drugs cause high blood coagulation and low fibrinolysis and thrombosis; impair the blood flow in bone,

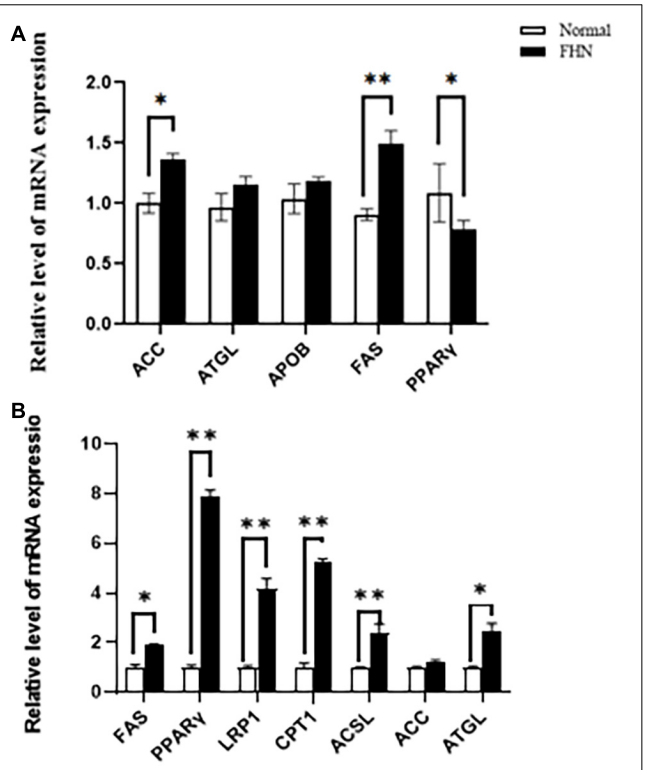

FIGURE 11 | The changes of the mRNA expression of the target genes related to lipid metabolism in the liver **(A)** and femoral head **(B)** at the age of 5 weeks. *indicates a significant difference ($P < 0.05$). **indicates an extremely significant difference ($P < 0.01$).

leading to ischemia, hypoxia, and the necrosis of bone cells; destroy the structure and function of bone tissue; and, finally, result in avascular necrosis of the femoral head (Glueck et al., 2005). Previous studies have found that lipids are distributed in bone marrow and mineralized tissues and may play important roles in regulating the physiological functions of bone fatty acids, cholesterol, phospholipids, and several endogenous metabolites [such as prostaglandins and oxysterols (During et al., 2015)] that play important roles in bone cell survival and function, bone mineralization, and key signaling pathways. Therefore, they can be considered as important regulators of bone homeostasis (Kiyoi, 2018). However, on the other hand, fatty acids have toxic effects and can impair bone health (Innes and Calder, 2018).

Most of the findings still remain restricted to humans and mice. However, in recent years, broilers have been used as a model animal for leg disorder research. This study used naturally affected broilers as a model to study the relationship between lipid metabolism disorders and femoral head necrosis during the pathogenesis of FHN in broilers. In fast-growing broilers, the incidence of FHN is higher at 4∼6 weeks due to the linear increase in body weight in these periods. Compared with the normal broilers, the body weight of the FHN birds significantly decreased because it was difficult for the FHN birds to access feed and water. We found that many of the naturally FHN-affected broilers were unwilling to walk or stand, and there were also a few broilers that looked normal in appearance and gait, but an autopsy showed that these birds were affected by FHN. Therefore, it was a golden standard to diagnose FHN based on pathological changes, clinical signs, and gait observation. In addition, bone quality is an important indicator of bone health and can be assessed through the determination of bone parameters (Fonseca et al., 2014). The bone strength and density of broilers with FHN were significantly decreased. This situation was also directly manifested in the abnormal gait of the FHN chickens, which was prone to fracture during autopsy. Serum ALP, Ca, and P showed a downward trend. The abnormal increase in BALP and TRACP indicated that the balance between bone formation and bone resorption was disturbed. In this work, the occurrence of FHN directly affected the maintenance of long bone volumes in broilers, especially the femur.

Lipid metabolism disorder appeared in broilers with FHN. The indicators of liver function were significantly higher in the FHN-affected birds. Histopathology showed that lipid droplets and steatosis appeared in the liver of the FHN birds. Combined with the manifestations of hyperlipidemia in the plasma, TC, TG, and LDL-C were increased, and HDL-C was decreased, indicating that the broiler chickens with FHN had a lipid metabolism disorder. When FHN developed, the body was in a state of lipid accumulation. The bone itself is equipped with enzymes and receptors for the absorption and utilization of fatty acids. The intake of chylomicrons of bone accounts for 17% of the liver, which is higher than that of other catabolic organs, such as muscle and the heart (Niemeier et al., 2008). Importantly, a femoral shaft rich in osteoblasts/osteocytes has a higher residual uptake of chylomicrons than bone marrow (Bartelt et al., 2017). This shows that the femur can absorb circulating lipoproteins and free fatty acids. We observed lipid droplets in the subchondral bone of the femoral head in the FHN birds. The potential role of bones in fatty acid metabolism is emphasized in the pathogenesis of FHN.

Previously, some people performed gene-chip analysis in hormonal osteonecrosis model rats and found that genes related to fatty acid synthesis in the femoral head were up-regulated (Yue et al., 2018). This finding is similar to our current results. The Acsl1 and CPT1 genes were up-regulated, and the FAS expression was down-regulated. More similarly, the PPAR gene also showed down-regulation, like FHN in the other animals. PPARγ is a widely expressed nuclear transcription factor, which plays an important role in the differentiation of bone marrow mesenchymal stem cells (Kim and Ko, 2014; Yuan et al., 2018). It promotes audiogenic differentiation at the expense of inhibiting osteogenic differentiation (Wang et al., 2017). Most studies reported that the main reason for glucocorticoid-induced FHN is an abnormal audiogenic osteogenic differentiation of bone marrow mesenchymal stem cells, which is manifested by an increased differentiation of adipocytes and inhibition of osteoblast differentiation (Yu et al., 2016). We speculate that the femoral head of FHN broilers may also have a similar abnormal pathological change and an increased fat accumulation in the femoral head. In addition, the expression of the lrp1 gene was up-regulated. It was reported that in the culture of osteoblast

models, LRP1 promoted the endocytosis of triglycerides and cholesterol containing chylomicron residues (Frey et al., 2014). The polymorphism of the gene encoding this receptor is related to bone density and to the maintenance of bone stability (Sims et al., 2008; Frey et al., 2014). LRP1 regulates osteoblast and osteoclast activities through the Wnt pathway. The Wnt pathway is the opposite of PPARγ, which also controls the osteogenic-adipogenic differentiation of bone marrow mesenchymal stem cells and promotes the proliferation and differentiation of osteoblasts (Zhang et al., 2015; Chen et al., 2016; Yao et al., 2017). In this work, the osteogenic-adipogenic differentiation of femurs in FHN broilers was disrupted, many fat cells appeared, the fatty acid metabolism increased, and the lipotoxic effect of fatty acids caused the necrosis of bone cells and osteoblasts. However, the reason for the destruction of the balance of osteogenic-adipogenic differentiation was not yet known, and further research in this direction needs to be conducted.

In summary, when femoral head necrosis occurred in fast-growing broilers, it was accompanied by lipid metabolism disorders. The affected femoral head had a lipid accumulation and changes in the expression of lipid metabolism-related genes, which may be involved in the PPAR pathway. A lot of work needs to be conducted to figure out the factors leading to femoral head necrosis in broilers, and the mechanisms of lipid regulation involved in osteocyte function and signal pathways need to be investigated.

DATA AVAILABILITY STATEMENT

The raw data supporting the conclusions of this article will be made available by the authors, without undue reservation.

ETHICS STATEMENT

The animal study was reviewed and approved by #NJAU-Poult-2020092403, approved on September 24, 2020.

AUTHOR CONTRIBUTIONS

RF helped with the experimental design and this writing. KL helped with the sampling and the data analysis. All authors have read and agreed to the published version of the manuscript.

FUNDING

This work was supported by the National Key R&D Program of China (Project No. 2017YFD0502205), the National Natural Science Foundation of China (Grant 32072936), and the Priority Academic Program Development of Jiangsu Higher Education Institutions (PAPD).

REFERENCES

Alekos, N. S., Moorer, M. C., and Riddle, R. C. (2020). Dual Effects of Lipid Metabolism on Osteoblast Function. *Front. Endocrinol.* 11:578194. doi: 10.3389/fendo.2020.578194

Applegate, T. J., and Lilburn, M. S. (2002). Growth of the femur and tibia of a commercial broiler line. *Poultry Sci.* 81, 1289–1294. doi: 10.1093/ps/81.9.1289

Bartelt, A., Koehne, T., Toedter, K., Reimer, R., Mueller, B., Behler-Janbeck, F., et al. (2017). Quantification of Bone Fatty Acid Metabolism and Its Regulation by Adipocyte Lipoprotein Lipase. *Int. J. Mol. Sci.* 18:1264. doi: 10.3390/ijms18061264

Bermeo, S., Gunaratnam, K., and Duque, G. (2014). Fat and Bone Interactions. *Curr. Osteopor. Rep.* 12, 235–242.

Brewer, H. B. Jr., Lux, S. E., Ronan, R., and John, K. M. (1972). Amino acid sequence of human apoLp-Gln-II (apoA-II), an apolipoprotein isolated from the high-density lipoprotein complex. *Proc. Natl. Acad. Sci. U S A.* 69, 1304–1308. doi: 10.1073/pnas.69.5.1304

Chamani, S., Liberale, L., Mobasheri, L., Montecucco, F., Al-Rasadi, K., Jamialahmadi, T., et al. (2021). The role of statins in the differentiation and function of bone cells. *Eur. J. Clin. Invest.* 2021:e13534.

Chen, X., Wang, C., Zhang, K., Xie, Y., Ji, X., Huang, H., et al. (2016). Reduced femoral bone mass in both diet-induced and genetic hyperlipidemia mice. *Bone* 93, 104–112. doi: 10.1016/j.bone.2016.09.016

Chi, J. H., Shin, M. S., and Lee, B. J. (2019). Identification of hypertriglyceridemia based on bone density, body fat mass, and anthropometry in a Korean population. *BMC Cardiovas. Disord.* 19:66. doi: 10.1186/s12872-019-1050-2

Dirksen, T. R., and Marinetti, G. V. (1970). Lipids of bovine enamel and dentin and human bone. *Calcified Tissue Res.* 6, 1–10. doi: 10.1007/bf02196179

Dolegowska, B., Machoy, Z., and Chlubek, D. (2006). Profiles of fatty acids in different bone structures of growing chicks. *Vet. Res. Communic.* 30, 735–747. doi: 10.1007/s11259-006-3362-9

Durairaj, V., Okimoto, R., Rasaputra, K., Clark, F. D., and Rath, N. C. (2009). Histopathology and Serum Clinical Chemistry Evaluation of Broilers with Femoral Head Separation Disorder. *Avian Dis.* 53, 21–25. doi: 10.1637/8367-051908-reg.1

During, A. J. B. (2020). Osteoporosis: A role for lipids. *Biochimie* 178, 49–55. doi: 10.1016/j.biochi.2020.08.004

During, A., Penel, G., and Hardouin, P. (2015). Understanding the local actions of lipids in bone physiology. *Prog. Lipid Res.* 59, 126–146. doi: 10.1016/j.plipres.2015.06.002

Fonseca, H., Moreira-Goncalves, D., Coriolano, H.-J. A., and Duarte, J. A. (2014). Bone Quality: The Determinants of Bone Strength and Fragility. *Sports Med.* 44, 37–53. doi: 10.1007/s40279-013-0100-7

Frey, J., Li, Z., Ellis, J., Farber, C., Aja, S., Wolfgang, M., et al. (2014). Wnt-Lrp5 signaling regulates fatty acid metabolism in the osteoblast. *J. Bone Mineral Res.* 29, S12–S12.

Glueck, C. J., Freiberg, R. A., Sieve, L., and Wang, P. (2005). Enoxaparin prevents progression of stages I and II osteonecrosis of the hip. *Clin. Orthopaed. Related Res.* 2005, 164–170. doi: 10.1097/01.blo.0000157539.67567.03

Gu, L., Lai, X., Wang, Y., Zhang, J., and Liu, J. J. M. (2019). A community-based study of the relationship between calcaneal bone mineral density and systemic parameters of blood glucose and lipids. *Medicine* 98:e16096. doi: 10.1097/md.0000000000016096

Guo, Y., Tang, H., Wang, X., Li, W., Wang, Y., Yan, F., et al. (2019). Clinical assessment of growth performance, bone morphometry, bone quality, and serum indicators in broilers affected by valgus-varus deformity. *Poultry Sci.* 98, 4433–4440. doi: 10.3382/ps/pez269

Havenstein, G. B., Ferket, P. R., and Qureshi, M. A. (2003). Growth, livability, and feed conversion of 1957 versus 2001 broilers when fed representative 1957 and 2001 broiler diets. *Poultry Sci.* 82, 1500–1508. doi: 10.1093/ps/82.10.1500

Huang, S. C., Zhang, J. L., Rehman, M. U., Tong, X. L., Qiu, G., Jiang, X., et al. (2018). Role and regulation of growth plate vascularization during coupling with osteogenesis in tibial dyschondroplasia of chickens. *Sci. Rep.* 8:3680. doi: 10.1038/s41598-018-22109-y

Innes, J. K., and Calder, P. C. (2018). Omega-6 fatty acids and inflammation. *Prostaglandins Leukotrienes Essential Fatty Acids* 132, 41–48. doi: 10.1016/j.plefa.2018.03.004

Julian, R. J. (2005). Production and growth related disorders and other metabolic diseases of poultry - A review. *Vet. J.* 169, 350–369. doi: 10.1016/j.tvjl.2004.04.015

Jahejo, A., Zhang, D., Niu, S., Mangi, R., Khan, A., Qadir, M., et al. (2020). Transcriptome-based screening of intracellular pathways and angiogenesis reated genes at different stages of thiram induced tibial lesions in broiler chickens. *BMC Genom.* 21:50. doi: 10.1186/s12864-020-6456-9

Kim, J., and Ko, J. (2014). A novel PPAR gamma(2) modulator sLZIP controls the balance between adipogenesis and osteogenesis during mesenchymal stem cell differentiation. *Cell Death Different.* 21, 1642–1655. doi: 10.1038/cdd.2014.80

Kiyoi, T. (2018). Bone Resorption Activity in Mature Osteoclasts. *Methods Mol. Biol.* 1868, 215–222. doi: 10.1007/978-1-4939-8802-0_22

Kestin, S., Knowles, T., Tinch, A., and Gregory, N. J. T. V. R. (1992). Prevalence of leg weakness in broiler chickens and its relationship with genotype. *Vet. Rec.* 131, 190–194. doi: 10.1136/vr.131.9.190

Lee, J. S., Lee, L. S., Rob, H. L., Kim, C. H., Jung, J. S., and Suh, K. T. (2006). Alterations in the differentiation ability of mesenchymal stem cells in patients with nontraumatic osteonecrosis of the femoral head: Comparative analysis according to the risk factor. *J. Orthopaed. Rese.* 24, 604–609. doi: 10.1002/jor.20078

Li, P. F., Zhou, Z. L., Shi, C. Y., and Hou, J. F. (2015). Downregulation of basic fibroblast growth factor is associated with femoral head necrosis in broilers. *Poultry Sci.* 94, 1052–1059. doi: 10.3382/ps/pev071

Liu, K., Wang, K., Wang, L., and Zhou, Z. J. P. S. (2021). Changes of lipid and bone metabolism in broilers with spontaneous femoral head necrosis. *Poult Sci.* 100:100808. doi: 10.1016/j.psj.2020.10.062

Niemeier, A., Niedzielska, D., Secer, R., Schilling, A., Merkel, M., Enrich, C., et al. (2008). Uptake of postprandial lipoproteins into bone in vivo: Impact on osteoblast function. *Bone* 43, 230–237. doi: 10.1016/j.bone.2008.03.022

Nuzzo, V., De Milita, A. M., Ferraro, T., Monaco, A., Florio, E., Miano, P., et al. (2009). Analysis of Skeletal Status by Quantitative Ultrasonometry in a Cohort of Postmenopausal Women with High Blood Cholesterol Without Documented Osteoporosis. *Ultrasound Med. Biol.* 35, 717–722. doi: 10.1016/j.ultrasmedbio.2008.11.003

Packialakshmi, B., Liyanage, R., Lay, J. Jr., Okimoto, R., and Rath, N. (2015a). Prednisolone-induced predisposition to femoral head separation and the accompanying plasma protein changes in chickens. *Biomark. Insights* 10, 1–8.

Packialakshmi, B., Rath, N. C., Huff, W. E., and Huff, G. R. (2015b). Poultry Femoral Head Separation and Necrosis: A Review. *Avian Dis.* 59, 349–354. doi: 10.1637/11082-040715-review.1

Pousinis, P., Gowler, P., Burston, J., Ortori, C., Chapman, V., and Barrett, D. A. (2020). Lipidomic identification of plasma lipids associated with pain behaviour and pathology in a mouse model of osteoarthritis. *Metabolomics* 16:32.

Saoji, R., Das, R. S., Desai, M., Pasi, A., Sachdeva, G., Das, T. K., et al. (2018). Association of high-density lipoprotein, triglycerides, and homocysteine with bone mineral density in young Indian tribal women. *Arch. Osteoporos.* 13:108.

Sims, A.-M., Shephard, N., Carter, K., Doan, T., Dowling, A., Duncan, E. L., et al. (2008). Genetic analyses in a sample of individuals with high or low BMD shows association with multiple Wnt pathway genes. *J. Bone Mineral Res.* 23, 499–506. doi: 10.1359/jbmr.071113

Teitelbaum, S. L. (2000). Bone resorption by osteoclasts. *Science* 289, 1504–1508. doi: 10.1126/science.289.5484.1504

Wang, A., Ren, M., and Wang, J. (2018). The pathogenesis of steroid-induced osteonecrosis of the femoral head: A systematic review of the literature. *Gene* 671, 103–109. doi: 10.1016/j.gene.2018.05.091

Wang, T., Teng, S., Zhang, Y., Wang, F., Ding, H., and Guo, L. (2017). Role of mesenchymal stem cells on differentiation in steroid-induced avascular necrosis of the femoral head. *Exp. Therapeut. Med.* 13, 669–675. doi: 10.3892/etm.2016.3991

Wolinsky, I., and Guggenheim, K. (1970). Lipid metabolism of chick epiphyseal bone and cartilage. *Calcified Tissue Res.* 6, 113–119. doi: 10.1007/bf02196190

Yamamoto, T., Irisa, T., Sugioka, Y., and Sueishi, K. (1997). Effects of pulse methylprednisolone on bone and marrow tissues - Corticosteroid-induced osteonecrosis in rabbits. *Arthritis Rheumat.* 40, 2055–2064. doi: 10.1002/art.1780401119

Yang, X., Cui, Z., Zhang, H., Wei, X., Feng, G., Liu, L., et al. (2019). Causal link between lipid profile and bone mineral density: A Mendelian randomization study. *Bone* 127, 37–43. doi: 10.1016/j.bone.2019.05.037

Yao, Q., Yu, C., Zhang, X., Zhang, K., Guo, J., and Song, L. (2017). Wnt/beta-catenin signaling in osteoblasts regulates global energy metabolism. *Bone* 97, 175–183. doi: 10.1016/j.bone.2017.01.028

Yu, Z., Fan, L., Li, J., Ge, Z., Dang, X., and Wang, K. (2016). Lithium prevents rat steroid-related osteonecrosis of the femoral head by beta-catenin activation. *Endocrine* 52, 380–390. doi: 10.1007/s12020-015-0747-y

Yuan, N., Li, J., Li, M., Ji, W., Ge, Z., Fan, L., et al. (2018). BADGE, a synthetic antagonist for PPAR gamma, prevents steroid-related osteonecrosis in a rabbit model. *BMC Musculoskel. Disord.* 19:129. doi: 10.1186/s12891-018-2050-6

Yue, J. A., Wan, F., Zhang, Q., Wen, P., Cheng, L., Li, P., et al. (2018). Effect of glucocorticoids on miRNA expression spectrum of rat femoral head microcirculation endothelial cells. *Gene* 651, 126–133. doi: 10.1016/j.gene.2018.01.057

Zhang, C., Zou, Y.-L., Ma, J., Dang, X.-Q., and Wang, K.-Z. (2015). Apoptosis associated with Wnt/beta-catenin pathway leads to steroid-induced avascular necrosis of femoral head. *BMC Musculoskel. Disord.* 16:132. doi: 10.1186/s12891-015-0606-2

Conflict of Interest: The authors declare that the research was conducted in the absence of any commercial or financial relationships that could be construed as a potential conflict of interest.

frontiers | Frontiers in Physiology

ORIGINAL RESEARCH
published: 28 April 2022
doi: 10.3389/fphys.2022.887381

Dietary Energy and Protein Levels During the Prelay Period on Production Performance, Egg Quality, Expression of Genes in Hypothalamus-Pituitary-Ovary Axis, and Bone Parameters in Aged Laying Hens

Qian Xin[1†], Ning Ma[1†], Hongchao Jiao[1], Xiaojuan Wang[1], Haifang Li[2], Yunlei Zhou[3], Jingpeng Zhao[1] and Hai Lin[1*]*

[1]*Shandong Provincial Key Laboratory of Animal Biotechnology and Disease Control and Prevention, College of Animal Science and Veterinary Medicine, Shandong Agricultural University, Tai'an, China,* [2]*College of Life Sciences, Shandong Agricultural University, Tai'an, China,* [3]*College of Chemistry and Material Science, Shandong Agricultural University, Tai'an, China*

OPEN ACCESS

Edited by:
Anthony Pokoo-Aikins, USDA ARS, United States

Reviewed by:
Shourong Shi, Poultry Institute (CAAS), China
Qiufeng Zeng, Sichuan Agricultural University, China

***Correspondence:**
Hai Lin
hailin@sdau.edu.cn
Jingpeng Zhao
zjp1299@163.com

[†]These authors have contributed equally to this work and share first authorship

Specialty section:
This article was submitted to Avian Physiology, a section of the journal Frontiers in Physiology

Received: *01 March 2022*
Accepted: *12 April 2022*
Published: *28 April 2022*

Citation:
Xin Q, Ma N, Jiao H, Wang X, Li H, Zhou Y, Zhao J and Lin H (2022) Dietary Energy and Protein Levels During the Prelay Period on Production Performance, Egg Quality, Expression of Genes in Hypothalamus-Pituitary-Ovary Axis, and Bone Parameters in Aged Laying Hens. Front. Physiol. 13:887381. doi: 10.3389/fphys.2022.887381

Nutrition during the pre-lay period takes effect on the production performance in the laying flock. This study evaluated the effects of dietary energy and protein levels in pre-lay diet on performance during the whole laying period and the egg quality, bone quality, and mRNA expression of hypothalamus-pituitary-gonadal (HPG) axis-related genes of hens at the end of the laying cycle. A total of 1,856 15-wk old Hy-Line brown pullets were randomly assigned to one of the four dietary treatments: using a 2 × 2 factorial arrangement with 2 energy levels (2,700 and 2,800 kcal/kg ME, respectively) and 2 protein levels (15 and 16.5% CP, respectively). Pullets were fed *ad libitum* from 15 to 20 wk and from 20 wk onward, fed with a similar laying diet till 72 wk of age. At 72 wk, the expression of genes in the hypothalamus, pituitary, ovarian, and follicles and bone quality was evaluated. At 72wk, there were no differences in production performance, BW, organ index, and ovarian parameters among the dietary treatments. High-CP diet increased the egg shape index and eggshell thickness ($p < 0.05$), but the eggshell breaking strength, Haugh unit, and albumen height did not differ among the treatments. Neither dietary energy nor protein level took an effect of bone quality. Low-energy diet increased the mRNA expression of gonadotropin-releasing hormone-1 (*GnRH-1*) in the hypothalamus ($p < 0.05$). The mRNA expression level of estrogen receptor-1 (*ESR-1*) in the hypothalamus and ovary

Abbreviations: ADPN, Adiponectin; AgRP, agouti-gelated protein; ALP, alkaline phosphatase; BM, breast muscle; Ca, calcium; CART, cocaine-and amphetamine-regulated transcript; CYP17A1, cytochrome family 17 subfamily A polypeptide 1; CYP19A1, cytochrome P450 family 19 subfamily A polypeptide 1; DF, dominant follicles; DXA, dual-energy x-ray absorptiometry; E_2, estradiol; FSH, follicle-stimulating hormone; GHRH, growth Hormone Releasing Hormone; GnRH, gonadotropin-releasing hormone and; GnIH, gonadotropin inhibitory hormone; HPG, hypothalamic-pituitary-gonadal; IGF-1, insulin-like growth factor-1; LEPR, leptin receptor; LH, luteinizing hormone; LM, leg muscle; LWF, large white follicles; NPY, neuropeptide Y; OVR, oocyte vitellogenesis receptor; P, phosphorus; P_4, progesterone; POMC, pro-opiomelanocortin; SIRT1, sirtuin1; SYF, small yellow follicles.

was elevated by the 2,700 ME-15%CP diet ($p < 0.05$). The expression of cytochrome family 17 subfamily A polypeptide 1 (*CYP17A1*) in the large white follicle (LWF), small yellow follicles (SYF) and dominant follicle (DF) was decreased by the 2,800 kcal/kg diet ($p < 0.05$). These results indicate that the prelay diet had no influence on the production performance but had minimal effect on the eggshell characteristics and bone parameters. These results suggest that the energy and protein level of the prelay diet changes the expression of HPG axis-related genes of hens around the end of the laying cycle without changing the circulating sex hormone profile. The effect of prelay diet on the endocrinal adjustment at the end of the laying cycle needs to be investigated further.

Keywords: bone quality, egg quality, energy, gene expression, protein

INTRODUCTION

Dietary manipulation during the prelay period can be an effective way of maintaining flock uniformity and enhancing production performance in the laying flock. The development of secondary reproductive organs and growth of ovarian follicles is thought to be between 4 and 6 wk before the first egg (16–18 wk of age) (Cave, 1984), and rapid physiological changes occur during the prelay phase (Sujatha et al., 2014). The diet's energy and protein content must be adjusted to ensure that hens consume enough nutrients needed to cope with growth and onset of egg production (Bain et al., 2016). Preliminary evidence has demonstrated that the increase of energy and protein levels in the prelay diet increases production performance in laying hens (Lilburn and Myers-Miller, 1990; Sujatha et al., 2014). Cave (1984) reported that a high-protein prelay diet could remarkably increase egg production in laying hens. However, little attention has been given to this critical stage in the management of laying hens.

It is known that an increase in egg size is associated with an increase in dietary protein intake during the production phase (Gunawardana et al., 2008). However, the protein intake needed for development during the prelay phase and maintaining persistency in lay is unknown. Furthermore, earlier studies have reported that dietary energy intake restriction delays the sexual maturity of broiler breeders and layers (Isaacks et al., 1960; Hollands and Gowe, 1961; Fuller and Dunahoo, 1962; Gowe et al., 1965; Fuller et al., 1969). However, due to constant selection and genetic improvement, the nutrient requirement should be continuously optimized (Han et al., 2017; Saxena et al., 2020).

In birds, like other vertebrates, the hypothalamic-pituitary-gonadal (HPG) axis governs egg production by regulating the cyclic production of gonadotropins [follicle-stimulating hormone (FSH) and luteinizing hormone (LH)] and steroid hormones and the selection of a dominant follicle for ovulation (Mikhael et al., 2019). In the hypothalamus, gonadotropin-releasing hormone (GnRH) and gonadotropin inhibitory hormone (GnIH) act on the pituitary gland to either stimulate or inhibit the production of gonadotropins, respectively (Tsutsui et al., 2000; Bédécarrats et al., 2009; Bain et al., 2016). GnRH stimulates the pituitary gland to synthesize FSH and LH, which stimulates the developed gonads to synthesize sex steroids hormones for initiating sexual maturity (Tsutsui et al., 2000; Bain et al., 2016). But, GnIH inhibits the synthesis of FSH and LH. A recent research has shown that high energy diet activated the HPG axis and stimulated the secretion of reproductive hormones in broiler breeder pullets (Hadinia et al., 2020). However, little is known on the effect of prelay dietary energy and protein level on hormone levels.

Egg production performance of modern laying hens has improved significantly during the last decade. Prolonging the laying period of laying hens has become a new breeding goal, that is, the "long life" layer, which will be capable of producing 500 eggs in a laying cycle of 100 weeks (Bain et al., 2016; Gautron et al., 2021). Osteoporosis is a major and prevalent welfare condition in laying hens caused by bone loss due to absorption of structural and medullary bone for calcium needed for eggshell production (Webster, 2004). Osteoporosis has led to increased fracture, especially during depopulation and transportation of spent-layers, causing carcass condemnation (Rath et al., 2000; Webster, 2004). In laying hens, protein-energy enrichment diets may help maintain bone mass and bone strength prior to sexual maturity (Rath et al., 2000). Previous studies had demonstrated that bone quality achieved before sexual maturity lasted through the production phase and was maintained in aged laying hens (Casey-Trott et al., 2017).

We hypothesized that manipulating energy and protein levels during the prelay period will improve production performance, maintain the persistency in lay with quality eggs, and maintain bone quality until the end of the first laying cycle. Therefore, this study aimed to evaluate the effects of dietary energy and protein levels fed during the prelay period on performance, egg quality, expression genes in the HPG axis, and bone quality of aged laying hens.

MATERIALS AND METHODS

Approval for this study was granted by the Institutional Animal Care and Use Committee of Shandong Agricultural University prior to the commencement of the trial.

Experimental Design and Animal Management

A total of one thousand eight hundred and fifty-six 15 wk Hy-Line Brown pullets were used for this trial. The experiment was a

TABLE 1 | Experimental diets and nutrient compositions.

Energy	Treatments				
	2,700 kcal/kg		2,800 kcal/kg		Laying
Protein	**15%**	**16.5%**	**15%**	**16.5%**	
Corn	63	61	60	60	64
Soybean meal	17	22	17	22.5	23
Oil	-	-	2	1.5	1
Bran	15	12	16	11	-
Limestone	1.75	1.75	1.75	1.75	9.4
Choline chloride	0.07	0.07	0.07	0.07	0.07
Mono-dicalcium phosphte	0.6	0.6	0.6	0.6	0.8
Salt	0.3	0.3	0.3	0.3	0.32
Medical Stone	1.96	1.96	1.96	1.96	0.94
Lysine	0.1	0.1	0.1	0.1	0.16
Methionine	0.08	0.08	0.08	0.08	0.16
Vitamin premix	0.04[a]	0.04[a]	0.04[a]	0.04[a]	0.05[b]
Mineral premix	0.1[c]	0.1[c]	0.1[c]	0.1[c]	0.1[d]
Nutrient composition					
Crude protein[e]	15.07	16.86	14.89	16.82	15.60
Metabolizable energy, Kcal/kg	2,700	2,700	2,800	2,800	2,700
Ca, %	0.89	0.89	0.89	0.89	3.57
Available P, %	0.55	0.55	0.55	0.55	0.48
Lysine, %	0.80	0.80	0.80	0.80	0.85
Methionine, %	0.32	0.32	0.32	0.32	0.41

[a]*Provided per kg of premix: vitamin A, 180,000 IU; vitamin D, 60,000 IU; vitamin E, 500 mg; vitamin K, 50 mg; vitamin B1, 50 mg; vitamin B2, 120 mg; vitamin B6, 60 mg; pantothenate, 200 mg; nicotinamide, 600 mg; folic acid, 16 mg; biotin, 4 mg.*
[b]*Provided per kg of premix: Cu, 0.24 g; Fe, 1 g; Mn, 2.00 g; Zn, 1.80 g; I, 13 mg; Se, 5.60 mg; Co., 10 mg.*
[c]*Provided per kg of premix: vitamin A, 230,000 IU; vitamin D, 75,000 IU; vitamin E, 500 mg; vitamin K, 86 mg; vitamin B1, 60 mg; vitamin B2, 150 mg; vitamin B6, 75 mg; vitamin B1, 1 mg; pantothenate, 200 mg; nicotinamide, 750 mg; folic acid, 35 mg; biotin, 4 mg.*
[d]*Provided per kg of premix: Cu, 300 g; Fe, 1.5 g; Mn, 2.4 g; Zn, 2.3 g; I, 20 mg; Se, 10 mg; Co., 12 mg.*
[e]*Measured value.*

2 × 2 factorial arrangement with two dietary energy levels (2,700 vs. 2,800 kcal/kg ME) and two dietary protein levels (15 and 16.5% CP). Each treatment was replicated 4 times with 116 pullets per replicate, all the rearing facilities were kept the same. The birds were reared in cages with 2 birds per cage. The dimensions of each cage were 45 × 35 × 35 cm (length × width × height) and equipped with a nipple drinker and feeding trough. The room temperature was maintained at 20 ± 1°C throughout the trial. Light was maintained at 10 h/d at 15 wk of age and increased gradually with 1 h/wk till 16 h/d at 30 wk. Pullets were fed experimental diets from 15 to 20 weeks of age and fed the same laying diet till the end of the experiment. All birds had free access to water and feed throughout the trial period. The formulated diets and nutrient compositions are presented in **Table 1**. The same batch of corn, soybean meal, bran and oil was used throughout the experiment to ensure the consistency of feed composition throughout the experiment.

Production Performance

All eggs laid were counted and weighed daily starting from the first egg until the end of the experiment (72 wk). Egg production and egg weight were recorded daily; egg mass was calculated by multiplying the egg production by the egg weight.

Egg Quality

At 72 wk, 20 eggs per replicate were randomly selected for egg quality analysis. Egg length (mm) and width (mm) were measured using a digital vernier caliper, and egg shape index was calculated by dividing the egg length by the egg width. Eggshell thickness (mm) was measured at the equator, sharp, and blunt end of the egg using an eggshell thickness gauge (ROBOTMATION, Japan). Egg Shell breaking strength was determined using eggshell force gauge (ROBOTMATION, Japan). Haugh unit, yolk color, and albumen height were measured using Egg Multi Tester (EMT-5200, ROBOTMATION, Japan).

Sample Collection

At the end of the experiment (72 wk), thirty-two hens (2 per replicate) were randomly selected for analysis. Blood samples were collected by venipuncture via the brachial vein into a non-coated vacutainer tube. Subsequently, blood was centrifuged at 3,500 *g* for 10 min at 4°C, and serum was recovered and stored at -20°C till further analysis.

After the blood sample was obtained, the hens were sacrificed and dissected, and the hypothalamus, pituitary, and follicles with average sizes [dominant follicles; small yellow follicles (SYF); and large white follicles (LWF)], the yolk was drained from each follicle and the follicle was everted to collect the theca interna layer and the remaining theca externa layer was removed. Tissue samples were immediately snap-frozen in liquid nitrogen and stored at −80 °C for RNA extraction. The breast muscle (BM; total of pectoralis major and pectoralis minor), leg muscle (LM; total leg muscle of the left leg), liver, abdominal fat pad, ovary, oviduct, magnum, and eggshell gland were excised and weighed. The left tibia and femur were dissected, cleaned of all adhering muscles and connective tissue, and then weighed to obtain the absolute weight. The total length and diameter of the tibia and femur were measured using a digital vernier caliper. Tibia and femur length was defined as the distance between the proximal and distal epiphysis. The tibia and femur diameter was measured at the mid-diaphysis at approximately 50% of the bone length. The tibia and femur were then kept in individual labeled zip-lock plastic bags and stored at −20°C till further analysis. The relative bone, muscle, and organ weight was calculated and expressed in percentage relative to the live body weight.

Measurement of Serum Hormones and Biochemical Parameters

The concentrations of calcium (Ca), phosphorus (P), and activity of alkaline phosphatase (ALP) in serum were measured using Hitachi L-7020 fully automatic biochemical analyzer (Tokyo, Japan) and commercial kits (Jiancheng Bioengineering Institute, Nanjing, China). Serum concentrations of estradiol (E2), FSH, LH, and progesterone (P4)were determined by RIA using kits obtained from Union Medical & Pharmaceutical Tech (Tianjin, China). The E_2 sensitivity of the assay was 1.4 Pg/ml, the FSH sensitivity of the assay was 0.46 mIU/ml, the LH sensitivity of the assay was 0.4 mIU/ml, the P_4 sensitivity of the assay was 0.05 ng/ml, and all samples were included in the same assay to

TABLE 2 | Primers used for real-time quantitative PCR.

Gene name	Genbank number	Primers position	PCR primers sequences (5′→3′)
ADPN	NM_206991	Forward	ACCCAGACACAGATGACCGTT
		Reverse	GAGCAAGAGCAGAGGTAGGAGT
AgRP	XM_025154207.2	Forward	GGAACCGCAGGCATTGTC
		Reverse	GTAGCAGAAGGCGTTGAAGAA
CART	XM_003643097.5	Forward	CCGCACTACGAGAAGAAG
		Reverse	AGGCACTTGAGAAGAAAGG
CYP17A1	NM_001001901.3	Forward	GCTGAAGCGATGCCTGAAGGTC
		Reverse	GGCTCAAGAGGGCTGTTGTTCTC
CYP19A1	XM_046924620.1	Forward	GCCAGTTGCCACAGTGCCTATC
		Reverse	GGCCCAATTCCCATGCAGTATCC
ESR1	NM_205183	Forward	TATTGATGATCGGCTTAGTCTGGG
		Reverse	CGAGCAGCAGTAGCCAGTAGCA
FSHβ	NM_204257	Forward	GCTTCACAAGGGATCCGGTA
		Reverse	TGAAGGAGCAGTAGGATGGC
FSHR	NM_205079	Forward	CACCAATGCCACAGAACTGAGAT
		Reverse	GCACCTTATGGACGACGGGT
GAPDH	NM_204305	Forward	CTACACACGGACACTTCAAG
		Reverse	ACAAACATGGGGGCATCAG
GH	NM_204359	Forward	CTGGAAGAAGGGATCCAAGCC
		Reverse	TAGGTGGGTCTGAGGAGCTG
GHR	NM_001001293	Forward	AGGCTCCTGAGTGACGATCATCTG
		Reverse	GCTTGCACTGAAGTCTGTCTCTGG
Ghrelin	NM_001001131	Forward	CCTTGGGACAGAAACTGCTC
		Reverse	CACCAATTTCAAAAGGAACG
GHRH	XM_015296360	Forward	AGTCACAAGCTCCATCTCCTCTCC
		Reverse	CTGGGCTGCTCTCACTGTTTCTG
GnIH	NM_204363	Forward	GCCGAGTGCTTATTTGCCTTTGAG
		Reverse	TCACATCCCTGGTTCAGACTCCTG
GnIHR	NM_204362.1	Forward	AGTGGCCTGGTACAGGGCATGTCT
		Reverse	CAATGCGGGCATACATGACGACAA
GnRH1	NM_001080877	Forward	TGGGTTTGTTGATGGTGTTGT
		Reverse	ATTTTCCAGCGGGAAGAGTTG
GnRH1R	NM_204653	Forward	ACGGAGGGGGACACCAAC
		Reverse	GCCCAGCACTGCTGTATTGC
IGF1R	NM_205032	Forward	TTCAGGAACCAAAGGGCGA
		Reverse	TGTAATCTGGAGGGCGATACC
LEPR	NM_204323	Forward	TTTGCTGTTGGGCTTTCTTCAC
		Reverse	AACCAGACCGGCTCCGTACA
LHβ	XM_025153997	Forward	GTGACAGTGGCGGTGGAGAA
		Reverse	CCCAAAGGGCTGCGGTA
LHR	AB009283	Forward	AGCCTTCCTGCTTTGTCTG
		Reverse	ATCGTTGTGTATCCGCCTG
NPY	NM_205473.1	Forward	TGCTGACTTTCGCCTTGTCG
		Reverse	GTGATGAGGTTGATGTAGTGCC
OVR	NM_205229	Forward	ACTGTGAGGATGGGTCTGACGA
		Reverse	TGGGATACACTGGGTTGACTGAG
POMC	XM_015285103.3	Forward	CGCTACGGCGGCTTCA
		Reverse	TCTTGTAGGCGCTTTTGACGAT
SIRT1	XM_015288090	Forward	CGGAAACAATACCTCCACCTGA
		Reverse	GAAGTCTACAGCAAGGCGAGCA

avoid intra assay variability. The intra assay coefficient of variation was less than 10%.

RNA Extraction, cDNA Synthesis, and Quantitative Real-Time PCR

Total ribonucleic acid (RNA) was extracted from the hypothalamus, pituitary, ovary, and follicles using the NcmZol reagent (NCM Biotech), following the manufacturer's instructions. The quantity and quality of RNA were measured using a NanoDrop Spectrophotometer (DeNovix). Subsequently, complementary deoxyribose nucleic acid (cDNA) was synthesized using PrimeScript RT Master Mix (TaKaRa Biotechnology). The primers were designed using Primer 5.0 software (SPS Inc., CA, United States) and synthesized by Sangon Biotechnology (Shanghai, China) and shown in **Table 2**. Quantitative RT-PCR analysis was performed on ABI 7,500 (Applied Biosystems). The cDNA was amplified in a 20 μL PCR reaction system containing 0.2 μM of each specific primer (Sangon, China) and of the SYBR Green master mix

TABLE 3 | Effect of dietary metabolizable energy (E) and crude protein (P) levels during the prelay period (15–20 weeks of age) on production performance in laying hens at 72 weeks.

Parameters	Energy[a]	Protein[a]			SEM	Factor	*p*-Value
		15%	16.5%	Mean			
Laying rate, %[b]	2,700 kcal/kg	91.9	92.6	92.3	0.45	E	0.938
	2,800 kcal/kg	92.6	92.0	92.3	0.45	P	0.912
	Mean	92.3	92.3		0.63	E×P	0.326
Egg weight, g	2,700 kcal/kg	63.1	63.1	63.1	0.11	E	0.284
	2,800 kcal/kg	63.4	63.1	63.3	0.11	P	0.419
	Mean	63.3	63.1		0.16	E×P	0.329
Egg mass, g/d	2,700 kcal/kg	57.7	58.0	57.9	0.42	E	0.852
	2,800 kcal/kg	58.3	57.8	58.1	0.42	P	0.708
	Mean	58.0	57.9		0.59	E×P	0.510
Feed intake, g/d[b]	2,700 kcal/kg	118.8	117.8	118.3	1.57	E	0.900
	2,800 kcal/kg	121.0	116.7	118.9	1.57	P	0.316
	Mean	119.9	117.3		2.22	E×P	0.559

[a]*Treatments were applied during prelay stage (15–20 wk of age). The same layer diet was fed after 20 wk of age.*
[b]*Total egg production from 24 to 72 weeks of age (n = 4).*

TABLE 4 | Effect of dietary metabolizable energy (E) and crude protein (P) levels during the prelay period (15–20 weeks of age) on egg quality of laying hens at 72 wk of age.

Parameters	Energy[a]	Protein[a]			SEM	Factor	*p*-Value
		15%	16.5%	Mean			
Egg shape index	2,700 kcal/kg	1.33	1.31	1.32	0.004	E	0.861
	2,800 kcal/kg	1.32	1.32	1.32	0.004	P	0.024
	Mean	1.33[a]	1.31[b]		0.006	E×P	0.195
Eggshell thickness, mm	2,700 kcal/kg	0.32	0.34	0.33	0.003	E	0.909
	2,800 kcal/kg	0.33	0.33	0.33	0.003	P	0.037
	Mean	0.32[a]	0.33[b]		0.004	E×P	0.116
Eggshell breaking strength, kg·f	2,700 kcal/kg	3.14	3.62	3.38	0.10	E	0.310
	2,800 kcal/kg	3.24	3.22	3.23	0.10	P	0.129
	Mean	3.19	3.42		0.15	E×P	0.098
Albumen height, mm	2,700 kcal/kg	6.57	6.62	6.59	0.09	E	0.414
	2,800 kcal/kg	6.33	6.66	6.49	0.09	P	0.133
	Mean	6.45	6.63		0.12	E×P	0.262
Yolk color	2,700 kcal/kg	6.13[a]	6.07[b]	6.12	0.13	E	0.043
	2,800 kcal/kg	6.55	6.43	6.49	0.13	P	0.615
	Mean	6.35	6.25		0.19	E×P	0.909
Haugh units	2,700 kcal/kg	77.79	78.35	78.07	0.67	E	0.327
	2,800 kcal/kg	76.17	78.10	77.14	0.67	P	0.193
	Mean	76.98	78.22		0.95	E×P	0.470

[a]*Treatments were applied during prelay stage (15–20 week of age). The same layer diet was fed after 20 week of age.*
[a,b] *Means within a row with different letters are significantly different at* $p < 0.05$.

(TaKaRa Biotechnology) according to the manufacturer's instructions. GAPDH was used as a housekeeping gene, and the gene expression levels were determined using the comparative $2^{-\Delta\Delta CT}$ method (Livak and Schmittgen, 2001).

Bone Quality Analysis

The excised bones were subjected to densitometry using the dual-energy x-ray absorptiometry (DXA) method on InAlyzer (Medikors LAB., Seoul, Korea). After the DXA analysis, bones were subjected to mechanical test analysis using a three-point method according to the method described by Song et al. (2020). Briefly, the bones were thawed to room temperature before the mechanical testing. The bone was rested in the anterior-posterior plane on two support points with 40 mm distance between the two support points (4 cm span) with a 1 N preload before loading to failure at a rate of 2 mm/min. The test was carried out by a microcomputer-controlled electronic universal testing machine (Jinan Shi JinNeng). Bone strength was calculated according to the formula "aw = $(8*F*L)/\pi/d^3$, where F is the maximum force needed for fracture, L is the spacing between two support points, and d is the diameter of the bone.

After the bone-bending strength analysis, the bone volume was determined based on a modified procedure described by Cui et al. (2019). Briefly, the bone was inserted into a 100 ml measuring cylinder previously filled with some water. The bone volume was calculated by subtracting the initial volume from the final volume. Subsequently, the bones were

TABLE 5 | Effect of dietary metabolizable energy (E) and crude protein (P) levels during the prelay period (15–20 weeks of age) on body weight, relative muscle and organ weight of laying hens at 72 wk of age.

Parameters	Energy[a]	Protein[a]			SEM	Factor	*p*-Value
		15%	16.5%	Mean			
BW, kg[b]	2,700 kcal/kg	2.16	2.03	2.15	0.04	E	0.296
	2,800 kcal/kg	2.16	2.14	2.09	0.04	P	0.146
	Mean	2.16	2.08		0.05	E×P	0.348
BM, %[c]	2,700 kcal/kg	10.97	11.16	11.06	0.28	E	0.414
	2,800 kcal/kg	10.61	10.84	10.73	0.28	P	0.610
	Mean	10.79	10.99		0.39	E×P	0.958
LM, %	2,700 kcal/kg	7.01	6.75	6.86	0.07	E	0.598
	2,800 kcal/kg	6.91	6.96	6.94	0.07	P	0.519
	Mean	6.96	6.85		0.10	E×P	0.174
Liver weight, %	2,700 kcal/kg	1.87	2.03	1.95	0.07	E	0.884
	2,800 kcal/kg	1.87	2.08	1.97	0.07	P	0.119
	Mean	1.87	2.05		0.11	E×P	0.771
Abdominal fat weight, %	2,700 kcal/kg	5.67	5.18	5.43	0.40	E	0.631
	2,800 kcal/kg	5.91	5.50	5.71	0.40	P	0.444
	Mean	5.79	5.34		0.57	E×P	0.945
Ovary weight, %	2,700 kcal/kg	0.014	0.013	0.013	0.001	E	0.957
	2,800 kcal/kg	0.014	0.013	0.013	0.001	P	0.385
	Mean	0.014	0.013		0.001	E×P	0.926
Oviduct, %	2,700 kcal/kg	4.12	4.21	4.17	0.26	E	0.926
	2,800 kcal/kg	3.65	4.61	4.13	0.26	P	0.182
	Mean	3.89	4.41		0.37	E×P	0.259
Magnum, g	2,700 kcal/kg	63.80	58.27	61.09	6.18	E	0.744
	2,800 kcal/kg	51.44	64.78	58.11	6.18	P	0.663
	Mean	57.62	61.52		8.74	E×P	0.302
Eggshell gland, g	2,700 kcal/kg	22.89	23.65	23.27	1.77	E	0.319
	2,800 kcal/kg	23.87	27.86	25.87	1.77	P	0.361
	Mean	23.38	25.76		2.50	E×P	0.530

[a]*Treatments were applied during prelay stage (15–20 week of age). The same layer diet was fed after 20 week of age.*
[b]*BW, at 72week of age; BW, body weight; BM, breast muscle; LM, leg muscle; (*n = 4*).*
[c]*Muscle and Organ weights expressed as % live weight.*

TABLE 6 | Effect of dietary metabolizable energy (E) and crude protein (P) levels during the prelay period (15–20 weeks of age) on ovarian parameters of laying hens at 72 week of age.

Parameters	Energy[a]	Protein[a]			SEM	Factor	*p*-Value
		15%	16.5%	Mean			
Number of dominant follicles	2,700 kcal/kg	5.63	5.50	5.56	0.29	E	1.000
	2,800 kcal/kg	5.75	5.38	5.56	0.29	P	0.555
	Mean	5.69	5.44		0.41	E×P	0.767
Weight of dominant follicles, g	2,700 kcal/kg	38.40	37.93	38.16	2.78	E	0.417
	2,800 kcal/kg	41.13	41.83	41.48	2.78	P	0.978
	Mean	39.76	39.88		3.94	E×P	0.884
Number of small yellow follicles	2,700 kcal/kg	18.25	17.00	17.63	1.04	E	0.309
	2,800 kcal/kg	19.38	19.00	19.19	1.04	P	0.591
	Mean	18.81	18.00		1.47	E×P	0.771
Weight of small yellow follicles, g	2,700 kcal/kg	2.95	2.65	2.80	0.28	E	0.550
	2,800 kcal/kg	3.20	2.89	3.04	0.28	P	0.455
	Mean	3.08	2.77		0.40	E×P	0.988
Number of large white follicles	2,700 kcal/kg	28.25	22.88	25.56	1.30	E	0.510
	2,800 kcal/kg	25.63	23.00	24.31	1.30	P	0.051
	Mean	26.94	22.94		1.84	E×P	0.469
Weight of large white follicles, g	2,700 kcal/kg	0.84	1.01	0.92	0.12	E	0.383
	2,800 kcal/kg	0.80	0.73	0.77	0.12	P	0.762
	Mean	0.82	0.89		0.18	E×P	0.503

[a]*Treatments were applied during prelay stage (15–20 week of age). The same layer diet was fed after 20 week of age.*

TABLE 7 | Effect of dietary metabolizable energy (E) and crude protein (P) levels during the prelay period (15–20 weeks of age) on serum parameters in laying hens at 72 week of age.

Parameters	Energy[a]	Protein[a]			SEM	Factor	*p*-Value
		15%	16.5%	Mean			
Ca, mmol/L	2,700 kcal/kg	8.84	8.42	8.63	0.67	E	0.557
	2,800 kcal/kg	7.99	10.41	9.20	0.67	P	0.310
	Mean	8.41	9.41		0.92	ExP	0.158
P, mmol/L	2,700 kcal/kg	1.61	1.77	1.69	0.17	E	0.283
	2,800 kcal/kg	1.38	2.56	1.97	0.17	P	0.019
	Mean	1.50[b]	2.16[a]		0.25	ExP	0.063
TP, g/L	2,700 kcal/kg	53.49	53.38	53.43	2.35	E	0.824
	2,800 kcal/kg	49.24	56.11	52.68	2.35	P	0.328
	Mean	51.36	55.74		3.32	ExP	0.313
ALP, U/L	2,700 kcal/kg	762.5	978.8	870.6	264.4	E	0.469
	2,800 kcal/kg	504.0	677.5	590.8	264.4	P	0.612
	Mean	633.3	828.1		374.0	ExP	0.955
E_2, Pg/mL	2,700 kcal/kg	309.28	404.13	356.70	33.10	E	0.455
	2,800 kcal/kg	299.35	330.85	315.10	33.10	P	0.264
	Mean	304.31	367.49		53.88	ExP	0.568
FSH, mIU/mL	2,700 kcal/kg	2.33	4.83	3.58	0.56	E	0.360
	2,800 kcal/kg	3.00	2.65	2.83	0.56	P	0.198
	Mean	2.66	3.74		0.79	ExP	0.098
LH, mIU/mL	2,700 kcal/kg	4.94	5.58	5.26	0.51	E	0.806
	2,800 kcal/kg	4.93	5.94	5.44	0.51	P	0.277
	Mean	4.93	5.76		0.72	ExP	0.805
P_4, ng/mL	2,700 kcal/kg	1.36	0.75	1.06	0.21	E	0.789
	2,800 kcal/kg	1.15	0.81	0.98	0.21	P	0.135
	Mean	1.25	0.78		0.30	ExP	0.657

[a]*Treatments were applied during prelay stage (15–20 week of age). The same layer diet was fed after 20 wk of age.*

[a,b] *Means within a row with different letters are significantly different at* p < *0.05.*

Ca, calcium; P, phosphorus; TP, total protein; ALP, alkaline phosphatase; E_2, estradiol; FSH, follicle-stimulating hormone; LH, luteinizing hormone; P_4, progesterone (n = *4).*

degreased by immersing in 2:1 ethanol: benzene mixture for 96 h, air-dried under the fume hood for 24 h, then oven-dried at 105°C for 24 h and weighed to obtain the defatted dry weight. Subsequently, dry-defatted bones were placed in a muffle furnace at 550°C for ash content determination. The percentage of ash was calculated and expressed as a percentage of the dry-defatted bone weight. Bone ash concentration was calculated by dividing the ash weight by the volume of each bone.

Statistical Analysis

Statistical analysis was performed using SAS software. For the production performance, egg quality, serum hormones and biochemical parameters, body weight, carcass weight, ovarian parameters and bone parameters, a two-way ANOVA model (version 8e; SAS Institute, Cary, NC) was used to estimate the main effect of energy and protein as well as their interaction. Results were expressed as means and standard errors. $p < 0.05$ was considered statistically significant.

RESULTS

Laying Performance

The egg production, egg weight, egg mass, and feed intake did not differ among the dietary treatments ($p > 0.05$, **Table 3**).

Egg Quality

Compared with the 15% CP group, the egg shape index and eggshell thickness were significantly higher in the 16.5% group ($p < 0.05$, **Table 4**). The yolk color was not affected by dietary protein level ($p > 0.05$), but decreased with a low-energy diet compared with a high-energy diet ($p < 0.05$). However, dietary energy and protein level did not affect the eggshell breaking strength, the albumen height, and Haugh units ($p > 0.05$).

Body Weight and Carcass Weight and Ovarian Parameters

BW, relative organ and muscle weight: BM, LM, and ovarian parameters did not differ among treatments ($p > 0.05$, **Table 5**, **6**).

Serum Parameters in Laying Hens

There was no energy and protein level and their interaction effect on serum Ca concentration ($p > 0.05$, **Table 7**). Compared with the 15% CP group, the serum P concentration was significantly higher in the 16.5% CP group ($p < 0.05$), and the interaction of energy/protein level showed a trend to influence on P concentration ($p = 0.063$). However, different levels of ME and CP and interaction had no significant effect on the concentration of serum TP, ALP, E_2, FSH, LH, and P_4 ($p > 0.05$, **Table 7**).

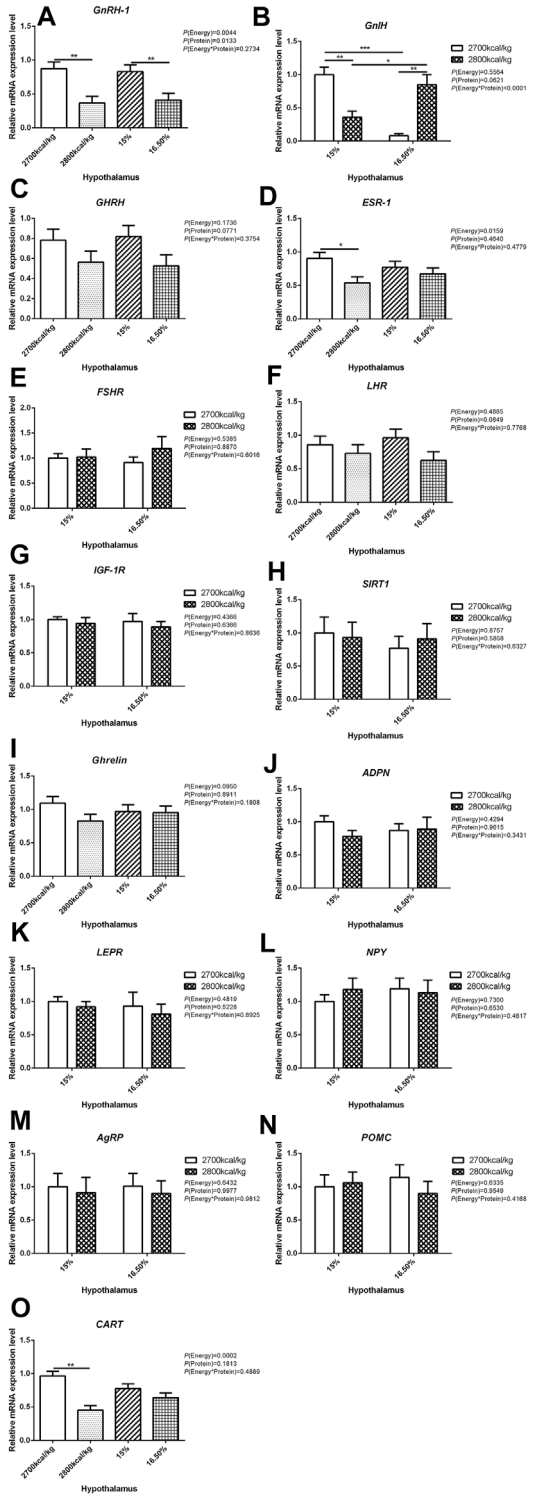

FIGURE 1 | Effect of dietary metabolizable energy (E) and crude protein (P) levels during the prelay period (15–20 weeks of age) on the mRNA expression of genes *GnRH-1* **(A)**, *GnIH* **(B)**, *GHRH* **(C)**, *ESR-1* **(D)**, *FSHR* **(E)**, *LHR* **(F)**, *IGF-1R* **(G)**, *SIRT1* **(H)**, *Ghrelin* **(I)**, *ADPN* **(J)**, *LEPR* **(K)**, *NPY* **(L)**, *AgRP* **(M)**, *POMC* **(N)**, and *CART* **(O)** in the hypothalamus of hens. Data represent the mean ± SD (n = 4); $*p < 0.05$, $**p < 0.01$, $***p < 0.0001$.

The mRNA Expression of Genes in the Hypothalamus-Pituitary-Ovarian Axis

The mRNA expression level of *GnRH-1*, *ESR-1*, and *CART* in the hypothalamus decreased when the dietary energy level increased from 2,700 kcal/kg to 2,800 kcal/kg ($p < 0.05$; **Figures 1A,D,O**) while the mRNA expression level of *GnRH-1* and *LHR* in the hypothalamus decreased when dietary protein level increased from 15% to 16.5% ($p < 0.05$; **Figure 1A**). However, the interaction between dietary energy and protein levels only affected the mRNA expression level of *GnIH*. When the protein level of diet was 15%, the mRNA expression of *GnIH* decreased with the increase in dietary energy level, while the protein level was 16.5%, the expression of *GnIH* increased ($p < 0.05$; **Figure 1B**). The mRNA expression level of *GHRH*, *FSHR*, *IGF-1R*, *SIRT1*, *Ghrelin*, *ADPN*, *LEPR*, *NPY*, *AgRP*, and *POMC* in the hypothalamus was not influenced by the dietary energy and protein levels and their interaction (**Figures 1C,E,G–N**).

In the pituitary, the mRNA expression level of *FSH* and *GH* were affected by the interaction between the dietary energy and protein level ($p < 0.05$; **Figures 2A,C**). When the protein level of diet was 15%, the mRNA expression of *FSH* increased with the increase in dietary energy level, while the mRNA expression of *GH* decreased ($p < 0.05$; **Figures 2A,C**). The expression of LH was decreased by dietary protein ($p < 0.05$) but not by energy and the interaction of energy and protein level ($p > 0.05$, **Figure 2B**). The mRNA expression level of *GnRH-1R*, *GnIHR*, *ESR-1*, and *IGF-1R* in the pituitary was not influenced by the dietary energy and protein levels and their interaction (**Figures 2D–G**).

In the ovary, the mRNA expression level of *CYP17A1* was affected by the interaction between the dietary energy and protein level ($p < 0.05$; **Figure 3A**). When the protein level of diet was 15%, the mRNA expression of *CYP17A1* decreased with the increase in dietary energy level ($p < 0.05$; **Figure 3A**). In the ovary, compared with hens fed with 2,700 kcal/kg diet, the mRNA expression level of *ESR-1* was significantly decreased by 2,800 kcal/kg diet ($p < 0.05$; **Figure 3C**). The mRNA expression level of *LHR* in the ovary increased when the dietary energy level increased from 2,700 kcal/kg to 2,800 kcal/kg ($p < 0.05$; **Figure 3E**). The mRNA expression level of *CYP19A1* and *FSHR* in the ovary was not influenced by dietary energy level, dietary protein level, and their interaction (**Figures 3B,D**).

The mRNA Expression in the Follicles

The mRNA expression level of *CYP17A1* and *CYP19A1* in the large white follicles decreased when dietary energy level increased from 2,700 kcal/kg to 2,800 kcal/kg ($p < 0.05$; **Figures 4A,B**), and the mRNA expression level of *CYP19A1* was decreased then dietary protein level increased from 15 to 16.50% ($p < 0.05$, **Figure 4B**). The mRNA expression level of *ESR-1*, *FSHR*, *LHR*, and *OVR* in the large white follicles was not influenced by the dietary energy and protein level and their interaction (**Figures 4C–F**). In the small yellow follicles, the mRNA expression level of *CYP17A1* and *CYP19A1* were affected by the interaction between the dietary energy and protein level ($p < 0.05$; **Figures 5A,B**). When the protein level of diet was 15%, the mRNA expression of *CYP17A1* and *CYP19A1* decreased with the increase in dietary energy level ($p < 0.05$; **Figures 5A,B**). In the small yellow follicles, the mRNA expression level of *ESR-1* tended to be decreased when the dietary energy level increased from 2,700 kcal/kg

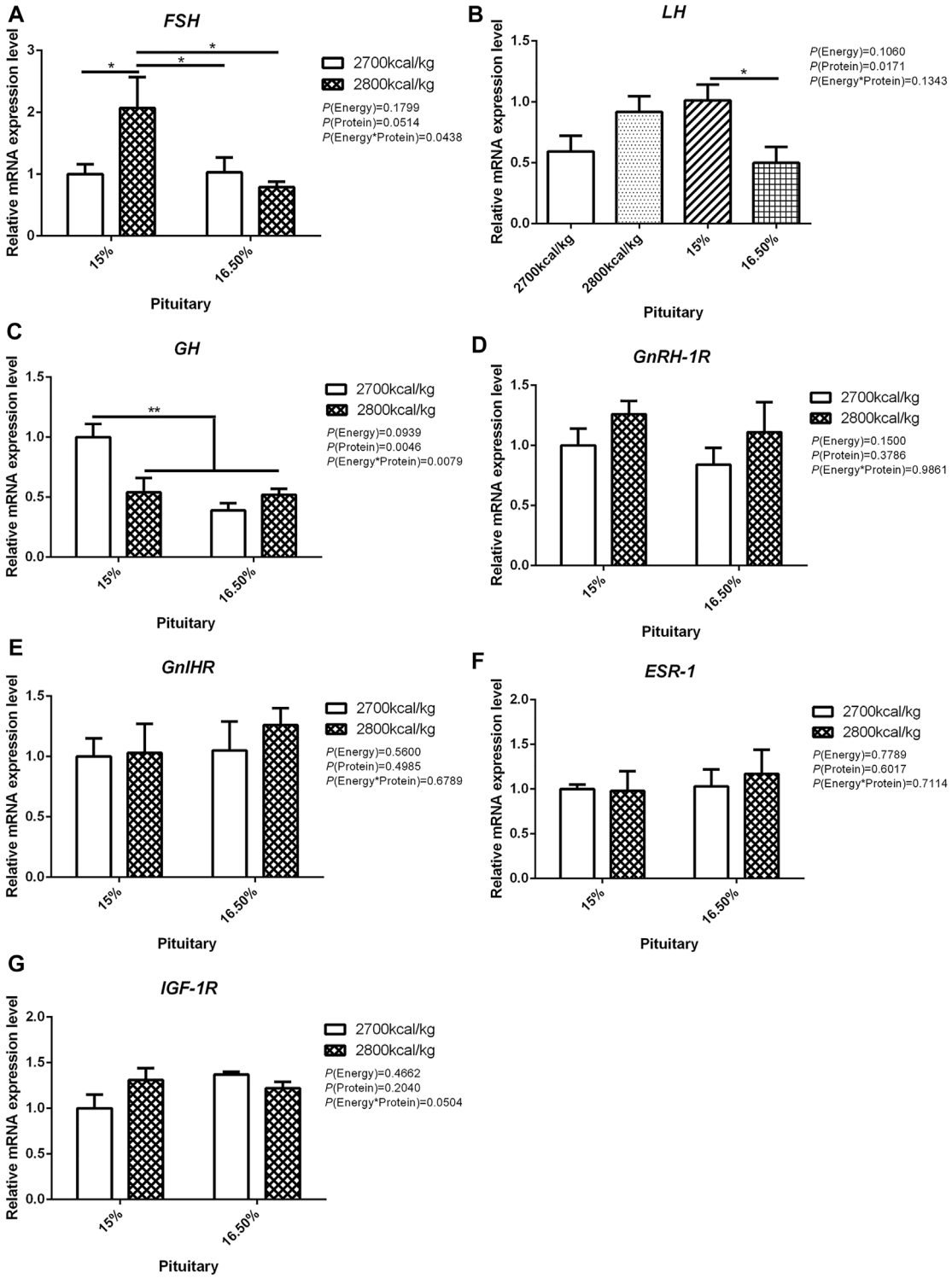

FIGURE 2 | Effect of dietary metabolizable energy (E) and crude protein (P) levels during the prelay period (15–20 weeks of age) on the mRNA expression of genes *FSH* **(A)**, *LH* **(B)**, *GH* **(C)**, *GnRH-1R* **(D)**, *GnIHR* **(E)**, *ESR-1* **(F)**, and *IGF-1R* **(G)** in the pituitary of hens. Data represent the mean ± SD (n = 4); $*p < 0.05$, $**p < 0.01$.

to 2,800 kcal/kg (p = 0.054)and increased when the dietary protein level increased from 15 to 16.5% ($p < 0.05$; **Figure 5C**). The mRNA expression level of *FSHR*, *LHR* and *OVR* in the small yellow follicles was not influenced by the dietary energy and protein levels, and their interaction (**Figures 5D–F**). In the dominant follicles, the mRNA expression level of *CYP17A1*, *CYP19A1*, and *OVR* decreased when the

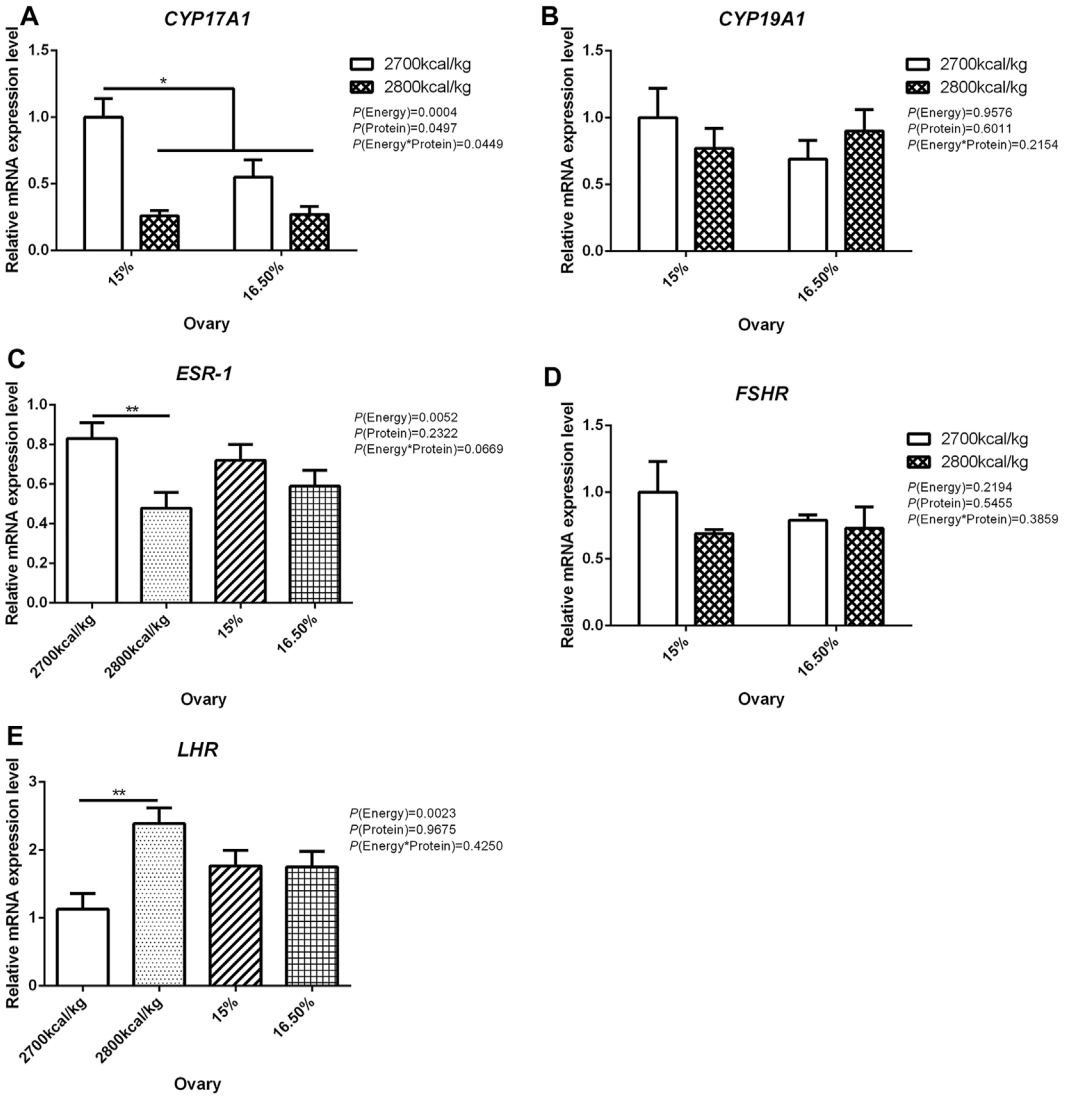

FIGURE 3 | Effect of dietary metabolizable energy (E) and crude protein (P) levels during the prelay period (15–20 weeks of age) on the mRNA expression of genes *CYP17A1* **(A)**, *CYP19A1* **(B)**, *ESR-1* **(C)**, *FSHR* **(D)**, and *LHR* **(E)** in the ovary of hens. Data represent the mean ± SD (n = 4); $*p < 0.05$, $**p < 0.01$.

dietary energy level increased from 2,700 kcal/kg to 2,800 kcal/kg ($p < 0.05$; **Figures 6A,B,F**). When the dietary protein level increased from 15 to 16.5%, the mRNA expression level of *ESR-1* show a trend to decrease ($p = 0.055$; **Figure 6C**) whereas *CYP17A1* and *OVR* decreased ($p < 0.05$; **Figures 6A,F**). The mRNA expression level of *FSHR* and *LHR* in the dominant follicles was not influenced by the dietary energy and protein level, and their interaction (**Figures 6D,E**).

Bone Parameters

The effects of energy and protein levels on bone physical characteristics, bone mineral density (BMD), and bone-bending strength (BBS) are shown in **Table 8**. At 72 wk, the length and width of bone, relative bone weight, BMD, and BBS of the tibia were not affected by energy or protein level ($p > 0.05$), nor was there any interaction effect ($p > 0.05$).

Ash Content

The effects of energy and protein levels on ash weight, ash concentration, and ash percentage of femur and tibia are shown in **Table 9**. At 72 wk of age, there was no effect of energy or protein level on the ash weight and ash concentration of femur and tibia ($p > 0.05$). There was an energy/protein interaction on both femur and tibial ash weight ($p < 0.05$); the hen fed with the 2,800 ME-16.5%CP diet or 2,700 ME-15%CP diet had a higher ash weight ($p < 0.05$).

DISCUSSION

In the current study, egg production was not influenced by dietary energy and protein levels during the prelay period, and all dietary treatment groups reached 50% production at similar ages (24 wk of age). In addition, egg weight and egg mass was similar among the

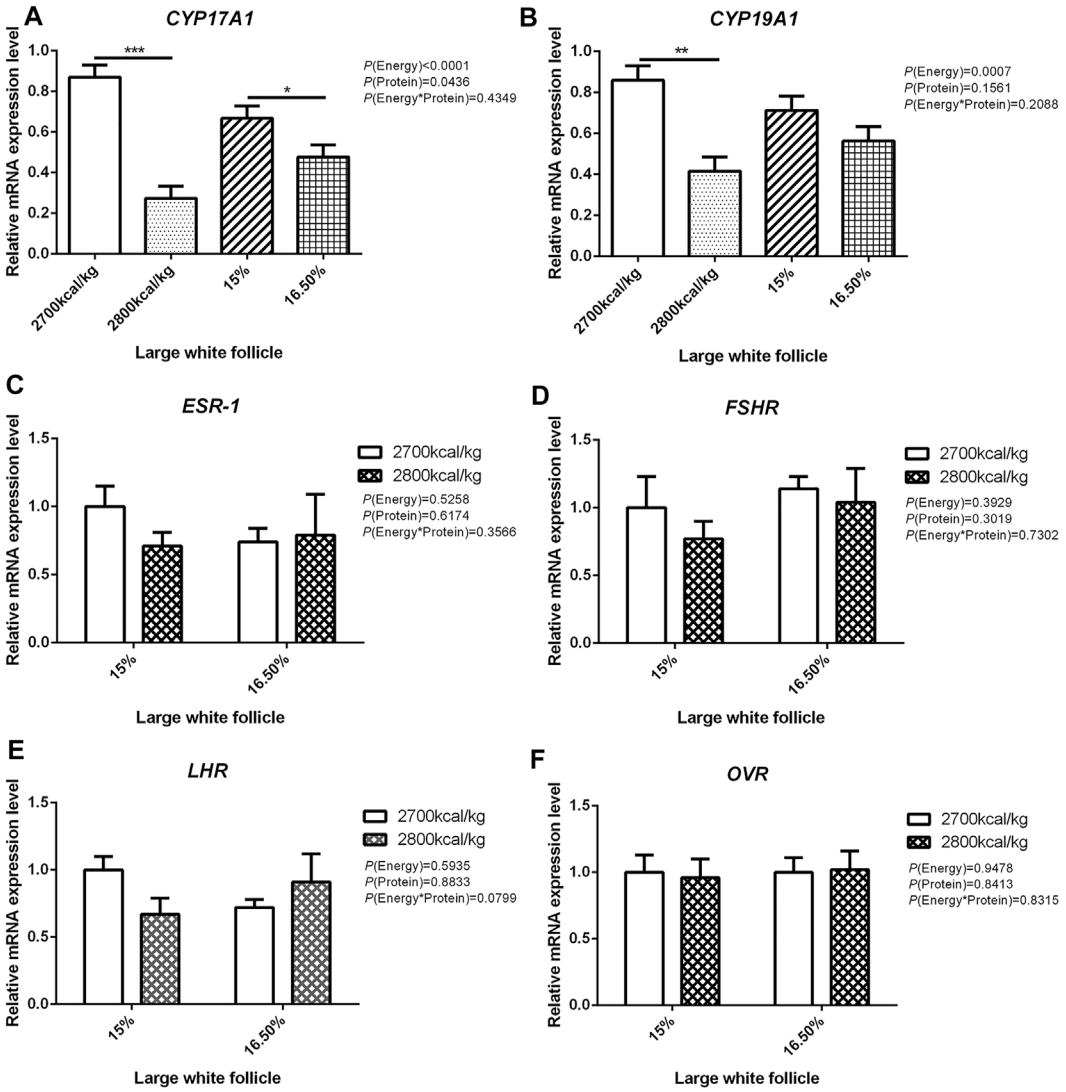

FIGURE 4 | Effect of dietary metabolizable energy (E) and crude protein (P) levels during the prelay period (15–20 weeks of age) on the mRNA expression of genes *CYP17A1* **(A)**, *CYP19A1* **(B)**, *ESR-1* **(C)**, *FSHR* **(D)**, *LHR* **(E)**, and *OVR* **(F)**in the large white follicles of hens. Data represent the mean ± SD ($n = 4$); $*p < 0.05$, $**p < 0.01$, $***p < 0.0001$.

treatment, neither influenced by the energy level nor protein level. These findings are in line with those found in the literature, where dietary protein levels prior to sexual maturity did not influence egg production (Hussein et al., 1996; Keshavarz, 1998). However, a previous study has shown a positive effect of prelay diet on production performance (Sujatha et al., 2014). They reported that an increase in energy and protein levels in a prelay diet improves production performance. The reason for the discrepancy between experimental results is not apparent but is likely to be due to the difference in the energy level. Sujatha et al. (2014) increased the energy level from 2,500 to 2,700 kcal/kg, whereas the dietary treatment in this experiment was 2,700 and 2,800 kcal/kg. This suggests that 2,700 kcal/kg energy meets the growth requirement, and further increase to 2,800 kcal does not affect the production performance. In addition, the difference in egg-type strains used for the study can be a reason for the discrepancy in the result. Hy-Line brown pullets were used in our study, whereas White Leghorn pullets were used for their study.

Earlier studies reported that increasing the energy level of the diet from 2,850 kcal/kg to 3,050 kcal/kg did not influence the eggshell quality and Haugh units (Junqueira et al., 2006). This is consistent with the result of the current study. Yolk color has a considerable influence on the marketability of eggs; the color of the yolk depends on the fat-soluble carotenoids and xanthophylls (Gunawardana et al., 2008; Pérez-Bonilla et al., 2012). We observed that the yolk color increased with the increase of the dietary energy level. Similar findings were reported by Pérez-Bonilla et al. (2012), who found that yolk pigmentation increased linearly with an increase in energy concentration of the diet even though all diets had similar levels of pigmenting additives and

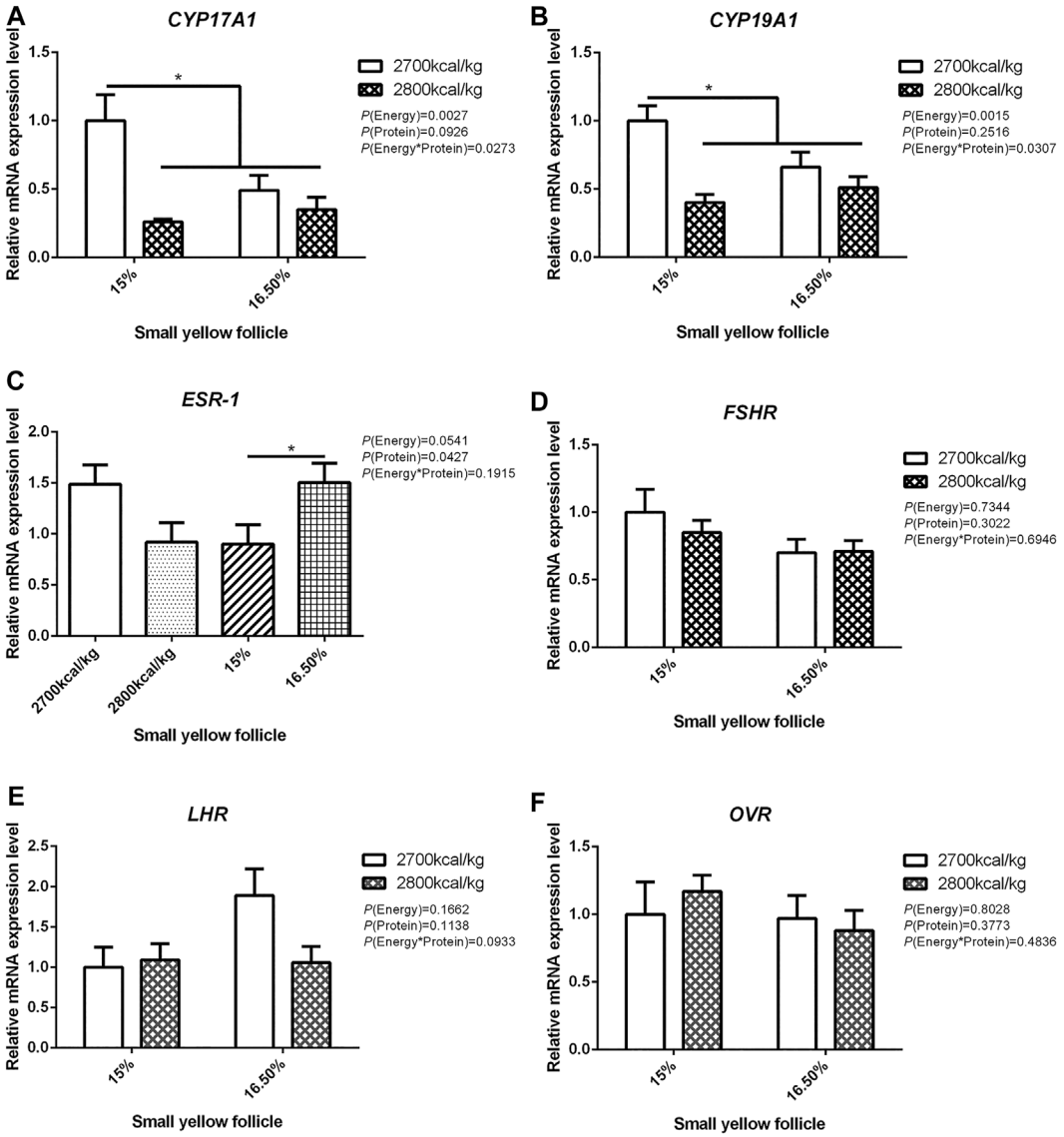

FIGURE 5 | Effect of dietary metabolizable energy (E) and crude protein (P) levels during the prelay period (15–20 weeks of age) on the mRNA expression of genes *CYP17A1* **(A)**, *CYP19A1* **(B)**, *ESR-1* **(C)**, *FSHR* **(D)**, *LHR* **(E)**, and *OVR* **(F)** in the small yellow follicles of hens. Data represent the mean ± SD (n = 4); $*p < 0.05$.

corn. The BW and relative organ weight at the end-of-lay was similar among the dietary treatments suggesting that dietary energy and protein levels during the prelay period had no effect on the BW and relative organ weight at the end-of-lay. This observation corroborates those of Lilburn and Myers-Miller (1990), who found that protein intake during the prelay period (18–25 wk) did not influence BW and carcass parameters in broiler breeder pullets. Furthermore, Joseph et al. (2000) found that increased CP levels in the diet of prelay broiler breeders had no influence on BW and relative organ weight.

In poultry, ovulation and egg production are mainly regulated by the HPG axis, in which the endocrine system plays a dominant role. The hypothalamus is the main site of the regulatory axis. The regulation of energy homeostasis is inseparable from the central nervous system, especially the hypothalamus. In the present study, the endocrine system in the HPG axis was evaluated in aged hens around the end of the laying cycle. Sharp et al. (1992) found that LH in plasma and pituitary decreased and LH responsiveness to GnRH decreased in laying hens with low laying rate or no production. Earlier studies have demonstrated that dietary energy levels may promote the secretion of GnRH, FSH, LH, and E_2 to promote follicular development and reproductive performance (Scaramuzzi et al., 2006; Romano et al., 2007; Zhou et al., 2010). Similarly, the plasma LH and FSH concentrations of broiler breeder pullets fed with high energy diet increased compared to the low energy diet (Hadinia et al., 2020). It was found that the decrease in egg production was related to the decrease of LH and FSH in the SYF

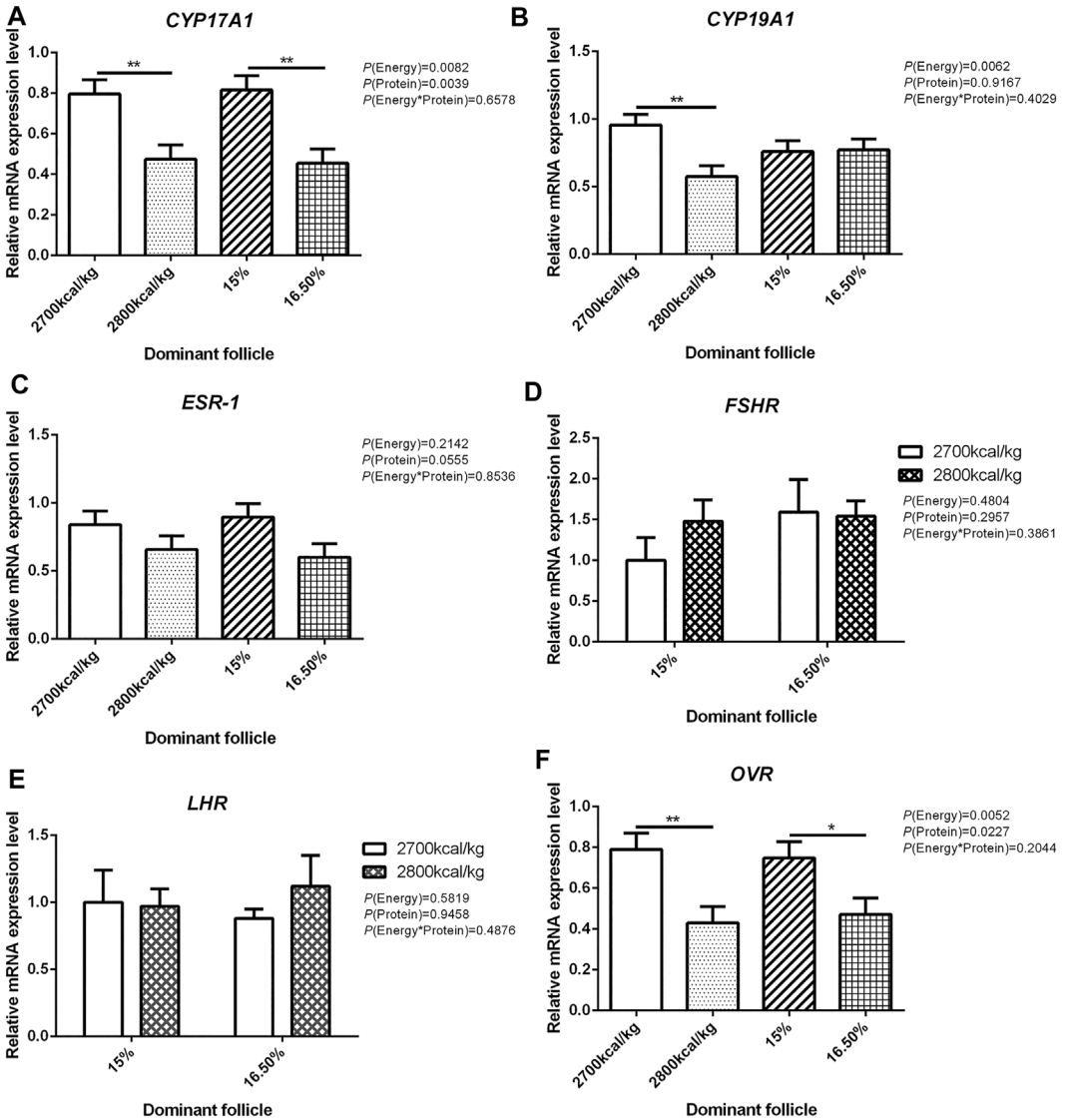

FIGURE 6 | Effect of dietary metabolizable energy (E) and crude protein (P) levels during the prelay period (15–20 weeks of age) on the mRNA expression of genes *CYP17A1* **(A)**, *CYP19A1* **(B)**, *ESR-1* **(C)**, *FSHR* **(D)**, *LHR* **(E)**, and *OVR* **(F)** in the dominant follicles of hens. Data represent the mean ± SD ($n = 4$); $*p < 0.05$, $**p < 0.01$.

and plasma (Sharp et al., 1992; Ciccone et al., 2005). Tanabe et al. (1981) and Wang and Johnson (1993) found that high LH level was associated with high laying rate in laying hens. However, our results showed that the dietary treatment did not significantly influence the serum concentration of E_2 and LH of aged hens. This could explain the similarity in the production performance among the dietary treatment. It has been found that the decrease of plasma LH is related to the decrease of *GnRH-1* mRNA in the hypothalamus of aging layers with ovarian degeneration (Dunn et al., 1996). In our experiment, there was no change in the concentration of serum LH. The *GnRH-1* mRNA in the hypothalamus was the highest in hens fed with 2,700 kcal/kg diet or 15% CP diet. In the pituitary, the mRNA expression level of *LH* is up-regulated in the 15% CP diet and showed a trend to be increased by 2,700 kcal/kg diet. We think that the increase of GnRH-1 secretion in the hypothalamus leads to the increase of *LH* mRNA level in the pituitary.

The development of ovarian follicles is mainly regulated by FSH and LH secreted by the pituitary gland. It was found that FSH treatment alone could increase FSH binding capacity and *FSHR* mRNA level, promote follicular development, and ovulation in hypophysectomized rats pre-treated with estrogen (Galway et al., 1990). It has been reported that high dietary energy levels can promote *FSHR* and *LHR* gene mRNA expression in the ovary (Zhou et al., 2009). Our study found that the mRNA expression level of *LH* in the pituitary was the highest in the group with 15% CP whereas the expression of *LHR* in the ovary, LWF, SYF, and DF was not obvious altered, indicating that dietary protein play a minor role in affecting

TABLE 8 | Effect of dietary metabolizable energy (E) and crude protein (P) levels during the prelay period (15–20 weeks of age) on bone parameters in laying hens at 72 week of age.

Parameters	Energy[a]	Protein[a]			SEM	Factor	*p*-Value
		15%	16.5%	Mean			
Femur							
Length, mm	2,700 kcal/kg	70.3	69.9	70.06	5.46	E	0.168
	2,800 kcal/kg	82.3	80.5	81.38	5.46	P	0.893
	Mean	76.25	75.19		7.72	E×P	0.931
Width, mm	2,700 kcal/kg	6.66	7.56	7.11	0.37	E	0.272
	2,800 kcal/kg	7.66	7.77	7.71	0.37	P	0.356
	Mean	7.16	7.66		0.52	E×P	0.470
Weight, %	2,700 kcal/kg	0.44	0.45	0.45	0.01	E	0.646
	2,800 kcal/kg	0.43	0.44	0.43	0.01	P	0.763
	Mean	0.44	0.44		0.02	E×P	0.711
BMD, g/cm2	2,700 kcal/kg	0.31	0.31	0.33	0.01	E	0.213
	2,800 kcal/kg	0.32	0.34	0.31	0.01	P	0.631
	Mean	0.32	0.32		0.02	E×P	0.454
BBS, MPa	2,700 kcal/kg	0.04	0.04	0.04	0.003	E	0.994
	2,800 kcal/kg	0.04	0.04	0.04	0.003	P	0.853
	Mean	0.04	0.04		0.004	E×P	0.660
Tibia							
Length, mm	2,700 kcal/kg	117.4	114.4	115.9	4.87	E	0.531
	2,800 kcal/kg	120.6	102.3	111.4	4.87	P	0.147
	Mean	119.0	108.3		6.89	E×P	0.286
Width, mm	2,700 kcal/kg	6.54	6.36	6.45	0.14	E	0.808
	2,800 kcal/kg	6.62	6.39	6.50	0.14	P	0.325
	Mean	6.58	6.38		0.20	E×P	0.903
Weight, %	2,700 kcal/kg	0.51	0.51	0.51	0.01	E	0.164
	2,800 kcal/kg	0.52	0.54	0.53	0.01	P	0.462
	Mean	0.52	0.53		0.02	E×P	0.507
BMD, g/cm2	2,700 kcal/kg	0.29	0.26	0.28	0.01	E	0.216
	2,800 kcal/kg	0.28	0.31	0.29	0.01	P	0.955
	Mean	0.28	0.29		0.02	E×P	0.108
BBS, MPa	2,700 kcal/kg	0.06	0.06	0.06	0.009	E	0.451
	2,800 kcal/kg	0.07	0.08	0.07	0.009	P	0.678
	Mean	0.06	0.07		0.01	E×P	0.550

[a]*Treatments were applied during prelay stage (15–20 week of age). The same layer diet was fed after 20 week of age.*
BMD, bone mineral density; BBS, bone bending strength, n = *4.*

the expression of *LH*. In contrast, the mRNA level of *LHR* in the ovary was lower in 2,700 kcal/kg groups, suggesting that dietary energy is an important factor affecting the expression of *LH*. The mRNA level of *ESR-1* in the hypothalamus and ovary was highest in the 2,700 kcal/kg groups, which may be caused by positive feedback regulation of the HPG axis. Moreover, the increased *ESR-1* mRNA level by 16.5% CP diet in SYF was not observed in LWF or DF, suggesting that the response of ESR-1 is dependent of the stage of follicle development.

During the laying cycle, only one yolk follicle is selected as the dominant follicle and enters the stage of development, becoming the pre-ovulatory follicle, and then the follicles develop in the order of size until ovulation (Onagbesan et al., 2009). The more follicles selected to enter the development stage, the longer the laying cycle and the higher the laying performance of poultry. The decrease in egg production is related to the decrease of collection of ovarian eggs running to yolk follicles (Waddington et al., 1985; Palmer and Bahr, 1992). Previous studies have shown that feeding regimes can influence the development of ovarian follicles, and broiler breeder hens fed ad libitum had more pre-ovulatory ovarian follicles (Bacon et al., 1972; Hocking et al., 1987; Yu et al., 1992). However, there was no significant difference in the number and weight of follicles of different grades among the groups in this study. Similar findings were reported by Joseph et al. (2000), where CP level in prelay diet had no remarkable effect on ovarian parameters.

Estrogen is mainly secreted by theca cells and granulosa cells of the ovary, which regulates the development of follicle, reproductive tract, and ovulation (Ormerod and Galea, 2001). Estrogen plays a decisive role in the formation of dominant follicles. The dominant follicles with high estrogen content and more FSH receptors can further develop into mature follicles, while the follicles with low estrogen synthesis and less FSHR tend to atresia and eventually apoptosis (Onagbesan et al., 2009). In our experiment, we detected the reproductive hormone-associated key genes: *CYP17A1* and *CYP19A1*, and the mRNA expression level of *CYP17A1* in the LWF, SYF and DF was the highest in the 2,700 kcal/kg groups, while *ESR-1* was not changed, suggesting the stimulating effect of dietary energy on *CYP17A1* transcription.

In laying hens, structural bone loss is associated with medullary bone remodeling during Ca mobilization for

TABLE 9 | Effect of dietary metabolizable energy (E) and crude protein (P) levels during the prelay period (15–20 weeks of age) on bone ash in laying hens at 72 week of age.

Parameters	Energy[a]	Protein[a]			SEM	Factor	*p*-Value
		15%	16.5%	Mean			
Femur							
Ash weight, g	2,700 kcal/kg	2.62^{x}	2.20^{y}	2.41	0.07	E	0.714
	2,800 kcal/kg	2.38^{xy}	2.52^{x}	2.45	0.07	P	0.204
	Mean	2.50	2.36		0.10	E×P	0.019
Ash concentration, g/cm^3	2,700 kcal/kg	0.36	0.31	0.33	0.02	E	0.708
	2,800 kcal/kg	0.34	0.35	0.34	0.02	P	0.480
	Mean	0.35	0.33		0.03	E×P	0.236
Ash, %	2,700 kcal/kg	46.95	44.26	45.61	1.90	E	0.983
	2,800 kcal/kg	45.96	45.38	45.67	1.90	P	0.555
	Mean	46.45	44.82		2.69	E×P	0.702
Tibia							
Ash weight, g	2,700 kcal/kg	4.12^{x}	3.68^{y}	3.65	0.16	E	0.606
	2,800 kcal/kg	3.68^{xy}	3.86^{x}	3.77	0.16	P	0.129
	Mean	3.90	3.52		0.23	E×P	0.032
Ash concentration, g/cm^3	2,700 kcal/kg	0.44	0.38	0.41	0.01	E	0.549
	2,800 kcal/kg	0.40	0.40	0.40	0.01	P	0.097
	Mean	0.42	0.39		0.02	E×P	0.118
Ash, %	2,700 kcal/kg	52.19	51.03	51.01	1.15	E	0.655
	2,800 kcal/kg	51.03	49.49	50.26	1.15	P	0.252
	Mean	51.61	49.66		1.62	E×P	0.801

[a]*Treatments were applied during prelay stage (15–20 week of age). The same layer diet was fed after 20 week of age.*

[x,y] *Mean within interaction with different letters are significantly different at* $p < 0.05$, $n = 4$.

eggshell formation (Cransberg et al., 2001). Earlier studies have reported that eggshell quality and bone quality are related (Whitehead, 2004; Kim et al., 2012). In the current study, dietary treatments had minimal effects on bone physical characteristics. The finding suggests that the development of femur and tibia is not influenced in the range of tested dietary protein and energy levelsbetween15 wk to 20 wk of age. In previous studies, it is reported that the tibia grows till 25 wk of age (Rath et al., 2000), while different bones responded differently to experimental treatments (Baird et al., 2008; Regmi et al., 2015). The effect of dietary protein and energy level on bone development remains to be elucidated. ALP is an important biomarker for measuring osteoblastic proliferation and bone formation and plays a critical role in bone mineralization (Zhang et al., 2019). In this study, serum ALP activity was similar at the end-of-lay among the different dietary treatment groups indicating a similarity in osteoblastic activity. The results of this study showed that the dietary energy and protein level fed during the prelay period did not affect the BMD and BBS at the end-of-lay, possibly because the prelay diet was fed from 15 to 20 weeks, and during this period, bone formation is targeted towards medullary bone that lacks structural integrity compared to cortical bone (Whitehead, 2004). This is consistent with the observation that dietary protein did not affect bone strength in broiler chickens (Muszyński et al., 2018). Furthermore, the current results corroborate a previous report by Hassan et al. (2013) that BMD and BBS of organic laying hens were not significantly influenced by different dietary energy and protein levels in the diet. Contrary to our result, Jiang et al. (2013) reported that hens fed with high energy diet have lower BMD and BBS. Bone mineralization analysis showed that birds fed with the 15% CP diet had higher tibia ash weight and ash concentration values, likely due to the increase in tibia length in this group. In this study, we observed increased serum P level in 16.5% CP diet. This result was consistent with the observation in broilers by Cowieson et al. (2020), who reported that serum P was decreased by low-protein diet, which is speculated to be a result of reduced dietary P level in low-protein diet. In the present study, the experimental diets had the same amount of P, and hence, the effect of dietary protein level on P metabolism needs to be investigated further.

In conclusion, the results of this study showed that the egg production performance was not changed by the protein and energy levels of prelay diet. Increased dietary CP level in prelay diet increased the egg shape index, eggshell thickness, while the increased energy level increased the yolk pigmentation. The gene expression in the hypothalamus, pituitary, ovary, and follicles of aged hens was differently affected by dietary treatment, whereas the circulating levels of sex hormones were not changed. The long-term effect of prelay diet on the endocrinology of hens during the laying period needs to be investigated further.

DATA AVAILABILITY STATEMENT

The original contributions presented in the study are included in the article/Supplementary Materials, further inquiries can be directed to the corresponding authors.

ETHICS STATEMENT

The animal study was reviewed and approved by the Approval for this study was granted by the Institutional Animal Care and Use Committee of Shandong Agricultural University prior to the commencement of the trial.

AUTHOR CONTRIBUTIONS

All authors contributed to the study conception and design. QX, NM, XW and HL conceived and designed the experiments, wrote manuscript; QX performed the experiments and analyzed the data; JZ and YZ designed the experimental diet and gave suggestions to data analysis; HL and HJ provided essential reagents; and all authors commented on previous versions of the manuscript. All authors read and approved the final manuscript.

FUNDING

This work was supported by the Key Technologies Research and Development Program of China (grant number 2021YFD1300405), Key Technology Research and Development Program of Shandong Province (2019JZZY020602), and the Earmarked Fund for China Agriculture Research System (CARS-40-K09).

ACKNOWLEDGMENTS

We thank Ms. Zhao for her excellent experiment assistance. We thank Cecilia T. Oluwabiyi for her conceived and designed the experiments and analyzed the data. We greatly thank the reviewers for their valuable comments and suggestions to the paper.

REFERENCES

Bacon, W., Nestor, K., and Renner, P. (1972). Further Studies on Ovarian Follicular Development in Egg and Meat Type Turkeys. *Poult. Sci.* 51, 398–401. doi:10.3382/ps.0510398

Bain, M. M., Nys, Y., and Dunn, I. C. (2016). Increasing Persistency in Lay and Stabilising Egg Quality in Longer Laying Cycles. What are the Challenges? *Br. Poult. Sci.* 57, 330–338. doi:10.1080/00071668.2016.1161727

Baird, H. T., Eggett, D. L., and Fullmer, S. (2008). Varying Ratios of omega-6: omega-3 Fatty Acids on the Pre-and Postmortem Bone Mineral Density, Bone ash, and Bone Breaking Strength of Laying Chickens. *Poult. Sci.* 87, 323–328. doi:10.3382/ps.2007-00186

Bédécarrats, G. Y., McFarlane, H., Maddineni, S. R., and Ramachandran, R. (2009). Gonadotropin-Inhibitory Hormone Receptor Signaling and its Impact on Reproduction in Chickens. *Gen. Comp. Endocrinol.* 163, 7–11. doi:10.1016/j.ygcen.2009.03.010

Casey-Trott, T. M., Korver, D. R., Guerin, M. T., Sandilands, V., Torrey, S., and Widowski, T. M. (2017). Opportunities for Exercise during Pullet Rearing, Part II: Long-Term Effects on Bone Characteristics of Adult Laying Hens at the End-Of-Lay. *Poult. Sci.* 96, 2518–2527. doi:10.3382/ps/pex060

Cave, N. A. G. (1984). Effect of a High-Protein Diet Fed Prior to the Onset of Lay on Performance of Broiler Breeder Pullets. *Poult. Sci.* 63, 1823–1827. doi:10.3382/ps.0631823

Ciccone, N. A., Sharp, P. J., Wilson, P. W., and Dunn, I. C. (2005). Changes in Reproductive Neuroendocrine mRNAs with Decreasing Ovarian Function in Ageing Hens. *Gen. Comp. Endocrinol.* 144, 20–27. doi:10.1016/j.ygcen.2005.04.009

Cowieson, A. J., Perez-Maldonado, R., Kumar, A., and Toghyani, M. (2020). Possible Role of Available Phosphorus in Potentiating the Use of Low-Protein Diets for Broiler Chicken Production. *Poult. Sci.* 99, 6954–6963. doi:10.1016/j.psj.2020.09.045

Cransberg, P. H., Parkinson, G. B., Wilson, S., and Thorp, B. H. (2001). Sequential Studies of Skeletal Calcium Reserves and Structural Bone Volume in a Commercial Layer Flock. *Br. Poult. Sci.* 42, 260–265. doi:10.1080/00071660120048528

Cui, Y.-M., Wang, J., Zhang, H.-J., Feng, J., Wu, S.-G., and Qi, G.-H. (2019). Effect of Photoperiod on Growth Performance and Quality Characteristics of Tibia and Femur in Layer Ducks during the Pullet Phase. *Poult. Sci.* 98, 1190–1201. doi:10.3382/ps/pey496

Dunn, I. C., Beattie, K. K., Maney, D., Sang, H. M., Talbot, R. T., Wilson, P. W., et al. (1996). Regulation of Chicken Gonadotropin-Releasing Hormone-I mRNA in Incubating, Nest-Deprived and Laying Bantam Hens. *Neuroendocrinology* 63, 504–513. Available at: https://www.karger.com/Article/FullText/127079. doi:10.1159/000127079

Fuller, H. L., and Dunahoo, W. S. (1962). Restricted Feeding of Pullets. *Poult. Sci.* 41, 1306–1314. doi:10.3382/ps.0411306

Fuller, H. L., Potter, D. K., and Kirkland, W. (1969). Effect of Delayed Maturity and Carcass Fat on Reproductive Performance of Broiler Breeder Pullets. *Poult. Sci.* 48, 801–809. doi:10.3382/ps.0480801

Galway, A. B., Lapolt, P. S., Tsafriri, A., Dargan, C. M., Boime, I., and Hsueh, A. J. W. (1990). Recombinant Follicle-Stimulating Hormone Induces Ovulation and Tissue Plasminogen Activator Expression in Hypophysectomized Rats. *Endocrinology* 127, 3023–3028. doi:10.1210/endo-127-6-3023

Gautron, J., Réhault-Godbert, S., Van de Braak, T. G. H., and Dunn, I. C. (2021). Review: What are the Challenges Facing the Table Egg Industry in the Next Decades and what Can Be Done to Address Them? *Animal* 15, 100282. doi:10.1016/j.animal.2021.100282

Gowe, R. S., Strain, J. H., Crawford, R. D., Hill, A. T., Slen, S. B., and Mountain, W. F. (1965). Restricted Feeding of Growing Pullets. *Poult. Sci.* 44, 717–726. doi:10.3382/ps.0440717

Gunawardana, P., Roland, D. A., and Bryant, M. M. (2008). Effect of Energy and Protein on Performance, Egg Components, Egg Solids, Egg Quality, and Profits in Molted Hy-Line W-36 Hens. *J. Appl. Poult. Res.* 17, 432–439. doi:10.3382/japr.2007-00085

Hadinia, S. H., Carneiro, P. R. O., Fitzsimmons, C. J., Bédécarrats, G. Y., and Zuidhof, M. J. (2020). Post-Photostimulation Energy Intake Accelerated Pubertal Development in Broiler Breeder Pullets. *Poult. Sci.* 99, 2215–2229. doi:10.1016/j.psj.2019.11.065

Han, S., Wang, Y., Liu, L., Li, D., Liu, Z., Shen, X., et al. (2017). Influence of Three Lighting Regimes during Ten Weeks Growth Phase on Laying Performance, Plasma Levels- and Tissue Specific Gene Expression- of Reproductive Hormones in Pengxian Yellow Pullets. *PLoS One* 12, e0177358. doi:10.1371/journal.pone.0177358

Hassan, M. R., Choe, H. S., Jeong, Y. D., Hwangbo, J., and Ryu, K. S. (2013). Effect of Dietary Energy and Protein on the Performance, Egg Quality, Bone Mineral Density, Blood Properties and Yolk Fatty Acid Composition of Organic Laying Hens. *Ital. J. Anim. Sci.* 12, e10. doi:10.4081/ijas.2013.e10

Hocking, P. M., Gilbert, A. B., Walker, M., and Waddington, D. (1987). Ovarian Follicular Structure of white Leghorns Fedad Libitumand dwarf and Normal Broiler Breeders Fedad Libitumor Restricted until Point of Lay. *Br. Poult. Sci.* 28, 493–506. doi:10.1080/00071668708416983

Hollands, K. G., and Gowe, R. S. (1961). The Effect of Restricted and Full-Feeding during Confinement Rearing on First and Second Year Laying House Performance. *Poult. Sci.* 40, 574–583. doi:10.3382/ps.0400574

Hussein, A. S., Cantor, A. H., Pescatore, A. J., and Johnson, T. H. (1996). Effect of Dietary Protein and Energy Levels on Pullet Development. *Poult. Sci.* 75, 973–978. doi:10.3382/ps.0750973

Isaacks, R. E., Reid, B. L., Davies, R. E., Quisenbeery, J. H., and Couch, J. R. (1960). Restricted Feeding of Broiler Type Replacement Stock. *Poult. Sci.* 39, 339–346. doi:10.3382/ps.0390339

Jiang, S., Cui, L., Shi, C., Ke, X., Luo, J., and Hou, J. (2013). Effects of Dietary Energy and Calcium Levels on Performance, Egg Shell Quality and Bone Metabolism in Hens. *Vet. J.* 198, 252–258. doi:10.1016/j.tvjl.2013.07.017

Joseph, N. S., Robinson, F. E., Korver, D. R., and Renema, R. A. (2000). Effect of Dietary Protein Intake during the Pullet-To-Breeder Transition Period on Early Egg Weight and Production in Broiler Breeders. *Poult. Sci.* 79, 1790–1796. doi:10.1093/ps/79.12.1790

Junqueira, O. M., De Laurentiz, A. C., Da Silva Filardi, R., Rodrigues, E. A., and Casartelli, E. M. C. (2006). Effects of Energy and Protein Levels on Egg Quality and Performance of Laying Hens at Early Second Production Cycle. *J. Appl. Poult. Res.* 15, 110–115. doi:10.1093/japr/15.1.110

Keshavarz, K. (1998). The Effect of Light Regimen, Floor Space, and Energy and Protein Levels during the Growing Period on Body Weight and Early Egg Size. *Poult. Sci.* 77, 1266–1279. doi:10.1093/ps/77.9.1266

Kim, W. K., Bloomfield, S. A., Sugiyama, T., and Ricke, S. C. (2012). Concepts and Methods for Understanding Bone Metabolism in Laying Hens. *World's Poult. Sci. J.* 68, 71–82. doi:10.1017/S0043933912000086

Lilburn, M. S., and Myers-Miller, D. J. (1990). Dietary Effects on Body Composition and Subsequent Production Characteristics in Broiler Breeder Hens. *Poult. Sci.* 69, 1126–1132. doi:10.3382/ps.0691126

Livak, K. J., and Schmittgen, T. D. (2001). Analysis of Relative Gene Expression Data Using Real-Time Quantitative PCR and the 2−ΔΔCT Method. *Methods* 25, 402–408. doi:10.1006/meth.2001.1262

Mikhael, S., Punjala-Patel, A., and Gavrilova-Jordan, L. (2019). Hypothalamic-Pituitary-Ovarian Axis Disorders Impacting Female Fertility. *Biomedicines* 7, 5. doi:10.3390/biomedicines7010005

Muszyński, S., Tomaszewska, E., Dobrowolski, P., Kwiecień, M., Wiącek, D., Świetlicka, I., et al. (2018). Analysis of Bone Osteometry, Mineralization, Mechanical and Histomorphometrical Properties of Tibiotarsus in Broiler Chickens Demonstrates a Influence of Dietary Chickpea Seeds (Cicer Arietinum L.) Inclusion as a Primary Protein Source. *PLoS One* 13, e0208921. doi:10.1371/journal.pone.0208921

Onagbesan, O., Bruggeman, V., and Decuypere, E. (2009). Intra-Ovarian Growth Factors Regulating Ovarian Function in Avian Species: A Review. *Anim. Reprod. Sci.* 111, 121–140. doi:10.1016/j.anireprosci.2008.09.017

Ormerod, B. K., and Galea, L. A. M. (2001). Reproductive Status Influences Cell Proliferation and Cell Survival in the Dentate Gyrus of Adult Female Meadow Voles: A Possible Regulatory Role for Estradiol. *Neuroscience* 102, 369–379. doi:10.1016/s0306-4522(00)00474-7

Palmer, S. S., and Bahr, J. M. (1992). Follicle Stimulating Hormone Increases Serum Oestradial-17ß Concentrations, Number of Growing Follicles and Yolk Deposition in Aging Hens (*Gallus Gallus Domesticus*) with Decreased Egg Production. *Br. Poult. Sci.* 33, 403–414. doi:10.1080/00071669208417478

Pérez-Bonilla, A., Novoa, S., García, J., Mohiti-Asli, M., Frikha, M., and Mateos, G. G. (2012). Effects of Energy Concentration of the Diet on Productive Performance and Egg Quality of Brown Egg-Laying Hens Differing in Initial Body Weight. *Poult. Sci.* 91, 3156–3166. doi:10.3382/ps.2012-02526

Rath, N. C., Huff, G. R., Huff, W. E., and Balog, J. M. (2000). Factors Regulating Bone Maturity and Strength in Poultry. *Poult. Sci.* 79, 1024–1032. doi:10.1093/ps/79.7.1024

Regmi, P., Deland, T. S., Steibel, J. P., Robison, C. I., Haut, R. C., Orth, M. W., et al. (2015). Effect of Rearing Environment on Bone Growth of Pullets. *Poult. Sci.* 94, 502–511. doi:10.3382/ps/peu041

Romano, M., Barnabe, V., Kastelic, J., De Oliveira, C., and Romano, R. (2007). Follicular Dynamics in Heifers during Pre-pubertal and Pubertal Period Kept under Two Levels of Dietary Energy Intake. *Reprod. Domest. Anim.* 42, 616–622. doi:10.1111/j.1439-0531.2006.00832.x

Saxena, R., Saxena, V. K., Tripathi, V., Mir, N. A., Dev, K., Begum, J., et al. (2020). Dynamics of Gene Expression of Hormones Involved in the Growth of Broiler Chickens in Response to the Dietary Protein and Energy Changes. *Gen. Comp. Endocrinol.* 288, 113377. doi:10.1016/j.ygcen.2019.113377

Scaramuzzi, R. J., Campbell, B. K., Downing, J. A., Kendall, N. R., Khalid, M., Muñoz-Gutiérrez, M., et al. (2006). A Review of the Effects of Supplementary Nutrition in the Ewe on the Concentrations of Reproductive and Metabolic Hormones and the Mechanisms that Regulate Folliculogenesis and Ovulation Rate. *Reprod. Nutr. Dev.* 46, 339–354. doi:10.1051/rnd:2006016

Sharp, P. J., Dunn, I. C., and Cerolini, S. (1992). Neuroendocrine Control of Reduced Persistence of Egg-Laying in Domestic Hens: Evidence for the Development of Photorefractoriness. *Reproduction* 94, 221–235. doi:10.1530/jrf.0.0940221

Song, M., Lin, X., Zhao, J., Wang, X., Jiao, H., Li, H., et al. (2020). High Frequency Vaccination-Induced Immune Stress Reduces Bone Strength with the Involvement of Activated Osteoclastogenesis in Layer Pullets. *Poult. Sci.* 99, 734–743. doi:10.1016/j.psj.2019.12.023

Sujatha, T., Rajini, R. A., and Prabakaran, R. (2014). Efficacy of Pre-lay Diet. *J. Appl. Anim. Res.* 42, 57–64. doi:10.1080/09712119.2013.822803

Tanabe, Y., Nakamura, T., Tanase, H., and Doi, O. (1981). Comparisons of Plasma LH, Progesterone, Testosterone and Estradiol Concentrations in Male and Female Chickens (*Gallus Domesticus*) from 28 to 1141 Days of Age. *Endocrinol. Japon* 28, 605–613. doi:10.1507/endocrj1954.28.605

Tsutsui, K., Saigoh, E., Ukena, K., Teranishi, H., Fujisawa, Y., Kikuchi, M., et al. (2000). A Novel Avian Hypothalamic Peptide Inhibiting Gonadotropin Release. *Biochem. Biophys. Res. Commun.* 275, 661–667. doi:10.1006/bbrc.2000.3350

Waddington, D., Perry, M. M., Gilbert, A. B., and Hardie, M. A. (1985). Follicular Growth and Atresia in the Ovaries of Hens (*Gallus Domesticus*) with Diminished Egg Production Rates. *Reproduction* 74, 399–405. doi:10.1530/jrf.0.0740399

Wang, S.-Y., and Johnson, P. A. (1993). Increase in Ovarian α-Inhibin Gene Expression and Plasma Immunoreactive Inhibin Level Is Correlated with a Decrease in Ovulation Rate in the Domestic Hen. *Gen. Comp. Endocrinol.* 91, 52–58. doi:10.1006/gcen.1993.1103

Webster, A. B. (2004). Welfare Implications of Avian Osteoporosis. *Poult. Sci.* 83, 184–192. doi:10.1093/ps/83.2.184

Whitehead, C. C. (2004). Overview of Bone Biology in the Egg-Laying Hen. *Poult. Sci.* 83, 193–199. doi:10.1093/ps/83.2.193

Yu, M. W., Robinson, F. E., and Etches, R. J. (1992). Effect of Feed Allowance during Rearing and Breeding on Female Broiler Breeders. *Poult. Sci.* 71, 1762–1767. doi:10.3382/ps.0711762

Zhang, H. Y., Zeng, Q. F., Bai, S. P., Wang, J. P., Ding, X. M., Xuan, Y., et al. (2019). Study on the Morphology and Mineralization of the Tibia in Meat Ducks from 1 to 56 D. *Poult. Sci.* 98, 3355–3364. doi:10.3382/ps/pez121

Zhou, D. S., Fang, Z. F., Wu, D., Zhuo, Y., Xu, S. Y., Wang, Y. Z., et al. (2010). Dietary Energy Source and Feeding Levels during the Rearing Period Affect Ovarian Follicular Development and Oocyte Maturation in Gilts. *Theriogenology* 74, 202–211. doi:10.1016/j.theriogenology.2010.02.002

Zhou, X., Yu, M. Y., Liu, L. W., Yi, K. L., Li, C. J., Chen, L., et al. (2009). Effects of Dietary Energy Level on Ovarian Expression of mRNAs for Luteinizing Hormone Receptor and Follicle-Stimulating Hormone Receptor in Prepubertal Gilts. *Chin. J. Vet. Sci.* 29, 97–105.

Conflict of Interest: The authors declare that the research was conducted in the absence of any commercial or financial relationships that could be construed as a potential conflict of interest.

Publisher's Note: All claims expressed in this article are solely those of the authors and do not necessarily represent those of their affiliated organizations, or those of the publisher, the editors and the reviewers. Any product that may be evaluated in this article, or claim that may be made by its manufacturer, is not guaranteed or endorsed by the publisher.

frontiers | Frontiers in Physiology

ORIGINAL RESEARCH
published: 12 May 2022
doi: 10.3389/fphys.2022.887207

Integrated Fecal Microbiome and Metabolomics Reveals a Novel Potential Biomarker for Predicting Tibial Dyschondroplasia in Chickens

Shucheng Huang[1], Chaodong Zhang[1], Tingting Xu[1], Aftab Shaukat[2], Yanfeng He[1], Pan Chen[1], Luxi Lin[1], Ke Yue[1], Qinqin Cao[1] and Xishuai Tong[3]*

[1]College of Veterinary Medicine, Henan Agricultural University, Zhengzhou, China, [2]National Center for International Research on Animal Genetics, Breeding and Reproduction (NCIRAGBR), Huazhong Agricultural University, Wuhan, China, [3]Institutes of Agricultural Science and Technology Development (Joint International Research Laboratory of Agriculture and Agri-Product Safety of the Ministry of Education of China)/College of Veterinary Medicine, Yangzhou University, Yangzhou, China

Tibial dyschondroplasia (TD) is a metabolic tibial-tarsal disorder occurring in fast-growing poultry, and its diagnosis is mainly based on an invasive method. Here, we profiled the fecal gut microbiome and metabolome of broilers with and without TD to identify potential non-invasive and non-stress biomarkers of TD. First, TD broilers with the most pronounced clinical signs during the experiment were screened and faecal samples were collected for integrated microbiome and metabolomics analysis. Moreover, the diagnostic potential of identified biomarkers was further validated throughout the experiment. It was noted that the microbial and metabolic signatures of TD broilers differed from those of normal broilers. TD broilers were characterized by enriched bacterial OTUs of the genus *Klebsiella*, and depleted genera [*Ruminococcus*], *Dorea*, *Ruminococcus*, *Oscillospira*, *Ochrobactrum*, and *Sediminibacterium*. In addition, a total of 189 fecal differential metabolites were identified, mainly enriched in the purine, vitamin and amino acid metabolism, which were closely associated with differential microbiota and tibia-related indicators. Furthermore, three fecal metabolites were screened, including 4-hydroxybenzaldehyde, which distinguished TD from normal broilers with extremely high specificity and was superior to serum bone markers. These results indicated that gut microbiota equilibrium might influence the pathogenesis of TD by modulating host metabolism, and the identified fecal metabolite 4-hydroxybenzaldehyde might be a potential and non-invasive biomarker for predicting TD in chickens.

Keywords: tibial dyschondroplasia, gut microbiome, metabolome, diagnosis, biomarker

OPEN ACCESS

Edited by:
Kazuhisa Honda,
Kobe University, Japan

Reviewed by:
Yanhui Han,
University of Massachusetts Amherst, United States
Shozo Tomonaga,
Kyoto University, Japan

****Correspondence:***
Shucheng Huang
huang.sc@henau.edu.cn

Specialty section:
This article was submitted to Avian Physiology, a section of the journal Frontiers in Physiology

Received: *01 March 2022*
Accepted: *19 April 2022*
Published: *12 May 2022*

Citation:
Huang S, Zhang C, Xu T, Shaukat A, He Y, Chen P, Lin L, Yue K, Cao Q and Tong X (2022) Integrated Fecal Microbiome and Metabolomics Reveals a Novel Potential Biomarker for Predicting Tibial Dyschondroplasia in Chickens. Front. Physiol. 13:887207. doi: 10.3389/fphys.2022.887207

Abbreviations: AA, arbor acres; ALP, alkaline phosphatase; AUC, area under the ROC curve; Ca, calcium; ELISA, enzyme-linked immunosorbent assay; LDA, linear discriminant analysis; LEfSe, linear discriminant analysis; OPLS-DA, orthogonal partial least squares discriminant analysis; P, phosphorus; PCA, principal analysis; PLS-DA, partial least squares discriminant analysis; ROC, receiver operating characteristic; TD, tibial chondrodysplasia; TGP, tibia growth plate; TGPI, tibia growth plate index; TRACP, tartrate-resistant acid phosphatase; VIP, variable importance in project.

INTRODUCTION

Tibial dyschondroplasia (TD) is a metabolic cartilage disease that can occur in humans or animals, including poultry, especially broilers and turkeys, accompanied by a rapid growth rate (Poulos, 1978; Leach and Monsonego-Ornan, 2007; Xu et al., 2021). It is characterized by an abnormality in the bone growth plate. This cartilage template is not properly resorbed but replaced by bone, a common cause of deformity and lameness in the broiler chicken (Farquharson and Jefferies, 2000; Rath et al., 2005; Huang et al., 2018). Evidence shows that 12.5 billion birds worldwide have leg problems each year (Almeida Paz et al., 2010). Derakhshanfar *et al.* found that TD affects the skeletal system of 30% of meat chickens and 90% of turkeys (Derakhshanfar et al., 2013). In addition, the abnormalities of growth and development of the skeleton in poultry indirectly lead to reduce gross profits (about 10%–40%) in the poultry industry (Almeida Paz et al., 2010). But, it is challenging to accurately assess the prevalence of TD in broiler management due to its sub-clinical signs and symptoms (Groves and Muir, 2017). However, the formation of broiler TD causes leg weakness, dyskinesias and leg deformities that ultimately prevent standing (Genin et al., 2012; Huang et al., 2019), thus compromising the welfare of the chickens.

Broilers with apparent leg disease can be easily diagnosed based on clinical manifestations, but the condition is usually severe and has no therapeutic value. The most effective method for diagnosing TD in broilers is mainly based on an invasive technique, namely observation of morphological changes in the tibial growth plate (Farquharson and Jefferies, 2000; Rath et al., 2007; Huang et al., 2018). In addition, radiological methods can be used for assessment of broiler TD, but there is a delay in the early diagnosis of sub-clinical TD in broilers and it is complex and time-consuming for the farms (Poulos, 1978; Pelicia et al., 2012). It is well known that early diagnosis is essential for the treatment of metabolic and developmental diseases (Edwards and Veltmann, 1983). Therefore, a non-invasive, low-stress or non-stress method is desired for the darly diagnosis of TD in broiler chickens.

The microbiome that resides in the gastrointestinal tract reflects physiological and metabolic properties. These microorganisms live symbiotically with the host to produce microbial metabolites, forming the host-microbe metabolic axis, which plays a vital role in animal nutritional metabolism and immune homeostasis, including the occurrence and development of disease (Zaiss et al., 2019; Zheng et al., 2019; Kim et al., 2020; Wang et al., 2020; Ling et al., 2021; Murga-Garrido et al., 2021). More evidence has demonstrated that gut microbiota is a critical regulator in bone and that alterations in microbiota composition can contribute to pathological bone loss or reduced bone mineral density. While the changes in microbiota composition can improve calcium absorption and mineral levels by adding nutritional supplements, suggesting that gut microbiota directly and indirectly affects bone metabolism (Di Stefano et al., 2001; Stotzer et al., 2003; Chen et al., 2017; Lu et al., 2021). Furthermore, previous studies have shown significant changes in the structure of the gut microbiota of broiler chickens affected by TD (Tong et al., 2018). Until now, the gut microbial characteristics of broiler TD have not been fully elucidated. Recent studies have highlighted that the detection of characteristics of 16S rRNA gene profiling in gut microbiota provides a plentiful thread for the diagnosis and assessment of diseases, and serves as a predictor or a monitor of disease prognosis of therapeutic intervention (Pan et al., 2020; Hao et al., 2021). This approach may inspire the identification of predictive microbial markers of TD in broilers. Although 16S rRNA gene sequencing technology has been successfully applied in clinical diagnosis, the phylogenetic resolution of the 16S rRNA gene is limited that restricts the universality and significance of these studies (Rodriguez-R et al., 2018; Zhu et al., 2021). The gut metabolome, rather than the gut microbiota itself, may also directly involve TD formation (He et al., 2020; Lu et al., 2021; Xu et al., 2021). Furthermore, fecal metabolomics is derived not only from microbial metabolism that accounts for 15%, but also jointly from diet and host metabolism (HolmesLi et al., 2012; Kim et al., 2020; Murga-Garrido et al., 2021), which provides a complementary functional readout of microbial activity, and combining these two omics-approaches is a mature strategy for identifying potentially disease-related gut microbes and their functional metabolites (Klein et al., 2016; Stewart et al., 2017).

To address these challenges, we analyzed the microbial compositions and metabolic changes of fecal samples in the thiram-induced TD chicken model by combined 16S rRNA gene sequencing and UPLC/MS/MS-based metabolomics. Previous studies have confirmed that the analysis of these two methods is a well-established strategy for uncovering both gut microbial composition and functional features in various diseases (Zheng et al., 2019; Kim et al., 2020; Wang et al., 2020; Chen et al., 2021). Therefore, based on this well-established strategy, we identified the microbial and metabolic signatures of TD in broilers to explore their reciprocal interactions in the gut ecosystem stability of TD. The relationship between altered gut microbes, fecal metabolites and tibia-related indexes (e.g., tibia weight, tibia length, tibia diameter, and tibia growth plate width) was evaluated. Moreover, based on these multi-omic data, we identified three novel differential fecal metabolite biomarkers that can accurately distinguish TD in broiler chickens.

RESULTS

Changes in the Tibiae and Their Growth Plate in Broilers With TD

To determine the changes in tibia-related parameters in broilers in the CON and TD groups, tibia weight, tibia length and tibia diameter were measured (**Figures 1A–F**). The tibia weight and length of broiler chickens in the TD group were markedly ($p < 0.001$ and $p < 0.001$, respectively) decreased compared to the CON group on days 11 and 15. Similarly, the tibia mean diameter of broiler chickens with TD was also significantly ($p = 0.001$, $p < 0.001$, and $p = 0.005$, respectively) decreased during the experiment compared to normal broiler chickens of CON group. Our previous study showed the dynamics of cartilaginous growth plates in broiler chickens play central

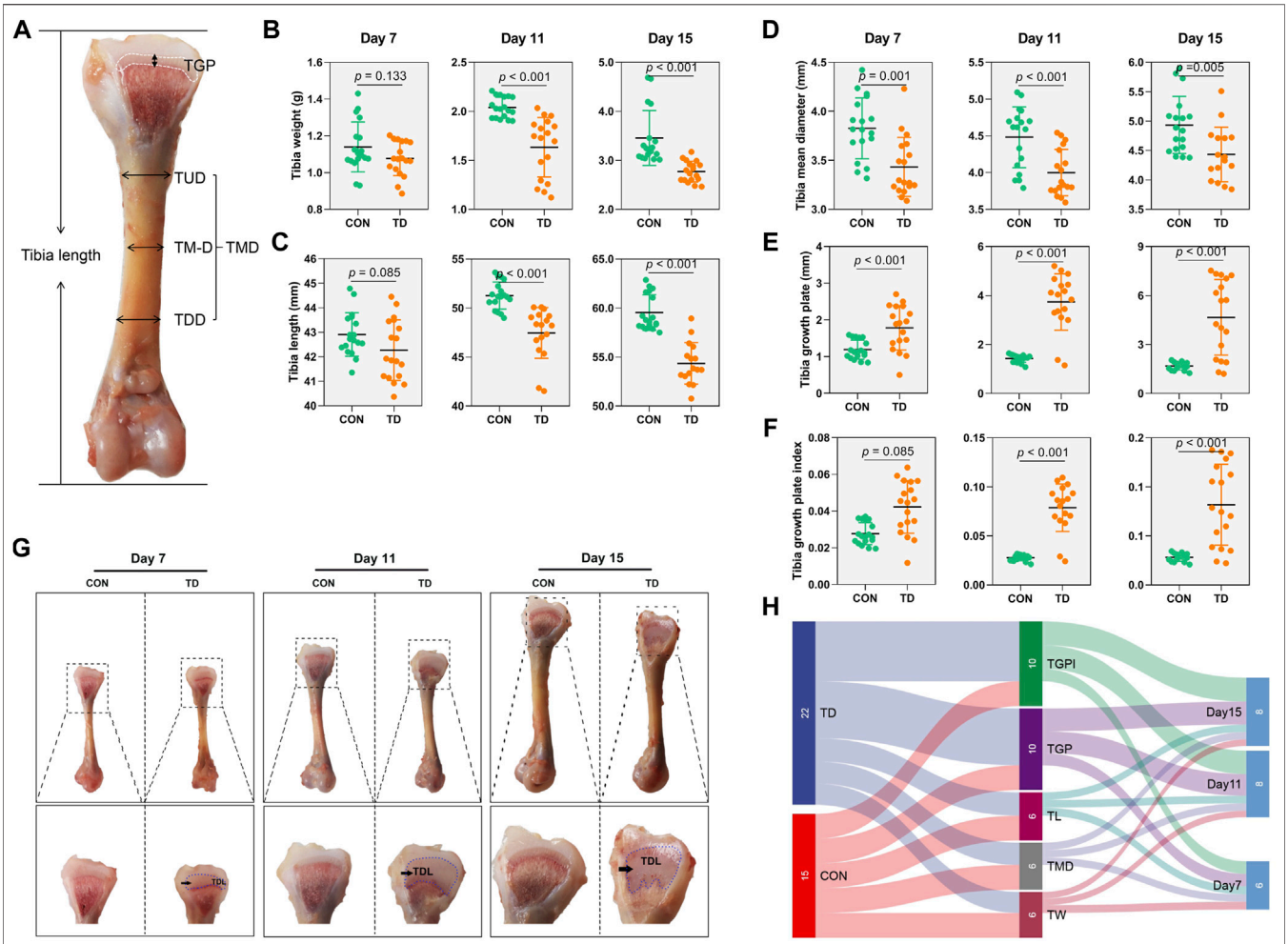

FIGURE 1 | Tibia related-parameters of broiler chickens. **(A)** Standard for the measurement of tibia length, TUD (Upper 1/2 diameter of the tibia), TMD (tibia mid-diameter), and TLD (Lower 1/2 diameter of the tibia). TMD (tibia mean diameter) comes from the average of the TUD, TMD, and TLD. **(B–F)** The tibia weight, tibia length, tibia mean diameter (TMD), tibia growth plate, and tibia growth plate index were recorded and compared between the CON and TD groups from 7-, 11-, and 15-day-old broiler chickens. A statistical difference of p-value less than 0.05; data represent means ± SD, two-tailed unpaired Student's t-test. N = 18. **(G)** Morphological observation of the tibial growth plate in the CON and TD groups from 7-, 11-, and 15-day-old broiler chickens. The black arrows indicate TD lesion. **(H)** Sankey diagram depicting tibia related-parameters by test point in the CON and TD groups of broiler chickens.

roles in the proper development and growth of the tibiae (Huang et al., 2018). The morphological observation found that the width of the tibia growth plate (TGP) in the TD group was significantly widened on days 7 and 11 compared to the CON group (**Figure 1G**). On day 15, the TGP width of the TD group was significantly increased and the area of the TD lesion was increased (**Figure 1G**). Quantitative histomorphology analysis of the bone showed that the TGP width and its index were markedly higher in the TD group than the CON group on days 7, 11 and 15 (**Figures 1E,F**). These results collectively demonstrated that tibia-related parameters were obviously altered in TD broilers.

Sankey diagram is a specific type of flow diagram that usually displays the flows and quantities from one set of values to the other proportion, and is used to further determine which experimental stage of TD broiler chickens tibia-related parameters changed most significantly. The results showed that the width of tibia growth plate and its index accounted for a high proportion of tibia-related parameters, mainly derived from the TD group. In addition, the proportion of tibia-related parameters was much more significant on days 10 and 15 than that on day 7 (**Figure 1H**), indicating that the tibia growth plates of TD broilers showed the most observable changes on days 11 and 15 than on day 7.

Fecal Microbial Structure of Two Groups in Broiler Chickens

The analysis of tibia-related parameters showed significant changes in TD symptoms in broilers on days 11 and 15. Faecal samples are a non-invasive way to screen biomarkers for poultry (Zhu et al., 2021). Therefore, we further screen the potential biomarkers of TD broilers from 11 days of age. 16S

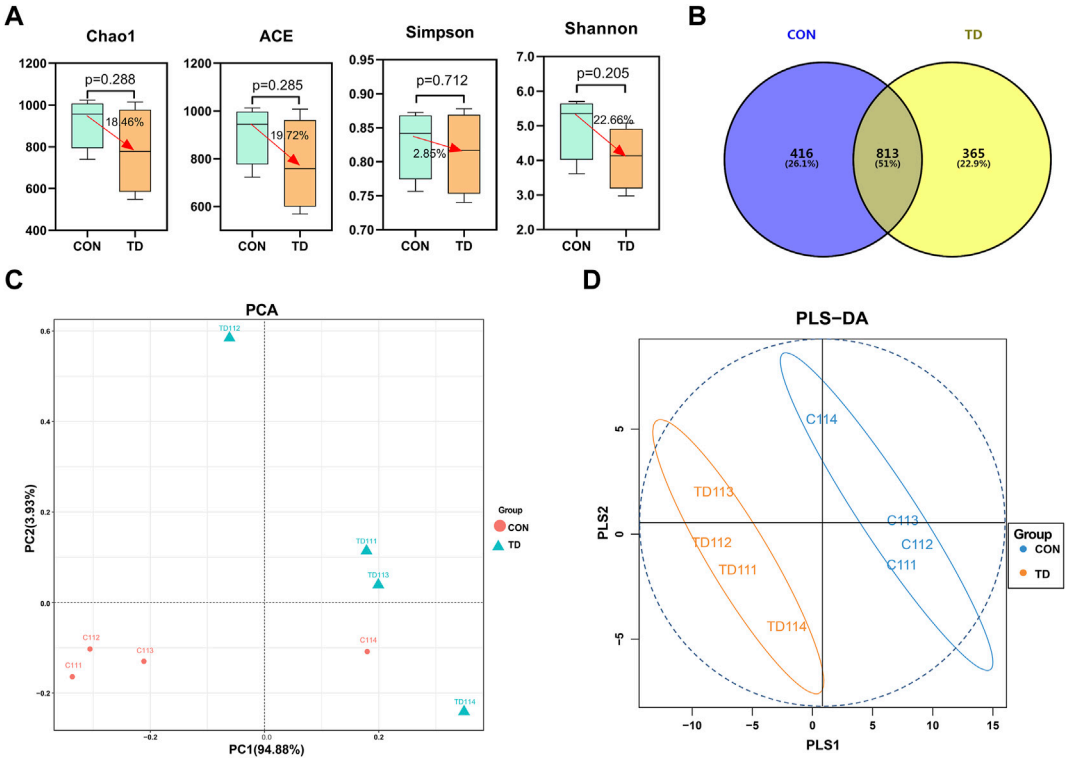

FIGURE 2 | Fecal microbial overall structure of broiler chickens. **(A)** Chao1, ACE, Simpson, and Shannon indices from the CON and TD groups were used to analyze the alpha diversity. Statistical analysis was performed by Kruskal-Willis test, a *p*-value lower than 0.05 (<0.05) has statistically significant, N = 4. **(B)** The Venn diagram showed the common and unique OTUs in the CON and TD groups of broiler chickens. **(C)** Unweighted Unifrac PCA estimates for the gut microbiota of the CON group (red) and TD group (green). **(D)** OPLS-DA analysis of gut-microbiota in the CON group (green) and TD group (orange-yellow) of broiler chickens.

rRNA gene sequencing examined the gut microbiota in the feces of both the CON and TD groups. The α-diversity analyzed using different indexes, including the Chao1 index, ACE index, Simpson index, and Shannon index, showed that there was decrease (18.46, 19.72, 2.85, and 22.66%, respectively) in the indexes of gut microbiota listed in the TD group, but the difference was not significant as compared with the CON group ($p > 0.05$) as shown in **Figure 2A**. The Venn diagram (**Figure 2B**) shows that 365 unique OTUs in the TD group compared with the CON group, accounting for approximately 22.9%. To analyze the differences between the CON and TD groups, the bioinformatics analysis methods of unweighted unifrac PCA and OPLS-DA model were performed to evaluate the gut microbiota in feces (**Figures 2C,D**). The constructed PCA and OPLS-DA score plots showed a clear separation between the CON and TD groups, indicating a significant difference in fecal microbial structure.

Difference Analysis of Microbiota Composition Between the CON and TD Groups

Next, we compared the relative abundance features of each group of bacterial taxa to distinguish specific alterations in microbiota. As shown in **Figures 3A,B**, five phyla with the highest average relative abundance, including the Firmicutes, Proteobacteria, Tenericutes, Actinobacteria and Bacteroidetes, and the proportion of the phyla Proteobacteria (2.82%), Actinobacteria (0.20%) and Bacteroidetes (0.18%) in the CON group was lower than in the TD group (7.09, 0.70, and 0.28%, respectively). Still, the phyla Firmicutes (95.82%) and Tenericutes (0.90%) in the CON group were higher than those in the TD group (91.72 and 0.13%, respectively) (see **Supplementary Material S1**). In addition, the genera between the CON and TD groups were distinctly enriched in *Lactobacillus*, *Ruminococcus* [*Ruminococcus*], *Blautia*, *Oscillospira*, *Dorea*, *Candidatus_Arthromitus*, *Kurthia*, *Coprococcus*, *Ochrobactrum*, *Coprobacillus*, *Agrobacterium*, *Sediminibacterium* and *Eggerthella* (**Figure 3B**, **Supplementary Material S2**).

Differential bacterial taxa between the two groups were further identified using the LEfSe analysis (**Figures 3C,D**), an algorithm for high-dimensional biomarker discovery and interpretation. The LDA was employed to determine the data and effects on the different species. LEfSe analysis identified 50 discriminative features (genus level; LDA score >2, $p < 0.05$), and the relative abundance was significantly different between the CON and TD groups. Among them, *Klebsiella, Arthrobacter, Lvsinibacillus, Citrobacter, Sphingobacterium, Myroides, Oceanobacillus, Wautersiella* and *Serratia* were concentrated in TD broilers; while *Ruminococcus*, *Oscillospira*, *Dorea*, butyrate-producing genera *Ochrobacturm*, *Coprococcus*, *Brevibacterium*, *Sediminibacterium*, *Eggerthella*,

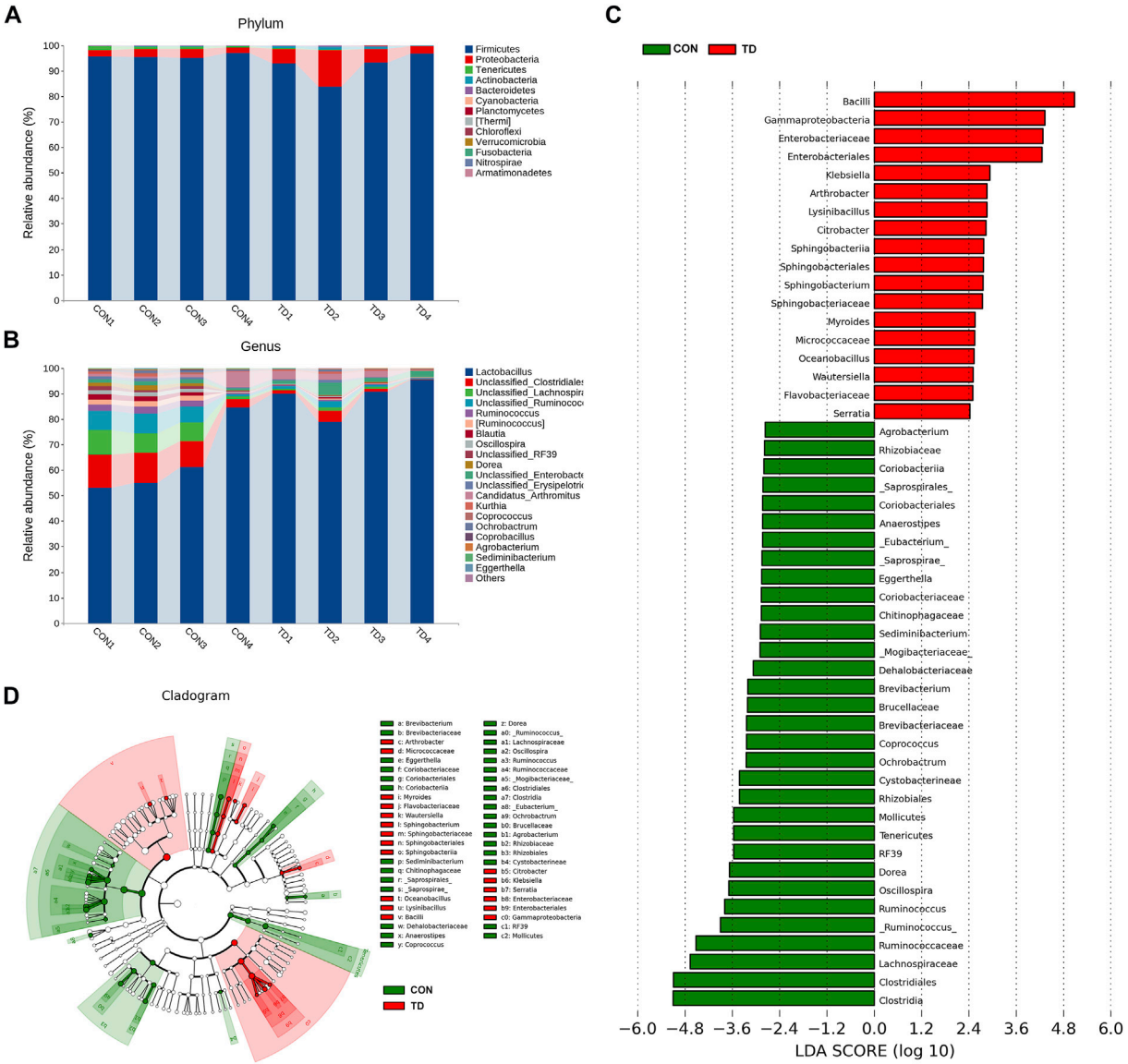

FIGURE 3 | Fecal microbial composition of broiler chickens. **(A,B)** Relative abundance of microbiota at the phylum level and the genus level (Top 20) in CON and TD groups. **(C,D)** LDA score and cladogram of LDA effect size (LEfSe) comparison analysis between the CON and TD groups. As indicated, the red, green shading represents bacterial taxa that were significantly higher in either the CON or TD group. The selection of discriminative taxa between the CON and TD groups was based on an LDA score cutoff of 2.0, and differences in the relative abundances of taxa were statistically determined based on a Wilcoxon's signed-rank test at a significance level of 0.05 (N = 4).

_Eubacterium, *Anaerostipes* and *Agrobacterium* were concentrated in normal broilers (see **Supplementary Material S3**). These results indicated that the fecal microbial composition of TD broiler chickens has been significantly changed compared to that of normal broiler chickens.

Screening of Differential Fecal Microbiota in TD Broiler Chickens

The random forest analysis was performed to screen the top20 important species, showing the highest important species, including the *Lactobacillus*, Clostridiaceae, Ruminococcaceae, Clostridiales, Lachnospiraceae, *RF39 [Ruminococcus]*, *Dorea*, *Ruminococcus*, *Cupriavidus*, Enterobacteriaceae, *Oscillospira*, *Ochrobactrum* [Mogibacteriaceae], *Sediminibacterium*, *Blautia*, *Methyolbacterium*, *Clostridium*, *Acinetobacter* and *Klebsiella* (**Figure 4A**). In addition, Venn diagram analysis of the LEfSe identified 50 characteristic species (LDA score >2; $p < 0.05$) and the top 20 species in importance scores by random forest analysis showed that 12 species were screened, and we noted the higher abundances of Clostridiales ($p = 0.013$), Lachnospiraceae ($p = 0.023$), Ruminococcaceae ($p = 0.030$) *[Ruminococcus]* ($p = 0.020$), *Dorea* ($p =$

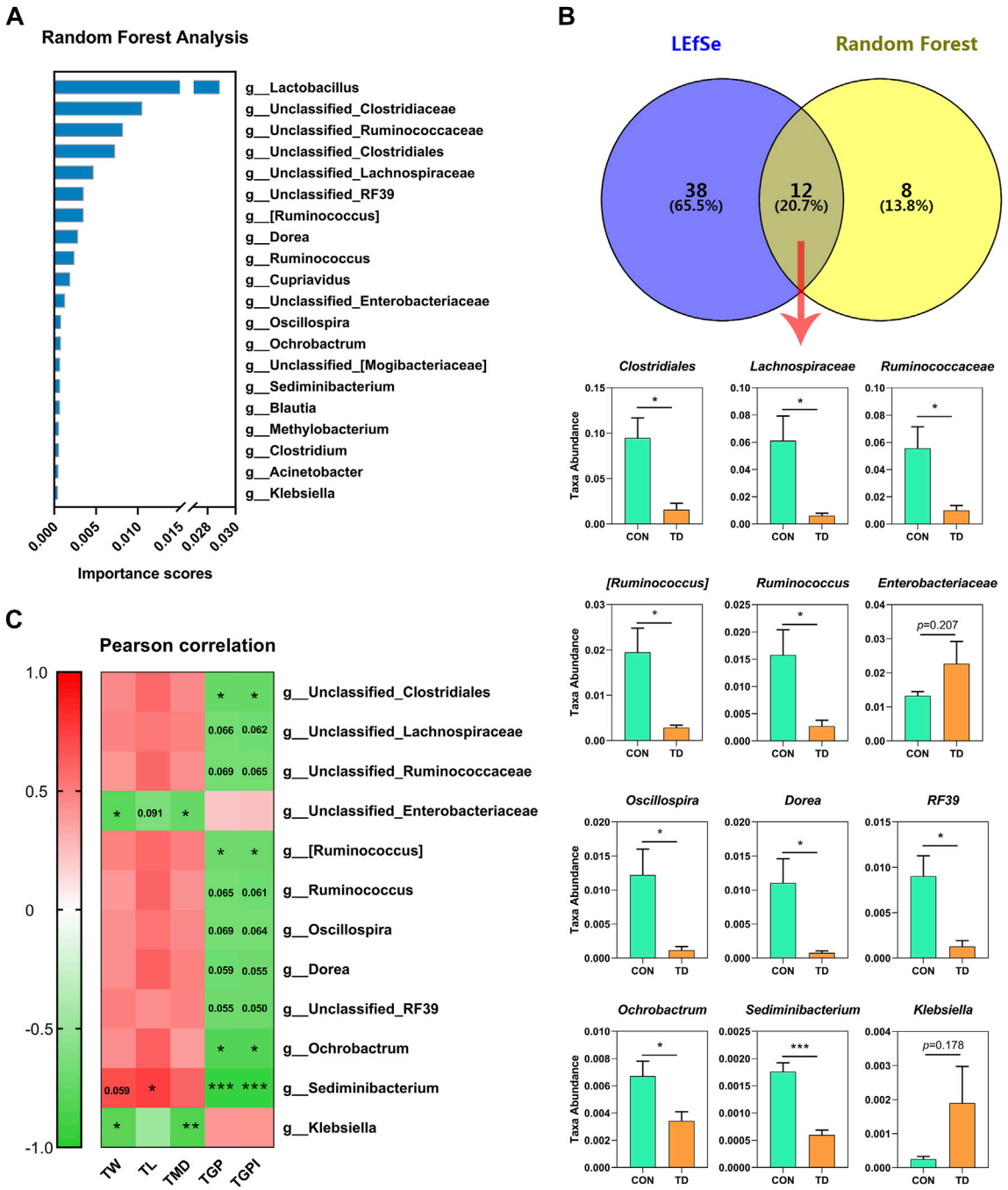

FIGURE 4 | Analysis of differential fecal microbiota in broiler chickens with TD. **(A)** Random forest analysis on fecal microbiome of CON and TD groups of broiler chickens. The *y*-axis, from top to bottom, displays the taxa (TOP 20) ranked by their importance (Mean Decrease Accuracy) for the group classification. **(B)** Venn analysis was performed to screen differential fecal microbiota through LEfSe and random forest model. The overlapping part of the Venn diagram represents the number of differential fecal microbiota in common between groups, and statistical analysis was performed on the relative abundances of the twelve differential bacterial families between groups and significantly different in terms of abundance by the Student's *t*-test (N = 4). The asterisks indicate statistically significant differences and correspond to $p < 0.05$ (*) and $p < 0.001$ (***). **(C)** Pearson correlation analysis between the differential fecal microbiota and tibia-related parameters of broiler chickens with TD. The asterisks indicate statistically significant differences and correspond to $p < 0.05$ (*), $p < 0.01$ (**), and $p < 0.001$ (***). A *p*-value higher than 0.05 (>0.05) represents not statistically significant.

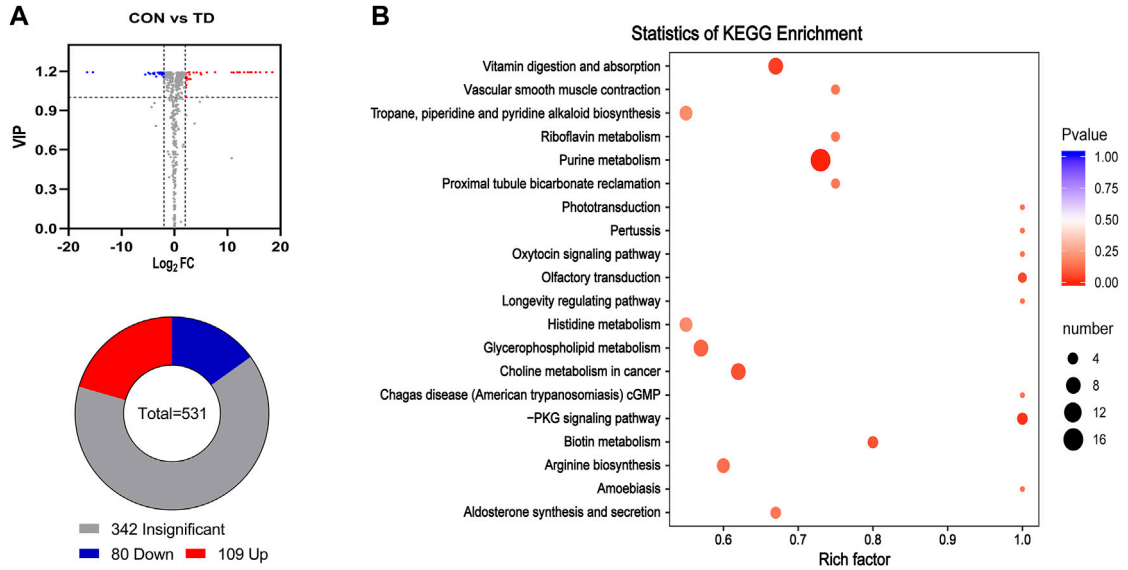

FIGURE 5 | Differential metabolites in feces of broiler chickens with TD. **(A)** Volcano plot analysis of fecal metabolites. Some significantly differential metabolites were selected out by using the criteria of FC ≧2 or FC ≦ 0.5 and VIP≧1 in the volcano plot. Significantly differential metabolites were shown as a red (up) or blue (down) dot, whereas a gray dot represented non-significant difference of metabolites. The number of differential metabolites is shown using a pie chart. **(B)** Potential metabolic pathways analysis based on significantly differential metabolites in feces from the CON and TD group chickens. The bubble size indicates the number of significant differential metabolites enriched in this pathway, and the point with the different gradation of color (from red to blue) represents the scope of *p*-value. The bigger size of each circle indicates a higher degree of enrichment, and the lower *p*-value represents a more significant degree of enrichment.

0.028), *Ruminococcus* ($p = 0.032$), *RF39* ($p = 0.016$), *Oscillospira* ($p = 0.028$), *Ochrobactrum* ($p = 0.043$), *and Sediminibacterium* ($p < 0.001$) in the TD group were clearly lower than those in the CON group, while the abundances of Enterobacteriaceae ($p = 0.206$) *and Klebsiella* ($p = 0.178$) in the TD group were increased compared with the CON group (**Figure 4B**). Next, the results of Pearson correlation analysis revealed that the tibia growth plate width and its index were correlated with Clostridiales (r = −0.728 and −0.736; $p = 0.040$ and 0.037, respectively) [*Ruminococcus*] (r = −0.710 and −0.717; $p = 0.048$ and 0.045, respectively), *Sediminibacterium* (r = −0.913 and −0.917; $p = 0.002$ and 0.001, respectively), *Ochrobactrum* (r = −0.813 and −0.811; $p = 0.014$ and 0.015, respectively) as shown in **Figure 4C**. In addition, tibia-related indicators were positively correlated with *Sediminibacterium* (r = 0.689, 0.742 and 0.605; $p = 0.059$, 0.035 and 0.112, respectively), and negatively correlated with Enterobacteriaceae (r = −0.799, −0.634 and −0.743; $p = 0.017$, 0.091 and 0.035, respectively) *and Klebsiella* (r = −0.806, −0.461 and −0.846; $p = 0.016$, 0.250 and 0.008, respectively) (**Figure 4C**). These results indicated that tibial growth and tibia growth plate quality are closely related to the differential faecal microbiota of TD broiler chickens.

Analysis of Fecal Differential Metabolites of TD Broiler Chickens

The gut microbiota identified by 16S rRNA gene sequencing can only reach the genus level and has limitations as a potential biomarker, but metabolites derived from differential faecal microbiota become the optative choice (Kim et al., 2020). Next, to explore the composition of fecal metabolites, metabolomic analysis of the faecal samples was performed using UPLC-MS/MS. The results showed that a total of 531 metabolites were identified between the CON and TD groups (see **Supplementary Material S4**). PCA analysis revealed that the three biological replicates from the two groups clustered together in different regions, indicating significant differences in metabolism between the two groups (see **Supplementary Figure S1A**). Additionally, the supervised OPLS-DA method was performed to assess the faecal samples. The OPLS-DA score plot showed a clear separation with high reliability using the permutation test (Q2Y = 0.998) between the CON and TD groups (see **Supplementary Figure S1B**). The differential metabolites of the comparison groups were screened by combining the criteria of fold-change ≥ 2 or ≤0.5 and VIP value ≥1 of the metabolites. The results presented a total of 189 differentially produced metabolites, including 80 downregulated and 109 upregulated, as illustrated in the Volcano plot and Pie chart (**Figure 5A**, see **Supplementary Material S5**). Meanwhile, these differential metabolites between the two groups were mapped to the KEGG database for functional clustering analysis, and the results showed that the differentially expressed metabolites were mainly enriched in purine metabolism, vitamin digestion and absorption, glycerophospholipid metabolism, cGMP-PKG signaling pathway, biotin metabolism, etc. (**Figure 5B**).

The difference analysis was used for comparisons of differential metabolites and the log2 fold change (log2FC ≥ 2.5 or ≤ −2.5) represented the comparison against the reference group based on OPLS-DA (**Figure 6A**). Compared with the CON group, the differential metabolites with the highest abundance in the TD groups were the thiamine (log2FC = 18.46), N-alpha-acetyl-L-asparagine (log2FC = 17.31),

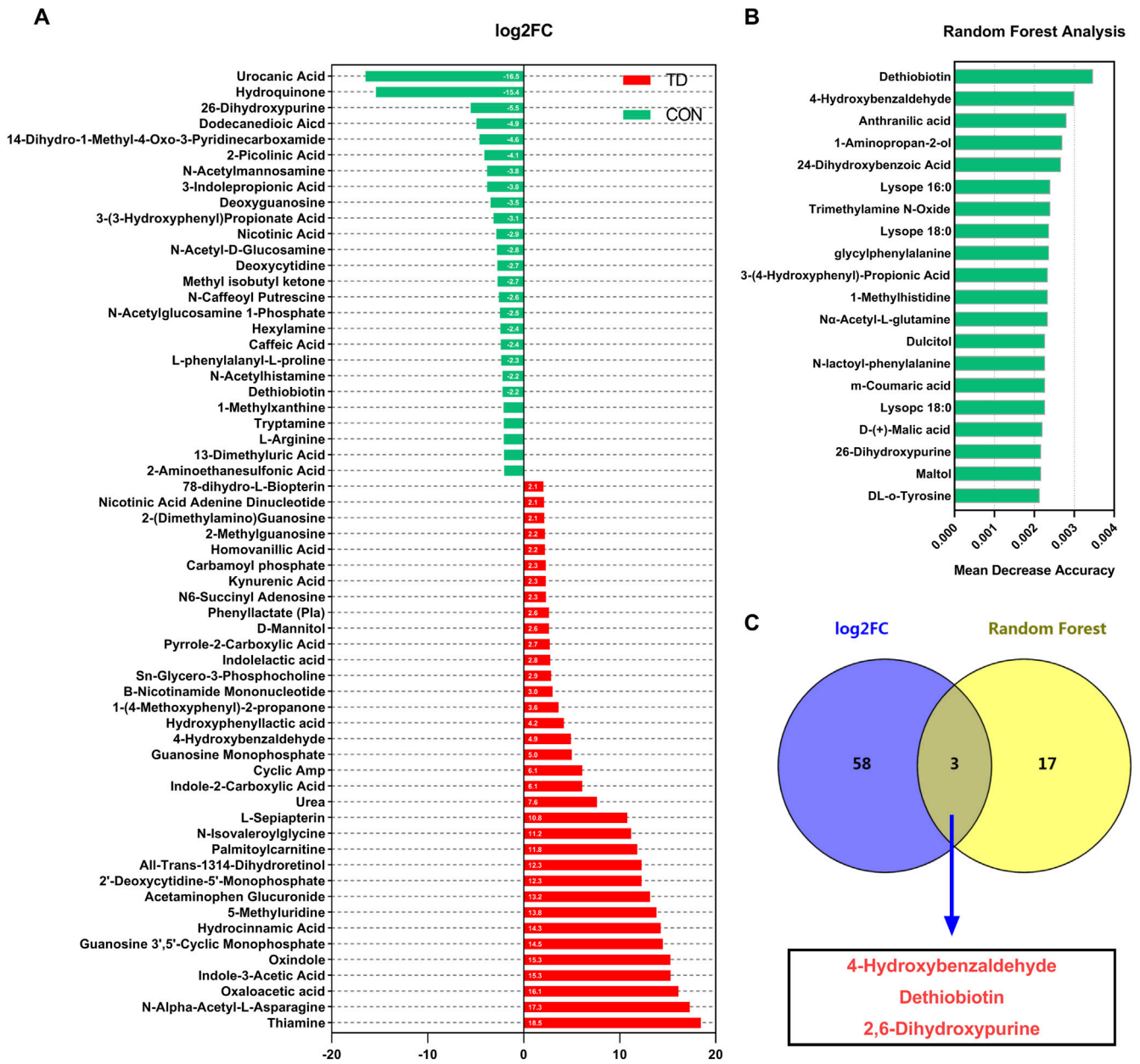

FIGURE 6 | Screening of differential metabolites in feces of broiler chickens. **(A)** Visualization of log2-transformed read counts of differentially metabolites in feces between the CON and TD groups ($|\log2(FC)| \geq 2.5$ and $p < 0.05$, FC stands for fold-change, N = 4). **(B)** Random forest analysis of differential metabolites in feces of broilers in the CON and TD groups. The *y*-axis, from top to bottom, displays the taxa (TOP 20) ranked by their importance (Mean Decrease Accuracy) for the group classification **(C)** Venn analysis was performed to screen differential fecal metabolites through log2FC and random forest model. The overlapping part of the Venn diagram represents the number of differential fecal microbiota in common between groups.

oxaloacetic acid (log2FC = 16.12), indole-3-acetic acid (log2FC = 15.31), oxindole (log2FC = 15.28), guanosine 3′,5′-cyclic monophosphate (log2FC = 14.50), hydrocinnamic acid (log2FC = 14.27), 5-methyluridine (log2FC = 13.84), acetaminophen glucuronide (log2FC = 13.17) and 2′-deoxycytidine-5′-monophosphate (log2FC = 12.27), while the content of urocanic acid, hydroquinone, 2,6-dihydroxypurine and dodecanedioic acid were lower (**Figure 6A**). These results indicated that the fecal metabolites of broilers with TD were significantly fluctuated. Then, the top 20 important metabolites were screened using random forest analysis, including the dethiobiotin, 4-hydroxybenzaldehyde, anthranilic acid, 1-aminopropan-2-ol, 2, 4-dihydroxybenzoic acid, lysope (16: 0), trimethylamine N-Oxide, lysope (18: 0), glycylphenylalanine, 3-(4-hydroxyphenyl)-propionic acid, 1-methylhistidine, Nα-acetyl-L-glutamine, dulcitol, N-lactoyl-phenylalanine, M-coumaric

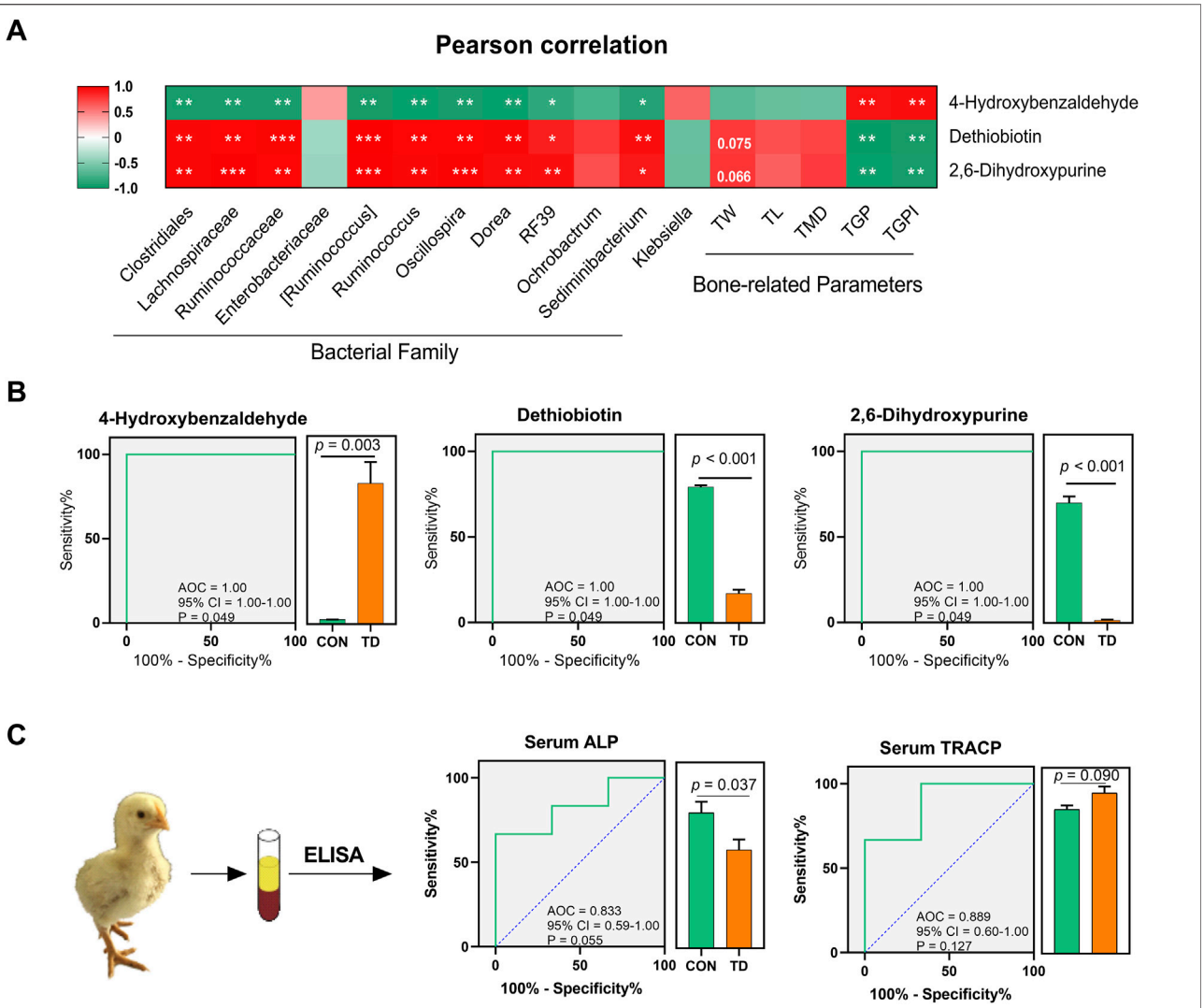

FIGURE 7 | Fecal metabolite biomarkers for the diagnosis of TD broiler chickens. **(A)** Pearson correlation analysis between the differential microbiota and metabolites, differential metabolites and tibia-related parameters in feces of broiler chickens with TD. The asterisks indicate statistically significant differences and correspond to $p < 0.05$ (*), $p < 0.01$ (**), and $p < 0.001$ (***). A p-value higher than 0.05 (>0.05) represents statistically non-significant (N = 4). **(B)** Curves of ROC of differential metabolite biomarkers for diagnosis of TD in an independent test set. An AUC close to 1.0 indicates high sensitivity and specificity and statistical analysis was performed on the relative abundances of the three differential metabolites between groups by the Student's t-test, a p-value < 0.05 was considered to be significant (N = 4). **(C)** ROC curve of serum ALP and TRACP for diagnosis of TD (N = 3).

acid, lysopc (18: 0), D-(+)-malic acid, 2, 6-dihydroxypurine, daltol, DL-o-tyrosine, N-acetyl-L-tyrosine and biopterin (**Figure 6B**). Moreover, Venn diagram analysis of OPLS-DA (identified 61 characteristic metabolites (log2FC ≥ 2.5 or ≤ -2.5)) and random forest analysis (the top 20 important metabolites) showed that three potential biomarkers were screened, including 4-Hydroxybenzaldehyde, Dethiobiotin, and 2,6-Dihydroxypurine (**Figure 6C**).

Predictive Ability of Fecal Metabolites for TD Broiler Chickens

Pearson analysis was performed to unveil the correlations between the abundance of 12 differential fecal microbiota, three differential fecal metabolites, and tibia-related parameters in the host (**Figure 7A**). The results revealed that dethiobiotin and 2,6-dihydroxypurine were positively correlated with the relative abundances of several important bacterial genera, including the Clostridiales, Lachnospiraceae, Ruminococcaceae [*Ruminococcus*], *Dorea*, *Ruminococcus*, *RF39*, *Oscillospira*, and *Sediminibacterium*. However, 4-hydroxybenzaldehyde was negatively correlated with these important bacterial genus (**Figure 7A**). More interestingly, the damage indexes (TGP and TGPI) of the tibial growth plate of TD broilers were negatively correlated with the differential metabolites dethiobiotin and 2,6-dihydroxypurine, whereas the damage indexes of the tibial growth plate were positively correlated with 4-hydroxybenzaldehyde (**Figure 7A**).

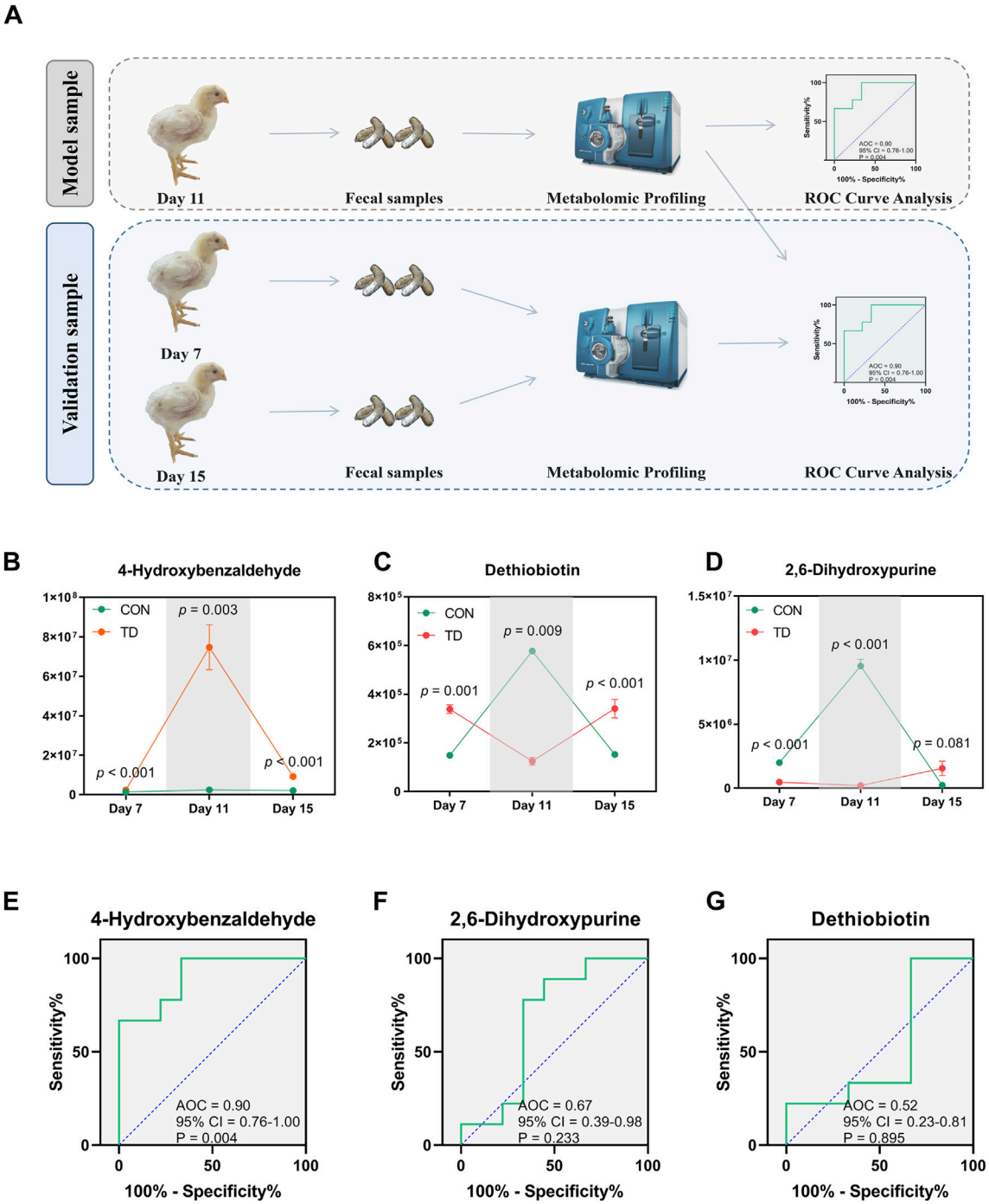

FIGURE 8 | Validation and evaluation of the predictive power of the three metabolites. **(A)** Design of verification experimental approach. **(B–D)** Statistical analysis was performed on the relative abundances of the three differential metabolites between groups by the Student's *t*-test, a *p*-value < 0.05 was considered to be significant (N = 4). **(E–G)** Curves of ROC of differential metabolite biomarkers for diagnosis of TD during the entire trial. An AUC close to 1.0 indicates high sensitivity and specificity, a *p*-value < 0.05 was considered to be significant (N = 4).

These results indicated that damage to the tibia growth plate in TD broilers is associated with changes in differential metabolites, which is also closely related to the gut-microbiota in feces.

Receiver operating characteristic (ROC) curve analysis was performed to evaluate the predictive ability and diagnostic performance of differential fecal metabolites in distinguishing TD from normal broiler chickens. Three metabolites with higher

importance scores among the differential fecal metabolites, namely 4-hydroxybenzaldehyde, dethiobiotin, and 2,6-dihydroxypurine, were screened and their ROC analysis showed high values of sensitivity, specificity and the area under the curve (AUC) (AUC = 1, $p = 0.049$; **Figure 7B**).

Serum ALP and TRACP are important indicators for the assessment of normal bone function. Serum ALP secreted by osteoblast has been extensively studied as a biomarker of bone disease, which is essential for osteoid formation and mineralization. TRACP secreted by osteoclasts is a sensitive index of bone resorption, and its activity correlates with resorptive activity in bone diseases (Li et al., 2010). ROC curves of bone funtion biomarkers are shown in **Figure 7C**, the AUCs of the serum ALP and TRACP were 0.83 and 0.89, respectively; these serum biomarkers can distinguish the TD from normal broilers, which is lower than the predictive ability of the differentially fecal metabolites. To further validate the predictive ability of these three biomarkers, we sequenced the feces from normal and TD broilers on days 7 and 15 based on metabolomics (**Figure 8A**). Verification and evaluation of the predictive ability in the three potential biomarkers were assessed based on ROC curve analysis, the results showed that the abundance of 4-hydroxybenzaldehyde, dethiobiotin, and 2,6-dihydroxypurine were significantly different ($p < 0.05$; **Figures 8B–D**) and their AUCs were 0.90 (95% CI = 0.76–1.00; $p = 0.004$), 0.52 (95% CI = 0.23–0.81; $p = 0.895$), and 0.67 (95% CI = 0.39–0.98; $p = 0.233$) during the entire trial, respectively (**Figures 8E–G**). These results indicated that differential fecal metabolites, especially 4-hydroxybenzaldehyde, which is closely related to differential gut-microbiota, could be used as a valuable biomarker for the assessment and diagnosis of broiler chickens with TD.

DISCUSSION

In this study, we investigated the faecal gut microbiome structure and composition of normal and TD broilers as well as the changes of fecal metabolites by metabonomics, and further analyzed for correlation with tibiae and their growth plate-related indexes. The results indicated significant differences in the overall structure and composition of fecal microbiota between the two groups. The proportion of the phyla Firmicutes and Tenericutes in the TD broilers was lower than that in the normal broilers. Furthermore, broiler chickens with TD are characterized by enriched *Klebsiella*, and depleted genera *[Ruminococcus], Dorea, Ruminococcus, Oscillospira, Ochrobactrum, and Sediminibacterium,* as well as disturbances of fecal purine metabolism, vitamin metabolism, and amino acid metabolism. Interestingly, the abundance of [*Ruminococcus*], *Sediminibacterium, and Ochrobactrum* was negatively correlated with tibia growth plate width and tibia-related parameters. Tibia related-parameters were positively correlatied with *Sediminibacterium,* whereas negatively correlated with *Klebsiella,* which provides information on abnormal growth and development of tibias and their growth plates in TD broilers associated with changes in the gut microbiota affecting the metabolism of fecal metabolites. We further screened three fecal differential metabolites closely associated with the differential microbiota and tibia related-indicators based on log2FC and random forest analysis for ROC analysis, which were highly specificity and superior to serum bone markers. Furthermore, verification and evaluation of the predictive ability of the three potential biomarkers during the entire trial found that the AUC of 4-Hydroxybenzaldehyde was 0.90. Therefore, our findings indicated that gut microbiota disturbances or dysbiosis could potentially contribute to TD pathogenesis by modulating abnormal production of fecal metabolism, and fecal metabolite 4-Hydroxybenzaldehyde as a biomarker may be valuable for the assessment and diagnosis of broiler chickens with TD.

Broiler chickens are a poultry breed that is very susceptible to stress due to the genetic selection of broilers for rapid growth and increased breast yields. Therefore, some invasive diagnostic methods are not certainly the best choice in broilers, especially for diagnosing the TD broilers accompanied with sub-clinical symptoms. There is growing evidence that biomarker discovery is a key target for many microbiome and metabolome studies as they implicate potentials for developing sensitive, non-invasive, and scalable early diagnosis (Tsoukalas et al., 2021; Zhu et al., 2021). Moreover, abnormal bone development or pathological bone loss is closely associated with alterations in microbiota composition (Castaneda et al., 2020; Lu et al., 2021). In the present study, we noted that the width of the tibial growth plate, mainly contributed by TD broilers, accounted for the largest proportion of all bone phenotypes. The most significant changes in all bone phenotypes occurred on days 11 and 15 using morphological observation and Sankey diagram analysis. Accordingly, the feces of TD broilers on day 11 were more representative for subsequent biomarker screening.

The richness and diversity of the intestinal bacterial species are essential elements of the animal intestinal microbiome (McKinney et al., 2020). In the current study, the alpha diversity of the faecal microbial community was found to be significantly lower in the TD group than in the CON group by faecal microbiome sequencing. Moreover, the structure and composition of the faecal microbiome of the TD and CON groups were markedly different, indicating the presence of gut microbial dysbiosis in TD broilers (Zhu et al., 2021). Previous studies have revealed that gut microbiota homeostasis is among the most important factors for the host to resist the invasion of pathogenic bacteria and perform various biological functions. Conversely, dysbacteriosis has emerged as a hidden risk factor that can generate bioactive metabolites, enzymes, or small molecules that affect host physiology and pose a great threat to host health (Biver et al., 2019; Wang et al., 2019; Meng et al., 2020). Although the gut microbiota changes dynamically, significant alterations in the microbial community can cause dysbacteriosis and affect intestinal barrier function (Liu et al., 2020). In addition, gut-derived bacterial metabolites can penetrate through the gut into the bloodstream disrupting the bioenergetic machinery of host cells, which provides an essential pathway for the gut microbiota to regulate anatomically distant organs (Lu et al., 2021; Tomasova et al., 2021). Therefore, the effect of changes in microbiome structure and composition on bone physiological functions has gradually attracted attention (Chen et al., 2017; Castaneda et al., 2020; Hao et al., 2021; Ling et al., 2021).

In the this study, the category of predominant phyla in the faecal microbiome of broiler chickens were Firmicutes, Proteobacteria, and Tenericutes, which are different from mammals and humans and indicate a special gut microbiota in broilers (Sánchez-Alcoholado et al., 2020; Zhang et al., 2020). Among them, Firmicutes is mainly composed of Gram-positive bacteria, such as *Lactococcus* and *Lactobacillus, etc.,* most of which are considered to be beneficial bacteria that contribute to maintain the balance of gut microbiota and prevent pathogenic invasion (Garneau et al., 2008). More meaningful for us is that we noticed a relatively low proportion of the phyla Firmicutes and Tenericutes in TD broilers compared with the normal broilers. Moreover, TD broiler chickens were characterized by enriched genus *Klebsiella*, and depleted the genera [*Ruminococcus*], *Dorea, Ruminococcus, Oscillospira, Ochrobactrum, and Sediminibacterium,* as well as disturbances of fecal purne, vitamin, and amino acid metabolism. The Gram-negative *bacillus* of the genus *Klebsiella* is widely distributed in the gastrointestinal tract and respiratory tract, which may result in organ inflammation, and even the septicemia (Fendukly et al., 2003).

In contrast, the genus *Ruminococcus* can effectively decompose and ferment the cellulose, hemicellulose, and polysaccharides in foods into acetate and succinate (La Reau and Suen, 2018), and *Ochrobactrum* strains can indirectly influence the propionic acid decomposition through the production of vitamin B12, which plays a crucial role in maintaining the functionality and morphology of intestinal epithelial cells, regulating systemic bone mass and preventing pathological bone loss (Watson et al., 2016; Wang et al., 2017; Lucas et al., 2018; Zimmermann et al., 2019). A recent publication has highlighted that lower enrichment of Ruminococcaceae was negatively correlated with the presence of osteoporosis, which is consistent with our findings and provides strong evidence for an association between gut microbiota and bone in humans (Ling et al., 2021). In addition, the genus *Sediminibacterium* has been reported to be closely associated with fat deposition in chickens (Kong et al., 2020). The decrease of these genera in TD broilers will inevitably affect the normal function of the intestinal tract and the production of SCFAs, which may potentially contribute to the pathogenesis of TD. More interestingly, the abundance of [*Ruminococcus*], *Sediminibacterium,* and *Ochrobactrum* was negatively correlated with the width of the tibia growth plate and its index TGPI. Tibia related-parameters were positively correlated with *Sediminibacterium* and negatively correlated with *Klebsiella,* which further provides evidence that abnormal growth and development of the tibiae and their growth plates in TD broiler chickens are associated with changes in the gut microbiota and affect the metabolism of fecal metabolites.

The results demonstrated that the metabolites of TD broilers are different from those of normal broilers, especially amino acid metabolomics, organic acid derivatives, indole derivatives, vitamins, and carbohydrate metabolomics. Previous studies have shown that gut metabolites affect the balance of intestinal microecology and regulate anatomically distant biological effects by penetrating from the intestine into the bloodstream (Lu et al., 2021; Tomasova et al., 2021). Indole derivatives were first described as one of the microbiota-derived metabolites that contribute to intestinal homeostasis in humans and animals by modulating the immune function of the host (Schiering et al., 2017; Xiao et al., 2020). The previous studies have described the skeletal effect of SCFAs, as key regulatory metabolites produced by the gut microbiota, showing that butyrate promotes mineralized nodule formation and osteoprotegerin expression (Katono et al., 2008; Lu et al., 2021). Next, 189 fecal differential metabolites, mainly enriched in purine metabolism, vitamin metabolism and amino acid metabolism, etc., were screened and closely correlated with the differential gut microbiota and tibia-related indicators. In birds, uric acid, a purine compound, serves as the end product of nitrogen catabolism originating from the microbes, is rapidly cleared from the blood by the kidneys. Purines have been shown to be involved in continuous bone remodeling by bone cells, allowing the skeleton to grow and repair itself, which is achieved in a balance of osteoclasts and osteoblasts, eventually purine metabolism likely contributing to dynamic bone homeostasis (Schwartz, 1978; Stentoft et al., 2015; Zuccarini et al., 2021). Studies on the vitamin metabolism affecting bone growth and development mainly focused on vitamin D, which is associated with osteoporosis (Binkley, 2012). Besides, vitamin B, such as thiamine, folate (vitamin B9), and cobalamin (vitamin B12), are also associated with bone metabolism and bone quality, and contribute to fracture risk by affecting homocysteine/folate metabolism (Ahn et al., 2020). An emerging report through fecal and serum metabolomics analyses also implies that amino acid metabolism is clearly associated with the identified microbial biomarkers and osteoporosis, respectively (Ling et al., 2021). Therefore, these enriched metabolisms are closely related to bone homeostasis, and the occurrence of TD in broilers may be associated with metabolite changes in related pathways. The detection of relevant differential metabolites may be a biomarker for early diagnosis or prediction of TD in broilers.

ROC curves are currently used as a fundamental tool for medical diagnostics (Zheng et al., 2019; Wang et al., 2020), and are rarely used in veterinary medicine. Here, we selected the three fecal metabolites based on the log2FC and the random forest analysis, and the isolated metabolic markers could robustly distinguish TD broilers from normal broilers. Furthermore, the separate metabolic markers showed extremely high specificity in TD broilers, better than serum bone markers, including serum ALP and TRACP. Further validation revealed that 4-hydroxybenzaldehyde was significantly increased in TD broilers and had a higher specificity throughout the broilers suffering from TD. These findings suggested that separate fecal metabolic biomarker has a non-invasive diagnostic potential for TD.

Despite many novel insights, our study has certain limitations. First, our study results cannot conclusively determine the causal relationship between the imbalance of faecal microbial community and TD, and the causal contribution of the gut microbiota and its corresponding metabolites to TD. Therefore, a multitude of more direct experimental evidence is needed for further verification, such as gut microbiota transplantation study, intervention study of differential metabolites, etc. (Witkowski et al., 2020). In addition, further animal experiments are needed to explore how the interactions between microbial species and metabolites, specific gut

microbiota-dependent regulatory pathways, and downstream differential metabolites may affect TD pathogenesis. The 16S rRNA sequencing technology has relatively limitations in this study. Therefore, further experiments will use larger cohorts and integrated data of different levels to analyze the taxonomy, composition, pathways, and functions of gut microbiome in TD broiler chickens using a high-resolution shotgun metagenomic data sequencing approach. On these foundations, robust microbial biomarkers were established to diagnose TD in broiler chickens. Furthermore, it is important to collect more clinical faecal samples from nature TD broilers to screen the differential gut microbiota and fecal metabolites and verify our existing findings. Notably, the fecal sample sampling process is susceptible to interference from other factors and therefore requires a high level of fecal sample collection process. These are crucial to optimize biomarkers and to evaluate the sensitivity and accuracy of predicting the occurrence of TD in chickens.

In conclusion, we summarized the characteristics and interaction analysis of altered tibia related-parameters and their growth plate morphology, faecal microbiota, and metabolites in TD broilers by using multi-omics data. We found that the dysbiosis of the gut microbiota may participate in the pathogenesis of TD by regulating the host's fecal metabolism. Moreover, we identified 4-hydroxybenzaldehyde as a key biomarker to distinguish TD broilers from normal broilers and to assess the severity of boiler chickens suffering from TD. Our findings may provide a new potential path for understanding the pathogenesis of TD, and it is possible to develop a non-invasive and non-stress tool for early diagnosis of broiler TD.

MATERIALS AND METHODS

Animals

A total of 180 one-day-old healthy Arbor Acres (AA) broilers were purchased from an intensive commercial broiler farm located in Kaifeng City (Henan, China). They were housed in cages in the livestock laboratory of the Henan Agricultural University (Henan, China). The chickens were reared and performed according to the standard AA broiler management manual as previously described (Huang et al., 2018).

All animal experiments and procedures were performed in strict accordance with the guidance of the Animal Care and Use Committee of Henan Agricultural University and the Care and Use of Laboratory Animals of the College of Veterinary Medicine (approved no: 17–0126), none of the chickens exhibited signs of distress before their death during the experiment. Besides, all the possible measures were carried out to ensure the welfare of the broiler chickens.

TD Establishment

All broilers were allowed to adapt to the environment before the further experiment. Broilers were randomly divided into two separate groups: 15 chicks per cage, total four replicates per group. The grouping of the chickens was as: the control group (CON) and the thiram-induced TD chicken group (TD; the addition of 100 mg/kg of thiram from day 4 to day 7, then followed by feeding with a normal diet until the end of the experiment). All experiments lasted for 15 days, with *ad libitum* provision of feed and water.

Sample Collection

Ten broilers were randomly selected from each group for weighing on days 7, 11 and 15 of the experiment, respectively. Blood samples were obtained from the wing vein using heparinized syringes and the serum sample was centrifugated at 3,000 rpm for 10 min at 4°C and stored at −20°C.

Chicks were sacrificed by cervical dislocation in the CON and TD groups. Then, tibia specimens were retrieved for measurement of tibia-related parameters, and the growth plate was stripped from the articular cartilage of the proximal tibia using a surgical knife for morphological analysis of the tibial growth plate as in our previous studies (Huang et al., 2017; Huang et al., 2018). Furthermore, faecal samples were collected from the chickens of both groups on days 7, 11, and 15 to analyze the microbiome and metabolome. The sterile cotton swabs were used to take the upper half of freshly removed chicken feces (within 5 min) in a 2 ml sterile eppendrof (EP) tube, mixed and stored at −80°C. To reduce the difference in sampling time, the first group was sampled in turn until the last group was sampled. We mixed the faeces of 4–6 different broilers into one faecal sample and used four mixed faecal samples per group for subsequent 16S rRNA sequencing and metabolomic analyses to reduce sampling error.

Measurement of Tibial Parameters

All tibial specimens from chinkens were collected to analyze the weight (g), length (mm), mean diameter (mm) and growth plate width (mm) of the tibia. These bone histomorphometry parameters were determined by an electronic balance sensitive to 0.001 g (#FA1204N; Jinghai Instrument Co., Ltd. Shanghai, China) and Digital Calipers (#SATA91511; TATA Company, Shanghai, China), respectively. In addition, the tibia growth plate index (TGPI, mm/mm) was determined as the width of the tibia growth plate in the broiler. Tibia mean diameter was calculated as the average of the TUD (upper 1/2 diameter of the tibia), TMD (tibia mid-diameter), and TLD (lower 1/2 diameter of the tibia) (**Figure 1A**).

Analysis of Serum Biochemical Parameters

To determine the levels of calcium (Ca) and phosphorus (P) in serum samples from the CON and TD groups, the electrolyte indicators were quantified by a veterinary reagent tray (Chengdu Puli Taisheng Technology Co., Ltd, Chengdu, China). Quantitative assays were performed with a portable, fully automated veterinary biochemistry analyzer (#SMT-120 V; Seamaty Technology Co., Ltd, Chengdu, China).

Quantification of TRACP and ALP in Serum

Serum concentrations of alkaline phosphatase (ALP) and tartrate-resistant acid phosphatase (TRACP) were measured by an enzyme-linked immunosorbent assay (ELISA) kit (Nanjing Jiancheng Biotechnology Co. Ltd, Nanjing, China) according to the manufacturer's instructions. The optical density values of

each well were determined within 15 min at a wavelength of 450 nm using microplate reader (Model: 30086376 Spark, Tecan Group Ltd, Mannedorf, Switzerland).

Analysis of 16S rRNA Gene Sequencing

According to the manufacturer's instructions, faecal microbial genome DNA was extracted using a QIAamp DNA tool mini kit (Qiagen, Hilden, Germany). The V3 and V4 hypervariable regions of the bacterial 16S rRNA were PCR-amplified using bacterial primers 338 (forward: 5′-ACTCCTACGGGAGGCAGCA-3′) and 806 (reverse: 5′-GGACTACHVGGGTWTCTAAT-3′). The amplicons were purified and quantified using Agencourt AMPure Beads and the PicoGreen dsDNA Assay Kit (Invitrogen, Carlsbad, CA, United States), respectively. TheDNA libraries were constructed and then sequencing was performed on an Illumina Miseq 250 platform (Illumina Inc. San Diego, CA, United States) according to the standard protocols by Shanghai Personalbio Technology Co., Ltd, China. Raw Illumina read data for all samples were deposited in the NCBI Sequence Read Archive with the accession code PRJNA755075.

As previously described, the bioinformatics analysis procedure of raw reads was performed (Kong et al., 2020). The bacterial community was compared with their beta diversity using the distance matrices generated from the principal component analysis (PCA) and partial least squares discriminant analysis (PLS-DA). The key bacterial taxa responsible for discrimination between the two groups were identified using linear discriminant analysis (LEfSe) with linear discriminant analysis (LDA) score >2.0 based on the Galaxy online analysis platform (http://huttenhower.sph.harvard.edu/galaxy/). The random forest classifier was performed by 10-fold cross-validation to predict the discrimination between the CON and TD groups in broilers.

Analysis of Widely Targeted Metabolomics

Metabolomic analysis was conducted by a commercial service company (Wuhan Metware Biotechnology Co., Ltd, Wuhan, China) following previously reported methods (Huang et al., 2021). Briefly, 50 mg faecal samples were processed with 1,000 μL methanol/water (ice-cold, 70%, v/v) and 5 μl 2-chlorophenylalanine (1 μg/ml). Two pre-cooled sterile steel balls were added to the sample mixture at −20°C for 2 min and homogenized at 30 Hz for 3 min. The sample mixture was centrifuged at 12,000 g for 10 min at 4°C. The supernatant was collected and filtered through a 0.22 μm filter membrane, and quality control (QC) analysis of samples was performed before UPLC-MS/MS analysis (see **Supplementary Material S2**).

All data analyses were based on the self-built MWDB database (Metware Biotechnology Co., Ltd. Wuhan, China). PCA analysis and orthogonal partial least squares discriminant analysis (OPLS-DA) were performed for the identified metabolites. UPLC-MS/MS analyses were performed, and differentially accumulated metabolites with fold change (FC) ≥ 2 or ≤0.5 and variable importance in project (VIP) ≥ 1 were used as criteria for screening potential biomarkers. In addition, KEGG annotation and enrichment analysis were performed according to our previously described methods [64].

Statistical Analysis

GraphPad Prism version 8 (GraphPad Software, La Jolla, CA, United States) was used to perform statistical analysis and drawing. All data are presented as the means ± SD. Comparisons between groups were conducted using two tailed unpaired student's *t*-test. Correlations between the altered gut microbes, significantly different faecal metabolites, and tibia related-indexes (e.g., tibia weight, tibia length, tibia diameter and tibia growth plate width) in the CON and TD groups were analyzed by Pearson correlation test and meanwhile visualized by using GraphPad Prism software. Receiver operating characteristic (ROC) curve analysis obtained (GraphPad Prism V.8) for the display of the constructed models, then the area under the ROC curve (AUC) was used to designate the ROC effect. $p < 0.05$ was considered to significant.

DATA AVAILABILITY STATEMENT

The data presented in the study are deposited in the National Center for Biotechnology Information (NCBI) repository, accession number PRJNA755075.

ETHICS STATEMENT

The animal study was reviewed and approved by The Animal Care and Use Committee of Henan Agricultural University.

AUTHOR CONTRIBUTIONS

SCH: Conceptualization, Supervision, Resources, Writing—review and editing. YFH: Data curation, Formal analysis, Writing—original draft. QQC: Data curation, Methodology, Investigation. PC, LXL, KY, CDZ, and TTX: Methodology, Data curation, and Investigation. AS and XT: Formal analysis, Writing—review andamp; editing.

FUNDING

This study was supported by the Postdoctoral Science Foundation of China (No. 2020M672234), the Outstanding Talents of Henan Agricultural University (No.30500421), and Key Scientific Research Project of Henan Higher Education Institutions of China (No. 21A230013).

SUPPLEMENTARY MATERIAL

The Supplementary Material for this article can be found online at: https://www.frontiersin.org/articles/10.3389/fphys.2022.887207/full#supplementary-material

REFERENCES

Ahn, T.-K., Kim, J. O., An, H. J., Park, H. S., Choi, U. Y., Sohn, S., et al. (2020). 3'-UTR Polymorphisms of Vitamin B-Related Genes Are Associated with Osteoporosis and Osteoporotic Vertebral Compression Fractures (OVCFs) in Postmenopausal Women. *Genes* 11, 612. doi:10.3390/genes11060612

Almeida Paz, I., Garcia, R., Bernardi, R., Nääs, I., Caldara, F., Freitas, L., et al. (2010). Selecting Appropriate Bedding to Reduce Locomotion Problems in Broilers. *Rev. Bras. Cienc. Avic.* 12, 189–195. doi:10.1590/S1516-635X2010000300008

Binkley, N. (2012). Vitamin D and Osteoporosis-Related Fracture. *Archives Biochem. Biophysics* 523, 115–122. doi:10.1016/j.abb.2012.02.004

Biver, E., Berenbaum, F., Valdes, A. M., Araujo de Carvalho, I., Bindels, L. B., Brandi, M. L., et al. (2019). Gut Microbiota and Osteoarthritis Management: An Expert Consensus of the European Society for Clinical and Economic Aspects of Osteoporosis, Osteoarthritis and Musculoskeletal Diseases (ESCEO). *Ageing Res. Rev.* 55, 100946. doi:10.1016/j.arr.2019.100946

Castaneda, M., Strong, J. M., Alabi, D. A., and Hernandez, C. J. (2020). The Gut Microbiome and Bone Strength. *Curr. Osteoporos. Rep.* 18, 677–683. doi:10.1007/s11914-020-00627-x

Chen, Y.-C., Greenbaum, J., Shen, H., and Deng, H.-W. (2017). Association between Gut Microbiota and Bone Health: Potential Mechanisms and Prospective. *J. Clin. Endocrinol. Metab.* 102, 3635–3646. doi:10.1210/jc.2017-00513

Chen, F., Chen, Z., Chen, M., Chen, G., Huang, Q., Yang, X., et al. (2021). Reduced Stress-Associated FKBP5 DNA Methylation Together with Gut Microbiota Dysbiosis Is Linked with the Progression of Obese PCOS Patients. *npj Biofilms Microbiomes* 7, 60. doi:10.1038/s41522-021-00231-6

Derakhshanfar, A., Kheirandish, R., Alidadi, S., and Bidadkosh, A. (2013). Study of Long Effects of Administration of Aspirin (Acetylsalicylic Acid) on Bone in Broiler Chickens. *Comp. Clin. Pathol.* 22, 1201–1204. doi:10.1007/s00580-012-1550-2

Di Stefano, M., Veneto, G., Malservisi, S., and Corazza, G. R. (2001). Small Intestine Bacterial Overgrowth and Metabolic Bone Disease. *Dig. Dis. Sci.* 46, 1077–1082. doi:10.1023/a:1010722314493

Edwards, H. M., and Veltmann, J. R. (1983). The Role of Calcium and Phosphorus in the Etiology of Tibial Dyschondroplasia in Young Chicks. *J. Nutr.* 113, 1568–1575. doi:10.1093/jn/113.8.1568

Farquharson, C., and Jefferies, D. (2000). Chondrocytes and Longitudinal Bone Growth: the Development of Tibial Dyschondroplasia. *Poult. Sci.* 79, 994–1004. doi:10.1093/PS/79.7.994

Fendukly, F., Karlsson, I., Hanson, H. S., Kronvall, G., and Dornbusch, K. (2003). Patterns of Mutations in Target Genes in Septicemia Isolates of *Escherichia coli* and *Klebsiella pneumoniae* with Resistance or Reduced Susceptibility to Ciprofloxacin. *Apmis* 111, 857–866. doi:10.1034/j.1600-0463.2003.1110904.x

Garneau, J. E., Tremblay, D. M., and Moineau, S. (2008). Characterization of 1706, a Virulent Phage from Lactococcus Lactis with Similarities to Prophages from Other Firmicutes. *Virology* 373, 298–309. doi:10.1016/j.virol.2007.12.002

Genin, O., Hasdai, A., Shinder, D., and Pines, M. (2012). The Effect of Inhibition of Heat-Shock Proteins on Thiram-Induced Tibial Dyschondroplasia. *Poult. Sci.* 91, 1619–1626. doi:10.3382/ps.2012-02207

Groves, P. J., and Muir, W. I. (2017). Earlier Hatching Time Predisposes Cobb Broiler Chickens to Tibial Dyschondroplasia. *Animal* 11, 112–120. doi:10.1017/S1751731116001105

Hao, X., Shang, X., Liu, J., Chi, R., Zhang, J., and Xu, T. (2021). The Gut Microbiota in Osteoarthritis: where Do We Stand and what Can We Do? *Arthritis Res. Ther.* 23, 42. doi:10.1186/s13075-021-02427-9

He, J., Xu, S., Zhang, B., Xiao, C., Chen, Z., Si, F., et al. (2020). Gut Microbiota and Metabolite Alterations Associated with Reduced Bone Mineral Density or Bone Metabolic Indexes in Postmenopausal Osteoporosis. *Aging* 12, 8583–8604. doi:10.18632/aging.103168

HolmesLi, E. J. V., Li, J. V., Marchesi, J. R., and Nicholson, J. K. (2012). Gut Microbiota Composition and Activity in Relation to Host Metabolic Phenotype and Disease Risk. *Cell Metab.* 16, 559–564. doi:10.1016/j.cmet.2012.10.007

Huang, S.-c., Rehman, M. U., Lan, Y.-f., Qiu, G., Zhang, H., Iqbal, M. K., et al. (2017). Tibial Dyschondroplasia Is Highly Associated with Suppression of Tibial Angiogenesis through Regulating the HIF-1α/VEGF/VEGFR Signaling Pathway in Chickens. *Sci. Rep.* 7, 9089. doi:10.1038/s41598-017-09664-6

Huang, S.-c., Zhang, L.-h., Zhang, J.-l., Rehman, M. U., Tong, X.-l., Qiu, G., et al. (2018). Role and Regulation of Growth Plate Vascularization during Coupling with Osteogenesis in Tibial Dyschondroplasia of Chickens. *Sci. Rep.* 8, 3680. doi:10.1038/s41598-018-22109-y

Huang, S., Kong, A., Cao, Q., Tong, Z., and Wang, X. (2019). The Role of Blood Vessels in Broiler Chickens with Tibial Dyschondroplasia. *Poult. Sci.* 98, 6527–6532. doi:10.3382/ps/pez497

Huang, S.-c., Cao, Q.-q., Cao, Y.-b., Yang, Y.-r., Xu, T.-t., Yue, K., et al. (2021). Morinda Officinalis Polysaccharides Improve Meat Quality by Reducing Oxidative Damage in Chickens Suffering from Tibial Dyschondroplasia. *Food Chem.* 344, 128688. doi:10.1016/j.foodchem.2020.128688

Katono, T., Kawato, T., Tanabe, N., Suzuki, N., Iida, T., Morozumi, A., et al. (2008). Sodium Butyrate Stimulates Mineralized Nodule Formation and Osteoprotegerin Expression by Human Osteoblasts. *Archives Oral Biol.* 53, 903–909. doi:10.1016/j.archoralbio.2008.02.016

Kim, M., Vogtmann, E., Ahlquist, D. A., Devens, M. E., Kisiel, J. B., Taylor, W. R., et al. (2020). Fecal Metabolomic Signatures in Colorectal Adenoma Patients Are Associated with Gut Microbiota and Early Events of Colorectal Cancer Pathogenesis. *Mbio* 11, e3119–86. doi:10.1128/mBio.03186-19

Klein, M. S., Newell, C., Bomhof, M. R., Reimer, R. A., Hittel, D. S., Rho, J. M., et al. (2016). Metabolomic Modeling to Monitor Host Responsiveness to Gut Microbiota Manipulation in the BTBRT+tf/j Mouse. *J. Proteome Res.* 15, 1143–1150. doi:10.1021/acs.jproteome.5b01025

Kong, A., Zhang, C., Cao, Y., Cao, Q., Liu, F., Yang, Y., et al. (2020). The Fungicide Thiram Perturbs Gut Microbiota Community and Causes Lipid Metabolism Disorder in Chickens. *Ecotoxicol. Environ. Saf.* 206, 111400. doi:10.1016/j.ecoenv.2020.111400

La Reau, A. J., and Suen, G. (2018). The Ruminococci: Key Symbionts of the Gut Ecosystem. *J. Microbiol.* 56, 199–208. doi:10.1007/s12275-018-8024-4

Leach, R. M., and Monsonego-Ornan, E. (2007). Tibial Dyschondroplasia 40 Years Later. *Poult. Sci.* 86, 2053–2058. doi:10.1093/PS/86.10.2053

Li, C., Jiang, Z., and Liu, X. (2010). Biochemical Mechanism of Gallium on Prevention of Fatal Cage-Layer Osteoporosis. *Biol. Trace Elem. Res.* 134, 195–202. doi:10.1007/s12011-009-8467-x

Ling, C.-w., Miao, Z., Xiao, M.-l., Zhou, H., Jiang, Z., Fu, Y., et al. (2021). The Association of Gut Microbiota with Osteoporosis Is Mediated by Amino Acid Metabolism: Multiomics in a Large Cohort. *J. Clin. Endocrinol. Metab.* 106, e3852–e3864. doi:10.1210/clinem/dgab492

Liu, Z., Li, A., Wang, Y., Iqbal, M., Zheng, A., Zhao, M., et al. (2020). Comparative Analysis of Microbial Community Structure between Healthy and Aeromonas Veronii-Infected Yangtze Finless Porpoise. *Microb. Cell Fact.* 19, 123. doi:10.1186/s12934-020-01383-4

Lu, L., Chen, X., Liu, Y., and Yu, X. (2021). Gut Microbiota and Bone Metabolism. *FASEB J.* 35, e21740. doi:10.1096/fj.202100451R

Lucas, S., Omata, Y., Hofmann, J., Böttcher, M., Iljazovic, A., Sarter, K., et al. (2018). Short-chain Fatty Acids Regulate Systemic Bone Mass and Protect from Pathological Bone Loss. *Nat. Commun.* 9, 55. doi:10.1038/s41467-017-02490-4

McKinney, C. A., Oliveira, B. C. M., Bedenice, D., Paradis, M.-R., Mazan, M., Sage, S., et al. (2020). The Fecal Microbiota of Healthy Donor Horses and Geriatric Recipients Undergoing Fecal Microbial Transplantation for the Treatment of Diarrhea. *Plos One* 15, e0230148. doi:10.1371/journal.pone.0230148

Meng, X., Zhang, G., Cao, H., Yu, D., Fang, X., Vos, W. M., et al. (2020). Gut Dysbacteriosis and Intestinal Disease: Mechanism and Treatment. *J. Appl. Microbiol.* 129, 787–805. doi:10.1111/jam.14661

Murga-Garrido, S. M., Hong, Q., Cross, T.-W. L., Hutchison, E. R., Han, J., Thomas, S. P., et al. (2021). Gut Microbiome Variation Modulates the Effects of Dietary Fiber on Host Metabolism. *Microbiome* 9, 117. doi:10.1186/s40168-021-01061-6

Pan, R., Zhang, X., Gao, J., Yi, W., Wei, Q., and Su, H. (2020). Analysis of the Diversity of Intestinal Microbiome and its Potential Value as a Biomarker in Patients with Schizophrenia: A Cohort Study. *Psychiatry Res.* 291, 113260. doi:10.1016/j.psychres.2020.113260

Pelicia, K., Aparecido Jr, I., Garcia, E., Molino, A., Santos, G., Berto, D., et al. (2012). Evaluation of a Radiographic Method to Detect Tibial Dyschondroplasia

Lesions in Broilers. *Rev. Bras. Cienc. Avic.* 14, 129–135. doi:10.1590/S1516-635X2012000200007

Poulos, P. W. (1978). Tibial Dyschondroplasia (Osteochondrosis) in the turkey. A Morphologic Investigation. *Acta Radiol. Suppl.* 358, 197–227.

Rath, N. C., Richards, M. P., Huff, W. E., Huff, G. R., and Balog, J. M. (2005). Changes in the Tibial Growth Plates of Chickens with Thiram-Induced Dyschondroplasia. *J. Comp. Pathology* 133, 41–52. doi:10.1016/J.JCPA.2005.01.005

Rath, N. C., Kannan, L., Pillai, P. B., Huff, W. E., Huff, G. R., Horst, R. L., et al. (2007). Evaluation of the Efficacy of Vitamin D3 or its Metabolites on Thiram-Induced Tibial Dyschondroplasia in Chickens. *Res. Veterinary Sci.* 83, 244–250. doi:10.1016/J.RVSC.2006.12.008

Rodriguez-R, L. M., Castro, J. C., Kyrpides, N. C., Cole, J. R., Tiedje, J. M., and Konstantinidis, K. T. (2018). How Much Do rRNA Gene Surveys Underestimate Extant Bacterial Diversity? *Appl. Environ. Microbiol.* 84, e00014–18. doi:10.1128/AEM.00014-18

Sánchez-Alcoholado, L., Ordóñez, R., Otero, A., Plaza-Andrade, I., Laborda-Illanes, A., Medina, J. A., et al. (2020). Gut Microbiota-Mediated Inflammation and Gut Permeability in Patients with Obesity and Colorectal Cancer. *Ijms* 21, 6782. doi:10.3390/ijms21186782

Schiering, C., Wincent, E., Metidji, A., Iseppon, A., Li, Y., Potocnik, A. J., et al. (2017). Feedback Control of AHR Signalling Regulates Intestinal Immunity. *Nature* 542, 242–245. doi:10.1038/nature21080

Schwartz, M. (1978). [59] Thymidine Phosphorylase from *Escherichia coli*. *Methods Enzymol.* 51, 442–445. doi:10.1016/s0076-6879(78)51061-6

Stentoft, C., Røjen, B. A., Jensen, S. K., Kristensen, N. B., Vestergaard, M., and Larsen, M. (2015). Absorption and Intermediary Metabolism of Purines and Pyrimidines in Lactating Dairy Cows. *Br. J. Nutr.* 113, 560–573. doi:10.1017/S0007114514004000

Stewart, C. J., Mansbach, J. M., Wong, M. C., Ajami, N. J., Petrosino, J. F., Camargo, C. A., et al. (2017). Associations of Nasopharyngeal Metabolome and Microbiome with Severity Among Infants with Bronchiolitis. A Multiomic Analysis. *Am. J. Respir. Crit. Care Med.* 196, 882–891. doi:10.1164/rccm.201701-0071OC

Stotzer, P. O., Johansson, C., Mellström, D., Lindstedt, G., and Kilander, A. F. (2003). Bone Mineral Density in Patients with Small Intestinal Bacterial Overgrowth. *Hepatogastroenterology* 50, 1415–1418.

Tomasova, L., Grman, M., Ondrias, K., and Ufnal, M. (2021). The Impact of Gut Microbiota Metabolites on Cellular Bioenergetics and Cardiometabolic Health. *Nutr. Metab. (Lond)* 18, 72. doi:10.1186/s12986-021-00598-5

Tong, X., Rehman, M. U., Huang, S., Jiang, X., Zhang, H., and Li, J. (2018). Comparative Analysis of Gut Microbial Community in Healthy and Tibial Dyschondroplasia Affected Chickens by High Throughput Sequencing. *Microb. Pathog.* 118, 133–139. doi:10.1016/j.micpath.2018.03.001

Tsoukalas, D., Sarandi, E., and Georgaki, S. (2021). The Snapshot of Metabolic Health in Evaluating Micronutrient Status, the Risk of Infection and Clinical Outcome of COVID-19. *Clin. Nutr. ESPEN* 44, 173–187. doi:10.1016/j.clnesp.2021.06.011

Wang, X., Ye, T., Chen, W.-J., Lv, Y., Hao, Z., Chen, J., et al. (2017). Structural Shift of Gut Microbiota during Chemo-Preventive Effects of Epigallocatechin Gallate on Colorectal Carcinogenesis in Mice. *Wjg* 23, 8128–8139. doi:10.3748/wjg.v23.i46.8128

Wang, Y., Li, A., Zhang, L., Waqas, M., Mehmood, K., Iqbal, M., et al. (2019). Probiotic Potential of Lactobacillus on the Intestinal Microflora against *Escherichia coli* Induced Mice Model through High-Throughput Sequencing. *Microb. Pathog.* 137, 103760. doi:10.1016/j.micpath.2019.103760

Wang, X., Liu, H., Li, Y., Huang, S., Zhang, L., Cao, C., et al. (2020). Altered Gut Bacterial and Metabolic Signatures and Their Interaction in Gestational Diabetes Mellitus. *Gut microbes* 12, e1840765. doi:10.1080/19490976.2020.1840765

Watson, E., Olin-Sandoval, V., Hoy, M. J., Li, C.-H., Louisse, T., Yao, V., et al. (2016). Metabolic Network Rewiring of Propionate Flux Compensates Vitamin B12 Deficiency in *C. elegans*. *Elife* 5, e17670. doi:10.7554/eLife.17670

Witkowski, M., Weeks, T. L., and Hazen, S. L. (2020). Gut Microbiota and Cardiovascular Disease. *Circ. Res.* 127, 553–570. doi:10.1161/CIRCRESAHA.120.316242

Xiao, H.-w., Cui, M., Li, Y., Dong, J.-l., Zhang, S.-q., Zhu, C.-c., et al. (2020). Gut Microbiota-Derived Indole 3-propionic Acid Protects against Radiation Toxicity via Retaining Acyl-CoA-Binding Protein. *Microbiome* 8, 69. doi:10.1186/s40168-020-00845-6

Xu, T., Yue, K., Zhang, C., Tong, X., Lin, L., Cao, Q., et al. (2021). Probiotics Treatment of Leg Diseases in Broiler Chickens: a Review. *Probiotics Antimicro. Prot.* 1–11. doi:10.1007/s12602-021-09869-2

Zaiss, M. M., Jones, R. M., Schett, G., and Pacifici, R. (2019). The Gut-Bone axis: How Bacterial Metabolites Bridge the Distance. *J. Clin. Investig.* 129, 3018–3028. doi:10.1172/JCI128521

Zhang, L., Jiang, X., Li, A., Waqas, M., Gao, X., Li, K., et al. (2020). Characterization of the Microbial Community Structure in Intestinal Segments of Yak (Bos Grunniens). *Anaerobe* 61, 102115. doi:10.1016/j.anaerobe.2019.102115

Zheng, P., Li, Y., Wu, J., Zhang, H., Huang, Y., Tan, X., et al. (2019). Perturbed Microbial Ecology in Myasthenia Gravis: Evidence from the Gut Microbiome and Fecal Metabolome. *Adv. Sci.* 6, 1901441. doi:10.1002/advs.201901441

Zhu, Q., Hou, Q., Huang, S., Ou, Q., Huo, D., Vázquez-Baeza, Y., et al. (2021). Compositional and Genetic Alterations in Graves' Disease Gut Microbiome Reveal Specific Diagnostic Biomarkers. *Isme J.* 15, 3399–3411. doi:10.1038/s41396-021-01016-7

Zimmermann, J., Obeng, N., Yang, W., Pees, B., Petersen, C., Waschina, S., et al. (2019). The Functional Repertoire Contained within the Native Microbiota of the Model Nematode *Caenorhabditis elegans*. *Isme J.* 14, 26–38. doi:10.1038/s41396-019-0504-y

Zuccarini, M., Giuliani, P., Caciagli, F., Ciccarelli, R., and Di Iorio, P. (2021). In Search of a Role for Extracellular Purine Enzymes in Bone Function. *Biomolecules* 11, 679. doi:10.3390/biom11050679

Conflict of Interest: The authors declare that the research was conducted in the absence of any commercial or financial relationships that could be construed as a potential conflict of interest.

Publisher's Note: All claims expressed in this article are solely those of the authors and do not necessarily represent those of their affiliated organizations, or those of the publisher, the editors and the reviewers. Any product that may be evaluated in this article, or claim that may be made by its manufacturer, is not guaranteed or endorsed by the publisher.

frontiers | Frontiers in Physiology

ORIGINAL RESEARCH
published: 18 July 2022
doi: 10.3389/fphys.2022.945740

Long Bone Mineral Loss, Bone Microstructural Changes and Oxidative Stress After *Eimeria* Challenge in Broilers

Y. H. Tompkins[1], *P. Teng*[1], *R. Pazdro*[2] *and W. K. Kim*[1]*

[1]Department of Poultry Science, University of Georgia, Athens, GA, United States, [2]Department of Foods and Nutrition, University of Georgia, Athens, GA, United States

The objective of this study was to evaluate the impact of coccidiosis on bone quality and antioxidant status in the liver and bone marrow of broiler chickens. A total of 360 13-day old male broilers (Cobb 500) were randomly assigned to different groups (negative control, low, medium-low, medium-high, and highest dose groups) and orally gavaged with different concentrations of *Eimeria* oocysts solution. Broiler tibia and tibia bone marrow were collected at 6 days post-infection (6 dpi) for bone 3-D structural analyses and the gene expression related to osteogenesis, oxidative stress, and adipogenesis using micro-computed tomography (micro-CT) and real-time qPCR analysis, respectively. Metaphyseal bone mineral density and content were reduced in response to the increase of *Eimeria* challenge dose, and poor trabecular bone traits were observed in the high inoculation group. However, there were no significant structural changes in metaphyseal cortical bone. Medium-high *Eimeria* challenge dose significantly increased level of peroxisome proliferator-activated receptor gamma (*PPARG*, $p < 0.05$) and decreased levels of bone gamma-carboxyglutamate protein coding gene (*BGLAP*, $p < 0.05$) and fatty acid synthase coding gene (*FASN*, $p < 0.05$) in bone marrow. An increased mRNA level of superoxide dismutase type 1 (*SOD1*, $p < 0.05$) and heme oxygenase 1 (*HMOX1*, $p < 0.05$), and increased enzyme activity of superoxide dismutase (SOD, $p < 0.05$) were found in bone marrow of *Eimeria* challenged groups compared with that of non-infected control. Similarly, enzyme activity of SOD and the mRNA level of *SOD1*, *HMOX1* and aflatoxin aldehyde reductase (*AKE7A2*) were increased in the liver of infected broilers ($p < 0.05$), whereas glutathione (GSH) content was lower in the medium-high challenge group ($p < 0.05$) compared with non-challenged control. Moreover, the mRNA expression of catalase (*CAT*) and nuclear factor kappa B1 (*NFKB1*) showed dose-depend response in the liver, where expression of *CAT* and *NFKB1* was upregulated in the low challenge group but decreased with the higher *Eimeria* challenge dosage ($p < 0.05$). In conclusion, high challenge dose of *Eimeria* infection negatively affected the long bone development. The structural changes of tibia and decreased mineral content were mainly located at the trabecular bone of metaphyseal area. The change of redox and impaired antioxidant status following the *Eimeria* infection were observed in the liver and bone marrow of broilers.

Keywords: *eimeria*, bone health, bone mineral loss, bone quality, oxidative stress, broiler bone

OPEN ACCESS

Edited by:
Anthony Pokoo-Aikins, USDA ARS, United States

Reviewed by:
Katarzyna B. Miska, Agricultural Research Service (USDA), United States
Shawky Mohamed Aboelhadid, Beni-Suef University, Egypt
Muhammad Shahid, University of the Punjab, Pakistan

***Correspondence:**
W. K. Kim
wkkim@uga.edu

Specialty section:
This article was submitted to Avian Physiology, a section of the journal Frontiers in Physiology

Received: *16 May 2022*
Accepted: *14 June 2022*
Published: *18 July 2022*

Citation:
Tompkins YH, Teng P, Pazdro R and Kim WK (2022) Long Bone Mineral Loss, Bone Microstructural Changes and Oxidative Stress After Eimeria Challenge in Broilers. Front. Physiol. 13:945740. doi: 10.3389/fphys.2022.945740

INTRODUCTION

Avian coccidiosis is one of the top prevalent enteric diseases in the poultry industry. Especially in the modern broiler production, the high-density, small confinement, warm, and humid animal housing accelerate the dispersal, transmission, and outbreak of coccidiosis, making this issue hard to eradicate (Chapman 2014; Blake et al., 2020). Coccidiosis is a parasite disease caused by parasites of the genus *Eimeria* that can cause intestinal damage leading to inflammation and nutrient malabsorption (Gautier et al., 2019). The infection with *Eimeria* spp. results in growth retardation and mortality, which creates 13 billion dollars in losses by its detriment to production and increases the cost (Amerah and Ravindran, 2015). The prevention and control of coccidiosis outbreaks are not only achieved by careful management practices, but also the use of in-feed anticoccidial drugs or vaccines, alone or in combination. However, because of the market demand, the use of antibiotic-free diets leads to numerous challenges, such as control and treatment of enteric and systemic diseases (Dalloul and Lillehoj, 2006; Blake and Tomley, 2014; Cervantes, 2015). Other than anorexia or nutrient malabsorption, the pathogenicity of coccidiosis is also associated with the response from immune system which generates reactive oxygen species (ROS) in chicken (Georgieva et al., 2006; Georgieva et al., 2011; Gautier et al., 2019). The parasite infection causes an imbalance between endogenous antioxidant defense and free radical production, which leads to depletion of antioxidant enzymes and reduction of glutathione (GSH) level (Surai, 2019). The unbalanced status results in increased lipid peroxidation and DNA damage which can cause apoptosis of intestinal cells and affect the health status and productivity of poultry (Estevez, 2015; Mishra and Jha, 2019). The first lines of antioxidant defense system including catalase (CAT), superoxide dismutase (SOD), and glutathione peroxidase (GPX) are indispensable for protecting the body from the damage caused by free radicals, especially superoxide anion radicals, during *Eimeria* infection (Georgieva et al., 2006). Dietary manipulations, such as optimizing amino acids profile or adding dietary supplements are potential strategies to support broilers against coccidiosis induced oxidative stress (Arczewska-Wlosek et al., 2018; Gautier et al., 2019). In broilers, nutrient supplements such as vitamins, antioxidants, and trace minerals can alleviate the negative effect caused by oxidative stress (Arczewska-Wlosek et al., 2018; Santos et al., 2020).

Meanwhile, the incidence of physical abnormalities in bone of broilers has been noted. Because the fast-growing broilers are characterized by poor calcification and high porosity of long bone, severe duodenum and upper jejunum damage caused by *Eimeria* infection intensifies the bone health issues in the modern poultry industry (Sakkas et al., 2018; Oikeh et al., 2019). Bone mineral loss caused by *Eimeria* spp. in broilers has been previously linked to nutrition malabsorption, especially the reduced absorption of calcium, phosphate, and several important trace minerals for optimal bone growth (Turk and Stephens, 1967; Turk and Stephens, 1969; Turk and Stephens, 1970; Turk, 1973; Joyner et al., 1975). Recent studies have revealed a more profound understanding in regards to bone loss after *Eimeria* infection, where suppressed fat absorption resulted in depressed levels of fat-soluble vitamins; thus, an increase in bone resorption level was detected (Akbari Moghaddam Kakhki et al., 2019; Sakkas et al., 2019). Studies in human and mice also indicated that oxidative stress response caused by gastrointestinal infection could lead to inhibition of mineralization and osteogenesis, and activation of bone resorption, subsequently causing bone loss and structural changes (Basu et al., 2001; Domazetovic et al., 2017). Bone architectural organization is an independent marker that can precisely reflect bone turnover, however, how does the *Eimeria* infection change biomechanical properties on the specific bone region has not been documented extensively to date, and the etiology behind it is not fully understood (Brandi, 2009; Henkelmann et al., 2017). We reported that the increasing infection severity of *Eimeria* spp. linearly reduced nutrient digestibility and body weight of birds. The increased gut permeability and lesion scores in response to the graded levels of *Eimeria* infection were also found and presented in our recent publication (Teng et al., 2020). The objective of this study was to further evaluate the negative impact of coccidiosis on bone traits in broiler chickens. A new approach, micro-CT scanning and analyses, was taken in assessing the three-dimensional structure to provide in-depth and comprehensive understanding the pathogenetic mechanisms of bone disorders with acute intestinal pathogen infections in avian species.

MATERIALS AND METHODS

Ethics Statement

All experiments followed the guidelines of the Institutional Animal Care and Use Committee and was conducted at the Poultry Research Farm, University of Georgia, Athens, GA. The protocol was approved by the Institutional Animal Care and Use Committee at the University of Georgia.

Experimental Design

Management and diet formulation as previously described (Teng et al., 2020). Briefly, a total of 360 male broiler chicks were randomly allocated to five treatments with six replicates and twelve birds per cage. The birds were gavaged with 1 ml of water for a control and 1 ml of different concentrations of *Eimeria* solutions for challenge groups at 13 days of age. Mixed *Eimeria* spp. oocyst solutions were pre-prepared for the Low group as the lowest challenge dose with 6,250 oocysts of *E. maxima*, 6,250 oocysts of *E. tenella* and 31,250 oocysts of *E. acervulina*; the Med-low group as the medium-low challenge dose with 12,500 oocysts of *E. maxima*, 12,500 oocysts of *E. tenella* and 62,500 oocysts of *E. acervulina*; the Med-high group as the medium-high challenge dose with 25,000 oocysts of *E. maxima*, 25,000 oocysts of *E. tenella* and 125,000 oocysts of *E. acervulina*; and the High group as the highest challenge dose with 50,000 oocysts of *E. maxima*, 50,000 oocysts of *E. tenella*, and 250,000 oocysts of *E. acervulina* (**Table 1**). All chicks were raised under the same environmental conditions according to the Cobb 500 broiler management guide (Cobb, 2019). All chicks were fed the same basal diet and allowed

TABLE 1 | *Eimeria* spp. challenge dosage (Unit: oocysts/chick).

Treatment group[a]	*E. maxima*	*E. tenella*	*E. acervulina*	Total Concentration	Challenge Dosage
Control	0	0	0	0	Non-challenge
Low	6,250	6,250	31,250	43,750	Lowest challenge dose
Med-low	12,500	12,500	62,500	87,500	Medium-low challenge dose
Med-high	25,000	25,000	125,000	175,000	Medium-high challenge dose
High	50,000	50,000	250,000	350,000	Highest challenge dose

[a]*Low, the lowest challenge dose; Med-low, the medium-low challenge dose; Med-high, the medium-high challenge dose; High, the highest challenge dose.*

to consume feed and water on an *ad libitum* basis. Starter (0–12 days of age) and grower (13–19 days of age) diets were formulated to meet Cobb 500 nutrient requirements as previously described (Teng et al., 2020). A total of 30 birds (1 bird per replicate cage) were selected and euthanized by cervical dislocation at six dpi (19 days of age), and tibia bone and liver samples were collected and snap-frozen in liquid nitrogen and kept in −80°C until processing.

Antioxidant Study by Enzyme-Linked Immunosorbent Assay

SOD and CAT enzyme activities in the liver and bone marrow of 30 samples (6 samples per treatment group) were analyzed using superoxide dismutase assay and catalase assay kits (Cayman chemical, Superoxide dismutase assay kit, item No. 706002, Catalase Assay Kit, item No. 707002, AnnArbor, MI, United States), following the manufacturer's instructions. Approximately 100 mg of each sample was homogenized in 1 ml of cold sample buffer (20 mM HEPES buffer, pH 7.2, 2 mM EGTA, 10 mM mannitol, and 70 mM sucrose). The homogenized sample was centrifuged at 1,500 × g for 5 minutes at 4°C, and the supernatant was collected for analyses. All supernatant samples were diluted by using the sample buffer before the ELISA assays. Samples were measured by spectrophotometer (SpectraMax ABS Plus, Softmax Pro seven software, Molecular devices, San Jose, CA) at wavelength of 450 nm for SOD activity assay, and at 540 nm for CAT assay. For protein quantification assay (Pierce™ BCA Protein Assay Kit, Ref. 23,227, Thermo Scientific, Rockford, IL, United States), the supernatants were diluted before the assay, and Bovine Serum Albumin (2 mg/ml) was used as the protein standard, and enzyme activity was normalized to the total protein content for the final calculation. The protein samples were diluted and placed in duplicate and read in a spectrophotometer (SpectraMax, San Jose, CA) at wavelength of 562 nm.

High-Performance Liquid Chromatography

High-performance liquid chromatography (HPLC) setting and reading for measuring antioxidative parameters were as previously described (Gould et al., 2018). Immediately after collecting liver and tibia marrow samples, all samples were snap-frozen in liquid nitrogen. Within 24 h, all harvested tissues were homogenized in PBS containing 10 mM diethylenetriaminepentaacetic acid (DTPA) and promptly acidified as previously described (Park et al., 2010). Samples were stored at -80 °C for HPLC analyses. Briefly, glutathione (GSH) and glutathione disulfide (GSSG) were quantified in each sample by HPLC coupled with electrochemical detection (Dionex Ultimate 3,000, Thermo Scientific, Waltham, MA, United States). The cell was set at + 1,600 mV with a cleaning potential of +1900 mV between the samples. The mobile phase consisted of 4.0% acetonitrile, 0.1% pentafluoropropionic acid, and 0.02% ammonium hydroxide. The flow rate was maintained at 0.5 ml/min, and injection volumes were set at 2.0 µl for bone marrow samples. Peaks were quantified using external GSH and GSSG standards and the Chromeleon Chromatography Data System Software (Dionex Version 7.2, Thermo Scientific, Germering, Germany). Total glutathione was determined by calculating GSH + 2GSSG, and levels of total glutathione, GSH, and GSSG were all standardized to total protein content (Pierce™ BCA Protein Assay Kit). The protein samples were diluted and placed in duplicate and read in a spectrophotometer (SpectraMax, San Jose, CA) at wavelength of 562 nm.

Micro-Computed Tomography

To evaluate bone morphologic changes in the broiler, 30 samples (6 samples per treatment group) were randomly chosen for micro-Computed Tomography (micro-CT) microarchitectural scanning. The right tibias were scanned according to a standard protocol at 80 kV and128 µA, and a 0.5 mm aluminum filter, and analyses were performed with a SkyScan 1,172 (SkyScan, Kontich, Belgium). The scanned images were captured with a 360° complete rotation and an 18 min of acquisition time at 26 µm pixel size. 2-D images were transferred to CTAn software (CTAn, SkyScan, Aartselaar, Belgium) for structure construction and quantification as previously described (Chen and Kim, 2020). Trabecular and cortical bones of the metaphysis were analyzed. The analysis parameters are listed in **Table 2**. All images were post-operated to isolate trabecular bone from cortical bone and preserve its morphology using a threshold of 800 manually. Average bone mineral content (BMC), bone mineral density (BMD), and bone micro-architectural parameters of each treatment group were taken from the same region of interest (ROI). The whole bone length and bone diaphysis width were measured by using CTAn ruler tool which measures straight line distance. Controlling the location, four measurements were conducted on each sample by using CTAn ruler tool, the mean thickness of cortical bone was used for statistical analysis.

TABLE 2 | Definition and description of bone microstructure by using micro-CT method (Bouxsein et al., 2010).

Abbreviation	Variable	Unit	Description
BMC	Bone mineral content	g	The amount of the solid objects (bone minerals that mostly included calcium and phosphorous) within the region of interest
BMD	Bone mineral density	g/mm^2	The ratio of bone minerals within a mixed bone-soft tissue region
TV	Total volume	mm^3	Volume of the entire region of interest
BV	Bone volume	mm^3	Volume of the region segmented as bone
BS	Bone surface	mm^2	Surface area of all solid objects (bone tissue) within the total tissue volume
BV/TV	Bone volume fraction	%	Ratio of the solid objects (bone tissue) volume to the total volume of the region of interest
BS/BV	Specific bone surface	mm^2/mm^3	Ratio of the segmented bone surface to the mineralized bone volume
BS/TV	Bone surface density	%	Ratio of the segmented bone surface to the total volume of the region of interest
Tb. N	Trabecular number	1/mm	Measure of the average number of trabeculae per unit length
Tb. Th	Trabecular thickness	mm	Mean thickness of trabeculae osseous structure. It assessed using direct 3D methods
Tb. Sp	Trabecular spacing	mm	Mean space between trabeculae (marrow space), assessed using direct 3D methods
SMI	Structure model index	-	An indicator of the structure of trabeculae; Parallel plates was defined as 0 and cylindrical rods was rated as 3
Tb.pf	Trabecular pattern factor	1/mm	Describes quantitatively trabecular connectivity
Conn. Dn	Connectivity density	$1/mm^3$	A measure of the degree of connectivity of trabeculae normalized by TV
Po (op)	Cortical porosity (open pore)	%	In a given cortical region, the volume of open pores (Po.V, mm^3) ÷ total volume of cortical bone compartment (Ct.V, mm^3)
Po.V (op)	Open pore volume	mm^3	The volume of the open pores
Po.V (tot)	Total pore volume	mm^3	The volume of all pores
Po (tot)	Total cortical porosity	%	In a given cortical region, the volume of pores (Po.V, mm^3) ÷ total volume of cortical bone compartment (Ct.V, mm^3)

TABLE 3 | Nucleotide sequences of the primers used for real-time qPCR.

Gene[a]	Primer Sequence (5′-3′)	Product length (bp)	Annealing temperature (°C)	Accession #	Gene references
GAPDH	F-GCTAAGGCTGTGGGGAAAGT R-TCAGCAGCAGCCTTCACTAC	161	55	NM_204,305.1	Su et al. (2020)
ACTB	F-CAACACAGTGCTGTCTGGTGGTA R-ATCGTACTCCTGCTTGCTGATCC	205	61	NM_205,518.1	Teng et al. (2020)
NFKB1	F-GAAGGAATCGTACCGGGAACA R-CTCAGAGGGCCTTGTGACAGTAA	131	59	XM_015,285,418.2	Su et al. (2020)
RUNX2	F-ACTTTGACAATAACTGTCCT R-GACCCCTACTCTCATACTGG	192	60	XM_015,285,081.2	Adhikari et al. (2020)
PPARG	F-GAGCCCAAGTTTGAGTTTGC R-TCTTCAATGGGCTTCACATTT	131	58	XM_025,154,400.1	Chen et al. (2021)
FASN	F-AGAGGCTTTGAAGCTCGGAC R-GGTGCCTGAATACTTGGGCT	127	60	NM_205,155.3	Su et al. (2020)
FABP4	F-GCAGAAGTGGGATGGCAAAG R- GTTCGCCTTCGGATCAGTCC	153	60	NM_204,290.1	Chen et al. (2021)
BGLAP	F-GGATGCTCGCAGTGCTAAAG R-CTCACACACCTCTCGTTGGG	142	57	NM_205,387.3	Adhikari et al. (2020)
SOD1	F-ATTACCGGCTTGTCTGATGG R-CCTCCCTTTGCAGTCACATT	173	58	NM_205,064.1	Oh et al. (2019)
CAT	F-ACTGCAAGGCGAAAGTGTTT R-GGCTATGGATGAAGGATGGA	222	60	NM_001,031,215.1	Oh et al. (2019)
AKR7A2	F-CAAACTGCAGGGTTCTCTTG R-GAAGTAGTTGGGGCAGTCGT	234	60	NM_205,344.1	Lee et al. (2018)
HMOX1	F-CTGGAGAAGGGTTGGCTTTCT R-GAAGCTCTGCCTTTGGCTGTA	166	60	XM_417,628.2	Oh et al. (2019)
GPX1	F-AACCAATTCGGGCACCAG R-CCGTTCACCTCGCACTTCTC	122	60	NM_001,277,853.2	Oh et al. (2019)

[a]*GAPDH: glyceraldehyde-3-phosphate dehydrogenase; ACTB: actin beta; PPARG: peroxisome proliferator-activated receptor gamma; FASN: fatty acid synthase; SREBP1: sterol regulatory element-binding transcription factor 1; BGLAP: bone gamma-carboxyglutamate protein; RUNX2: runt-related transcription factor 2; FABP4: adipose tissue fatty acid binding protein four; NFKB1: nuclear factor kappa B subunit one; CAT: catalase; SOD1: superoxide dismutase type 1; GPX1: glutathione peroxidase one; HMOX1: heme oxygenase one; and AKR7A2: aflatoxin aldehyde reductase.*

Real-Time qPCR Analysis for Gene Expression in the Bone Marrow

Right tibia bones were opened, and bone marrow samples were collected and stored at −80°C until RNA isolation (n = 6). Bone marrow and liver total RNA were extracted by using Qiazol reagents (Quiagen, Germantown, MD, United States) according to the manufacturer's instructions. Nano-Drop 1,000 Spectrophotometer (ThermoFisher Scientific, Pittsburgh, PA, United States) was used to determine the quantity of extracted RNA. The cDNA was synthesized from total RNA (2000 ng) using high-capacity cDNA reverse transcription kits (Thermo Fisher Scientific, Waltham, MA, United States). Real-time reverse transcription polymerase chain reaction (Real-time RT-PCR) was used to measure mRNA expression. Primers were designed using

the Primer-BLAST program (https://www.ncbi.nlm.nih.gov/tools/primer-blast/). The specificity of primers was validated by PCR product sequencing and previously published (**Table 3**). Primer quality was verified through melting curve analysis and gel electrophoresis in this study. Real-time qPCR was performed on an Applied Biosystems StepOnePlus™ (Thermo Fisher Scientific, Waltham, MA, United States) with iTaq™ universal SYBR Green Supermix (BioRad, Hercules, CA, United States) using the following conditions for all genes: 95°C for 10 min followed 40 cycles at 95°C for 15 s, annealing temperature (**Table 3**) for 20 s, and extending at 72°C for 1 minute.

The geomeantric means of glyceraldehyde-3-phosphate dehydrogenase (*GAPDH*) and actin beta (*ACTB*) were used as housekeeping genes for normalization, and the stability of the housekeeping genes was confirmed by their consistent Ct values among the treatments ($p > 0.1$) (Vandesompele et al., 2002). Details of primer sequences used for the experiment are presented in **Table 3**. Peroxisome proliferator-activated receptor gamma (*PPARG*), fatty acid synthase (*FASN*), adipose tissue fatty acid binding protein 4 (*FABP4*) and sterol regulatory element-binding transcription factor 1 (*SREBP1*) were used as early markers of adipogenic differentiation and fatty acid synthesis, and bone gamma-carboxyglutamate protein (*BGLAP*) and runt-related transcription factor 2 (*RUNX2*) were used as osteogenic marker genes in the bone marrow. Nuclear factor kappa B subunit 1 (*NFKB1*) and antioxidant enzyme protein coding genes including catalase (*CAT*), superoxide dismutase type 1(*SOD1*), glutathione peroxidase 1 (*GPX1*), heme oxygenase 1 (*HMOX1*), and aflatoxin aldehyde reductase (*AKR7A2*) were used to determine the antioxidant enzyme activity and oxidative stress status (Lee et al., 2018). Samples were run in triplicate, and relative gene expression data were analyzed using the $2^{-\Delta\Delta Ct}$ (Livak et al., 2001). The mean ΔCt of each marker gene from the control group was used to calculate the ΔΔCt value, and $2^{-\Delta\Delta Ct}$ expression levels were normalized to one for the control group, and expression levels of the other treatment groups were presented as fold change relative to the control group.

Statistical Analysis

All experimental data were expressed as mean with standard errors of the means (SEM). Data were tested for homogeneity of variances and normality of studentized residuals. The differences between the treatment groups were analyzed by one-way ANOVA, and the means were analyzed statistically by Tukey's test using JMP Pro14 (SAS Institute, Cary, NC, United States). A $p \leq 0.05$ was considered statistically significant, and $0.05 \leq p \leq 0.1$ were also presented to show the trending toward statistical significance (Thiese et al., 2016; Serdar et al., 2021). To evaluate the effects of increasing oocysts inoculation doses on responses of each parameter, the linear and quadratic regression were analyzed using an ordered logistic regression model with inoculated number of oocytes as a fixed factor and broiler per pen as the experimental unit. The comparisons between non-challenge control and pooled challenged groups (Low, Med-low, Med-high, and High) were calculated by unpaired *t*-test with Welch's correction. Pair wise correlations (JMP Pro14) were evaluated for bone micro-CT and antioxidant variables. Statistical significance was set at $p \leq 0.05$.

TABLE 4 | Tibia length, width, and cortical bone thickness.

Unit (mm)	Bone length	Bone width	Cortical bone thickness[a]
Control	54.497	4.959	0.841
Low	54.436	4.969	0.850
Med-low	55.413	4.958	0.898
Med-High	55.109	4.969	0.841
High	55.092	5.086	0.873
SEM	0.244	0.051	0.021
ANOVA	0.226	0.925	0.836

[a]*Cortical thickness: a mean thickness of cortical mid-shaft.*

RESULTS

Bone Microstructural Changes in Response to Increasing Doses of *Eimeria* Oocysts

There were no statistically significant differences in the whole tibia length, tibia diaphysis width and the thickness of cortical bone among treatment groups at six dpi (**Table 4**). And all the micro-CT results are presented in **Table 5**. For the total bone structure of metaphysis, the lowest BMC (ANOVA, $p = 0.025$; linear regression, $p = 0.012$, $R^2 = 0.205$), BMD (ANOVA, $p = 0.002$; linear regression, $p < 0.001$, $R^2 = 0.342$), and the lowest bone volume fraction (BV/TV; ANOVA, $p = 0.023$) ratio were detected in the High group in response to increased challenge dose.

The microstructure changes in metaphysis were mainly attributed to impaired trabecular bone traits caused by higher *Eimeria* challenge dosage, including lower BMC (**Figure 1**; ANOVA, $p = 0.001$; linear regression, $p < 0.001$, $R^2 = 0.362$), lower BMD (ANOVA, $p < 0.001$; linear regression, $p < 0.001$, $R^2 = 0.402$), smaller bone surface (BS; ANOVA, $p = 0.048$), lower trabecular number (Tb. N; ANOVA, $p = 0.025$; linear regression, $p = 0.021$, $R^2 = 0.177$), lower connectivity density (Conn. Dn; ANOVA, $p = 0.035$; linear regression, $p = 0.014$, $R^2 = 0.243$), and higher rating structure model index (SMI; ANOVA, $p = 0.002$; linear regression, $p < 0.001$, $R^2 = 0.387$), higher rating of trabecular pattern factor (Tb. pf; ANOVA, $p = 0.029$; linear regression, $p = 0.003$, $R^2 = 0.268$). However, the microstructure of metaphyseal cortical bone was not significantly affected by *Eimeria* infection (ANOVA, $p > 0.050$).

Gene Expression Changes of Bone Formation and Adipogenic Markers in the Bone Marrow

The expression of protein coding genes that are involved in bone formation or adipocyte differentiation was measured (**Figure 2**). For bone growth gene markers, results showed a significant downregulation of *BGLAP* with increased inoculation levels (ANOVA, $p = 0.020$; linear regression, $p = 0.029$, $R^2 = 0.396$), where the lowest level of *BGLAP* was detected in the Med-High

TABLE 5 | Tibial metaphysis microstructure changes with increasing challenge dose of mixed *Eimeria* spp. oocysts.

	Items[a,b]	Unit	Control	Low	Med-low	Med-High	High	SEM	ANOVA
Total	BMC	G	61.244 [ab]	70.906[a]	68.282 [ab]	67.241 [ab]	51.567[b]	2.139	0.025
	BMD	g/mm^2	0.209[a]	0.209[a]	0.215[a]	0.213[a]	0.170[b]	0.004	0.002
	TV	mm^3	295.216	339.192	318.777	312.631	303.064	6.177	0.284
	BV	mm^3	89.331	100.332	108.552	101.309	85.588	3.196	0.134
	BS	mm^2	1,260.402	1,419.550	1,415.952	1,333.981	1,116.761	48.366	0.250
	BV/TV	%	29.590 [ab]	29.628 [ab]	34.105[a]	32.069 [ab]	28.161[b]	0.667	0.023
	BS/BV	mm^2/mm^3	14.018	14.114	13.047	13.281	13.025	0.224	0.360
	BS/TV	%	4.160	4.171	4.454	4.236	3.671	0.105	0.202
Trabecular	BMC	G	2.812[a]	2.646[a]	1.839[ab]	2.462[a]	1.087[b]	0.161	0.001
	BMD	g/mm^2	0.087[a]	0.096[a]	0.068[ab]	0.083[a]	0.038[b]	0.005	<0.001
	TV	mm^3	178.487	205.576	174.901	178.060	188.858	3.882	0.065
	BV	mm^3	5.802	7.704	6.717	6.086	4.863	0.331	0.073
	BS	mm^2	295.527[a]	385.188[ab]	340.596 [ab]	321.624 [ab]	258.360[b]	14.230	0.048
	BV/TV	%	3.238	3.710	3.863	3.424	2.59072	0.156	0.075
	BS/BV	mm^2/mm^3	52.046	50.578	50.831	52.900	54.140	0.643	0.394
	Tb. N	1/mm	0.389 [ab]	0.435 [ab]	0.464[a]	0.421 [ab]	0.310[b]	0.017	0.025
	Tb. Th	Mm	0.082	0.085	0.083	0.081	0.083	0.001	0.846
	Tb. Sp	Mm	2.848	2.513	2.364	2.376	2.935	0.087	0.100
	SMI	-	2.622[b]	2.617[b]	2.577[b]	2.661 [ab]	2.759[a]	0.017	0.002
	Tb.pf	1/mm	18.814 [ab]	18.238 [ab]	17.943[b]	19.635 [ab]	21.084[a]	0.360	0.029
	Conn. Dn	1/mm^3	10.158 [ab]	11.076[a]	11.852 [ab]	10.389 [ab]	8.077[b]	0.407	0.035
Cortical	BMC	G	44.029	47.190	51.033	46.949	41.989	1.388	0.306
	BMD	g/mm^2	0.412	0.401	0.404	0.402	0.409	0.876	0.876
	TV	mm^3	108.061	118.168	126.627	117.158	103.270	3.955	0.386
	BV	mm^3	79.177	87.435	93.899	87.243	78.179	2.614	0.298
	BV/TV	%	73.945	74.158	74.263	74.701	76.121	0.537	0.741
	Po (op)	%	25.951	25.736	25.604	25.171	23.763	0.536	0.737
	Po.V (op)	mm^3	28.767	30.605	32.559	29.757	24.971	1.455	0.589
	Po.V (tot)	mm^3	28.884	30.733	32.727	29.915	25.091	1.462	0.588
	Po (tot)	%	26.055	25.842	25.738	25.299	23.879	0.537	0.741

[a]*Low, the lowest challenge dose; Med-low, the medium-low challenge*[a]*dose; Med-high, the medium-high challenge dose; High, the highest challenge dose.*

[b]*BMC, bone mineral content; BMD, bone mineral density; TV, total bone volume; BV, bone volume (TV, minus bone marrow volume); BS, bone surface area; BV/TV, bone volume/total volume; BS/BV, bone surface/total volume; BS/TV, bone surface/total volume; Tb. N, trabecular number; Tb. Th, trabecular bone thickness; Tb. sp, trabecular spacing; SMI, structural model index; Tb. Pf, trabecular pattern factor; Conn. dn, connectivity density; Po.V (tot), total volume of pore space; Po. V (op), volume of open pore; Po (tot), porosity rate (percent).*

[a, ab,b] *Treatments with different letters means a significantly difference between treatments by using Tukey's HSD, test,* $p < 0.05$, $N = 6$.

group. The mRNA expression of *RUNX2* was not affected by different doses of *Eimeria* oocysts challenge (ANOVA, $p > 0.100$). For adipogenic gene expression, the expression of *PPARG* was significantly increased by the Med-high dose of challenge when compared with the Control, the Low and the Med-low groups (**Figure 2**; ANOVA, $p = 0.047$). The expression of *SREBP1* (**Figure 2**; ANOVA, $p = 0.056$; linear regression, $p = 0.008$, $R^2 = 0.226$), *FABP4* (**Figure 2**; ANOVA, $p = 0.057$; linear regression, $p = 0.004$, $R^2 = 0.279$), and *FASN* (ANOVA, $p = 0.013$; linear regression, $p = 0.005$, $R^2 = 0.261$) were down-regulated in response to graded inoculation doses.

Antioxidant Status in the Bone Marrow in Response to *Eimeria* Challenge

In the bone marrow, SOD enzyme activity increased in response to graded levels of oocysts challenge and showed the highest response to the Med-high challenge dose (**Table 6**; ANOVA, $p = 0.027$). However, the CAT enzyme activity was not significantly affected by the *Eimeria* challenge (**Table 6**; $p > 0.050$) in bone marrow. The bone marrow GSSG levels did not significantly changed by *Eimeria* infection, but it exhibited a negative response to increasing inoculation doses (**Table 6**; ANOVA, $p > 0.050$; linear regression, $p = 0.039$, $R^2 = 0.150$). However, there were no significant differences in total glutathione content (GSH + 2GSSG), GSH content or GSH/GSSG ratios among the treatment groups (**Table 6**).

Additionally, mRNA expression of *CAT* was positively correlated with higher inoculation doses of the mixed *Eimeria* oocysts in bone marrow (**Figure 3**; ANOVA, $p > 0.050$; linear regression, $p = 0.040$, $R^2 = 0.124$), whereas there were no significant differences in expression of *HMOX1*, *SOD1*, *GPX1* or *NFKB1* among the treatments in bone marrow (**Figure 3**; ANOVA, $p > 0.050$; linear regression, $p > 0.050$). By pooling all infected groups (Low, Med-low, Med-high, and High) together and compared with the non-infected Control, *Eimeria* infection significantly increased the mRNA level of *SOD1* ($p = 0.036$) and *HMOX1* ($p = 0.006$).

Antioxidant Status in the Liver in Response to *Eimeria* Challenge

In the liver, CAT activity was not significantly affected by *Eimeria* infection (ANOVA, $p > 0.050$), but the activity of CAT was negatively correlated to the higher challenge dose of

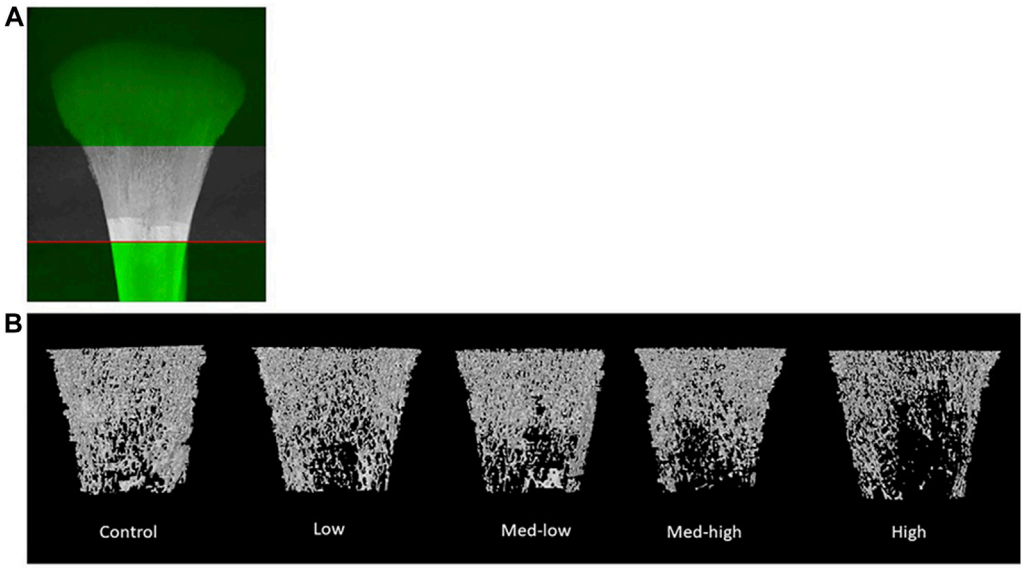

FIGURE 1 | (A) The selection of metaphyseal region of interest. **(B)** Representative reconstructed 2D images of broiler tibia metaphysis at six dpi (19 days of age). Metaphyseal structure analysis showed a lower bone mineral content and density coupled with impaired trabecular bone traits following the higher inoculation doses of *Eimeria*. The negative impact of Eimeria infection on bone traits was mainly located at metaphyseal trabecular bone.

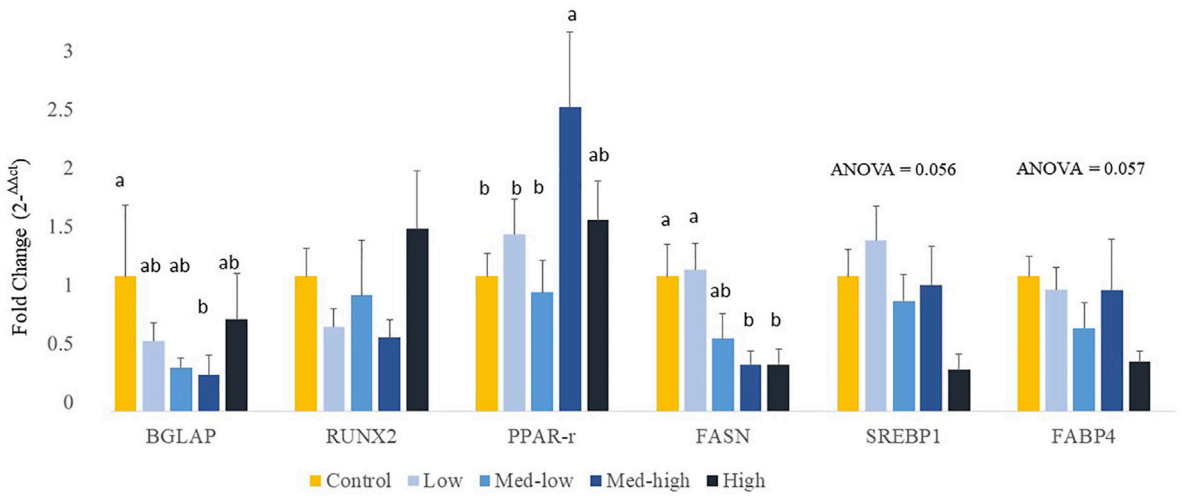

FIGURE 2 | Effects of increasing oocysts dose of *Eimeria* mix on osteogenesis, adipogenesis and fatty acid synthesis gene expression in bone marrow of broilers. Low, the lowest challenge dose; Med-low, the medium-low challenge dose; Med-high, the medium-high challenge dose; High, the highest challenge dose. BGLAP, bone gamma-carboxyglutamate protein; RUNX2, runt-related transcription factor 2; PPARG, peroxisome proliferator-activated receptor gamma; FASN, fatty acid synthase; SREBP1: sterol regulatory element-binding transcription factor 1; FABP4: adipose tissue fatty acid binding protein 4. [a, ab, b] Treatments with different letters means a significantly difference between treatments by using Tukey's HSD test, $p < 0.05$, N = 6.

Eimeria oocysts (**Table 7**; linear, $p = 0.043$, $R^2 = 0.143$). GSH content was significantly decreased by *Eimeria* infection and the lowest GSH content was observed in the Med-High group (**Table 7**; ANOVA, $p = 0.036$). By comparing infected groups (Low, Med-low, Med-high, High) with the non-infected Control, a significant higher SOD activity ($p < 0.001$) and numeric lower GSH content ($p = 0.091$) were detected in pooled *Eimeria*-infected groups.

Additionally, the expression of genes coding for front-line antioxidant enzymes was measured (**Figure 4**). The gene expression of antioxidant gene showed a dose dependent manner. More specifically, the Low challenge dose significantly increased the mRNA expression of CAT when compared with the Control, and the expression level was decreased with the high challenge dose of *Eimeria* oocysts (**Figure 4**; ANOVA, $p = 0.006$; linear regression, $p = 0.004$, $R^2 = 0.144$). The highest inoculation

TABLE 6 | Superoxide dismutase activity (SOD, U/g bone marrow), catalase activity (CAT, U/g bone marrow), GSH (μM/g), GSSG (μM/g) and GSH/GSSG ratio (μM/μM) concentrations in bone marrow at six dpi.

Items[a,*]	Unit	Control	Low	Med-low	Med-high	High	SEM	ANOVA	Non-challenge vs. challenge[b]
GSH	μM/g	18.145	20.891	19.154	14.762	15.318	1.260	0.495	0.469
GSSG	μM/g	0.487	0.506	0.613	0.360	0.353	0.034	0.069	0.224
GSH + 2GSSG	μM/g	19.119	21.903	20.379	15.482	16.025	1.296	0.452	0.453
GSH/GSSG	μM/μM	5.093	5.002	5.137	4.574	4.470	0.288	0.935	0.244
CAT	U/g	32.290	30.271	26.408	27.419	44.407	3.124	0.386	0.937
SOD	U/g	4.574[bc]	4.385[c]	5.616[ab]	5.892[a]	5.434[abc]	0.188	0.027	0.488

[a]*Low, the lowest challenge dose; Med-low, the medium-low challenge dose; Med-high, the medium-high challenge dose; High, the highest challenge dose.*
[b]*The comparisons between non-challenge control and pooled challenged groups (Low, Med-low, Med-high, and High) were calculated by unpaired* t*-test with Welch's correction.*
[c]*GSH, glutathione content; GSSG, oxidized glutathione content; GSH + 2GSSG: the total glutathione level; GSH/GSSG, the ratio of reduced glutathione content to oxidized glutathione content; CAT, catalase activity; SOD, superoxide dismutase.*
[a, ab, abc,c] *Treatments with different letters means a significantly difference between treatments by using Tukey's HSD, test,* $p < 0.05$, $N = 6$.

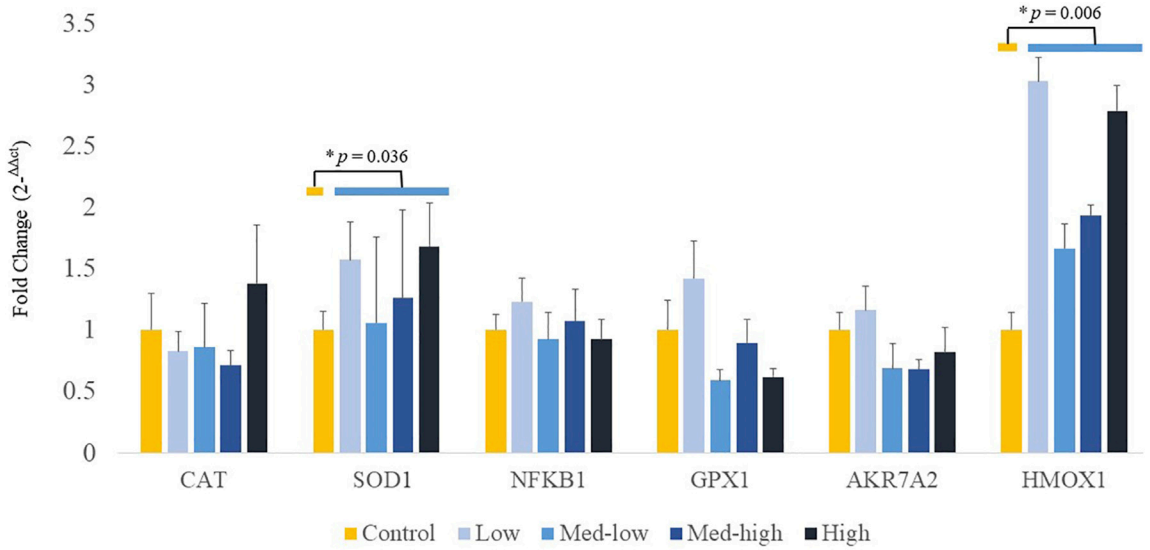

FIGURE 3 | Effects of increasing oocysts dose of *Eimeria* mix on the expression of antioxidant-related transcript genes in bone marrow of broilers. Low, the lowest challenge dose; Med-low, the medium-low challenge dose; Med-high, the medium-high challenge dose; High, the highest challenge dose. CAT, catalase; SOD1, superoxide dismutase 1; NFKB1: nuclear factor kappa B subunit 1; GPX1: glutathione peroxidase 1; HMOX1: heme oxygenase 1; and AKR7A2: aflatoxin aldehyde reductase. [a, ab, b] Treatments with different letters means a significantly difference between treatments by using Tukey's HSD test, $p < 0.05$, N = 6. * a significant difference between non-challenge control and pooled challenge groups (Low, Med-low, Med-high, and High) by using Welch's *t*-test, $p < 0.05$.

TABLE 7 | Superoxide dismutase activity (SOD, U/g), catalase activity (CAT, U/g) and GSH content (μM/g) in the liver at six dpi.

Items[a,b]	Unit	Control	Low	Med-low	Med-High	High	SEM	ANOVA	Non-challenge vs. challenge[c]
SOD	U/g	3,891.0	16,676.5	10,079.2	13,335.7	13,097.8	60.4	0.166	<0.001
CAT	U/g	6749.8	6851.56	4,361.84	5,402.07	5,253.27	2029.01	0.778	0.594
GSH	μM/g	11.562[a]	7.876 [ab]	6.710 [ab]	6.374[b]	7.688 [ab]	0.600	0.036	0.091

[a]*Low, the lowest challenge dose; Med-low, the medium-low challenge dose; Med-high, the medium-high challenge dose; High, the highest challenge dose.*
[b]*GSH, glutathione content; CAT, catalase activity; and SOD, superoxide dismutase.*
[c]*The comparisons between non-challenge control and pooled challenged grops (Low, Med-low, Med-high, and High) were calculated by unpaired* t*-test with Welch's correction.*
[a,ab,b] *Treatments with different letters means a significantly difference between treatments by using Tukey's HSD, test,* $p < 0.05$, $N = 6$.

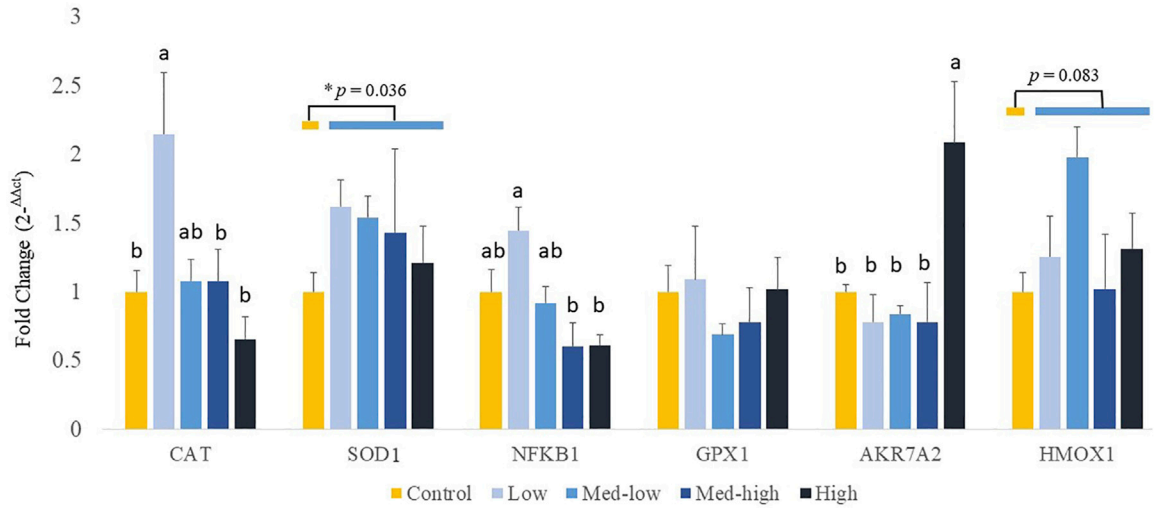

FIGURE 4 | Effects of increasing oocysts dose of *Eimeria* mix on antioxidant-related transcripts gene expression in the liver of broilers. Low, the lowest challenge dose; Med-low, the medium-low challenge dose; Med-high, the medium-high challenge dose; High, the highest challenge dose. CAT, catalase; SOD1, superoxide dismutase 1; NFKB1, nuclear factor kappa B subunit 1; GPX1, glutathione peroxidase 1; HMOX1, heme oxygenase 1; and AKR7A2, aflatoxin aldehyde reductase. [a, ab, b] Treatments with different letters means a significantly difference between treatments by using Tukey's HSD test, $p < 0.05$, N = 6. ***** a significant difference between non-challenge control and pooled challenge groups (Low, Med-low, Med-high, and High) by using Welch's *t*-test, $p < 0.05$.

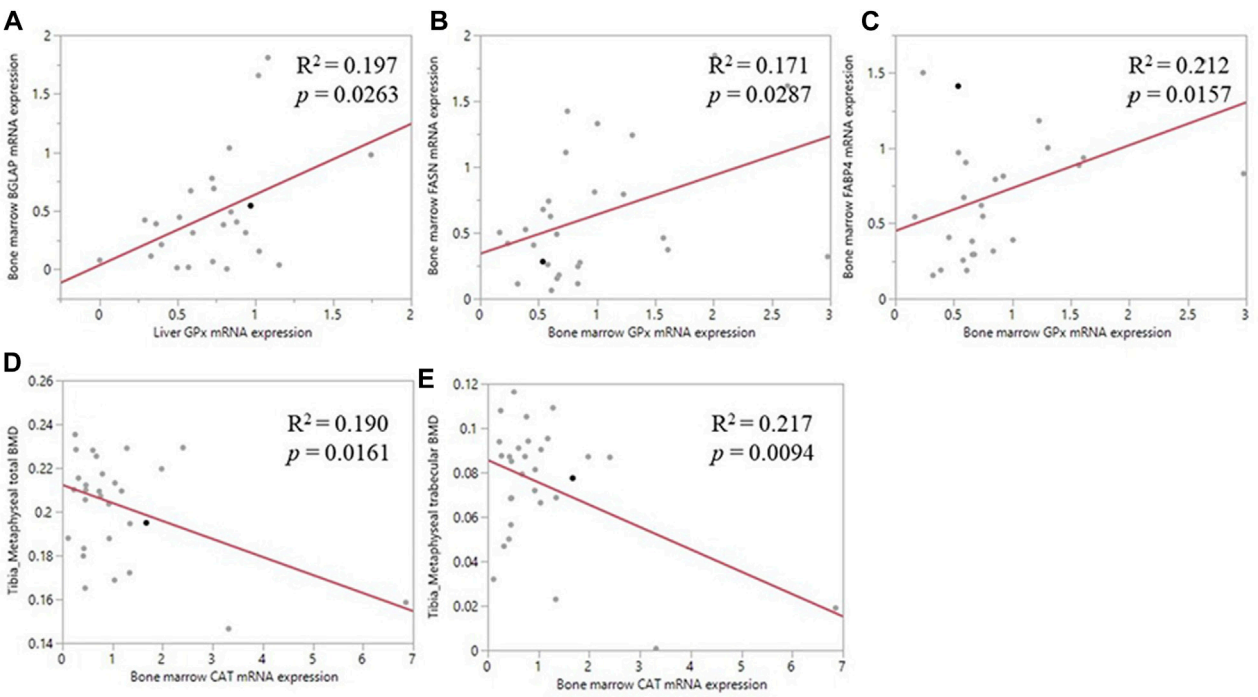

FIGURE 5 | Correlation of antioxidant enzyme mRNA expression and bone related parameters. **(A)** The positive correlation between liver *GPX1* mRNA level and the bone marrow *BGLAP* mRNA expression **(B)** The positive correlation between bone marrow *GPX1* mRNA expression and the bone marrow *FASN* mRNA expression **(C)** The positive correlation between bone marrow *GPX1* mRNA expression and the between bone marrow *FABP4* mRNA expression **(D)** The negative correlation between bone marrow *CAT* mRNA expression and tibia metaphyseal total BMD **(E)** The negative correlation between bone marrow *CAT* mRNA expression and tibia metaphyseal trabecular BMD.

dose of *Eimeria* oocysts upregulated the expression of *AKR7A2* (ANOVA, $p = 0.006$; linear regression, $p = 0.002$, $R^2 = 0.434$). The low challenge dose of *Eimeria* oocysts resulted in significantly higher *NFKB1* expression, compared to the Med-high and the High group (ANOVA, $p = 0.002$; linear regression, $p = 0.006$, $R^2 = 0.263$). No significant differences in the expression of *SOD1*, *GPX1*, and *HMOX1* were evident among the challenge doses ($p > 0.100$). By comparing infected groups with the non-infected Control, a significant higher level of *SOD1* ($p = 0.036$) and a numeric higher level of *HMOX1* ($p = 0.083$) were detected in the *Eimeria*-infected groups.

Correlation Between Antioxidant Enzymes Level and Bone Parameters

Pearson correlation analyses revealed a positive correlation between the liver *GPX1* mRNA level and bone marrow *BGLAP* mRNA level ($R^2 = 0.197$, $p = 0.026$; **Figure 5A**); between bone marrow *GPX1* mRNA and bone marrow *FASN* mRNA expression ($R^2 = 0.171$, $p = 0.029$; **Figure 5B**); and between bone marrow *GPX1* mRNA and bone marrow *FABP4* mRNA expression ($R^2 = 0.212$, $p = 0.016$; **Figure 5C**). Meanwhile, bone marrow *CAT* mRNA level was negatively correlated with tibia metaphyseal BMD ($R^2 = 0.190$, $p = 0.016$; **Figure 5D**) and trabecular BMD ($R^2 = 0.217$, $p = 0.009$; **Figure 5E**).

DISCUSSION

Based on current data, we concluded that high challenge dose of *Eimeria* infection negatively affected the long bone development. The structural changes of tibia and decreased mineral content were mainly located at the trabecular bone of metaphyseal area. The change of redox and impaired antioxidant status following the *Eimeria* infection were observed in the liver and bone marrow of broilers. Compared with the slower growing strains of broilers, bone formation and turnover are extremely rapid in the modern strains (Yair et al., 2017), that fast body weight gain places challenges to bone health in the modern broiler industry (Edwards, 2000; Fleming, 2008; Wideman, 2016; (Schmidt et al., 2009; Alrubaye et al., 2020). The rapid bone growth results in decreased mineral density, increased cortical porosity, and altered biomechanical properties of long bone in the modern broiler strains (Williams et al., 2004), that is partly responsible for broiler leg bone disorder that restricts the growth of broiler. Long bone homeostasis is closely associated intrinsic and extrinsic factors including nutrition status, physical stress (mechanical loading), immune status, hormonal status, genetics, management, and age of animals (Fleming, 2008; Rokavec and Zupan Semrov, 2020; Cao et al., 2021). Therefore, we propose that bone traits can be used as a dynamic indicator for growth and health status of poultry.

Bone is made up of two components: the organic matrix and the inorganic matrix (Rath and Durairaj, 2022). Crystals of calcium phosphate make up the bulk of the inorganic matrix, which is eventually counted as bone mineral content. The inorganic mineral content is the major component of the bone that provides stiffness and strength to the bone (Eliaz and Metoki, 2017), where quantitate bone mineral content is the easiest and most common way to reflect the bone health status. To date, researchers have conventionally focused on the changes in bone mineral content and density after *Eimeria* infection (Fetterer et al., 2013; Akbari Moghaddam Kakhki et al., 2019; Oikeh et al., 2019). Bone microarchitecture is a predictor for evaluating bone quality and health independent of bone mineral content (Brandi, 2009; Chen and Kim, 2020). However, few data exist on the poultry bone microstructure changes after *Eimeria* infection. Micro-CT is a precise and non-destructive evaluation approach that can provide a comprehensive overview of the morphological and architectural characteristics in poultry bones (Chen and Kim, 2020). In the current study, micro-CT was used in assessing the three-dimensional structure, which provides in-depth understanding behind the relationship between changes of bone traits and *Eimeria* infection. We mainly evaluated those parameters representing metaphyseal bone traits to reflect earlier bone changes under *Eimeria* spp. infection, because acute trabecular bone loss following infectious diseases or bone damage occurred almost exclusively within the metaphyseal compartment in human and poultry (Mubarak et al., 2009; Raehtz et al., 2018). Consistent with previous findings (Akbari Moghaddam Kakhki et al., 2019; Oikeh et al., 2019), the present results showed that a significant reduction in tibia metaphyseal bone mineral content and bone mineral density in the *Eimeria*-challenged groups, especially in the High challenge group of broilers as compared to the non-infected Control, demonstrated the impaired metaphyseal trabecular microstructure under parasite infection. The organization of the trabecular bone is not only a key to bone strength but also plays an important role in metabolic function (Seifert and Watkins, 1997). The trabecular bones are organized as a lattice structure that provides larger surface areas for osteoclast attachment, showing a higher turnover rate during bone resorption compared with cortical bones in rodent or human study (Baron et al., 1984; Qiu et al., 2019). Previous studies in mouse displayed a decreased total bone BV/TV, trabecular BV/TV, and trabecular BS, which indicated an accelerated trabecular bone turnover (Boskey and Imbert, 2017). As for both whole metaphyseal structure and trabecular bone structure in the current study, there were no statistical changes in bone mass (BV or TV) with different *Eimeria*-challenge dosages, whereas the total bone BMD and trabecular bone BMD were negatively correlated with increased inoculation doses of oocysts, and BMC decreased correspondingly. In the present study, the lower bone mineral content and density, and changed ratio of BV/TV at metaphyseal trabecular bone could be the outcome of trabecular bone remodeling in the High dose of *Eimeria* challenge group. Trabecular microstructure assay in this study also showed significant decreases in trabecular number (Tb. N) and connectivity density (Conn. Dn), and significant increases in SMI in tibia metaphyseal trabecular bone by *Eimeria* spp. challenge. The similar alteration of bone microstructures is also known in human bone microfracture, where small fractions that resulted from trauma, physical stress, or infection (Prat-Fabregat and Camacho-Carrasco, 2016;

Solomon et al., 2018). Bone trabecular microstructure traits such as SMI was designed to estimate the rod or plate-like trabecular geometry which describes the trabecular network (Hildebrand and Ruegsegger, 1997). Evaluation of SMI across human and rat studies suggests that higher SMI values represent a rod-like trabecular structure that indicates a poor weight-bearing ability; this structure could be observed in osteoporosis disease models (Borah et al., 2004; Akhter et al., 2007). Higher SMI values and lower numbers of trabeculae indicated a poor trabecular bone architecture in human (Greenwood et al., 2015). As for the current study, a higher SMI and lower number of trabeculae pointed out the poor-quality of the trabecular bone in *Eimeria* challenge groups, indicating that the bone mineral loss might have happened before any observation of phenotype abnormality of tibia bone during the *Eimeria* infection. At 19 days of age, the body weight of the broiler has yet to cause mechanical trauma on the tibia, thereby the immune response, nutrient deficiency or immune response associated energy cost resulted in the long bone structure abnormality and bone mineral loss. Although changes in bone microstructure during *Eimeria* infection may not necessarily cause bone damage during growth, it potentially enhances the risk of bone damage and the susceptibility to bone disease, with certain mechanical triggering and severe intestinal bacterial infection (Prisby et al., 2014; Wideman, 2016). Moreover, in the current study, the mRNA expression of bone related proteins in bone marrow is also in line with the micro-CT morphological observation. A reciprocal relationship between a key osteogenic marker, *BGLAP,* and a key adipogenic marker, *PPARG* was observed in the Med-high group that were challenged with second highest dose of *Eimeria* oocytes. Bone marrow adipose tissue content has adverse effects on bone quality and can serve as a relevant marker of a compromised bone integrity (Hardouin et al., 2016; Sundh et al., 2016; Kim et al., 2017). Previous studies indicated that higher *PPARG* expression could direct the mesenchymal stem cells (MSCs) differentiated into adipocytes instead of osteoblasts *in vitro* (Shockley et al., 2009; Hu et al., 2018). In the present study, the suppressed expression of *BGLAP* and increased expression of *PPARG* both indicated the impetus of fat growth instead of bone formation during *Eimeria* infection, confirming the negative impact of *Eimeria* infection on bone health from mRNA level. However, by *Eimeria* infection and intestinal damage, the dietary lipid malabsorption and low nutrient levels in high challenge dosage groups might predispose the suppression of fatty acid synthesis by decreasing the expression of *FASN* in bone marrow.

Broiler bone majorly develops in the first 3 weeks of life (Lilburn et al., 1994; Williams et al., 2000), which overlaps with the timeline when the oocyst shedding rapid accumulated (Chapman et al., 2014). For the etiology of bone loss after *Eimeria* infection, other than the main factors such as physical stress or nutritional deficiency, accumulating data documented the interaction between immune response, oxidative stress and bone mineral loss due to the crosstalk between the skeletal and the immune systems, and the important biological role of ROS in a variety of physiological systems (Takayanagi, 2007; Lorenzo et al., 2008). Reactive species play an important role in immune response. As for innate immunity, immune cells such as macrophages and neutrophils (heterophils in avian species) utilized phagocytic oxidative burst to destruct pathogens (Lauridsen, 2019; Mishra and Jha, 2019). However, unregulated ROS can damage host tissue homeostasis (Costantini and Moller 2009; Rehman et al., 2018). Coccidiosis can cause severe oxidative stress that elevates intracellular levels of reactive oxygen species (ROS) in broiler and other species (Sepp et al., 2012; Abdel-Haleem et al., 2017). *In vitro* studies in human and mouse cells have shown that ROS is an important activator for various cell signaling pathways, mediated MSCs differentiation and cell fate (Yang et al., 2013; Atashi et al., 2015). Accumulating evidence suggesting the alteration of the redox state causes systemic changes that can coordinate osteoblast differentiation or osteoclast activity that relat to the bone remodeling process in human and animal models (Domazetovic et al., 2017; Schreurs et al., 2020; Sheppard et al., 2022). The supplementation of trace minerals can alleviate the negative effect of oxidative stress and optimize the bone quality in human and broilers (Santos et al., 2020; Savaram Venkata et al., 2021). Infection with *E. tenella* or *E. acervulina* could increase serum CAT activity while it decreases serum GPX activity in broilers (Georgieva et al., 2006). In the present study, the changes in antioxidant enzyme activity and level of mRNA expression in the liver and bone marrow displayed a systemic oxidative stress in broilers after *Eimeria* infection. Moreover, significantly lower GSH levels were observed in the liver of *Eimeria* infected birds. The decreased defensive antioxidant abilities in higher *Eimeria* challenge dosage groups could partially be related to reduced intestinal absorption of antioxidants (Georgieva et al., 2006; Abdel-Haleem et al., 2017; Mishra and Jha, 2019). Moreover, in the present study, the mRNA expression pf *HMOX1* was upregulated by *Eimeria* infection. HMOX plays essential roles against oxidative stress by balancing body's systemic iron homeostasis and inflammation response (Otterbein and Choi, 2000; Immenschuh et al., 2010). *In vitro* studies have shown that upregulated *HMOX*1 inhibited the maturation and mineralization of osteoblasts (Lin et al., 2010), and HMOX enzyme was involved in the response of bone marrow macrophages to RANKL, which is an essential pathway for osteoclast formation (Florczyk-Soluch et al., 2018). Thus, the increased mRNA expression of *HMOX1* in bone marrow may be associated with oxidative- or inflammation-induced bone loss by either increasing the activity of osteoclast formation, inhibiting maturation of osteoblast, or both.

Unlike previous results that enzymatic antioxidant SOD was remarkably decreased in chicken serum in most cases of *Eimeria* spp. infection (Georgieva et al., 2006), we found the enzyme activity of SOD and mRNA expression of *SOD1* were significantly increased in the liver and bone marrow. Previous researchers have established that SOD has immunomodulatory function, and SOD3 is reported to downregulate several signaling cascades including nuclear factor kappa B (NFKB) transcription factors, thereby constraining the inflammatory responses in MSCs (Sah et al., 2020). In the present study, significantly downregulated mRNA expression of NFKB1 was coupled with upregulated mRNA expression of *SOD1* in the liver, indicating the constraining of inflammatory responses. SODs also play

significant role in MSCs differentiation and function (Nightingale et al., 2012; Shi et al., 2019). An *in vitro* study of human MSCs reported that the expression of *SOD3* was significantly increased under adipogenic differentiation, and overexpression of *SOD3* in MSCs promoted adipogenic differentiation of MSCs *in vitro* instead of osteogenic differentiation (Nightingale et al., 2012). Therefore, the increased SOD enzyme activity, increased mRNA expression of *SOD1*, and increased expression of *PPARG* both in the present study indicated that oxidative stress caused by *Eimeria* infection tilts the balance of MSC lineage specific differentiation in bone marrow more toward the adipogeneic differentiation.

Another crucial enzyme antioxidant, catalase (CAT), has been described as an important enzyme implicated in inflammation conditions (Georgieva et al., 2006). In present study, mRNA expression and activity of *CAT* were negatively correlated with higher challenge dose of *Eimeria* spp. in the liver. The Low group showed a higher level of *CAT* mRNA expression when compared with the Control, but higher *Eimeria* infection dosage did not change the expression of *CAT* in the liver. In bone marrow, mRNA expression of *CAT* was positively correlated with higher challenge dose of *Eimeria* spp. in bone marrow, where this result is similar with other studies that *Eimeria* infection decreased serum GPX activity but increased serum CAT activity (Georgieva et al., 2006; Georgieva et al., 2011). However, the enzyme activity of CAT in bone marrow was not affected by *Eimeria* spp. infection at six dpi, suggested that bone marrow is not a CAT active site during *Eimeria* infection, but lower level of *Eimeria* infection can stimulate synthesis of enzymatic antioxidant in bone marrow (Zhang et al., 2019). The high dose of inoculation might lead to apoptotic cell death that negatively impacts on protein level and mRNA level of CAT (Saha et al., 2020). Furthermore, the correlation analysis indicated that liver *GPX1* mRNA expression is positively correlated with bone marrow *BGLAP* mRNA expression, whereas bone marrow *CAT* mRNA expression was negatively correlated with tibia metaphysis BMD, emphasizing that the negative impact of *Eimeria* infection on bone quality might be associated with the occurrence of oxidative stress. However, while nutritional factors and animal husbandry play significant roles in determining antioxidant status and bone homeostasis**,** *in vitro* animal model is hard to provide direct evidence to explain the interaction between oxidative stress and bone remodeling in broilers. Further studies require comprehensive *in vitro* and in *ovo* investigation, which is necessary to confirm the functional significance of antioxidants in bone homeostasis, especially under parasite challenge models.

Recent studies also indicated that the immune status of individuals promoted the process of osteoclastic bone resorption that resulted in bone mineral loss, which is defined as osteoimmunology (Kamibayashi et al., 1995; Solomon et al., 2018). For example, in human clinical studies, the long-term investigation showed bone microarchitectural changes under infection of C virus (HCV), which increased the risk of fracture (Bedimo et al., 2018). Acute malaria infection severely suppresses bone homeostasis, which leads to increased RANKL expression and overstimulation of osteoclastogenesis which favors bone resorption (Lee et al., 2017). Trabecular bone microstructure is impaired in the proximal femur of human immunodeficiency virus-infected (HIV) men with normal bone mineral density (Kazakia et al., 2018). Decreased bone mass and abnormality in trabecular and cortical microarchitecture were observed in young men infected with HIV early in life (Yin et al., 2014). Related reports are very limited in poultry studies. Studies of acute inflammatory response caused by lipopolysaccharides (LPS) injection suppressed growth performance and altered bone homeostasis, which significantly decreased body weight and tibia breaking strength (Mireles et al., 2005). Immunosuppressive doses of dexamethasone triggered high incidences of turkey osteomyelitis complex in turkey poults and bone lesions in broilers (Wideman and Pevzner, 2012). All those studies indicated the link between health status and bone remodeling in broilers, suggesting immune status must be considered as another critical factor in the pathogenesis of bone abnormities under intestinal parasite infection.

DATA AVAILABILITY STATEMENT

The original contributions presented in the study are included in the article/Supplementary Materials, further inquiries can be directed to the corresponding author.

ETHICS STATEMENT

The animal study was reviewed and approved by The Institutional Animal Care and Use Committee at the University of Georgia.

AUTHOR CONTRIBUTIONS

All authors listed have made a substantial, direct and intellectual contribution to the work, and approved it for publication. YT, PT and WK conceived and designed this study. YT and PT contributed to broilers husbandry and sample collection, YT contributed to qRT-PCR, micro-CT assay and data analyses. RP contributed to HPLC assay. The paper was written through contribution and critical review of the manuscript by all authors (YT, PT, RP, and WK).

FUNDING

This study was financed in part by a cooperative agreement 58-6040-8-034 from United States Department of Agriculture-Agricultural Research Service.

REFERENCES

Abdel-Haleem, H. M., Aboelhadid, S. M., Sakran, T., El-Shahawy, G., El-Fayoumi, H., Al-Quraishy, S., et al. (2017). Gene Expression, Oxidative Stress and Apoptotic Changes in Rabbit Ileum Experimentally Infected with *Eimeria* Intestinalis. *Folia Parasitol. (Praha)* 64. 012. doi:10.14411/fp.2017.012

Adhikari, R., Chen, C., and Kim, W. K. (2020). Effect of 20(S)-hydroxycholesterol on Multilineage Differentiation of Mesenchymal Stem Cells Isolated from Compact Bones in Chicken. *Genes (Basel)* 11 (11), 1360. doi:10.3390/genes11111360

Akbari Moghaddam Kakhki, R., Lu, Z., Thanabalan, A., Leung, H., Mohammadigheisar, M., and Kiarie, E. (2019). *Eimeria* Challenge Adversely Affected Long Bone Attributes Linked to Increased Resorption in 14-Day-Old Broiler Chickens. *Poult. Sci.* 98 (4), 1615–1621. doi:10.3382/ps/pey527

Akhter, M. P., Lappe, J. M., Davies, K. M., and Recker, R. R. (2007). Transmenopausal Changes in the Trabecular Bone Structure. *Bone* 41 (1), 111–116. doi:10.1016/j.bone.2007.03.019

Alrubaye, A. A. K., Ekesi, N. S., Hasan, A., Koltes, D. A., Wideman, R. F., Jr., and Rhoads, D. D. (2020). Chondronecrosis with Osteomyelitis in Broilers: Further Defining a Bacterial Challenge Model Using Standard Litter Flooring and Protection with Probiotics. *Poult. Sci.* 99, 6474–6480. doi:10.1016/j.psj.2020.08.067

Amerah, A. M., and Ravindran, V. (2015). Effect of Coccidia Challenge and Natural Betaine Supplementation on Performance, Nutrient Utilization, and Intestinal Lesion Scores of Broiler Chickens Fed Suboptimal Level of Dietary Methionine. *Poult. Sci.* 94 (4), 673–680. doi:10.3382/ps/pev022

Arczewska-Wlosek, A., Swiatkiewicz, S., Ognik, K., and Jozefiak, D. (2018). Effect of Dietary Crude Protein Level and Supplemental Herbal Extract Blend on Selected Blood Variables in Broiler Chickens Vaccinated against Coccidiosis. *Anim. (Basel)* 8 (11). doi:10.3390/ani8110208

Atashi, F., Modarressi, A., and Pepper, M. S. (2015). The Role of Reactive Oxygen Species in Mesenchymal Stem Cell Adipogenic and Osteogenic Differentiation: a Review. *Stem Cells Dev.* 24, 1150–1163. doi:10.1089/scd.2014.0484

Baron, R., Tross, R., and Vignery, A. (1984). Evidence of Sequential Remodeling in Rat Trabecular Bone: Morphology, Dynamic Histomorphometry, and Changes during Skeletal Maturation. *Anat. Rec.* 208 (1), 137–145. doi:10.1002/ar.1092080114

Basu, S., Michaëlsson, K., Olofsson, H., Johansson, S., and Melhus, H. (2001). Association between Oxidative Stress and Bone Mineral Density. *Biochem. Biophysical Res. Commun.* 288 (1), 275–279. doi:10.1006/bbrc.2001.5747

Bedimo, R. J., Adams-Huet, B., Poindexter, J., Brown, G., Farukhi, I., Castanon, R., et al. (2018). The Differential Effects of Human Immunodeficiency Virus and Hepatitis C Virus on Bone Microarchitecture and Fracture Risk. *Clin. Infect. Dis.* 66 (9), 1442–1447. doi:10.1093/cid/cix1011

Blake, D. P., Knox, J., Dehaeck, B., Huntington, B., Rathinam, T., Ravipati, V., et al. (2020). Re-calculating the Cost of Coccidiosis in Chickens. *Vet. Res.* 51, 115. doi:10.1186/s13567-020-00837-2

Blake, D. P., and Tomley, F. M. (2014). Securing Poultry Production from the Ever-Present Eimeria Challenge. *Trends Parasitol.* 30 (1), 12–19. doi:10.1016/j.pt.2013.10.003

Borah, B., Dufresne, T. E., Chmielewski, P. A., Johnson, T. D., Chines, A., and Manhart, M. D. (2004). Risedronate Preserves Bone Architecture in Postmenopausal Women with Osteoporosis as Measured by Three-Dimensional Microcomputed Tomography. *Bone* 34 (4), 736–746. doi:10.1016/j.bone.2003.12.013

Boskey, A. L., and Imbert, L. (2017). Bone Quality Changes Associated with Aging and Disease: a Review. *Ann. N.Y. Acad. Sci.* 1410 (1), 93–106. doi:10.1111/nyas.13572

Bouxsein, M. L., Boyd, S. K., Christiansen, B. A., Guldberg, R. E., Jepsen, K. J., and Müller, R. (2010). Guidelines for Assessment of Bone Microstructure in Rodents Using Micro-computed Tomography. *J. Bone Min. Res.* 25, 1468–1486. doi:10.1002/jbmr.141

Brandi, M. L. (2009). Microarchitecture, the Key to Bone Quality. *Rheumatol. Oxf.* 48 (4), iv3–8. doi:10.1093/rheumatology/kep273

Cao, S., Li, T., Shao, Y., Zhang, L., Lu, L., Zhang, R., et al. (2021). Regulation of Bone Phosphorus Retention and Bone Development Possibly by Related Hormones and Local Bone-Derived Regulators in Broiler Chicks. *J. Anim. Sci. Biotechnol.* 12 (1), 88. doi:10.1186/s40104-021-00610-1

Cervantes, H. M. (2015). Antibiotic-free Poultry Production: Is it Sustainable? *J. Appl. Poult. Res.* 24 (1), 91–97. doi:10.3382/japr/pfv006

Chapman, H. D. (2014). Milestones in Avian Coccidiosis Research: a Review. *Poult. Sci.* 93, 501–511. doi:10.3382/ps.2013-03634

Chen, C., and Kim, W. K. (2020). The Application of Micro-CT in Egg-Laying Hen Bone Analysis: Introducing an Automated Bone Separation Algorithm. *Poult. Sci.* 99, 5175–5183. doi:10.1016/j.psj.2020.08.047

Chen, C., White, D. L., Marshall, B., and Kim, W. K. (2021). Role of 25-Hydroxyvitamin D3 and 1,25-Dihydroxyvitamin D3 in Chicken Embryo Osteogenesis, Adipogenesis, Myogenesis, and Vitamin D3 Metabolism. *Front. Physiol.* 12, 637629.

Cobb (2019). *Role of 25-Hydroxyvitamin D3 and 1,25-Dihydroxyvitamin D3 in Chicken Embryo Osteogenesis, Adipogenesis, Myogenesis, and Vitamin D3 Metabolism*. Siloam Springs, AR: Cobb-Vantress.

Costantini, D., and Møller, A. P. (2009). Does Immune Response Cause Oxidative Stress in Birds? A Meta-Analysis. *Comp. Biochem. Physiology Part A Mol. Integr. Physiology* 153, 339–344. doi:10.1016/j.cbpa.2009.03.010

Dalloul, R. A., and Lillehoj, H. S. (2006). Poultry Coccidiosis: Recent Advancements in Control Measures and Vaccine Development. *Expert Rev. Vaccines* 5 (1), 143–163. doi:10.1586/14760584.5.1.143

Domazetovic, V., Marcucci, G., Iantomasi, T., Brandi, M. L., and Vincenzini, M. T. (2017). Oxidative Stress in Bone Remodeling: Role of Antioxidants. *ccmbm* 14, 209–216. doi:10.11138/ccmbm/2017.14.1.209

Edwards, H. M. (2000). Nutrition and Skeletal Problems in Poultry. *Poult. Sci.* 79 (7), 1018–1023. doi:10.1093/ps/79.7.1018

Eliaz, N., and Metoki, N. (2017). Calcium Phosphate Bioceramics: A Review of Their History, Structure, Properties, Coating Technologies and Biomedical Applications. *Mater. (Basel)* 10 (4). 334, doi:10.3390/ma10040334

Estévez, M. (2015). Oxidative Damage to Poultry: from Farm to Fork. *Poult. Sci.* 94, 1368–1378. doi:10.3382/ps/pev094

Fetterer, R. H., Miska, K. B., Mitchell, A. D., and Jenkins, M. C. (2013). The Use of Dual-Energy X-Ray Absorptiometry to Assess the Impact of Eimeria Infections in Broiler Chicks. *Avian Dis.* 57(2), 199–204.

Fleming, R. H. (2008). Nutritional Factors Affecting Poultry Bone Health. *Proc. Nutr. Soc.* 67 (2), 177–183. doi:10.1017/s0029665108007015

Florczyk-Soluch, U., Józefczuk, E., Stępniewski, J., Bukowska-Strakova, K., Mendel, M., Viscardi, M., et al. (2018). Various Roles of Heme Oxygenase-1 in Response of Bone Marrow Macrophages to RANKL and in the Early Stage of Osteoclastogenesis. *Sci. Rep.* 8, 10797. doi:10.1038/s41598-018-29122-1

Gautier, A. E., Latorre, J. D., Matsler, P. L., and Rochell, S. J. (2019). Longitudinal Characterization of Coccidiosis Control Methods on Live Performance and Nutrient Utilization in Broilers. *Front. Vet. Sci.* 6, 468. doi:10.3389/fvets.2019.00468

Georgieva, N. V., Gabrashanska, M., Koinarski, V., and Yaneva, Z. (2011). Zinc Supplementation against Eimeria Acervulina-Induced Oxidative Damage in Broiler Chickens. *Vet. Med. Int.* 2011, 647124. doi:10.4061/2011/647124

Georgieva, N. V., Koinarski, V., and Gadjeva, V. (2006). Antioxidant Status during the Course of Eimeria Tenella Infection in Broiler Chickens. *Veterinary J.* 172, 488–492. doi:10.1016/j.tvjl.2005.07.016

Gould, R. L., Zhou, Y., Yakaitis, C. L., Love, K., Reeves, J., Kong, W., et al. (2018). Heritability of the Aged Glutathione Phenotype Is Dependent on Tissue of Origin. *Mamm. Genome* 29 (9-10), 619–631. doi:10.1007/s00335-018-9759-2

Greenwood, C., Clement, J. G., Dicken, A. J., Evans, J. P. O., Lyburn, I. D., Martin, R. M., et al. (2015). The Micro-architecture of Human Cancellous Bone from Fracture Neck of Femur Patients in Relation to the Structural Integrity and Fracture Toughness of the Tissue. *Bone Rep.* 3, 67–75. doi:10.1016/j.bonr.2015.10.001

Hardouin, P., Rharass, T., and Lucas, S. (2016). Bone Marrow Adipose Tissue: To Be or Not To Be a Typical Adipose Tissue?. *Front. Endocrinol. (Lausanne)* 7, 85.

Henkelmann, R., Frosch, K.-H., Frosch, K.-H., Glaab, R., Lill, H., Schoepp, C., et al. (2017). Infection Following Fractures of the Proximal Tibia - a Systematic Review of Incidence and Outcome. *BMC Musculoskelet. Disord.* 18 (1), 481. doi:10.1186/s12891-017-1847-z

Hildebrand, T., and Rüegsegger, P. (1997). Quantification of Bone Microarchitecture with the Structure Model Index. *Comput. Methods Biomechanics Biomed. Eng.* 1 (1), 15–23. doi:10.1080/01495739708936692

Hu, L., Yin, C., Zhao, F., Ali, A., Ma, J., and Qian, A. (2018). Mesenchymal Stem Cells: Cell Fate Decision to Osteoblast or Adipocyte and Application in Osteoporosis Treatment. *Int. J. Mol. Sci.* 19(2). 360 doi:10.3390/ijms19020360

Immenschuh, S., Baumgart-Vogt, E., and Mueller, S. (2010). Heme Oxygenase-1 and Iron in Liver Inflammation: a Complex Alliance. *Curr. Drug Targets* 11 (12), 1541–1550. doi:10.2174/1389450111009011541

Joyner, L. P., Patterson, D. S. P., Berrett, S., Boarer, C. D. H., Cheong, F. H., and Norton, C. C. (1975). Amino-acid Malabsorption and Intestinal Leakage of Plasma-Proteins in Young Chicks Infected with *Eimeria Acervulina*. *Avian Pathol.* 4 (1), 17–33. doi:10.1080/03079457508418129

Kamibayashi, L., Wyss, U. P., Cooke, T. D. V., and Zee, B. (1995). Trabecular Microstructure in the Medial Condyle of the Proximal Tibia of Patients with Knee Osteoarthritis. *Bone* 17 (1), 27–35. doi:10.1016/8756-3282(95)00137-3

Kazakia, G. J., Carballido-Gamio, J., Lai, A., Nardo, L., Facchetti, L., Pasco, C., et al. (2018). Trabecular Bone Microstructure Is Impaired in the Proximal Femur of Human Immunodeficiency Virus-Infected Men with Normal Bone Mineral Density. *Quant. Imaging Med. Surg.* 8 (1), 5–13. doi:10.21037/qims.2017.10.10

Kim, T. Y., Schwartz, A. V., Li, X., Xu, K., Black, D. M., Petrenko, D. M., et al. (2017). Bone Marrow Fat Changes After Gastric Bypass Surgery Are Associated With Loss of Bone Mass. *J. Bone Miner. Res.* 32 (11), 2239–2247.

Lauridsen, C. (2019). From Oxidative Stress to Inflammation: Redox Balance and Immune System. *Poult. Sci.* 98, 4240–4246. doi:10.3382/ps/pey407

Lee, M. S. J., Maruyama, K., Fujita, Y., Konishi, A., Lelliott, P. M., Itagaki, S., et al. (2017). Plasmodium Products Persist in the Bone Marrow and Promote Chronic Bone Loss. *Sci. Immunol.* 2 (12). eaam8093, doi:10.1126/sciimmunol.aam8093

Lee, Y., Lee, S.-h., Lee, S.-J., Gadde, U. D., Oh, S.-T., Han, H., et al. (2018). Effects of Dietary Allium Hookeri Root on Growth Performance and Antioxidant Activity in Young Broiler Chickens. *Res. Veterinary Sci.* 118, 345–350. doi:10.1016/j.rvsc.2018.03.007

Lilburn, M. S. (1994). Skeletal Growth of Commercial Poultry Species. *Poult. Sci.* 73 (6), 897–903.

Lin, T. H., Tang, C. H., Hung, S. Y., Liu, S. H., Lin, Y. M., Fu, W. M., et al. (2010). Upregulation of Heme Oxygenase-1 Inhibits the Maturation and Mineralization of Osteoblasts. *J. Cell. Physiol.* 222, 757–768. doi:10.1002/jcp.22008

Livak, K. J., and Schmittgen, T. D. (1994). Analysis of Relative Gene Expression Data Using Real-Time Quantitative PCR and the 2(-Delta Delta C(T)) Method. *Methods* 25 (4), 402–408.

Lorenzo, J., Horowitz, M., and Choi, Y. (2008). Osteoimmunology: Interactions of the Bone and Immune System. *Endocr. Rev.* 29 (4), 403–440.

Mireles, A. J., Kim, S. M., and Klasing, K. C. (2005). An Acute Inflammatory Response Alters Bone Homeostasis, Body Composition, and the Humoral Immune Response of Broiler Chickens. *Poult. Sci.* 84, 553–560. doi:10.1093/ps/84.4.553

Mishra, B., and Jha, R. (2019). Oxidative Stress in the Poultry Gut: Potential Challenges and Interventions. *Front. Vet. Sci.* 6, 60. doi:10.3389/fvets.2019.00060

Mubarak, S. J., Kim, J. R., Edmonds, E. W., Pring, M. E., and Bastrom, T. P. (2009). Classification of Proximal Tibial Fractures in Children. *J. Pediatr. Orthop.* 3, 191–197. doi:10.1007/s11832-009-0167-8

Nightingale, H., Kemp, K., Gray, E., Hares, K., Mallam, E., Scolding, N., et al. (2012). Changes in Expression of the Antioxidant Enzyme SOD3 Occur Upon Differentiation of Human Bone Marrow-Derived Mesenchymal Stem Cells *In Vitro*. *Stem Cells Dev.* 21 (11), 2026–2035.

Oh, S., Lillehoj, H. S., Lee, Y., Bravo, D., and Lillehoj, E. P. (2019). Dietary Antibiotic Growth Promoters Down-Regulate Intestinal Inflammatory Cytokine Expression in Chickens Challenged with Lps or Co-infected with Eimeria Maxima and clostridium Perfringens. *Front. Vet. Sci.* 6, 420. doi:10.3389/fvets.2019.00420

Oikeh, I., Sakkas, P., Blake, D. P., and Kyriazakis, I. (2019). Interactions between Dietary Calcium and Phosphorus Level, and Vitamin D Source on Bone Mineralization, Performance, and Intestinal Morphology of Coccidia-Infected Broilers. *Poult. Sci.* 98 (11), 5679–5690. doi:10.3382/ps/pez350

Otterbein, L. E., and Choi, A. M. K. (2000). Heme Oxygenase: Colors of Defense against Cellular Stress. *Am. J. Physiology-Lung Cell. Mol. Physiology* 279, L1029–L1037. doi:10.1152/ajplung.2000.279.6.l1029

Park, H. J., Mah, E., and Bruno, R. S. (2010). Validation of High-Performance Liquid Chromatography-Boron-Doped Diamond Detection for Assessing Hepatic Glutathione Redox Status. *Anal. Biochem.* 407 (2), 151–159. doi:10.1016/j.ab.2010.08.012

Prat-Fabregat, S., and Camacho-Carrasco, P. (2016). Treatment Strategy for Tibial Plateau Fractures: an Update. *EFORT Open Rev.* 1 (5), 225–232. doi:10.1302/2058-5241.1.000031

Prisby, R., Menezes, T., Campbell, J., Benson, T., Samraj, E., Pevzner, I., et al. (2014). Kinetic Examination of Femoral Bone Modeling in Broilers. *Poult. Sci.* 93 (5), 1122–1129. doi:10.3382/ps.2013-03778

Qiu, Y., Tang, C., Serrano-Sosa, M., Hu, J., Zhu, J., Tang, G., et al. (2019). Bone Microarchitectural Parameters Can Detect Oxytocin Induced Changes Prior to Bone Density on Mitigating Bone Deterioration in Rabbit Osteoporosis Model Using Micro-CT. *BMC Musculoskelet. Disord.* 20 (1), 560. doi:10.1186/s12891-019-2861-0

Raehtz, S., Hargis, B. M., Kuttappan, V. A., Pamukcu, R., Bielke, L. R., and McCabe, L. R. (2018). High Molecular Weight Polymer Promotes Bone Health and Prevents Bone Loss under Salmonella Challenge in Broiler Chickens. *Front. Physiol.* 9, 384. doi:10.3389/fphys.2018.00384

Rath, N. C., and Durairaj, V. (2022). *Avian Bone Physiology and Poultry Bone Disorders" in Sturkie's Avian Physiology*. San Diego: Academic Press, 529–543.

Rehman, Z. U., Meng, C., Sun, Y., Safdar, A., Pasha, R. H., Munir, M., et al. (2018). Oxidative Stress in Poultry: Lessons from the Viral Infections. *Oxid. Med. Cell Longev.*, 2018(8), 1–514. doi:10.1155/2018/5123147

Rokavec, N., and Zupan Semrov, M. (2020). Psychological and Physiological Stress in Hens With Bone Damage. *Front. Vet. Sci.* 7, 589274.

Saha, S., Buttari, B., Panieri, E., Profumo, E., and Saso, L. (2020). An Overview of Nrf2 Signaling Pathway and its Role in Inflammation. *Molecules* 25(22). 5474 doi:10.3390/molecules25225474

Sakkas, P., Oikeh, I., Blake, D. P., Nolan, M. J., Bailey, R. A., Oxley, A., et al. (2018). Does Selection for Growth Rate in Broilers Affect Their Resistance and Tolerance to *Eimeria Maxima*? *Veterinary Parasitol.* 258, 88–98. doi:10.1016/j.vetpar.2018.06.014

Sakkas, P., Oikeh, I., Blake, D. P., Smith, S., and Kyriazakis, I. (2019). Dietary Vitamin D Improves Performance and Bone Mineralisation, but Increases Parasite Replication and Compromises Gut Health in *Eimeria*-Infected Broilers. *Br. J. Nutr.* 122 (6), 676–688. doi:10.1017/s0007114519001375

Santos, T. S. D., Teng, P.-Y., Yadav, S., Castro, F. L. d. S., Gould, R. L., Craig, S. W., et al. (2020). Effects of Inorganic Zn and Cu Supplementation on Gut Health in Broiler Chickens Challenged with *Eimeria* Spp. *Front. Vet. Sci.* 7, 230. doi:10.3389/fvets.2020.00230

Savaram Venkata, R. R., Bhukya, P., Raju, M., and Ullengala, R. (2021). Effect of Dietary Supplementation of Organic Trace Minerals at Reduced Concentrations on Performance, Bone Mineralization, and Antioxidant Variables in Broiler Chicken Reared in Two Different Seasons in a Tropical Region. *Biol. Trace Elem. Res.* 199 (10), 3817–3824.

Schmidt, C. J., Persia, M. E., Feierstein, E., Kingham, B., and Saylor, W. W. (2009). Comparison of a Modern Broiler Line and a Heritage Line Unselected since the 1950s. *Poult. Sci.* 88, 2610–2619. doi:10.3382/ps.2009-00055

Schreurs, A. S., Torres, S., Truong, T., Moyer, E. L., Kumar, A., Tahimic, C. G. T., et al. (2020). Skeletal Tissue Regulation by Catalase Overexpression in Mitochondria. *Am. J. Physiol. Cell Physiol.* 319 (4), C734–C745.

Seifert, M. F., and Watkins, B. A. (1997). Role of Dietary Lipid and Antioxidants in Bone Metabolism. *Nutr. Res.* 17 (7), 1209–1228. doi:10.1016/s0271-5317(97)00090-0

Sepp, T., Karu, U., Blount, J. D., Sild, E., Hõrak, M., and Horak, P. (2012). Coccidian Infection Causes Oxidative Damage in Greenfinches. *PLoS One* 7 (5), e36495. doi:10.1371/journal.pone.0036495

Serdar, C. C., Cihan, M., Yucel, D., and Serdar, M. A. (2021). Sample Size, Power and Effect Size Revisited: Simplified and Practical Approaches in Pre-clinical, Clinical and Laboratory Studies. *Biochem. Medica Cas. Hrvat. Drustva Med. Biokem.* 31, 010502. doi:10.11613/bm.2021.010502

Sheppard, A. J., Barfield, A. M., Barton, S., and Dong, Y. (2022). Understanding Reactive Oxygen Species in Bone Regeneration: a Glance at Potential Therapeutics and Bioengineering Applications. *Front. Bioeng. Biotechnol.* 10, 836764. doi:10.3389/fbioe.2022.836764

Shi, Y., Hu, X., Zhang, X., Cheng, J., Duan, X., Fu, X., et al. (2019). Superoxide Dismutase 3 Facilitates the Chondrogenesis of Bone Marrow-Derived Mesenchymal Stem Cells. *Biochem. Biophys. Res. Commun.* 509 (4), 983–987.

Shockley, K. R., Lazarenko, O. P., Czernik, P. J., Rosen, C. J., Churchill, G. A., and Lecka-Czernik, B. (2009). PPARγ2 Nuclear Receptor Controls Multiple Regulatory Pathways of Osteoblast Differentiation from Marrow Mesenchymal Stem Cells. *J. Cell. Biochem.* 106, 232–246. doi:10.1002/jcb.21994

Solomon, L. B., Kitchen, D., Anderson, P. H., Yang, D., Starczak, Y., Kogawa, M., et al. (2018). Time Dependent Loss of Trabecular Bone in Human Tibial Plateau Fractures. *J. Orthop. Res.* 36 (11), 2865–2875. doi:10.1002/jor.24057

Su, S., Wang, Y., Chen, C., Suh, M., Azain, M., and Kim, W. K. (2020). Fatty Acid Composition and Regulatory Gene Expression in Late-Term Embryos of ACRB and COBB Broilers. *Front. Vet. Sci.* 7, 317. doi:10.3389/fvets.2020.00317

Sundh, D., Rudang, R., Zoulakis, M., Nilsson, A. G., Darelid, A., and Lorentzon, M. (2016). A High Amount of Local Adipose Tissue is Associated With High Cortical Porosity and Low Bone Material Strength in Older Women. *J. Bone Miner. Res.* 31 (4), 749–757.

Surai, P. F., KochishII, Fisinin, V. I., and Kidd, M. T. (2019). Antioxidant Defence Systems and Oxidative Stress in Poultry Biology: An Update. *Antioxidants (Basel)* 8(7), 235. doi:10.3390/antiox8070235

Takayanagi, H. (2007). Osteoimmunology: Shared Mechanisms and Crosstalk Between the Immune and Bone Systems. *Nat. Rev. Immunol.* 7 (4), 292–304.

Teng, P.-Y., Yadav, S., Castro, F. L. d. S., Tompkins, Y. H., Fuller, A. L., and Kim, W. K. (2020). Graded *Eimeria* Challenge Linearly Regulated Growth Performance, Dynamic Change of Gastrointestinal Permeability, Apparent Ileal Digestibility, Intestinal Morphology, and Tight Junctions of Broiler Chickens. *Poult. Sci.* 99, 4203–4216. doi:10.1016/j.psj.2020.04.031

Thiese, M. S., Ronna, B., and Ott, U. (2016). P Value Interpretations and Considerations. *J. Thorac. Dis.* 8, E928–E931. doi:10.21037/jtd.2016.08.16

Turk, D. E. (1973). Calcium Absorption during Coccidial Infections in Chicks. *Poult. Sci.* 52 (3), 854–857. doi:10.3382/ps.0520854

Turk, D. E., and Stephens, J. F. (1969). Coccidial Infections of the Ileum, Colon, and Ceca of the Chick and Nutrient Absorption. *Poult. Sci.* 48 (2), 586–589. doi:10.3382/ps.0480586

Turk, D. E., and Stephens, J. F. (1970). Effects of Serial Inoculations with Eimeria Acervulina or Eimeria Necatrix upon Zinc and Oleic Acid Absorption in Chicks. *Poult. Sci.* 49 (2), 523–526. doi:10.3382/ps.0490523

Turk, D. E., and Stephens, J. F. (1967). Upper Intestinal Tract Infection Produced by E. Acervulina and Absorption of 65Zn and 131I-Labeled Oleic Acid. *J. Nutr.* 93 (2), 161–165. doi:10.1093/jn/93.2.161

Vandesompele, J., De Preter, K., Pattyn, F., Poppe, B., Van Roy, N., De Paepe, A., et al. (2002). Accurate Normalization of Real-Time Quantitative RT-PCR Data by Geometric Averaging of Multiple Internal Control Genes. *Genome Biol.* 3, RESEARCH0034. doi:10.1186/gb-2002-3-7-research0034

Wideman, R. F. (2016). Bacterial Chondronecrosis with Osteomyelitis and Lameness in Broilers: a Review. *Poult. Sci.* 95 (2), 325–344. doi:10.3382/ps/pev320

Wideman, R. F., Jr., and Pevzner, I. (2012). Dexamethasone Triggers Lameness Associated with Necrosis of the Proximal Tibial Head and Proximal Femoral Head in Broilers. *Poult. Sci.* 91 (10), 2464–2474. doi:10.3382/ps.2012-02386

Williams, B., Solomon, S., Waddington, D., Thorp, B., and Farquharson, C. (2000). Skeletal Development in the Meat-Type Chicken. *Br. Poult. Sci.* 41 (2), 141–149.

Williams, B., Waddington, D., Murray, D. H., and Farquharson, C. (2004). Bone Strength During Growth: Influence of Growth Rate on Cortical Porosity and Mineralization. *Calcif. Tissue Int.* 74 (3), 236–245.

Yair, R., Cahaner, A., Uni, Z., and Shahar, R. (2017). Maternal and Genetic Effects on Broiler Bone Properties during Incubation Period. *Poult. Sci.* 96, 2301–2311. doi:10.3382/ps/pex021

Yang, Y., Bazhin, A. V., Werner, J., and Karakhanova, S. (2013). Reactive Oxygen Species in the Immune System. *Int. Rev. Immunol.* 32, 249–270. doi:10.3109/08830185.2012.755176

Yin, M. T., Lund, E., Shah, J., Zhang, C. A., Foca, M., Neu, N., et al. (2014). Lower Peak Bone Mass and Abnormal Trabecular and Cortical Microarchitecture in Young Men Infected with HIV Early in Life. *AIDS* 28 (3), 345–353. doi:10.1097/qad.0000000000000070

Zhang, F., Peng, W., Zhang, J., Dong, W., Yuan, D., Zheng, Y., et al. (2019). New Strategy of Bone Marrow Mesenchymal Stem Cells against Oxidative Stress Injury via Nrf2 Pathway: Oxidative Stress Preconditioning. *J Cell. Biochem.* 120 (12), 19902–19914. doi:10.1002/jcb.29298

Conflict of Interest: The authors declare that the research was conducted in the absence of any commercial or financial relationships that could be construed as a potential conflict of interest.

Publisher's Note: All claims expressed in this article are solely those of the authors and do not necessarily represent those of their affiliated organizations, or those of the publisher, the editors, and the reviewers. Any product that may be evaluated in this article, or claim that may be made by its manufacturer, is not guaranteed or endorsed by the publisher.

frontiers | Frontiers in Physiology

TYPE Original Research
PUBLISHED 08 August 2022
DOI 10.3389/fphys.2022.941134

OPEN ACCESS

EDITED BY
Shu-cheng Huang,
Henan Agricultural University, China

REVIEWED BY
Wen-Chao Liu,
Guangdong Ocean University, China
Zhenlei Zhou,
Nanjing Agricultural University, China
Zhi-Qiang Du,
Yangtze University, China

*CORRESPONDENCE
Mônica Corrêa Ledur,
monica.ledur@embrapa.br

†Present address:
Jorge Augusto Petroli Marchesi,
MercoLab Laboratórios Ltda, Cascavel, Brazil

SPECIALTY SECTION
This article was submitted to Avian Physiology, a section of the journal Frontiers in Physiology

RECEIVED 11 May 2022
ACCEPTED 08 July 2022
PUBLISHED 08 August 2022

CITATION
Ibelli AMG, Peixoto JdO, Zanella R, Gouveia JJdS, Cantão ME, Coutinho LL, Marchesi JAP, Pizzol MSd, Marcelino DEP and Ledur MC (2022), Downregulation of growth plate genes involved with the onset of femoral head separation in young broilers. *Front. Physiol.* 13:941134. doi: 10.3389/fphys.2022.941134

Downregulation of growth plate genes involved with the onset of femoral head separation in young broilers

Adriana Mércia Guaratini Ibelli[1,2], Jane de Oliveira Peixoto[1,2], Ricardo Zanella[3], João José de Simoni Gouveia[4], Maurício Egídio Cantão[1], Luiz Lehmann Coutinho[5], Jorge Augusto Petroli Marchesi[6†], Mariane Spudeit dal Pizzol[7], Débora Ester Petry Marcelino[8] and Mônica Corrêa Ledur[1,7]*

[1]Embrapa Suínos e Aves, Concórdia, Brazil, [2]Programa de Pós-Graduação em Ciências Veterinárias, Universidade Estadual do Centro-Oeste, Guarapuava, Brazil, [3]Universidade de Passo Fundo, Passo Fundo, Brazil, [4]Universidade Federal do Vale do São Francisco, UNIVASF, Petrolina, Brazil, [5]Laboratório de Biotecnologia Animal, Escola Superior de Agricultura "Luiz de Queiroz", Universidade de SP, Piracicaba, Brazil, [6]Departamento de Genética, Faculdade de Medicina de Ribeirão Preto, Universidade de SP, Ribeirão Preto, Brazil, [7]Programa de Pós-Graduação Em Zootecnia, Universidade do Estado de SC, UDESC-Oeste, Chapecó, Brazil, [8]Faculdade de Concórdia FACC, Concórdia, Brazil

Femoral head separation (FHS) is characterized by the detachment of growth plate (GP) and articular cartilage, occurring in tibia and femur. However, the molecular mechanisms involved with this condition are not completely understood. Therefore, genes and biological processes (BP) involved with FHS were identified in 21-day-old broilers through RNA sequencing of the femoral GP. 13,487 genes were expressed in the chicken femoral head transcriptome of normal and FHS-affected broilers. From those, 34 were differentially expressed (DE; FDR ≤0.05) between groups, where all of them were downregulated in FHS-affected broilers. The main BP were enriched in receptor signaling pathways, ossification, bone mineralization and formation, skeletal morphogenesis, and vascularization. RNA-Seq datasets comparison of normal and FHS-affected broilers with 21, 35 and 42 days of age has shown three shared DE genes (*FBN2*, *C1QTNF8*, and *XYLT1*) in GP among ages. Twelve genes were exclusively DE at 21 days, where 10 have already been characterized (*SHISA3, FNDC1, ANGPTL7, LEPR, ENSGALG00000049529, OXTR, ENSGALG00000045154, COL16A1, RASD2, BOC, GDF10*, and *THSD7B*). Twelve SNPs were associated with FHS ($p < 0.0001$). Out of those, 5 were novel and 7 were existing variants located in 7 genes (*RARS, TFPI2, TTI1, MAP4K3, LINK54*, and *AREL1)*. We have shown that genes related to chondrogenesis and bone differentiation were downregulated in the GP of FHS-affected young broilers. Therefore, these findings evince that candidate genes pointed out in our study are probably related to the onset of FHS in broilers.

KEYWORDS

chickens, gene expression, FBN2, FHS, femoral head necrosis, RNA-seq

Introduction

Leg problems are considered one of the main issues in the chicken production (Li et al., 2015). The occurrence of these disorders in commercial flocks was estimated up to 30% depending on age, density, within others, having a huge impact on animal health and welfare (Knowles et al., 2008; Federici et al., 2016). Femoral head necrosis (FHN) can affect up to 75 and 88% of commercial broilers with 28 and 42 days of age, respectively, being reported as one of the major bone pathologies (McNamee and Smyth, 2000; Durairaj et al., 2009; Wideman, 2016; Liu K. et al., 2021). Some authors classified FHN depending on its severity, such as femoral head separation (FHS), when the growth plate is separated from cartilage and femoral head separation with growth plate lacerations (FHSL), when there are lesions in the femoral growth plate (Li et al., 2015; Packialakshmi et al., 2015). This condition is also known as bacterial chondronecrosis with osteomyelitis (BCO) when it is associated with bacterial infection (Jiang et al., 2015; Al-rubaye et al., 2017; Ramser et al., 2021).

The FHS is a multifactorial disorder, which could be caused by traumatic or non-traumatic factors (Liu K. et al., 2021). It is characterized by a degenerative skeletal problem presenting focal cell death, fibrotic thickening, and atrophic changes in the cartilage (Packialakshmi et al., 2015). Furthermore, some authors consider FHS as a primary cartilage defect, since reduced chondrocyte density was observed in the GP of affected broilers (Wilson et al., 2019). These failures lead to cartilage degeneration and necrosis, which predispose animals to develop FHN (Packialakshmi et al., 2015; Wilson et al., 2019). The growth plate chondrocytes are required to the proper development and growth of endochondral bones (Hallett et al., 2019). The disruption in homeostasis of bone formation and resorption through the imbalance of catabolic and anabolic factors (Wnt signaling, HIF expression, extracellular matrix production, within others) was described in broilers with 42 and 56 days of age (Yu et al., 2020). Therefore, the understanding of the GP molecular mechanisms is essential to clarify the genes responsible for triggering FHS/FHN in chickens.

Over the years, global gene expression studies have provided a better understanding of the putative acting genes in the two tissues that are the primary sites of femoral head disorders. From transcriptomes of the femur articular cartilage (AC) and growth plate (GP) of 35-day-old broilers (Peixoto et al., 2019; Hul et al., 2021; Goldoni et al., 2022), several candidate genes were prospected. Oliveira et al. (2020) also pointed out that osteochondral downregulated genes are potentially triggering BCO in tibia of 42-day-old broilers. Most of the studies with FHN/FHS in chickens are focused on understanding the ossification processes and, generally, in animals older than 35 days of age (Li et al., 2015; Paludo et al., 2017; Peixoto et al., 2019; Hul et al., 2021; Ramser et al., 2021, 2022), since the highest incidences of this condition occur at these ages (McNamee and Smyth, 2000; Paxton et al., 2014; Packialakshmi et al., 2015). Therefore, molecular mechanisms involved with femoral head separation in young age (21 days) broilers were identified using RNA sequencing, allowing highlighting genes and BP potentially related to the onset of this condition.

Material and methods

Experimental animals and sample collection

Cobb500 male broilers used in this study were raised in a standard system for commercial growing broilers with the management conditions following the recommendations for this line, with water and feed supplied *ad libitum*. At 21 days of age, 15 lameness and 10 normal standard broilers were weighed and euthanized by cervical dislocation followed by exsanguination, according to the ethical guidelines of the Embrapa Swine and Poultry Ethics Committee on Animal Utilization, under the protocol number 012/2012. Immediately after the slaughter, femurs were evaluated by the presence or absence of FHS, following the methodology described by Paludo et al. (2017). Chickens were considered with FHS when there was separation of the articular cartilage from the growth plate without any visual signal of necrosis, and normal when the AC remained attached to the GP. Samples of one of the femur proximal growth plates were collected individually, immerged in liquid nitrogen and stored at −80°C for further expression analysis.

Total RNA extraction and quantification

For the RNA-Seq analysis, 4 normal and 4 FHS-affected femur growth plates were chosen and 100 mg of this tissue was homogenized using a mortar with liquid nitrogen. The total RNA was extracted using Trizol (Life Technologies, Carlsbad, United States), according to the manufacturer's protocol, followed by a RNA cleanup step using the RNeasy mini kit (Qiagen, Hilden, Germany). RNA purity and concentration were measured using Biodrop spectrophotometer (Biodrop, UK, and integrity was evaluated using Bioanalyzer 2,100 (Agilent, Santa Clara, United States). Only samples with RIN >8.0 were considered for further analysis.

Library preparation and sequencing

Libraries were prepared using TruSeq RNA Sample Prep v2 Kit (Illumina, San Diego, United States) with 2 μg of total RNA, following the manufacturer´s protocol. The quality of the libraries was evaluated using Bioanalyzer 2,100 (Agilent, Santa

Clara, United States). Libraries were quantified through quantitative PCR using the KAPA Library Quantification kit (KAPA Biosystems, Wilmington, United States). After pooling the libraries, clustering and sequencing were performed in the Illumina HiSeq 2,500 sequencer (lllumina, San Diego, United States) producing 2 × 100 bp paired-end reads, at the Functional Genomics Center from ESALQ-USP, Piracicaba, São Paulo, Brazil.

RNA-seq data analysis

The RNA-seq analysis was performed using BAQCOM, an automated pipeline available at https://github.com/hanielcedraz/BAQCOM (accession on 15th February 2022). Low quality reads (QPhred ≤20), short reads (<70 bp) and Illumina sequence adapters were trimmed using Trimmomatic v0.39 (Bolger et al., 2014). After the quality control, sequence reads of each sample were mapped against the reference chicken genome (GRCg6a, Ensembl release 105) using STAR (Dobin et al., 2013). Reads counting was performed with HTseq-count (Anders et al., 2015), which also generated a count table for statistical analysis. The differentially expressed (DE) genes and heatmap were obtained using the limma package (Ritchie et al., 2015) from the R software (R Core Team, 2021). The Benjamini-Hochberg (BH) methodology (Benjamini and Hochberg, 1995) was applied to correct for multiple testing and genes with false discovery rate (FDR) ≤ 0.05 were considered DE. Negative and positive fold-changes indicate downregulation and upregulation of the genes in the FHS-affected group compared to control group.

Functional annotation analysis

Functional annotation of DE genes was performed using clusterProfiler (Wu et al., 2021) with MSigDB (Liberzon et al., 2011) and gene ontology with *Gallus gallus* information (org.Gg.eg.db) available at AnnotationDBbi (Pagès et al., 2022) and also in shinyGO v 0.75 (Ge et al., 2020). A search was also performed in the DAVID database, with all genes expressed in the samples used as background, and values of EASE ≤ 0.05 and *p*-values ≤ 0.05 were considered significant. A gene interaction analysis was performed with the STRING database (Szklarczyk et al., 2019) in Cytoscape v 3.9 (Shannon et al., 2003) with *G. gallus* organism using two approaches: 1) only with DE genes and 2) with DE genes plus 5 additional gene interactors.

Additionally, in order to verify the FHS gene expression profile among different ages, Ensembl IDs of DE genes identified in this study were compared with results from transcriptome studies of Peixoto et al. (2019), Oliveira et al. (2020), Hul et al. (2021) and Goldoni et al. (2022). These studies evaluated early stages of FHS at 35 days in growth plate and articular cartilage (Peixoto et al., 2019; Hul et al., 2021; Goldoni et al., 2022) and tibia head separation at 42 days of age (Oliveira et al., 2020).

qPCR validation

The qPCR analysis was performed with the same 8 GP samples used in the RNA-seq analysis: 4 normal and 4 FHS-affected broilers with 21 days of age. The RNA was extracted as previously described and cDNA synthesis was performed using the SuperScript III First–Strand Synthesis SuperMix kit (Invitrogen, Carslbad, United States). Primers for *COL14A1, FAM180A, ANGPTL5, FBN2, TNMD*, and *LEPR* candidate genes were used for RNA-Seq confirmation (Table 1). These genes were chosen based on their FDR, logFC, and biological function. Quantitative PCR reactions were performed in the QuantStudio 6 Flex equipment (Applied Biosystems), containing 1 × Mastermix (GoTaq qPCR Master Mix 2×, Promega), 0.16 µM of each F and R primer, 2 µl of cDNA at 1:10 dilution and ultrapure water to complete 15 µl of total reaction. The qPCR reactions were performed in duplicates and the Ct (cycle threshold) values were obtained for differential expression analysis in the REST program (Pfaffl et al., 2002), which uses a nonparametric randomization test to compare the studied groups. For this analysis, Ct means for each sample and gene were used and normalization was performed with *RPL4* and *RPL30* reference genes (Petry et al., 2018). Differential expression was considered significant when $p \leq 0.05$.

Unmapped read analysis

Part of the reads from RNA sequencing was not mapped in the chicken genome. To verify if those reads could be from microorganisms, the unmapped sequences were submitted to a metagenome taxonomic classification analysis with Metacache software v. 2.2.1 (Müller et al., 2017) with Refseq database version 20200820. Results from family and genera were further processed using the Phyloseq v.1.34.0 package (McMurdie and Holmes, 2013) from R, in which the raw tables were concatenated and only the taxa with more than 100 mapped reads across all samples and present in more than half of the samples were maintained. Abundance analysis was performed using a zero-inflated Gaussian (ZIG) mixed model after cumulative sum scaling (CSS) normalization using the metagenomeSeq package from R (Paulson et al., 2013). Differential abundance of the taxa between groups was considered significant when FDR ≤0.05. Graphics were generated with ggplot2 v. 3.3.3 package from R (Wickham, 2016). Metagenomic classification was registered in the Brazilian National System of Genetic Resources (SISGEN) under ID A62341D.

TABLE 1 Gene identification and primers used in the qPCR analysis.

Gene	Gene/ensembl ID	Primer squences (5′-3′)
COL14A1[a]	NM_205334.1	F: GTGATGTTGGAGCTCCTGGT
		R: CACACTTGACGAGCAACAGC
*FAM180A***	ENSGALG00000028459	F:GAGTAGAGCTATGCTTTACCCAGC
		R: CGAAGCCAGCTCCTCATCTT
ANGPTL5[a]	NM_001197236.1	F: TCAGGAAACGCAGGTGATGC
		R: AGTGCACACTGGCCTACATC
FBN2[+]	ENSGALG00000014686	F: TGCATCGATAGCCTGAAGGG
		R: CTAATTCACACCGCTCACATGG
TNMD	ENSGALG00000006821	F: CGACTACACGGAGAACGGG
		R: TGATACGGCAGATCACCCTG
LEPR[++]	ENSGALG00000011058	F: TGGTTTCGCACCGAAGAATG
		R: TTGCTTCAGGGTGCTTGACA
RPL4[a]	NM_001007479.1	F: TGTTTGCCCCAACCAAGACT
		R: CTCCTCAATGCGGTGACCTT
RPL30[a]	NM_001007967.1	F: ATGATTCGGCAAGGCAAAGC
		R: GTCAGAGTCACCTGGGTCAA

[a]Petry et al., 2018;**Peixoto et al., 2019, [+]Hul et al., 2021; [++]Paludo et al., 2017.

Variant identification using RNA-Seq data

RNA sequences obtained in this study, as well as sequences from other GP and cartilage from normal and FHS-affected samples from our previous studies (Peixoto et al., 2019; Oliveira et al., 2020; Hul et al., 2021; Goldoni et al., 2022) were used to verify the presence of variants involved with FHS. To this, sequences from femoral GP and AC of 35-day-old and tibia GP from 42-day-old broilers were downloaded from SRA database bioprojects # PRJNA352962, PRJNA350521, and PRJNA352716, respectively, totaling 24 samples (9 normal and 15 FHS-affected). Sequences were trimmed as described in the RNA-Seq analysis section, and mapping against the chicken reference genome (GRCg6a, Ensembl release 105) was performed using the two pass-mode in STAR software (Dobin et al., 2013). Variant identification was performed using the Genome Analysis Tool kit 3.6 (GATK), following the best practices guidelines for transcriptome variant analysis. Firstly, the genome index, read groups assignment and marking duplicates were performed using Picard tools 2.5 (https://broadinstitute.github.io/picard/index.html). The GATK was used for CIGAR string determination (SplitNCigarReads), reassigning mapping qualities, base recalibration, variants calling and filtering. The following filters were used to select variants: FS > 30.0, MQRankSum < −12.5, SNPcluster considering 3 variants in a 35bp window, QD < 5.0, MQ < 50.0, GQ < 5.0, QUAL ≥ 30.0, ReadPosRankSum < −8.0 and DP ≥ 300.0. Once the polymorphisms were identified by GATK, they were submitted to quality control analysis in plink 1.9 (Purcell et al., 2007; Steiß et al., 2012), where SNPs with genotyping rate <0.2 and minor allele frequencies (MAF) < 0.05 were removed from further analysis. Then, a case-control association analysis using permutation was performed to verify the presence of variants related to FHS phenotype. p-values ≤ 0.0001 were considered significant. Variant annotation was performed in Variant Effect Predictor (VEP) tool (McLaren et al., 2016) from Ensembl using the *G. gallus* genome (GRCg6a, Ensembl 105), considering the distance of 1,000 bp for upstream/downstream transcript assignment.

Results

Sequencing and mapping

RNA-Seq data from femoral head of all 8 samples generated approximately 22 million paired-end reads (2 × 100 pb) per sample. After the quality control, about 20.3 million of paired-end reads (Supplementary Table S1) were kept for further analysis. An average of 95.81 ± 0.27% (about 19.5 million) of the reads were mapped in the reference chicken genome (GRCg6a, Ensembl 105), where 77.58% of the reads were mapped in features.

Differential expression, annotation, and pathway analysis

The clustering of samples using the DE genes highlight the differences between FHS and normal groups (Figure 1A).

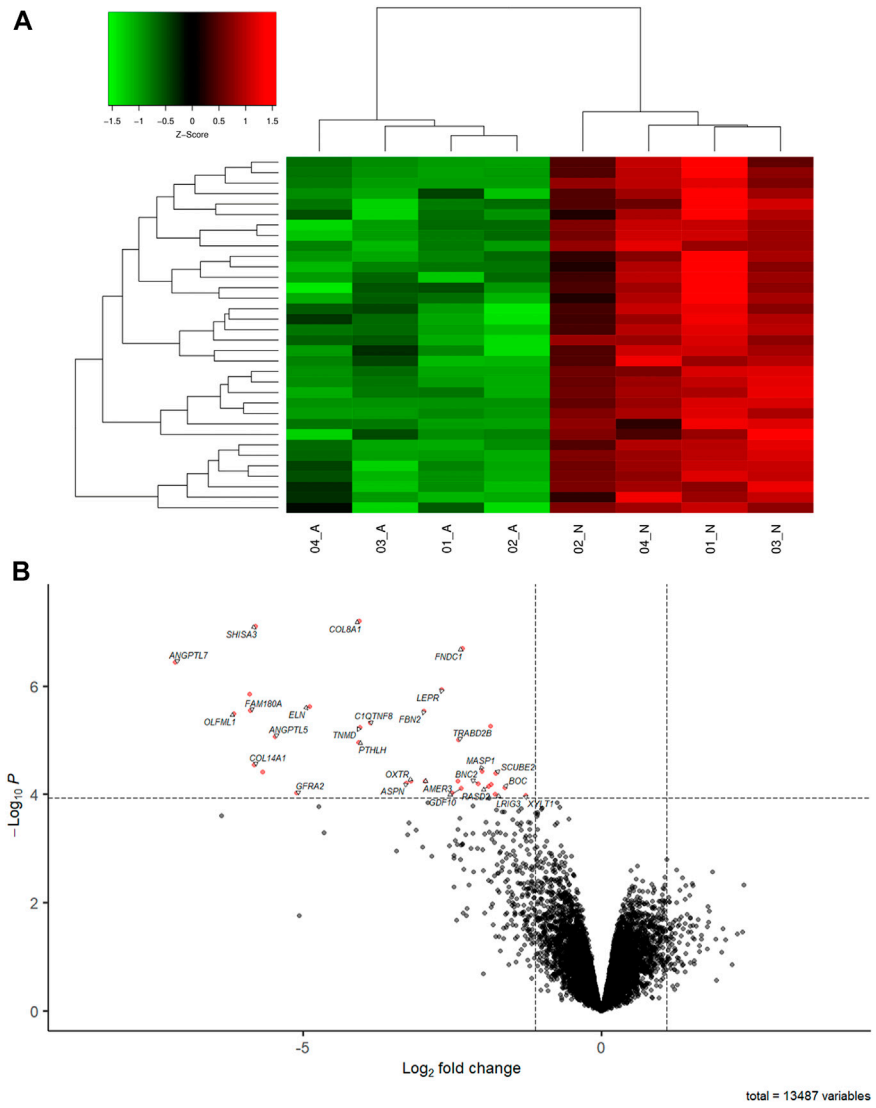

FIGURE 1
(A) Heatmap showing a hierarchical clustering of genes and samples of the DE genes between FHS-affected and control. The genes are presented in the rows and samples in the columns. Downregulated genes in the affected group are shown in red and upregulated in green. **(B)** Volcano plot showing the differentially expressed genes (red dot) in FHS-affected broilers.

13,487 genes (Supplementary Table S3) were expressed in the 21 days chicken femoral head transcriptome, corresponding to almost 55.40% of the total genes described in the *G. gallus* assembly GRCg6a. Out of those, 34 were differentially expressed (DE; Table 2) between the normal and FHS-affected broilers analyzed in this study. All of them were downregulated in the affected (Figure 1B) compared to the normal group.

Considering the DE genes, it was possible to observe 33 coding genes, being 29 known, 4 novel and 1 lncRNAs (ENSGALG00000045154). The sequences of 4 uncharacterized genes had similarities with fibronectin type III (ENSGALG00000015307, ENSGALG00000049529), immunoglobulin-like domain (ENSGALG00000054344), and concanavalin A-like lectin domain superfamily (ENSGALG00000054999).

In the DAVID ontology analysis, 20 genes (*ANGPTL7, ASPN, GDF10, TNMD, LRIG3, LEPR, FBN2, BNC2, BOC, COL8A1, PTHLH, TRABD2B, SCUBE2, GFRA2, AMER3*, and *SHISA3*) were attributed to biological processes, where most of them were related to receptor signaling pathways, ossification, bone mineralization and formation, and vascularization (Figure 2; Supplementary Table S4). Using the ShinyGO tool, *ANGPTL7, XYLT1, MASP1, FBN2, PTHLH, SCUBE2*, and *ELN* genes were in the extracellular region BP. The molecular

10.3389/fphys.2022.941134

TABLE 2 Differentially expressed genes downregulated in FHS-affected broilers, according to FDR.

T	Gene name	Gene description	LogFC	FDR
ENSGALG00000015253	*COL8A1*	collagen type VIII alpha 1 chain	−4.06	0.0005
ENSGALG00000045153	*SHISA3*	shisa family member 3	−5.79	0.0005
ENSGALG00000011663	*FNDC1*	fibronectin type III domain containing 1	−2.33	0.0009
ENSGALG00000003179	*ANGPTL7*	angiopoietin like 7	−7.14	0.0012
ENSGALG00000011058	*LEPR*	leptin receptor	−2.67	0.0031
ENSGALG00000049529			−5.90	0.0032
ENSGALG00000014686	*FBN2*	fibrillin 2	−2.97	0.0043
ENSGALG00000028459	*FAM180A*	family with sequence similarity 180 member A	−5.88	0.0043
ENSGALG00000032220	*ELN*	elastin	−4.88	0.0043
ENSGALG00000027184	*OLFML1*	olfactomedin like 1	−6.15	0.0044
ENSGALG00000005253	*C1QTNF8*	C1q and tumor necrosis factor related protein 8	−3.87	0.0059
ENSGALG00000006821	*TNMD*	tenomodulin	−4.05	0.0060
ENSGALG00000054999			−1.86	0.0060
ENSGALG00000017191	*ANGPTL5*	angiopoietin like 5	−5.47	0.0082
ENSGALG00000027655	*TRABD2B*	TraB domain containing 2B	−2.40	0.0088
ENSGALG00000017295	*PTHLH*	parathyroid hormone like hormone	−4.06	0.0092
ENSGALG00000037675	*COL14A1*	collagen type XIV alpha 1 chain	−5.82	0.0223
ENSGALG00000007419	*MASP1*	mannan binding lectin serine peptidase 1	−2.00	0.0273
ENSGALG00000015307	*ABI3BP*		−5.67	0.0273
ENSGALG00000032161	*SCUBE2*	signal peptide CUB domain and EGF like domain containing 2	−1.77	0.0273
ENSGALG00000003138	*OXTR*	oxytocin receptor	−3.20	0.0331
ENSGALG00000041501	*AMER3*	APC membrane recruitment protein 3	−2.96	0.0331
ENSGALG00000045154			−2.40	0.0331
ENSGALG00000004722	*ASPN*	biglycan	−3.27	0.0333
ENSGALG00000015101	*BNC2*	basonuclin 2	−2.07	0.0333
ENSGALG00000026836	*COL16A1*	collagen type XVI alpha 1 chain]	−1.84	0.0333
ENSGALG00000012542	*RASD2*	RASD family member 2	−1.90	0.0358
ENSGALG00000015152	*BOC*	BOC cell adhesion associated oncogene regulated	−1.62	0.0360
ENSGALG00000005985	*GDF10*	growth differentiation factor 10	−2.35	0.0361
ENSGALG00000032856	*GFRA2*	GDNF family receptor alpha 2	−5.10	0.0410
ENSGALG00000054344			−2.51	0.0410
ENSGALG00000009755	*LRIG3*	leucine rich repeats and immunoglobulin like domains 3	−1.78	0.0418
ENSGALG00000006757	*XYLT1*	xylosyltransferase 1	-1.27	0.0428
ENSGALG00000012362	*THSD7B*	thrombospondin type 1 domain containing 7B [	-1.88	0.0463

functions were mostly related to calcium ion binding and matrix constituent (Figure 2, Supplementary Table S4). Furthermore, these genes were characterized in fibronectin, collagen, immunoglobulin, and epidermal growth factor protein domains (Figure 2).

The gene network using *G. gallus* database was performed to verify the interactions among the DE genes, where 11 genes were grouped in two main branches (Figure 3A). Considering the gene network with the protein interactors, also 2 main branches were found (Figure 3B). Furthermore, 16 out of 34 DE genes were included in the gene network, being possible to observe that these genes are functionally associated, contributing to FHS phenotype.

Considering the transcriptome datasets from 21, 35, and 42 days of age, it was possible to observe that one gene was DE at all ages in the articular cartilage and growth plate (*FBN2*), while three genes (*FBN2, C1QTNF8* and *XYLT1*) where DE in GP at 21, 35, and 42 days of age (Figure 4). A total of 12 genes were exclusively DE at 21 days, where 10 have already been characterized (*SHISA3, FNDC1, ANGPTL7, LEPR,* ENSGALG00000049529, *OXTR,* ENSGALG00000045154, *COL16A1, RASD2, BOC, GDF10*, and *THSD7B*).

The genes evaluated in the qPCR analysis had the same expression profile when compared to the RNA-Seq results and were also DE between groups. The *COL14A1, FAM180A, ANGPTL5, FBN2*, and *LEPR* candidate genes were

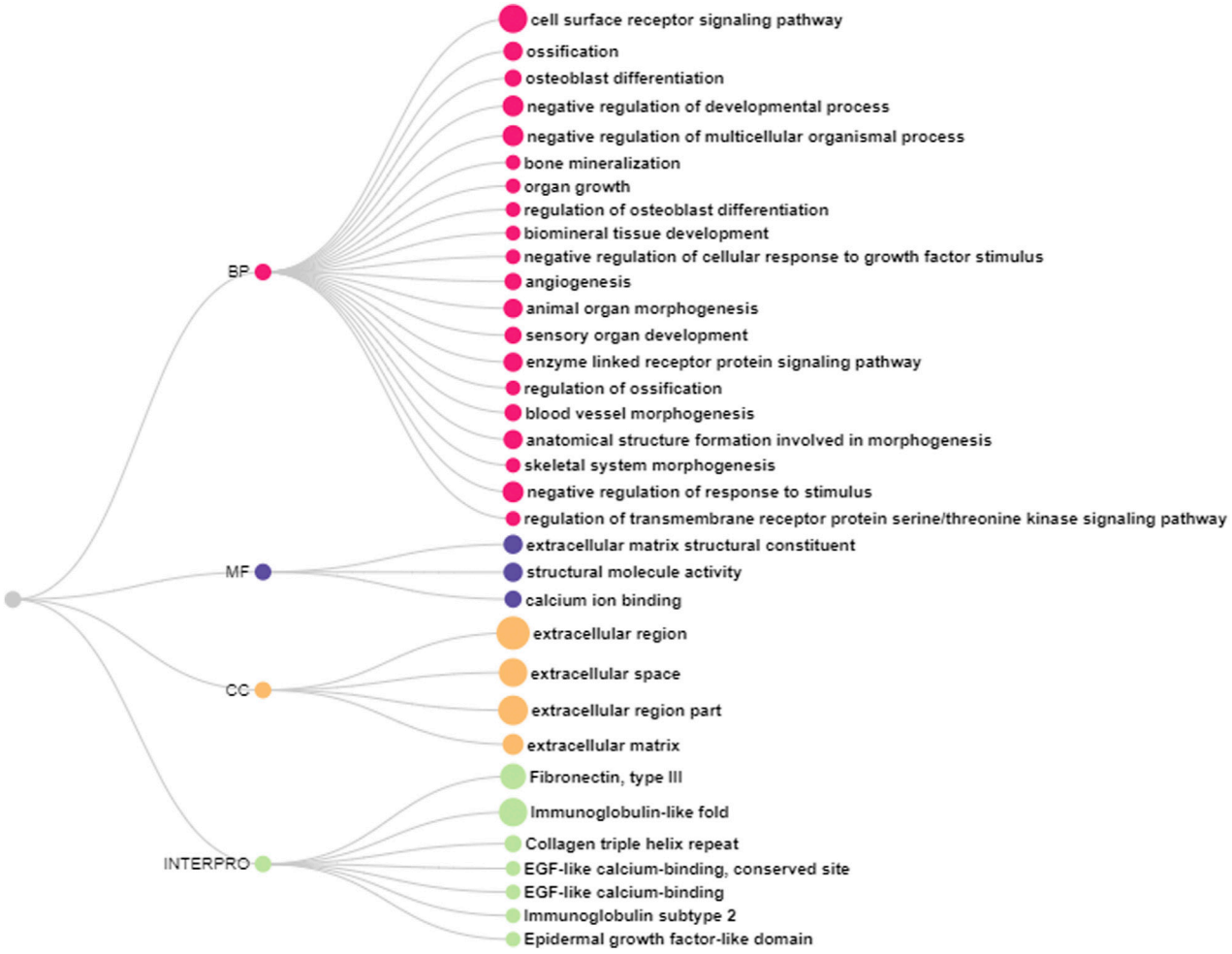

FIGURE 2
Biological processes (BP), molecular functions (MF), cell component (CC) and protein domains according to the Interpro enriched using DAVID database.

downregulated in the FHS-affected when compared to normal broilers, confirming the RNA-Seq analysis results (Table 3). The *TNMD* gene had a low expression, showing amplification (Ct mean = 36.7) in all normal samples, but it was detected in only one sample from the FHS-affected group (Ct mean = 39.2), therefore, it was not possible to perform the statistical analysis for this gene.

Variant identification

A total of 223,069 variants were identified in the 24 analyzed samples after GATK filtering. For association analysis, 8,316 and 45,615 variants were removed due to genotyping rate and MAF failures, respectively. A total of 168,672 SNPs were kept for association analysis, where 12 SNPs were associated with FHS ($p < 0.0001$). From those, 5 were novel and 7 were existing variants being located in 7 genes (*RARS, TFPI2, TTI1, MAP4K3, LINK5,4* and *AREL1)* (Table 4, Supplementary Table S5). The SNP located in the *TTI1* gene was a missense variant, while those in *RARS, TFPI2, LINK54*, and *AREL1* were synonymous. One SNP in the *MAP4K3* gene was located in an intron and three (4:46318416, 4:82213680 and 4:82216997) were in intergenic regions (Supplementary Tables S5, S6).

Unmapped reads identification

An average of 605,218 RNA reads/sample were unmapped in the chicken genome (Supplementary Table S2) and were submitted to a metagenome taxonomic classification analysis to check if they

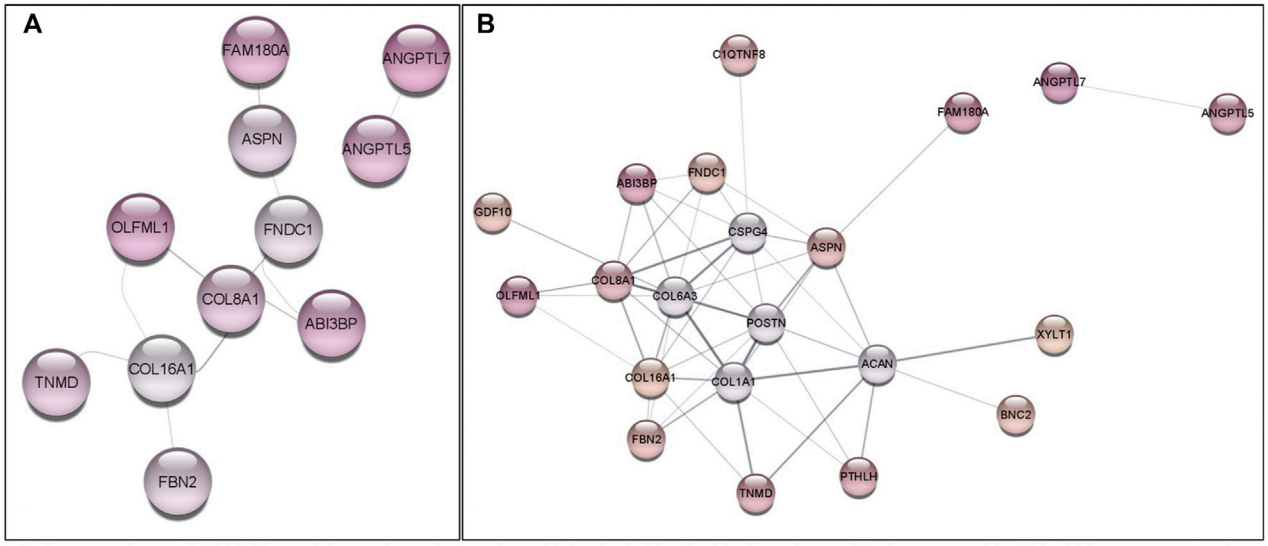

FIGURE 3
Gene network constructed with DE genes **(A)** and with DE genes plus up to 5 protein interactors **(B)** with the Gallus gallus information. Colored circles represent genes and connecting lines represent interactions among genes, according to Cytoscape Stringdb App. Colors indicate the downregulation expression levels, where darker colors have lower logFC levels in FHS-affected group. Gray circles **(B)** are protein interactors added to improve the gene network information.

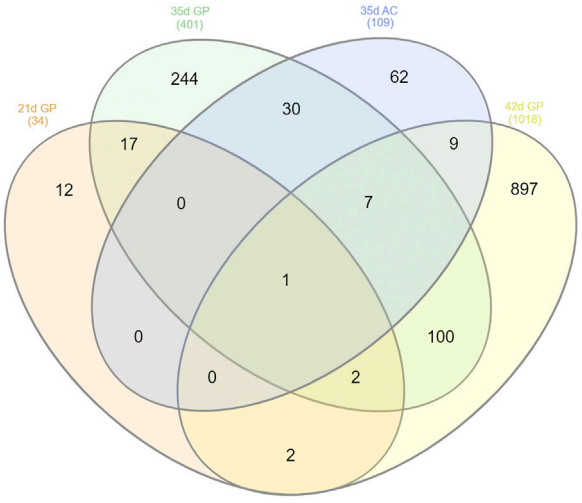

FIGURE 4
Venn diagram of DE genes in the femur GP of 21 and 35 days of age, tibia GP of 42 days of age and AC of 35 days of age.

matched with microorganisms sequences. About 23,608 (~3.8%) reads/sample were identified in 23 different families (Supplementary Table S7) where the most abundant were *Enterobacteriaceae, Comamonadaceae* and *Bacillaceae*, (Supplementary Table S7). Considering genus, 83 were identified and the most present were *Streptomyces, Pseudomonas, Proteus, Halomonas, Rhizobium, Stenotrophomonas, Shapirovirus, Corynebacterium, Acinetobacter*, and *Aeromonas* (Supplementary Figure S1). Although several groups were found in the analyzed samples, no differences were observed between normal and FHS-affected groups.

Discussion

The complexity of the FHS/FHN etiology and pathogenesis makes this condition one of the main problems affecting fast-growing broilers production (Prisby et al., 2014). FHS is characterized by the detachment of GP and AC, occurring in tibia and femur (Durairaj et al., 2009; Packialakshmi et al., 2015). Although some studies have been published in the last years with FHS, FHN, and BCO, including by our group, there are few of them approaching the molecular mechanisms involved with these conditions, especially with early ages (Li et al., 2015; Paludo et al., 2017; Peixoto et al., 2019; Oliveira et al., 2020; Liu K. et al., 2021; Hul et al., 2021; Ramser et al., 2021, 2022; Goldoni et al., 2022; Santos et al., 2022). To the best of our knowledge, this paper is the first attempt to compare normal and FHS-affected femoral head transcriptome in broilers with 21 days of age. The results presented here can contribute to deepen the understanding of FHS in chicken, clarifying BP, genes and variants involved with this condition, as well as to prospect the presence of microorganisms in the analyzed samples. Here, most of the enriched biological processes were related to ossification, developmental

TABLE 3 Relative gene expression and LogFC between FHS-affected.and control groups and results of differential expression analysis using REST.

Gene	Relative expression	Std. Error	95% C.I.	*p*-value	LogFC
Col14A1	0.015	0.007–0.035	0.004–0.049	0.01	−6.06
FAM180A	0.005	0.003–0.009	0.002–0.017	0.017	−7.64
ANGPTL5	0.015	0.007–0.027	0.004–0.047	0.001	−6.06
FBN2	0.396	0.245–0.649	0.192–0.931	0.03	−1.34
LEPR	0.131	0.098–0.176	0.076–0.214	0.001	−2.93

TABLE 4 SNPs associated with FHS in broilers.

SNP location	Gene symbol	Minor allele	Frequency of allele in cases	Frequency of allele in controls	Major allele	*p*-value	Odds ratio	Empirical *p*-value
2:23307098	*TFPI2*	A	0.03333		C	0.0000308	0.02759	0.00004691
3:16824258	*MAP4K3*	C	0.03333	0.4444	G	0.0004111	0.0431	0.00005369
4:46304089	*LIN54*	T	0.5333	0	A	0.0001478	NA	0.0000995
4:46315234	*LIN54*	A	0.5333	0	G	0.0001478	NA	0.0000995
4:46318356	—	A	0.5333	0	G	0.0001478	NA	0.0000995
4:46318416	—	C	0.5333	0	T	0.0001478	NA	0.0000995
4:82213680	—	G	0.1667	0.7222	A	0.0001186	0.07692	0.000092
4:82216997	*GRK4*	C	0.1667	0.7222	T	0.0001186	0.07692	0.000092
5:38228766	*AREL1*	A	0.03333	0.5625	G	0.0000341	0.02682	0.0000281
13:5487116	*RARS*	C	0.1667	0.7778	G	0.00002772	0.05714	0.00005413
13:5487611	*RARS*	G	0.1667	0.7778	A	0.00002772	0.05714	0.00005413
20:10404280	*TTI1*	A	0.6071	0.1111	G	0.0008542	12.36	0.00003559

processes, response to stimulus, extracellular matrix (ECM), angiogenesis, skeletal morphogenesis, within others. In these processes, collagen, angiopoietin-like, growth factors, fibronectins and tumor necrosis related genes were DE (Table 1). The skeletogenesis is initiated when mesenchymal precursor cells differentiate in cartilage and bone cells that grow by the endochondral ossification process (Goldring et al., 2006; Ağirdil, 2020). After hatch, mesenchymal cells in the GP initiate a proliferation to hypertrophic chondrocytes leading to cartilage formation, where chondrocytes will suffer chondrolysis and apoptosis, allowing vascular invasion and bone formation (Rath and Durairaj, 2022). The coordinated gene expression related to cell proliferation and differentiation, angiogenesis, apoptosis, local growth factors, hormones and cell signaling are needed (Goldring et al., 2006). In our study, 34 genes were DE between normal and FHS-affected 21 days old broilers, being downregulated in the affected group (Figure 1B; Table 2). Most of these genes were in BP related to ossification, chondrogenesis and angiogenesis (Figure 2), and the DE profile found in our study could help to understand the FHS pathogenesis. FHS has been characterized by focal death, atrophic changes in the cartilage (Packialakshmi et al., 2015), reduced chondrocyte density, presence of pyknotic nuclei and erythrocytes and the presence of inflammatory cells (Wilson et al., 2019). Here, several genes DE, such as collagens, *FBN2, ANGPTLs, FNDC1, C1QTNF8*, and *XYLT1* may corroborate with the hypothesis suggested by those authors.

GP zones have high metabolic activity, where chondrocytes pass from resting, proliferative, hypertrophic and terminal phases, leading to a healthy osteogenesis (Ağirdil, 2020). In the first phases, it is known that collagens such as *COL2A1* and *COL10A1* are essential to chondrocyte maturation (Ağirdil, 2020). The major constituent of the organic bone matrix and articular cartilage is the collagen protein, where the *COL2A1* is the main studied collagen (Hallett et al., 2019). This protein interacts with other collagens and proteins to create a network to form the ECM (Graham et al., 2000; Flowers et al., 2017), being highly expressed in the proliferation phase, while type X collagens are more expressed in the hypertrophic phases than in the other ones. In our study, three collagen genes, *COL14A1, COL8A1*, and *COL16A1*, were downregulated in the affected broilers, being, respectively, 7, 4, and 6.5 times less expressed in the FHS-affected than in the normal broilers (Table 1).

Furthermore, other collagen related genes, such as *FBN2* and *COL16A1* were also downregulated in the affected group. It is interesting to note that most of the genes in the network were grouped in one branch, where collagen genes were connectors (Figure 3). Although the endochondral ossification has been widely studied (Long and Ornitz, 2013), information on the genes involved in the endochondral ossification and FHS in chickens are still scarce. *COL14A1* has already been associated to calcium ligation and cell morphogenesis (Rojas-Peña et al., 2014), being highly expressed when submitted to mechanical stress (Manon-Jensen and Karsdal, 2016). *COL16A1* was associated to osteoarthritis in humans (Karlsson et al., 2010; Chou et al., 2013), while polymorphisms in *COL8A* gene were associated to the loss of function during embryogenesis leading to congenital vertebral malformations (Gray et al., 2014). The importance of *COL2A1* in the ECM, cartilage and bone replacement formation has been highlighted in several studies. Polymorphisms in this gene were found to increase the susceptibility to FHN in humans (Li et al., 2014), and its expression is essential to the fibrils formation on epiphyseal growth plate (Pouya and Kerachian, 2015). The downregulation of these collagen genes may influence the extracellular matrix formation, affecting the integrity of the collagen network (Heuijerjans et al., 2017), as well as the chondrocyte maturation, and, possibly, preventing the bone formation and, consequently, facilitating the FHS appearance in chickens.

Lack of angiogenesis and vascularization have also been associated to FHS in chickens (Durairaj et al., 2009; Prisby et al., 2014; Li et al., 2015; Packialakshmi et al., 2015; Paludo et al., 2017; Peixoto et al., 2019; Goldoni et al., 2022) and the DE genes *ANGPTL7, TNMD, LEPR*, and *COL8A1* were in BP related to these functions. The angiopoietin-like family is composed by 8 genes (*ANGPTL1* to *ANGPTL8*) encoding proteins structurally similar to angiopoietins, with functions related to glucose metabolism, hematopoiesis, fat metabolism and inflammation, participating in a multitude of physiological and pathophysiological processes. *ANGPTLs* differ from angiopoietins because they do not bind to their receptors (Santulli, 2014). In our study, 2 out of 8 known angiopoetin-like were DE between groups: *ANGPTL7* and *ANGPTL5*. The role of *ANGPTLs* in vascularization still needs to be better understood, since they may act as pro-angiogenic, anti-angiogenic and also VEGF-independent (Hato et al., 2008). *ANGPTL7* and *ANGPTL5* have a role in hematopoietic stem cell expansion (Zhang et al., 2006). *ANGPTL7* is believed to be a potent target of the WNT/β-catenin signaling pathway, which is essential to BMPs (bone morphogenetic proteins) activation in osteoblasts (Beederman et al., 2013; Osório, 2015). Moreover, the alteration of *ANGPTL7* influences the expression of several matrix proteins, such as fibronectin, collagens, myocillins and metalloproteinases (Santulli, 2014), encoded by genes that were also downregulated in our study and were grouped in enriched BP of ECM. The *TNMD* function is not well characterized, but this gene encodes a chondromodulin-I related protein, which increases chondrocyte growth and inhibits angiogenesis (Shukunami et al., 2005; TNMD, 2022). Another downregulated gene in broilers with 21 days of age was *LEPR*, which is involved with lipid metabolism and inflammatory response (Abete et al., 2009; Gogiraju et al., 2019). Mutations in this gene has already been associated to femoral head osteonecrosis in humans (Liu T. et al., 2021) and with bone integrity traits in broilers (Ibelli et al., 2014). Although there is no information on its role associated with FHS in chickens, in mice, *LEPR* was considered a negative modulator of bone mechanosensitivity, leading to a poor osteogenic response (Kapur et al., 2010).

The correct transportation of transmembrane adhesion molecules is important to maintain the articular cartilage and growth plate communication and, consequently, bone remodeling (Packialakshmi et al., 2015). In the current study, low expression levels of genes associated with ECM could favor the FHS condition. Among the genes DE in BP related to extracellular matrix were *ASPN, FBN2, COL8A1, COL14A1, COL16A1,* and *ELN*. The *ELN* was downregulated in FHS-affected broilers compared to normal ones in this study and in broilers with 35 days of age (Peixoto et al., 2019). This gene is associated with the production of a protein called tropoelastine, which is responsible for the elasticity of connective tissue found in cartilage, and acts as a precursor of osteoblast differentiation (Twine et al., 2014). Reduced *ELN* expression was associated to the risk of injury in the rat tendon (Kostrominova and Brooks, 2013).The A*SPN* gene encodes a small leucine-rich cartilage extracellular protein of proteoglycan family, regulating chondrogenesis and binding calcium to collagens (Mishra et al., 2019). A*SPN* is considered a biological marker for osteoarthritis development in humans and mice (Karlsson et al., 2010; Mishra et al., 2019). This gene also acts in osteoblast biomineralization activity, and its expression was increased in ECM (Zhu et al., 2012).

FHS occurrence is also affected by broilers age, increasing at older ages (Prisby et al., 2014). Our research group has been evaluating the FHS/FHN gene expression in several ages in femur (Paludo et al., 2017; Hul et al., 2021; Goldoni et al., 2022; Santos et al., 2022) and in tibia (Oliveira et al., 2020). In this way, trying to understand the genes more related with FHS onset, we have compared the common DE genes and also those exclusive to 21, 35, and 42 days of age in GP and AC. The *FBN2* was the only DE gene in all studied datasets: 21 and 35 days femur GP, 42 days tibia GP and 35 days AC (Figure 4; Supplementary Table S8). This gene was annotated in 23 of the 34 ontologies enriched in this study (Figure 2; Supplementary Table S4), including ossification, regulation of TGF, extracellular matrix and calcium binding. *FBN2* gene is one of the major components of ECM with a primary function of maintaining tissue structural integrity, which can affect several tissues, including skeletal system (Yu and Urban, 2013; Lee et al., 2019). In *FBN2*

knockout mice, a reduced osteoblast maturation was observed, preventing bone formation, and increasing bone resorption (Nistala et al., 2010), showing that this gene has an important role in stimulate osteoblast differentiation (Lee et al., 2019). In dogs, mutations in *FBN2* gene were associated with hip dysplasia (Friedenberg et al., 2011). In the analyzed datasets, the *FBN2* downregulation in the FHS-affected group could be preventing the optimal ossification of the GP and, since it occurred at 21, 35, and 42 days of age, this reinforces *FBN2* gene as candidate for FHS/FHN.

We also observed that three genes (*FBN2, XYLT1*, and *C1QTNF8*) were downregulated in GP of FHS-group of all analyzed ages. *XYLT1* encodes the xylosyltransferase enzyme, necessary for glycosaminoglycan (GAG) biosynthesis, and it is considered a key gene for chondrocyte maturation and skeletal length (Mis et al., 2014). In mice, *XYLT* anomalous expression, as well as mutations in this gene alters the GAG normal levels, affecting proteoglycan production and bone growth, leading to a pug dwarfism phenotype (Mis et al., 2014). Furthermore, it was demonstrated in zebrafish that bone formation around cartilage is space and time regulated, in which proteoglycans were responsible for this regulation, being crucial for skeletal development (Eames et al., 2011). There is a lack of information on the *C1QTNF8* (complement C1q Tumor Necrosis Factor-Related Protein 8) gene function in chickens. *C1QTNF8* is predicted to be part of a collagen trimmering and, in humans, it is considered a paralog of *C1QTNF6*. A DNA methylation analysis found that the *C1QTNF8* was differentially methylated in osteoarthritis (OA) subchondral bone (Jeffries et al., 2016), while its paralogous is a marker for OA in mouse, acting in host defense, inflammation and glucose metabolism (Murayama et al., 2014, 2015). Moreover, when comparing DE genes in GP from different ages, we observed that through aging, more shared DE genes were found between 21 and 35 days and between 35 and 42 days of age, than when 21 and 42 days were compared (Figure 4). When looking at the 12 exclusively DE genes between normal and FHS-affected broilers at 21 days of age (*SHISA3, FNDC1, ANGPTL7, LEPR, OXTR, COL16A1, BOC, E*NSGALG00000049529, *RASD2, GDF10* ENSGALG00000045154, and *THSD7B)*, they were mainly related to WNT and FGF signaling (Amanatullah et al., 2014), bone metabolism (Nilsson et al., 2007; Di Benedetto et al., 2014; Lui et al., 2018), angiogenesis (Shang et al., 2015; Huang et al., 2021), chondrogenesis (Sekiya et al., 2002; Paradise et al., 2018) and Hedgehog signaling pathway (Kavran et al., 2010; Xavier et al., 2016). In this way, it is possible to highlight that DE genes between normal and affected broilers at 21 days of age were mainly related to endochondral ossification, while when GP and AC at 35 and 42 days of age were evaluated (Peixoto et al., 2019; Oliveira et al., 2020; Hul et al., 2021; Goldoni et al., 2022), there were several DE genes related to other biological processes, such as inflammation, defense response, chemotaxis, within others. Therefore, the expression profiles found at 21 days of age are in agreement with other studies that found that one of the main issues regarding FHS/FHN is related to the femur maturation and mineralization (Prisby et al., 2014; Wilson et al., 2019), possibly due to fast-growth and lack of increasing bone volume in the same rate.

Variants in all datasets analyzed here were identified in the RNA-Seq and an odds ratio analysis was performed. Twelve SNPs in seven genes (*TFPI2, MAP4K3, LIN54, GRK4, AREL1, RARS*, and *TTI1*) were associated with FHS predisposition in chickens ($p < 0.0001$). A new SNP annotated as missense in the TELO2 Interacting Protein (*TTI1)* gene had an odds ratio of 12.36. The *TTI1* is an mTOR signaling that regulates cell growth and survival in response to nutrient and hormonal changes and activates the eukaryotic translation initiation factor 4E binding protein 1 (*eIF4E*) (Ronkina and Gaestel, 2022) from 4E-BP1, which is an inhibitor of cap-dependent translation (Katsara and Kolupaeva, 2018). The 4E-BP1 inhibition has already been associated to cartilage degeneration in rat osteoarthritic knees (Katsara and Kolupaeva, 2018). The other variants were intronic or synonymous, but it is interesting to note that, as the missense, they were found in genes mainly related to basal machinery of cells, such as *RARS1*, *LIN54, AREL1*, and *TFPI2. RARS1* is an Arginyl-TRNA Synthetase 1, *LIN54* is a key regulator of cell cycle genes, in which its depletion leads to growth defects (Schmit et al., 2009), the *AREL1* is a negative regulator of apoptosis, while *TFPI2* is related to vascular endothelial growth factor (Xu et al., 2006). Although with a small number of samples, the RNA-Seq data allowed us to identify putative functional variants that could contribute with the appearance of the analyzed condition. The SNPs discovered here should be validated in a large population to confirm them as genetic markers.

According to our results, several biological processes and genes involved with femur head separation in chickens were identified at an early age. Here, genes of the collagen and angiopoietin-like family, among others, were associated with this condition in *G. gallus* at 21 days of age. It was possible to show that several genes, such as *FBN2, XYLT1*, and *C1QTNF8* have an important role in the organic matrix bone formation, hypoxia, as well as its homeostasis. This indicates that changes associated with broiler rapid growth may affect genes related to osteogenesis, especially those involved with endochondral ossification, which might contribute to the onset of femoral head necrosis. Although it is difficult to state whether these genes are causing FHS or not, the approach used in this study allows comprehending how the early molecular changes are happening. Nevertheless, further studies are needed to clarify the expression pattern of these genes over time, to elucidate whether the alteration in expression occurs since the birth of the chicks, or if it is due to their rapid growth. Moreover, SNPs in candidate genes were prospected in the femoral GP of 21-day-old broilers, which can evince new approaches to reduce this condition in chickens. Understanding the genetic factors associated with bone formation and maintenance may lead to a better comprehension on how environmental and management factors can affect the necrosis process.

Conclusion

In this study, using RNA-seq analysis, we have shown that a set of genes related to chondrogenesis and bone differentiation were downregulated in the GP of FHS-affected young broilers. Among these genes, *FBN2, XYLT1*, and *C1QTNF8* can be highlighted since they were DE in the GP of various ages. SNPs were also identified in genes related to translation factors and cell growth, which could predispose the animals to FHS/FHN development. Furthermore, at 21 days of age, we also notice that the DE genes were more related to cartilage and bone morphogenesis, while in other ages (35 and 42 days), genes related to defense response, inflammation and chemotaxis were also found. Therefore, these findings evince that candidate genes pointed out in our study are probably related to the FHS progression in broilers.

Data availability statement

The datasets presented in this study can be found in online repositories. The names of the repository/repositories and accession number(s) can be found below: https://www.ncbi.nlm.nih.gov/, SRA Bioproject PRJNA288640.

Ethics statement

The animal study was reviewed and approved by the Ethics Committee on Animal Utilization of the Embrapa Swine and Poultry National Research Center.

Author contributions

JP, ML, RZ, and AI conceived and designed the experiment. JP, RZ, and ML were responsible for the data collection. AI, JM, MP, LC, and DM performed the laboratory experiment. AI, JG, and MC performed the data analysis. AI, JP, JG, MC, and ML interpreted the results and wrote the manuscript. All authors reviewed, edited and approved the final manuscript. JP, and ML were responsible for funding acquisition and supervision of the research.

Funding

This study was financed by the National Council for Scientific and Technological Development (CNPq), project numbers 400606/2012-7 and 407404/2013-9.

Acknowledgments

The authors are grateful to A. L. Tessmann for technical assistance. RZ was supported by a BJT grant n° 373167/2012-1 from the National Council for Scientific and Technological Development (CNPq). DEPM received a PIBIC/CNPq scholarship at Embrapa and MSDP received a FAPESC/CAPES scholarship at UDESC/Oeste. LLC, MCL, AMGI, and RZ are recipients of a productivity fellowship from CNPq. We thank the Coordenação de Aperfeiçoamento de Pessoal de Nível Superior (CAPES), Brazil—Finance Code 001 for the free access to the journals used in the literature review.

Conflict of interest

The authors declare that the research was conducted in the absence of any commercial or financial relationships that could be construed as a potential conflict of interest.

Publisher's note

All claims expressed in this article are solely those of the authors and do not necessarily represent those of their affiliated organizations, or those of the publisher, the editors and the reviewers. Any product that may be evaluated in this article, or claim that may be made by its manufacturer, is not guaranteed or endorsed by the publisher.

Supplementary material

The Supplementary Material for this article can be found online at: https://www.frontiersin.org/articles/10.3389/fphys.2022.941134/full#supplementary-material

References

Abete, I., Goyenechea, E., Crujeiras, A. B., and Martínez, J. A. (2009). Inflammatory state and stress condition in weight-lowering Lys109Arg LEPR gene polymorphism carriers. *Arch. Med. Res.* 40, 306–310. doi:10.1016/J.ARCMED.2009.03.005

Ağirdil, Y. (2020). The growth plate: A physiologic overview. *EFORT Open Rev.* 5, 498–507. doi:10.1302/2058-5241.5.190088

Al-rubaye, A. A. K., Ekesi, N. S., Zaki, S., Emami, N. K., Jr, R. F. W., Rhoads, D. D., et al. (2017). Chondronecrosis with osteomyelitis in broilers : Further defining a bacterial challenge model using the wire flooring model. *Poult. Sci.* 96, 332–340. doi:10.3382/ps/pew299

Amanatullah, D. F., Yamane, S., and Reddi, A. H. (2014). Distinct patterns of gene expression in the superficial, middle and deep zones of bovine articular cartilage. *J. Tissue Eng. Regen. Med.* 8, 505–514. doi:10.1002/TERM.1543

Anders, S., Pyl, P. T., and Huber, W. (2015). HTSeq--a Python framework to work with high-throughput sequencing data. *Bioinformatics* 31, 166–169. doi:10.1093/bioinformatics/btu638

Beederman, M., Lamplot, J. D., Nan, G., Wang, J., Liu, X., Yin, L., et al. (2013). BMP signaling in mesenchymal stem cell differentiation and bone formation. *J. Biomed. Sci. Eng.* 6, 32–52. doi:10.4236/JBISE.2013.68A1004

Benjamini, Y., and Hochberg, Y. (1995). Controlling the false discovery rate: A practical and powerful approach to multiple testing. *J. R. Stat. Soc. Ser. B* 57, 289–300. doi:10.1111/J.2517-6161.1995.TB02031.X

Bolger, A. M., Lohse, M., and Usadel, B. (2014). Trimmomatic: A flexible trimmer for Illumina sequence data. *Bioinformatics* 30, 2114–2120. doi:10.1093/bioinformatics/btu170

Chou, C. H., Lee, C. H., Lu, L. S., Song, I. W., Chuang, H. P., Kuo, S. Y., et al. (2013). Direct assessment of articular cartilage and underlying subchondral bone reveals a progressive gene expression change in human osteoarthritic knees. *Osteoarthr. Cartil.* 21, 450–461. doi:10.1016/J.JOCA.2012.11.016

Di Benedetto, A., Sun, L., Zambonin, C. G., Tamma, R., Nico, B., Calvano, C. D., et al. (2014). Osteoblast regulation via ligand-activated nuclear trafficking of the oxytocin receptor. *Proc. Natl. Acad. Sci. U. S. A.* 111, 16502–16507. doi:10.1073/PNAS.1419349111

Dobin, A., Davis, C. A., Schlesinger, F., Drenkow, J., Zaleski, C., Jha, S., et al. (2013). Star: Ultrafast universal RNA-seq aligner. *Bioinformatics* 29, 15–21. doi:10.1093/bioinformatics/bts635

Durairaj, V., Okimoto, R., Rasaputra, K., Clark, F. D., and Rath, N. C. (2009). Histopathology and serum clinical chemistry evaluation of broilers with femoral head separation disorder. *Avian Dis.* 53, 21–25. doi:10.1637/8367-051908-Reg.1

Eames, B. F., Yan, Y. L., Swartz, M. E., Levic, D. S., Knapik, E. W., Postlethwait, J. H., et al. (2011). Mutations in fam20b and xylt1 reveal that cartilage matrix controls timing of endochondral ossification by inhibiting chondrocyte maturation. *PLoS Genet.* 7, 1002246. doi:10.1371/JOURNAL.PGEN.1002246

Federici, J. F., Vanderhasselt, R., Sans, E. C. O., Tuyttens, F. A. M., Souza, A. P. O., Molento, C. F. M., et al. (2016). Assessment of broiler chicken welfare in southern Brazil. *Rev. Bras. Cienc. Avic.* 18, 133–140. doi:10.1590/18069061-2015-0022

Flowers, S. A., Zieba, A., Örnros, J., Jin, C., Rolfson, O., Björkman, L. I., et al. (2017). Lubricin binds cartilage proteins, cartilage oligomeric matrix protein, fibronectin and collagen II at the cartilage surface. *Sci. Rep.* 71 (7), 13149. doi:10.1038/s41598-017-13558-y

Friedenberg, S. G., Zhu, L., Zhang, Z., van den Foels, W. B., Schweitzer, P. A., Wang, W., et al. (2011). Evaluation of a fibrillin 2 gene haplotype associated with hip dysplasia and incipient osteoarthritis in dogs. *Am. J. Vet. Res.* 72, 530–540. doi:10.2460/AJVR.72.4.530

Ge, S. X., Jung, D., Jung, D., and Yao, R. (2020). ShinyGO: A graphical gene-set enrichment tool for animals and plants. *Bioinformatics* 36, 2628–2629. doi:10.1093/BIOINFORMATICS/BTZ931

Gogiraju, R., Hubert, A., Fahrer, J., Straub, B. K., Brandt, M., Wenzel, P., et al. (2019). Endothelial leptin receptor deletion promotes cardiac autophagy and angiogenesis following pressure overload by suppressing akt/mTOR signaling. *Circ. Heart Fail.* 12, e005622. doi:10.1161/CIRCHEARTFAILURE.118.005622

Goldoni, I., Ibelli, A. M. G., Fernandes, L. T., Peixoto, J., Hul, L. M., Cantão, M. E., et al. (2022). Comprehensive analyses of bone and cartilage transcriptomes evince ion transport, inflammation and cartilage development-related genes involved in chickens' femoral head separation. *Anim* 12, 788. doi:10.3390/ANI12060788

Goldring, M. B., Tsuchimochi, K., and Ijiri, K. (2006). The control of chondrogenesis. *J. Cell. Biochem.* 97, 33–44. doi:10.1002/JCB.20652

Graham, H. K., Holmes, D. F., Watson, R. B., and Kadler, K. E. (2000). Identification of collagen fibril fusion during vertebrate tendon morphogenesis. The process relies on unipolar fibrils and is regulated by collagen-proteoglycan interaction. *J. Mol. Biol.* 295, 891–902. doi:10.1006/JMBI.1999.3384

Gray, R. S., Wilm, T. P., Smith, J., Bagnat, M., Dale, R. M., Topczewski, J., et al. (2014). Loss of col8a1a function during zebrafish embryogenesis results in congenital vertebral malformations. *Dev. Biol.* 386, 72–85. doi:10.1016/J.YDBIO.2013.11.028

Hallett, S. A., Ono, W., and Ono, N. (2019). growth plate chondrocytes: Skeletal development, growth and beyond. *Int. J. Mol. Sci.* 20, 6009. doi:10.3390/IJMS20236009

Hato, T., Tabata, M., and Oike, Y. (2008). The role of angiopoietin-like proteins in angiogenesis and metabolism. *Trends cardiovasc. Med.* 18, 6–14. doi:10.1016/J.TCM.2007.10.003

Heuijerjans, A., Wilson, W., Ito, K., and van Donkelaar, C. C. (2017). The critical size of focal articular cartilage defects is associated with strains in the collagen fibers. *Clin. Biomech.* 50, 40–46. doi:10.1016/J.CLINBIOMECH.2017.09.015

Huang, H., Zhang, J., Ling, F., Huang, Y., Yang, M., Zhang, Y., et al. (2021). Leptin Receptor (LEPR) promotes proliferation, migration, and invasion and inhibits apoptosis in hepatocellular carcinoma by regulating ANXA7. *Cancer Cell Int.* 21, 4. doi:10.1186/s12935-020-01641-w

Hul, L. M., Ibelli, A. M. G., Savoldi, I. R., Marcelino, D. E. P., Fernandes, L. T., Peixoto, J. O., et al. (2021). Differentially expressed genes in the femur cartilage transcriptome clarify the understanding of femoral head separation in chickens. *Sci. Rep.* 11, 17965. doi:10.1038/s41598-021-97306-3

Ibelli, A. M. G., Peixoto, J. O., Marchesi, J. A. P., Coutinho, L. L., and Ledur, M. C. (2014). New insights on the influence of leptin receptor gene in bone traits in broilers. *Proc. World Congr. Genet. Appl. Livest. Prod.* 2014, 328.

Jeffries, M. A., Donica, M., Baker, L. W., Stevenson, M. E., Annan, A. C., Beth Humphrey, M., et al. (2016). Genome-Wide DNA methylation study identifies significant epigenomic changes in osteoarthritic subchondral bone and similarity to overlying cartilage. *Arthritis Rheumatol.* 68, 1403–1414. doi:10.1002/art.39555

Jiang, T., Mandal, R. K., Wideman, R. F., Khatiwara, A., Pevzner, I., Min Kwon, Y., et al. (2015). Molecular survey of bacterial communities associated with bacterial chondronecrosis with osteomyelitis (BCO) in broilers. *PLoS One* 10, e0124403. doi:10.1371/journal.pone.0124403

Kapur, S., Amoui, M., Kesavan, C., Wang, X., Mohan, S., Baylink, D. J., et al. (2010). Leptin receptor (lepr) is a negative modulator of bone mechanosensitivity and genetic variations in lepr may contribute to the differential osteogenic response to mechanical stimulation in the C57BL/6J and C3H/HeJ pair of mouse strains. *J. Biol. Chem.* 285, 37607–37618. doi:10.1074/JBC.M110.169714

Karlsson, C., Dehne, T., Lindahl, A., Brittberg, M., Pruss, A., Sittinger, M., et al. (2010). Genome-wide expression profiling reveals new candidate genes associated with osteoarthritis. *Osteoarthr. Cartil.* 18, 581–592. doi:10.1016/J.JOCA.2009.12.002

Katsara, O., and Kolupaeva, V. (2018). mTOR-mediated inactivation of 4E-BP1, an inhibitor of translation, precedes cartilage degeneration in rat osteoarthritic knees. *J. Orthop. Res.* 36, 2728–2735. doi:10.1002/JOR.24049

Kavran, J. M., Ward, M. D., Oladosu, O. O., Mulepati, S., and Leahy, D. J. (2010). All mammalian hedgehog proteins interact with cell adhesion molecule, down-regulated by oncogenes (CDO) and brother of CDO (BOC) in a conserved manner. *J. Biol. Chem.* 285, 24584–24590. doi:10.1074/jbc.M110.131680

Knowles, T. G., Kestin, S. C., Haslam, S. M., Brown, S. N., Green, L. E., Butterworth, A., et al. (2008). Leg disorders in broiler chickens: Prevalence, risk factors and prevention. *PLoS One* 3, e1545. doi:10.1371/journal.pone.0001545

Kostrominova, T. Y., and Brooks, S. V. (2013). Age-related changes in structure and extracellular matrix protein expression levels in rat tendons. *Age* 35, 2203–2214. doi:10.1007/S11357-013-9514-2

Lee, Y. J., Park, S. Y., Park, E. K., and Kim, J. E. (2019). Unique cartilage matrix-associated protein regulates fibrillin-2 expression and directly interacts with fibrillin-2 protein independent of calcium binding. *Biochem. Biophys. Res. Commun.* 511, 221–227. doi:10.1016/J.BBRC.2019.01.128

Li, N., Yu, J., Cao, X., Wu, Q. Y., Li, W. W., Li, T. F., et al. (2014). A novel p. Gly630Ser mutation of COL2A1 in a Chinese family with presentations of legg–calvé–perthes disease or avascular necrosis of the femoral head. *PLoS One* 9, e100505. doi:10.1371/JOURNAL.PONE.0100505

Li, P. F., Zhou, Z. L., Shi, C. Y., and Hou, J. F. (2015). Downregulation of basic fibroblast growth factor is associated with femoral head necrosis in broilers. *Poult. Sci.* 94, 1052–1059. doi:10.3382/ps/pev071

Liberzon, A., Subramanian, A., Pinchback, R., Thorvaldsdóttir, H., Tamayo, P., Mesirov, J. P., et al. (2011). Molecular signatures database (MSigDB) 3.0. *Bioinformatics* 27, 1739–1740. doi:10.1093/BIOINFORMATICS/BTR260

Liu, K., Wang, K., Wang, L., and Zhou, Z. (2021a). Changes of lipid and bone metabolism in broilers with spontaneous femoral head necrosis. *Poult. Sci.* 100, 100808. doi:10.1016/J.PSJ.2020.10.062

Liu, T., Cao, Y., Han, C., An, F., Wang, T., Sun, M., et al. (2021b). Association of MIR17HG and MIR155HG gene variants with steroid-induced osteonecrosis of the femoral head in the population of northern China. *J. Orthop. Surg. Res.* 16, 673. doi:10.1186/s13018-021-02669-y

Long, F., and Ornitz, D. M. (2013). Development of the endochondral skeleton. *Cold Spring Harb. Perspect. Biol.* 5, a008334. doi:10.1101/CSHPERSPECT.A008334

Lui, J. C., Jee, Y. H., Garrison, P., Iben, J. R., Yue, S., Ad, M., et al. (2018). Differential aging of growth plate cartilage underlies differences in bone length and thus helps determine skeletal proportions. *PLoS Biol.* 16, e2005263. doi:10.1371/JOURNAL.PBIO.2005263

Manon-Jensen, T., and Karsdal, M. A. (2016). "Chapter 14-type XIV collagen," in *Biochemistry of Collagens, Laminins and Elastin* (Cambridge, Massachusetts, EUA: Academic Press), 93–95.

McLaren, W., Gil, L., Hunt, S. E., Riat, H. S., Ritchie, G. R. S., Thormann, A., et al. (2016). The Ensembl variant Effect predictor. *Genome Biol.* 17, 122. doi:10.1186/s13059-016-0974-4

McMurdie, P. J., and Holmes, S. (2013). phyloseq: An R package for reproducible interactive analysis and graphics of microbiome census data. *PLoS One* 8, e61217. doi:10.1371/JOURNAL.PONE.0061217

McNamee, P. T., and Smyth, J. A. (2000). Bacterial chondronecrosis with osteomyelitis ('femoral head necrosis') of broiler chickens: A review. *Avian Pathol.* 29, 253–270. doi:10.1080/03079450050118386

Mis, E. K., Liem, K. F., Kong, Y., Schwartz, N. B., Domowicz, M., Weatherbee, S. D., et al. (2014). Forward genetics defines Xylt1 as a key, conserved regulator of early chondrocyte maturation and skeletal length. *Dev. Biol.* 385, 67–82. doi:10.1016/J.YDBIO.2013.10.014

Mishra, A., Awasthi, S., Raj, S., Mishra, P., and Srivastava, R. N. (2019). Identifying the role of ASPN and COMP genes in knee osteoarthritis development. *J. Orthop. Surg. Res.* 14, 337. doi:10.1186/s13018-019-1391-7

Müller, A., Hundt, C., Hildebrandt, A., Hankeln, T., and Schmidt, B. (2017). MetaCache: Context-aware classification of metagenomic reads using minhashing. *Bioinformatics* 33, 3740–3748. doi:10.1093/BIOINFORMATICS/BTX520

Murayama, M. A., Kakuta, S., Maruhashi, T., Shimizu, K., Seno, A., Kubo, S., et al. (2014). CTRP3 plays an important role in the development of collagen-induced arthritis in mice. *Biochem. Biophys. Res. Commun.* 443, 42–48. doi:10.1016/J.BBRC.2013.11.040

Murayama, M. A., Kakuta, S., Inoue, A., Umeda, N., Yonezawa, T., Maruhashi, T., et al. (2015). CTRP6 is an endogenous complement regulator that can effectively treat induced arthritis. *Nat. Commun.* 61 (6), 8483. doi:10.1038/ncomms9483

Nilsson, O., Parker, E. A., Hegde, A., Chau, M., Barnes, K. M., Baron, J., et al. (2007). Gradients in bone morphogenetic protein-related gene expression across the growth plate. *J. Endocrinol.* 193, 75–84. doi:10.1677/JOE.1.07099

Nistala, H., Lee-Arteaga, S., Smaldone, S., Siciliano, G., and Ramirez, F. (2010). Extracellular microfibrils control osteoblast-supported osteoclastogenesis by restricting TGFβ stimulation of RANKL production. *J. Biol. Chem.* 285, 34126–34133. doi:10.1074/JBC.M110.125328

Oliveira, H. C., Ibelli, A. M. G., Guimarães, S. E. F., Cantão, M. E., Peixoto, J. D. O., Coutinho, L. L., et al. (2020). RNA-seq reveals downregulated osteochondral genes potentially related to tibia bacterial chondronecrosis with osteomyelitis in broilers. *BMC Genet.* 21, 58. doi:10.1186/s12863-020-00862-2

Osório, J. (2015). Stem cells: Back to the origins--identifying the skeletal stem cell. *Nat. Rev. Endocrinol.* 113 (11), 132. doi:10.1038/nrendo.2015.14

Packialakshmi, B., Rath, N. C., Huff, W. E., and Huff, G. R. (2015). Poultry femoral head separation and necrosis: A review. *Avian Dis.* 59, 349–354. doi:10.1637/11082-040715-Review.1

Pagès, H., Carlson, J., Facon, S., and Li, L. (2022). AnnotationDbi: Manipulation of SQLite-based annotations in bioconductor. Available at: https://bioconductor.org/packages/release/bioc/html/AnnotationDbi.html (Accessed May 10, 2022).

Paludo, E., Ibelli, A. M. G., Peixoto, J. O., Tavernari, F. C., Lima-Rosa, C. A. V., Pandolfi, J. R. C., et al. (2017). The involvement of RUNX2 and SPARC genes in the bacterial chondronecrosis with osteomyelitis in broilers. *Animal* 11, 1063–1070. doi:10.1017/S1751731116002433

Paradise, C. R., Galeano-Garces, C., Galeano-Garces, D., Dudakovic, A., Milbrandt, T. A., Saris, D. B. F., et al. (2018). Molecular characterization of physis tissue by RNA sequencing. *Gene* 668, 87–96. doi:10.1016/J.GENE.2018.05.034

Paulson, J. N., Colin Stine, O., Bravo, H. C., and Pop, M. (2013). Differential abundance analysis for microbial marker-gene surveys. *Nat. Methods* 2013, 1200–1202. doi:10.1038/nmeth.2658

Paxton, H., Tickle, P. G., Rankin, J. W., Codd, J. R., and Hutchinson, J. R. (2014). Anatomical and biomechanical traits of broiler chickens across ontogeny. Part II. Body segment inertial properties and muscle architecture of the pelvic limb. *PeerJ* 2, e473. doi:10.7717/peerj.473

Peixoto, J. D. O., Savoldi, I. R., Ibelli, A. M. G., Cantão, M. E., Jaenisch, F. R. F., Giachetto, P. F., et al. (2019). Proximal femoral head transcriptome reveals novel candidate genes related to epiphysiolysis in broiler chickens. *BMC Genomics* 20, 1031. doi:10.1186/s12864-019-6411-9

Petry, B., Savoldi, I. R., Ibelli, A. M. G., Paludo, E., de Oliveira Peixoto, J., Jaenisch, F. R. F., et al. (2018). New genes involved in the Bacterial Chondronecrosis with Osteomyelitis in commercial broilers. *Livest. Sci.* 208, 33–39. doi:10.1016/j.livsci.2017.12.003

Pfaffl, M. W., Horgan, G. W., and Dempfle, L. (2002). Relative expression software tool (REST) for group-wise comparison and statistical analysis of relative expression results in real-time PCR. *Nucleic Acids Res.* 30, e36. doi:10.1093/NAR/30.9.E36

Pouya, F., and Kerachian, M. A. (2015). Avascular necrosis of the femoral head: Are any genes involved? *Arch. Bone Jt. Surg.* 3, 149–155.

Prisby, R., Menezes, T., Campbell, J., Benson, T., Samraj, E., Pevzner, I., et al. (2014). Kinetic examination of femoral bone modeling in broilers. *Poult. Sci.* 93, 1122–1129. doi:10.3382/PS.2013-03778

Purcell, S., Neale, B., Todd-Brown, K., Thomas, L., Ferreira, M. A. R., Bender, D., et al. (2007). Plink: A tool set for whole-genome association and population-based linkage analyses. *Am. J. Hum. Genet.* 81, 559–575. doi:10.1086/519795

R Core Team (2021). R: A language and environment for statistical computing. Available at: https://www.r-project.org.

Ramser, A., Greene, E., Wideman, R., and Dridi, S. (2021). Local and systemic cytokine, chemokine, and FGF profile in bacterial chondronecrosis with osteomyelitis (BCO)-Affected broilers. *Cells* 10, 3174. doi:10.3390/CELLS10113174

Ramser, A., Greene, E., Alrubaye, A. A. K., Wideman, R., and Dridi, S. (2022). Role of autophagy machinery dysregulation in bacterial chondronecrosis with osteomyelitis. *Poult. Sci.* 101, 101750. doi:10.1016/J.PSJ.2022.101750

Rath, N. C., and Durairaj, V. (2022). Avian bone physiology and poultry bone disorders. *Sturkie's Avian Physiol.* 2022, 549–563. doi:10.1016/B978-0-12-819770-7.00037-2

Ritchie, M. E., Phipson, B., Wu, D., Hu, Y., Law, C. W., Shi, W., et al. (2015). Limma powers differential expression analyses for RNA-sequencing and microarray studies. *Nucleic Acids Res.* 43, e47. doi:10.1093/NAR/GKV007

Rojas-Peña, M. L., Olivares-Navarrete, R., Hyzy, S., Arafat, D., Schwartz, Z., Boyan, B. D., et al. (2014). Characterization of distinct classes of differential gene expression in osteoblast cultures from non-syndromic craniosynostosis bone. *J. Genomics* 2, 121–130. doi:10.7150/JGEN.8833

Ronkina, N., and Gaestel, M. (2022). MAPK-activated protein kinases: Servant or partner? *Annu. Rev. Biochem.* 91, 505–540. doi:10.1146/ANNUREV-BIOCHEM-081720-114505

Santos, C. E., Peixoto, J. de O., Fernandes, L. T., Marcelino, D. E. P., Kawski, V. L., Neis, F. T., et al. (2022). Upregulated genes in articular cartilage may help to counteract femoral head separation in broilers with 21 days of age. *Res. Vet. Sci.* 147, 92–95. doi:10.1016/J.RVSC.2022.04.006

Santulli, G. (2014). Angiopoietin-like proteins: A comprehensive look. *Front. Endocrinol.* 5, 4. doi:10.3389/fendo.2014.00004

Schmit, F., Cremer, S., and Gaubatz, S. (2009). LIN54 is an essential core subunit of the DREAM/LINC complex that binds to the cdc2 promoter in a sequence-specific manner. *FEBS J.* 276, 5703–5716. doi:10.1111/J.1742-4658.2009.07261.X

Sekiya, I., Vuoristo, J. T., Larson, B. L., and Prockop, D. J. (2002). *In vitro* cartilage formation by human adult stem cells from bone marrow stroma defines the sequence of cellular and molecular events during chondrogenesis. *Proc. Natl. Acad. Sci. U. S. A.* 99, 4397–4402. doi:10.1073/PNAS.052716199

Shang, J., Fan, X., Shangguan, L., Liu, H., and Zhou, Y. (2015). Global gene expression profiling and alternative splicing events during the chondrogenic differentiation of human cartilage endplate-derived stem cells. *Biomed. Res. Int.* 2015, 604972. doi:10.1155/2015/604972

Shannon, P., Markiel, A., Ozier, O., Baliga, N. S., Wang, J. T., Ramage, D., et al. (2003). Cytoscape: A software environment for integrated models of biomolecular interaction networks. *Genome Res.* 13, 2498–2504. doi:10.1101/GR.1239303

Shukunami, C., Oshima, Y., and Hiraki, Y. (2005). Chondromodulin-I and tenomodulin: A new class of tissue-specific angiogenesis inhibitors found in hypovascular connective tissues. *Biochem. Biophys. Res. Commun.* 333, 299–307. doi:10.1016/J.BBRC.2005.05.133

Steiß, V., Letschert, T., Schäfer, H., and Pahl, R. (2012). PERMORY-MPI: A program for high-speed parallel permutation testing in genome-wide association studies. *Bioinformatics* 28, 1168–1169. doi:10.1093/BIOINFORMATICS/BTS086

Szklarczyk, D., Gable, A. L., Lyon, D., Junge, A., Wyder, S., Huerta-Cepas, J., et al. (2019). STRING v11: Protein-protein association networks with increased coverage, supporting functional discovery in genome-wide experimental datasets. *Nucleic Acids Res.* 47, D607–D613. doi:10.1093/nar/gky1131

TNMD (2022). GeneCards - hum. gene database. Available at: https://www.genecards.org/cgi-bin/carddisp.pl?gene=TNMD (Accessed May 5, 2022).

Twine, N. A., Chen, L., Pang, C. N., Wilkins, M. R., and Kassem, M. (2014). Identification of differentiation-stage specific markers that define the *ex vivo* osteoblastic phenotype. *Bone* 67, 23–32. doi:10.1016/J.BONE.2014.06.027

Wickham, H. (2016). "Elegant graphics for data analysis," in *ggplot2*. 2nd ed. (Berlin, Germany: Springer Cham). doi:10.1007/978-3-319-24277-4_9

Wideman, R. F. (2016). Bacterial chondronecrosis with osteomyelitis and lameness in broilers: A review. *Poult. Sci.* 95, 325–344. doi:10.3382/ps/pev320

Wilson, F. D., Stayer, P., Pace, L. W., Hoerr, F. J., and Magee, D. L. (2019). Disarticulation-associated femoral head separation in clinically normal broilers:

Histologic documentation of underlying and predisposing cartilage abnormalities. *Avian Dis.* 63, 495–505. doi:10.1637/19-00090.1

Wu, T., Hu, E., Xu, S., Chen, M., Guo, P., Dai, Z., et al. (2021). clusterProfiler 4.0: A universal enrichment tool for interpreting omics data. *Innov* 2. doi:10.1016/J.XINN.2021.100141

Xavier, G. M., Seppala, M., Barrell, W., Birjandi, A. A., Geoghegan, F., Cobourne, M. T., et al. (2016). Hedgehog receptor function during craniofacial development. *Dev. Biol.* 415, 198–215. doi:10.1016/J.YDBIO.2016.02.009

Xu, Z., Maiti, D., Kisiel, W., and Duh, E. J. (2006). Tissue factor pathway inhibitor-2 is upregulated by vascular endothelial growth factor and suppresses growth factor-induced proliferation of endothelial cells. *Arterioscler. Thromb. Vasc. Biol.* 26, 2819–2825. doi:10.1161/01.ATV.0000248731.55781.87

Yu, J., and Urban, J. (2013). Immunolocalisation of fibrillin microfibrils in the calf metacarpal and vertebral growth plate. *J. Anat.* 223, 641–650. doi:10.1111/JOA.12123

Yu, Y., Wang, S., and Zhou, Z. (2020). Cartilage homeostasis affects femoral head necrosis induced by methylprednisolone in broilers. *Int. J. Mol. Sci.* 202021, 4841. doi:10.3390/IJMS21144841

Zhang, C. C., Kaba, M., Ge, G., Xie, K., Tong, W., Hug, C., et al. (2006). Angiopoietin-like proteins stimulate *ex vivo* expansion of hematopoietic stem cells. *Nat. Med.* 12, 240–245. doi:10.1038/NM1342

Zhu, F., Friedman, M. S., Luo, W., Woolf, P., and Hankenson, K. D. (2012). The transcription factor osterix (SP7) regulates BMP6-induced human osteoblast differentiation. *J. Cell. Physiol.* 227, 2677–2685. doi:10.1002/JCP.23010

frontiers | Frontiers in Physiology

TYPE Original Research
PUBLISHED 31 August 2022
DOI 10.3389/fphys.2022.962330

OPEN ACCESS

EDITED BY
Chongxiao (Sean) Chen, North Carolina State University, United States

REVIEWED BY
Prafulla Regmi,
University of Georgia, United States
Zhonghou Wang,
UF-Scripps Biomedical Research, United States
Pramir Maharjan,
Tennessee State University, United States

*CORRESPONDENCE
Guang-hai Qi,
qiguanghai@caas.cn
Bao-ming Li,
libm@cau.edu.cn

SPECIALTY SECTION
This article was submitted to Avian Physiology, a section of the journal Frontiers in Physiology

RECEIVED 06 June 2022
ACCEPTED 01 August 2022
PUBLISHED 31 August 2022

CITATION
Fu Y, Wang J, Schroyen M, Chen G, Zhang H-j, Wu S-g, Li B-m and Qi G-h (2022), Effects of rearing systems on the eggshell quality, bone parameters and expression of genes related to bone remodeling in aged laying hens. *Front. Physiol.* 13:962330. doi: 10.3389/fphys.2022.962330

Effects of rearing systems on the eggshell quality, bone parameters and expression of genes related to bone remodeling in aged laying hens

Yu Fu[1,2], Jing Wang[1], Martine Schroyen[2], Gang Chen[3], Hai-jun Zhang[1], Shu-geng Wu[1], Bao-ming Li[3]* and Guang-hai Qi[1]*

[1]Key Laboratory of Feed Biotechnology, Ministry of Agriculture and Rural Affairs, Institute of Feed Research, Chinese Academy of Agricultural Sciences, Beijing, China, [2]Precision Livestock and Nutrition Laboratory, TERRA Teaching and Research Centre, Gembloux Agro-Bio Tech, University of Liège, Gembloux, Belgium, [3]Key Laboratory of Bio-environmental Engineering, Ministry of Agriculture and Rural Affairs, China Agricultural University, Beijing, China

Public concerns regarding animal welfare are changing the selection of rearing systems in laying hens. This study investigated the effects of rearing systems on eggshell quality, bone parameters and relative expression levels of genes related to bone remodeling in aged laying hens. A total of 2,952 55-day-old Jing Tint Six pullets were randomly assigned to place in the conventional caging system (CCS) or aviary system (AVS) and kept until 95 weeks of age. The AVS group delayed the decrease of eggshell quality and alleviated the symptoms of osteoporosis in the humerus rather than in the femur. Eggshell breaking strength, thickness, weight, weight ratio, stiffness and fracture toughness were decreased linearly with age (from 55 to 95 weeks of age, $p < 0.05$). The AVS group had higher eggshell breaking strength, stiffness and fracture toughness than the CCS group ($p < 0.05$). Higher total calcium and phosphorus per egg were presented in the AVS group at 95 weeks of age ($p < 0.05$). At 95 weeks of age, the AVS group had a humerus with higher weight, volume, length, midpoint perimeter, cortical index, fat-free dry weight, ash content, total calcium per bone, total phosphorus per bone, average bone mineral density, strength, stiffness and work to fracture compared to the CCS group ($p < 0.05$). Such differences did not appear in the femur. The relative expression levels of alkaline phosphatase (ALP) and osteocalcin (OCN) genes in the femur and hormone receptors (vitamin D receptor (VDR), estrogen receptor alpha (ERα) and fibroblast growth factor 23 (FGF23)) genes in the humerus were significantly upregulated ($p < 0.05$) in the AVS group. The level of tartrate-resistant acid phosphatase (TRAP) transcripts was also increased ($p < 0.05$) in the femur of the AVS group. Overall, compared with the CCS, the AVS alleviated the deterioration of eggshell and bone

qualities of aged laying hens, which may be related to the changes in the expression of genes associated with bone remodeling.

KEYWORDS

bone quality, eggshell quality, conventional caging system, laying hen, aviary system

Introduction

Although the caging system has an edge in reducing the risk for feather-pecking, cannibalism and mortality (Fossum et al., 2009; Kjaer, 2009), the conventional caging system (CCS) limits the movement of hens and not welfare friendly to birds in aspects of the expression of natural behaviors (Bessei, 2019). In recent decades, the CCS has been prohibited in some regions (e.g. the European Union, Switzerland, Argentina, Australia, Brazil and New Zealand) through legislations and mandatory measures, but it still remains widespread in some countries such as China, Canada and the United States (Bessei, 2019). The transition from the CCS to the alternative or cage-free systems is an inevitable trend under multiple pressures from animal welfare and the international market scrutiny.

Aviary system (AVS), a cage-free system, is a promising alternation, which provides more activity space and enrichments (e.g., perches, terraces and platforms) to increase opportunities of locomotion, develop skills to navigate and reduce the risk of abnormal behavioral development (Hester, 2014; Janczak and Riber, 2015; Campbell et al., 2016). It not only improves animal welfare, but also has a positive impact on bone strengthening (Regmi et al., 2015). An early investigation in the causes of bone loss noted CCS had a higher incidence of osteoporosis (OP) (King, 1965) that is associated with fracture and premature mortality (Whitehead, 2004). Pullets raised in AVS has been evidenced to have bones with higher mineralization and strength (Regmi et al., 2015; Casey-Trott et al., 2017), and such benefits for bones could persist into the late period of laying (until the 14th month of laying) (Leyendecker et al., 2005). Extended laying period (from 80 weeks of age to 100 weeks of age) is a commonly mentioned target in recent years (Pottgüter, 2016), which presents greater challenges for bone quality of laying hens, since the long-term mobilization of Ca related to eggshell formation may lead to the hen's skeletal Ca to be absorbed into its uterus during eggshell formation, resulting in bone mineral loss and inducing OP (Wilson and Thorp, 1998; Cransberg et al., 2001). Additionally, the changes in bone quality in return could affect eggshell quality, as 20%–40% of the eggshell Ca content are derived from bone resorption (Comar and Driggers, 1949; Clunies et al., 1993). However, less attention has been given to the effects of rearing systems on eggshell quality. Our current study speculates that hens kept in AVS for a long time may alleviate the deterioration of bone and eggshell qualities compared to those kept in the CCS, which benefits the achievement of extended laying period. Thus, it is necessary to further compare the effects of CCS and AVS on eggshell and bone qualities of aged laying hens (over 80 weeks of age).

Given the complicated interactions between bone and eggshell, the mechanism of rearing systems on avian skeleton quality has been poorly understood. Two special types of skeletons remained during evolution in birds, one of which is a light but firm skeleton (without medullary bone) such as the humerus in charge of the ability to fly, and the other is a long bone containing medullary bone such as the femur (Dacke et al., 2015). The supply of Ca in eggshell formation depends on the rapid mobilization of medullary bone, while the humerus (mainly cortical bone) contributes only a little (Dacke et al., 1993; Dacke et al., 2015). Thus, the humerus and the femur may undergo bone remodeling in different manners. Their joint analysis may contribute to revealing the effects and molecular mechanisms of rearing systems on bone remodeling and eggshell formation.

This study tracked the eggshell quality of hens kept in the CCS and AVS at the late laying period, followed by analyzing their bone quality at the end of laying period. It then focused on the levels of bone remodeling-related transcripts and uterine Ca transport-related transcripts to explore the molecular mechanisms of rearing systems on bone remodeling and eggshell formation. This study may provide references for the selection of rearing systems in laying hens.

Materials and methods

Birds and experimental design

A total of 2,952 55-day-old Jing Tint Six pullets with similar body weight were purchased from Beijing Huadu Yukou Poultry Industry Co., Ltd. of China and randomly assigned to CCS and AVS. Jing Tint Six was based on Rhode Island Red and White Leghorn and featured with pink eggs. Breeder recommended, to 80 weeks, total egg number is around 380, the average egg weight is about 55.8 g, the egg production of the peak laying period is over 95%, the livability is more than 95%, and the average daily feed intake is around 106 g during laying period, and average body weight at 80 weeks is around 1800 g. The CCS was a four-tier battery system, whereas the AVS was a four-tier aviary system. Three hundred and sixty of hens were placed in 30 cages (12 hens per cage) of CCS with a space allowance of 450 cm^2/hen; total cage area = 5,400 cm^2. Another 2,592 hens were placed in 6 units of AVS with floor space allowance of

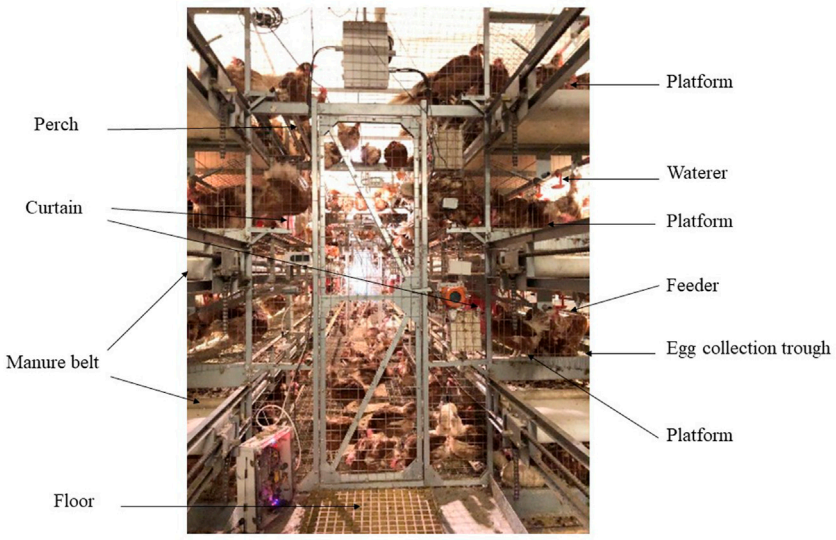

FIGURE 1
Image of aviary system employed in this study. The dimension (length × width × height) of the unit was 480 cm × 280 cm × 330 cm. Image depicts the main equipment inside the system (floor area 134,400 cm^2, total system area 396,144 cm^2), including feeders, waterers, perches, manure belts, litter area, nesting area and suspended platforms (261,744 cm^2).

311 cm^2/hen, and floor +3 layers suspended platforms space allowance of 917 cm^2/hen (floor area 134,400 cm^2, suspended platforms area 261,744 cm^2, total system area 396,144 cm^2). Each system was equally divided into six replicates, CCS had five cages per replicate and AVS had 1 unit per replicate. The dimension (length × width × height) of CCS cages and AVS units were 90 cm × 60 cm × 45 cm and 480 cm × 280 cm × 330 cm. As shown in Figure 1, the AVS had three levels of platforms above the floor, and each level contained two equally sized platforms on either side of the aviary unit interior. The perches of the same length as the platform were mounted on the upper platforms to increase opportunities for locomotion (Hester et al., 2014). Its nesting area was also installed in the platforms and separated by curtains. Each floor is equipped with the manure belt and egg collection trough. In the AVS, the floor and each level platform were equipped with feeders on both sides of the aviary unit, and waterlines with nipple waterers were suspended from the ceilings per level. The feeders and waterers of the CCS were fixed in the similar positions to the AVS.

The CCS and AVS were placed in one room of a research farm of China Agricultural University. This study was not terminated until the hens were 95 weeks of age. According to the nutrient requirements of the National Research Council (1994) and Chinese Feeding Standard of Chicken (Ministry of Agriculture of China, 2004), all pullets were fed a grower diet (CP = 15.5%, Ca = 0.8% and non-phytate p = 0.35%) until 18 weeks of age and changed to laying hen diets (19 weeks of age—the beginning of laying: CP = 17%, Ca = 2% and non-phytate p = 0.32%; the beginning of laying–55 weeks of age: CP:16.5%, Ca = 3.5% and non-phytate p = 0.32%; 55 weeks of age–95 weeks of age: CP = 15.5%, Ca = 3.8% and non-phytate p = 0.32%) later. All diets were purchased from a specialty feed mill. The detailed composition and nutrient levels of the diets were presented in the Supplementary Table S1. The analytical values of Ca and CP in diets from 55 to 95 weeks of age were 3.92% and 16.1%, respectively. All chickens were given feed and water *ad libitum* during the whole experiment. Two systems were given the same photoperiod (8–18 weeks of age: 9 h light/15 h dark, 15 lux; 18–30 weeks of age: increased stepwise to 16 h light/8 h dark, 30 lux; 30–95 weeks of age: 16 h light/8 h dark, 30 lux) and room temperature (15–23°C). The average daily egg production of the CCS and AVS for the whole laying period were 85.76% and 89.48%, respectively. And the average body weight at the end of trial was 1.894 kg in CCS and 1.752 kg in AVS.

Sample collection

Each replicate (5 cages for CCS, 1 unit for AVS) was a sampling unit and an experimental unit. On the final day of 55, 65, 75, 85 and 95 weeks of age, all eggs from each replicate were collected individually, and 10 eggs of them were randomly selected to determine eggshell quality. During each time point, 60 eggs were examined for each system. At the end of the trial, two individuals were chosen randomly from each replicate to sacrifice. The mucosa samples of uterus and duodenum were immediately removed and snap-frozen in liquid nitrogen. Moreover, humeri and femurs on both lateral sides were dissected out and removed from meat and fat. The left bones were stored at −20°C for compositional,

geometrical, morphological, or mechanical analyses. The right bones were truncated from their center. The proximal portion was immersed in formalin to fix. For the rest of the bone, a segment was cut in close proximity to the incision and snap-frozen in liquid nitrogen. Following collection, all samples frozen in liquid nitrogen were transferred to a freezer at −80°C until further analysis.

Egg size and eggshell quality

Sixty eggs from each group were selected for testing at each time point (6 replicates with 10 eggs per replicate). Egg length and width were measured using caliper for calculation of shape index (egg shape index = egg length/egg width). The determination of eggshell quality referred to earlier described methods (Mabe et al., 2003; Fu et al., 2021a). Eggshell thickness was measured with Egg Shell Thickness Gauge (Ramat Hasharon, Israel Orka Food Technology Ltd., Ramat Hasharon, Israel). Eggshell breaking strength was defined as the minimum force required to fracture each egg at a longitudinal compression speed of 5 mm/min. It was measured with Egg Force Reader (Ramat Hasharon, Israel Orka Food Technology Ltd., Ramat Hasharon, Israel) at room temperature with the following parameters: the speed of the cross head, 5 mm/min; rated load capacity, 50 N; overload tolerance, 100 N; accuracy, 0.001 kgf. Eggshell weight was weighted as w_1 after cleaning and drying in room temperature. The sum of dry weights of eggshells from each replicate was W_1. The weight ratio of eggshell was calculated as a percentage score for the weight of each eggshell to the weight of each egg. For eggshell stiffness, a Texture Lab Pro (TMS-Pro, Food Technology Ltd., SV, Sterling, VA, United States) was used with the parameters as follow: the load of sensor, 25 N; the applied load, 10 N; the speed of the cross head, 1 mm/min. According to a previous report (Mabe et al., 2003), eggshell elastic modulus and fracture toughness were calculated as follow: the elastic modulus (N/mm^2) = $[(0.153 \times I^3)–(0.907 \times I^2) + (1.866 \times I)–0.666]/0.444 \times (0.408 + 3.026 \times 2 \times T/w) \times (S_d \times w/2/T^2)$, the fracture toughness ($N/mm^{3/2}$) = $0.777 \times (2.388 + 2.9934 \times 12/w) \times F/T^{3/2}$, where I = egg shape index, T = eggshell thickness (mm), w = egg width (mm), Sd = eggshell stiffness (N/mm), F = breaking strength (N).

All eggshells from each replicate were mixed and crushed as one sample to analyze Ca and P contents according to the reported method (Fu et al., 2021b). Briefly, approximately 0.5 g of eggshell powder was taken and mixed with 3 mL nitric acid and 3 mL H_2O_2 in a burning cup and stood for 2 h. Then, the burning cup with eggshell was digested using a microwave digestion instrument (MDS-10, Shanghai Xinyi Instrument Technology Co., Ltd., Shanghai, China). After digesting, the solutions were transferred to 50 mL volumetric flasks and adjusted to 50 mL by rinsing 3 to 4 times deionized water. Flame atomic absorption spectrophotometry (Z2000, Hitachi Co., Ltd., Tokyo, Japan) was used to analyze the Ca content as C_1. The content of P was measured as C_2 with a spectrophotometer (UV-2700, Shimadzu, Japan). Total Ca and P per egg were calculated as follow: total Ca per egg = $W_1 * C_1$, total P per egg = $W_1 * C_2$.

Bone geometric characteristics

Each group consisted of 6 replicates with 2 birds per replicate. The left bones were thawed at 4°C overnight before weighing. The volume was defined as the amount of water displaced when the bone was placed in a measuring cylinder with water. The bone density was the weight divided by the volume. A vernier caliper and a string were used to measure the length and the midpoint perimeter of the bone. The mean relative wall thickness, the cortical cross-sectional area and the mean cortical index were measured using the proximal portion of the right bone (fixed with formalin) and calculated according to previous methods (Brzoska et al., 2005; Cui et al., 2019). Briefly, the horizontal external and internal cortical bone diameters of the mid-diaphyseal cross section were measured as H and h using a digital caliper, and the vertical external and internal cortical bone diameter of that were measured as B and b. The mean relative wall thickness, the cortical cross-sectional area and the mean cortical index were calculated according to the following formula:

$$\text{Mean relative wall thickness} = [(B - b)/b + (H - h)/h]/2$$

$$\text{Cortical cross–sectional area} = \pi\,(\mathrm{H} \times \mathrm{B} - \mathrm{h} \times \mathrm{b})/4$$

$$\text{Mean cortical index} = [(B - b)/B + (H - h)/H]/2$$

Bone mineral measurements

Following the analyses of geometric characteristics, three regions of each left bone (6 replicates per group, each replicate based on 2 birds) were used for analyzing bone mineral density (BMD) and bone mineral content (BMC) using a dual energy X-ray absorptiometry system (DTX-200, Osteometer MediTech, Hawthorne, CA, United States). The bone was divided into three aliquots and marked with lead needles. The point located near from the body was considered as proximal, and the other was distal. Similarly, the midpoint of the bone was also marked with a lead needle. Bone segments 0.5 cm above and below the lead marker were used to measure BMD and BMC.

Bone mechanical properties

After scanning, TMS-Pro was used to assess bone mechanical properties (strength, stiffness and work to fracture) using the three-point bending method reported by a previous study (Brzoska et al., 2005). Bone strength, stiffness and work to

TABLE 1 Definitions of the mechanical parameters.

Mechanical property	Definition
Bone strength	Minimum load to fracture the bone, descripting the resistance of the whole bone to fracture
Bone stiffness	The slope of the maximum elastic load-displacement curve, describing the resistance of the bone to deformation by a load
Work to fracture	The area under the load–displacement curve up to fracture, describing the amount of the total work done by imposed load to deform and fracture the bone or total energy absorbed by bone until fracture

fracture were defined in the Table 1 according to the previous studies (Ferretti et al., 2001; Brzoska et al., 2005; Cui et al., 2019). Six replicates were used for each group and each replicate contains 2 birds. The span of two support bars was 4 cm. The load of sensor was 1,000 N. The bone was vertically loaded at a displacement rate of 2 mm/min until bone fracture.

Bone components

Each group had 6 replicates and each replicate had 2 birds. The fracture bones were defatted completely and oven-dried at 65°C. The fat-free dry bone was weighed as W_2 and then burned in a muffle furnace until they were fully burned to obtain bone ashes. The bone ash content was determined through calculating the percentage of the ash weight versus the fat-free dry weight. The Ca and P contents in ash were analyzed following the same method described above (Eggshell Quality). Total Ca and P in bones were calculated according to the following formulas: total Ca/P per bone = the Ca/P content in ash × (the ash content × W_2).

Bone histomorphometry

Histomorphological analysis was performed in a blinded manner. The method of Goldner's Trichrome stain was adapted from a previous study (Farr et al., 2017). Femurs and humeri (6 replicates per group with 2 birds per replicate) were decalcified in EDTA until adequately softened. The softened bones were dehydrated, wax dipped, embedded and cut into 4-μm sections. The sections were deparaffinized and stained with Goldner staining solution suit (Servicebio technology Co. Ltd., Wuhan, China). Images were scanned with a panoramic slide scanner (3DHISTECH Ltd., Budapest, Hungary), and suitable areas of interest (AOI) in the proximal and middle parts of the bone were photographed with CaseViewer2.2 software (3DHISTECH Ltd., Budapest, Hungary). The AOI in proximal part of bone were defined as the entire epiphysis and metaphysis, and the AOI in the middle part of the bone was the mid-diaphyseal region (near the incision). Images of the epiphyseal region should contain the entire epiphyseal structure (including the outer cortical bone). Each image of metaphyseal and diaphyseal regions includes cortical bone on both sides. The regions were consistent across all bone samples. And, the same part was photographed at the same magnification.

The analysis of trabecular bone microarchitecture referred to a previous study (Lei et al., 2017) and was conducted with Image-Pro Plus 6.0 (Media Cybemetics, MD, United States) software. Tissue area (T.Ar), trabecular area (Tb.Ar) and trabecular perimeter (Tb.Pm) were measured. Trabecular number (Tb.N), trabecular thickness (Tb.Th), trabecular separation (Tb.Sp) and trabecular bone volume/tissue volume (BV/TV) were calculated using the following equations:

$$BV/TV = \mathrm{Tb}.Ar / \mathrm{T}.Ar \times 100\ (\%)$$
$$Tb.Th = (2000 / 1.199) \times (Tb.Ar / \mathrm{Tb}.Pm)\ (\mu m)$$
$$Tb.N = (1.199 / 2) \times (Tb.Pm / \mathrm{T}.Ar)\ (n/mm)$$
$$Tb.Sp = (2000 / 1.19) \times (T.Ar - \mathrm{Tb}.Ar) / \mathrm{Tb}.Pm\ (\mu m)$$

Quantification of calcium metabolism-related mRNA

The tissue samples (including humerus, femur, uterus and duodenum; six replicates per group with 2 birds per replicate) were ground in liquid nitrogen first. EASYspin Plus Bone Tissue RNA Kit (Aidlab Biotechnologies Co. Ltd., Beijing, China) was used to extract total RNA in the humerus and femur. The total RNA in uterine and duodenal tissues were extracted using TRIzol reagent (Tiangen Biotech Co. Ltd., Beijing, China). The integrity, purity and concentration of RNA were determined by agarose gel electrophoresis and a NanoDrop 2000 spectrophotometer (Thermo Fisher Scientific, Waltham, United States). The cDNA synthesis was done on 1.5 μg total RNA with Easy Script First-Strand cDNA Synthesis SuperMix kit (TransGen Biotech Co. Ltd., Beijing, China). The resulting cDNA was used for subsequent quantification.

Quantitative real-time PCR (qPCR) was carried out by Light Cycler 480 system (Roche, Basel, Switzerland) with SuperReal PreMix kit (Tiangen Biotech Co. Ltd., Beijing, China). The results were processed using $2^{-\Delta\Delta CT}$ method (Livak and Schmittgen, 2001). The sequences of primers were listed in Supplementary Table S2, the housekeeping gene used was avian β-actin.

10.3389/fphys.2022.962330

TABLE 2 Effect of rearing systems on eggshell quality of laying hens (55–95 weeks of age)[a].

Item	Egg size			Eggshell quality						
	Length (mm)	Width (mm)	Shape index (mm/mm)	Breaking strength (N)	Thickness (*0.01 mm)	Weight (g)	Weight ratio (%)	Stiffness (N/mm)	Elastic modulus (N/mm^2)	Fracture toughness ($N/mm^{3/2}$)
System										
CCS	5.84[a]	4.30[a]	1.36	34.95[b]	43.42	5.60	9.16	66.74[b]	4,689.23	305.05[b]
AVS	5.79[b]	4.28[b]	1.35	36.57[a]	43.84	5.54	9.24	67.66[a]	4,643.77	316.65[a]
SEM	0.10	0.04	0.02	0.39	0.21	0.02	0.04	0.56	29.41	2.42
Age, wk										
55	5.69	4.29	1.33	37.57	44.30	5.62	9.49	72.83	4,898.44	317.54
65	5.75	4.28	1.34	38.61	45.28	5.67	9.47	70.98	4,566.53	317.52
75	5.87	4.29	1.37	35.20	43.64	5.54	9.07	65.67	4,552.50	306.25
85	5.85	4.28	1.37	35.23	43.09	5.53	9.10	64.10	4,571.99	313.60
95	5.91	4.31	1.37	32.17	41.82	5.50	8.86	62.42	4,743.05	299.33
SEM	0.10	0.04	0.02	0.39	0.21	0.02	0.04	0.56	29.41	2.42
p-value										
System	<0.001	0.028	0.424	0.002	0.145	0.150	0.166	0.029	0.337	0.011
Age										
Linear	<0.001	0.347	<0.001	<0.001	<0.001	0.007	<0.001	<0.001	0.144	0.017
Quadratic	<0.001	0.293	<0.001	<0.001	<0.001	0.027	<0.001	<0.001	<0.001	0.053
System × Age	0.785	0.319	0.476	0.477	0.270	0.871	0.430	0.796	0.089	0.385

[a]Data represent means with standard error mean. There were six replicates per age in each group. CCS, conventional caging system; AVS, aviary system.
[a,b] Values within a column with no common superscripts differ significantly ($p < 0.05$).

Statistical analysis

The replicate was the experimental unit. All analyses were conducted with SAS 9.4 (SAS Inc.). The homogeneity of variances and the normality of the data were tested first. The Proc GLM procedure was used to examine the effects of rearing system, age and the interaction between these two factors on the data of eggshell quality. The linear and quadratic orthogonal polynomial contrasts were further conducted for age response. Eggshell components, bone qualities and qPCR mean values of two rearing systems were compared using *t*-test procedure. Differences were considered statistically significant at $p < 0.05$.

Results

Egg size and eggshell quality

The results of egg size and eggshell quality are presented in Table 2. Egg length and egg shape index were linearly and quadratically increased with age ($p < 0.05$). The eggs in the AVS group had longer length and width compared to those in the CCS group ($p < 0.05$). Eggshell breaking strength, thickness, weight, weight ratio, stiffness and fracture toughness were decreased linearly with age ($p < 0.05$). Additionally, quadratic effects of age were detected on the egg weight, egg shape index, eggshell breaking strength, thickness, weight, weight ratio, stiffness and elastic modulus ($p < 0.05$). The AVS group had higher eggshell breaking strength, stiffness and fracture toughness than the CCS group ($p < 0.05$).

In Figure 2, the results of eggshell component show that both total Ca and total P per egg in the AVS group were significantly higher than those in the CCS group ($p < 0.05$). In addition, eggshell Ca and P content were numerically higher in the AVS group compared to those in the CCS group, but the differences were not significant (Ca content, $p = 0.071$; P content, $p = 0.063$).

Bone geometric characteristics, and components

Figure 3 presents the differences in the geometric characteristics and components of the humerus and femur obtained from the AVS and CCS groups. Humeral weight, volume, length, midpoint perimeter and cortical index of the

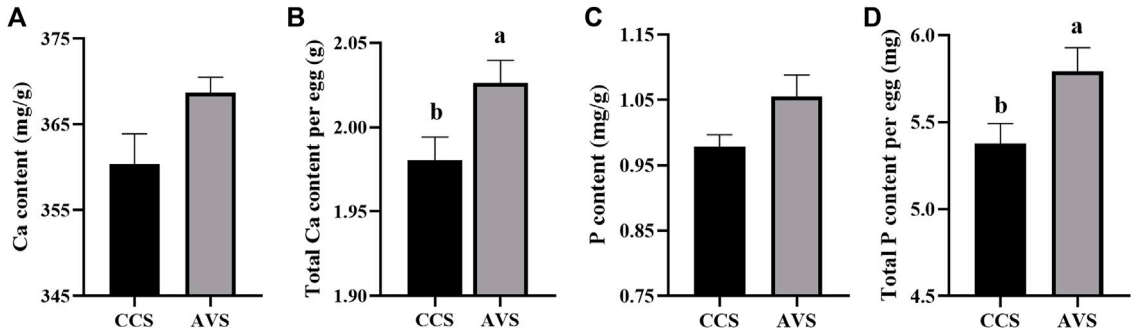

FIGURE 2
Effect of rearing systems on eggshell component of aged laying hens (95 weeks of age) (n = 6). **(A)** Ca content, **(B)** Total Ca per egg, **(C)** P content, **(D)** Total P per egg. CCS, conventional caging system; AVS, aviary system. a,b Bars with different letters differ significantly at $p < 0.05$.

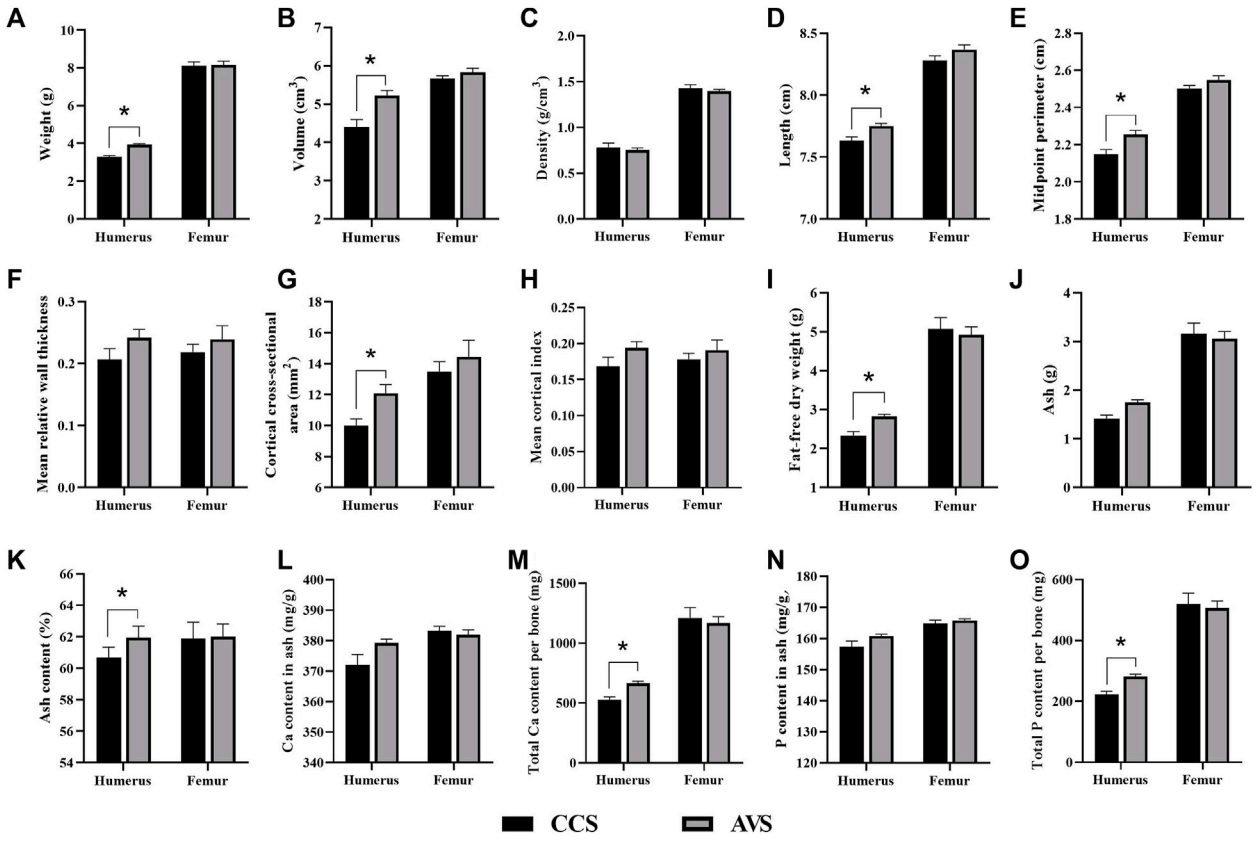

FIGURE 3
Effect of rearing systems on bone geometric characteristics **(A–H)** and component **(I-O)** in the aged laying hens (95 weeks of age) (n = 6). **(A)** Bone weight, **(B)** Volume, **(C)** Density, **(D)** Length, **(E)** Midpoint perimeter, **(F)** Mean relative wall thickness, **(G)** Cortical cross-sectional area, **(H)** Mean cortical index, **(I)** Fat-free dry weight, **(J)** Ash, **(K)** Ash content, **(L)** Ca content in ash, **(M)** Total Ca per bone, **(N)** P content in ash, **(O)** Total P per bone. CCS, conventional caging system; AVS, aviary system. Data represent means with standard error. *$p < 0.05$.

AVS group were obviously higher than those of the CCS group ($p < 0.05$). Compared to the CCS group, the AVS group had a humerus with higher fat-free dry weight, ash content, total Ca per bone and total P per bone ($p < 0.05$). There were no significant differences in the geometric characteristics and components of femur between the two groups ($p > 0.05$).

TABLE 3 Effect of rearing systems on mineral measurements of bones in aged laying hens (95 weeks of age)[a].

Items	CCS	AVS	*p*-value
Humerus			
Distal BMD (g/cm^2)	2.77 ± 0.04	2.82 ± 0.04	0.344
Midshaft BMD (g/cm^2)	2.81 ± 0.09	2.96 ± 0.04	0.141
Proximal BMD (g/cm^2)	2.73 ± 0.03	2.80 ± 0.06	0.257
Average BMD (g/cm^2)	2.77 ± 0.03[b]	2.86 ± 0.03[a]	0.042
Distal BMC (g)	2.50 ± 0.04	2.59 ± 0.06	0.268
Midshaft BMC (g)	1.62 ± 0.08	1.71 ± 0.04	0.296
Proximal BMC (g)	2.37 ± 0.03	2.49 ± 0.06	0.137
Average BMC (g)	2.16 ± 0.04	2.27 ± 0.05	0.134
Femur			
Distal BMD (g/cm^2)	2.72 ± 0.03[b]	2.82 ± 0.02[a]	0.046
Midshaft BMD (g/cm^2)	2.72 ± 0.09	2.87 ± 0.05	0.148
Proximal BMD (g/cm^2)	2.77 ± 0.04	2.89 ± 0.07	0.154
Average BMD (g/cm^2)	2.73 ± 0.04	2.84 ± 0.04	0.112
Distal BMC (g)	2.64 ± 0.04	2.71 ± 0.05	0.331
Midshaft BMC (g)	2.10 ± 0.06	2.23 ± 0.06	0.130
Proximal BMC (g)	2.62 ± 0.04	2.73 ± 0.08	0.238
Average BMC (g)	2.45 ± 0.04	2.56 ± 0.05	0.124

[a]Data represent means with standard error (n = 6). CCS, conventional caging system; AVS, aviary system; BMD, bone mineral density; BMC, bone mineral content.
[a,b] Values within a row with no common superscripts mean significant difference ($p < 0.05$).

TABLE 4 Effect of rearing systems on bone mechanical properties of aged laying hens (95 weeks of age)[a].

Items	CCS	AVS	*p*-value
Humerus			
strength (N)	130.15 ± 6.09[b]	182.44 ± 9.50[a]	0.001
stiffness (N/mm)	67.67 ± 4.58[b]	92.01 ± 6.45[a]	0.012
work to fracture (mJ)	139.20 ± 11.47[b]	217.19 ± 14.88[a]	0.002
Femur			
strength (N)	270.43 ± 20.18	263.27 ± 16.06	0.787
stiffness (N/mm)	188.33 ± 23.99	152.59 ± 6.96	0.183
work to fracture (mJ)	241.41 ± 22.76	287.82 ± 25.15	0.201

[a]Data represent means with standard error (n = 6). CCS, conventional caging system; AVS, aviary system.
[a,b]Values within a row with no common superscripts mean significant difference ($p < 0.05$).

Bone mineral measurements

Table 3 shows the comparative results of bone mineral measurements of laying hens. Compared to the CCS group, the AVS group had higher average BMD of the humerus ($p < 0.05$). The AVS group significantly increased distal BMD of the femur in comparison with the CCS group ($p < 0.05$).

Bone mechanical properties

As seen in the results summarized in Table 4, the strength, stiffness and work to fracture of the humerus in the AVS group were significantly higher than those in the CCS group ($p < 0.05$). However, these two groups did not differ significantly in femoral mechanical properties ($p > 0.05$).

Bone histomorphometry

The representative sections of the humeri and femurs stained with Goldner's Trichrome are shown in Figure 4 (A–D). The lateral margin of cortical bone was clear, while its medial edge lacked clear boundary with the adjacent trabecular bones. All humerus samples presented large cavities inside. In the humerus, most of trabecular bone and osteoid were distributed among the epiphysis, and a little in the metaphysis and diaphysis. The humerus of the AVS group had more trabecular bone and osteoid than that of the CCS group. The trabecular bone and osteoid of the femur were distributed throughout the bone cavity, accompanied by a few lacunae. Larger lacunae were observed in the femur of the AVS group compared to the CCS group. Figure 4 (E–L) shows the results of the blinded analysis of BV/TV, Tb.Th, Tb.N and Tb. Sp. There was a trend towards increased BV/TV ($p = 0.085$) in the humerus of the AVS group.

Quantification of bone remodeling-related mRNA in bone

The results of the expression levels of key genes involved in bone remodeling are shown in Figure 5. Compared to the CCS group, the AVS group significantly increased the relative mRNA expression levels of fibroblast growth factor 23 (FGF23), vitamin D receptor (VDR) and Estrogen receptor alpha (ERα) genes, but significantly decreased that of receptor activator of nuclear factor-kappa B (RANK) gene in humeri ($p < 0.05$). The relative mRNA expression levels of osteocalcin (OCN), alkaline phosphatase (ALP) and tartrate-resistant acid phosphatase (TRAP) genes in femurs were significantly upregulated in the AVS group compared to the CCS group ($p < 0.05$).

Quantification of Ca transport-related mRNA in duodenum and uterus

As seen in the results showed in Figure 6, no significant difference was observed in relative expression level of calbindin (CALB) in the mucosa of duodenum ($p > 0.05$). The AVS group significantly increased the transient receptor

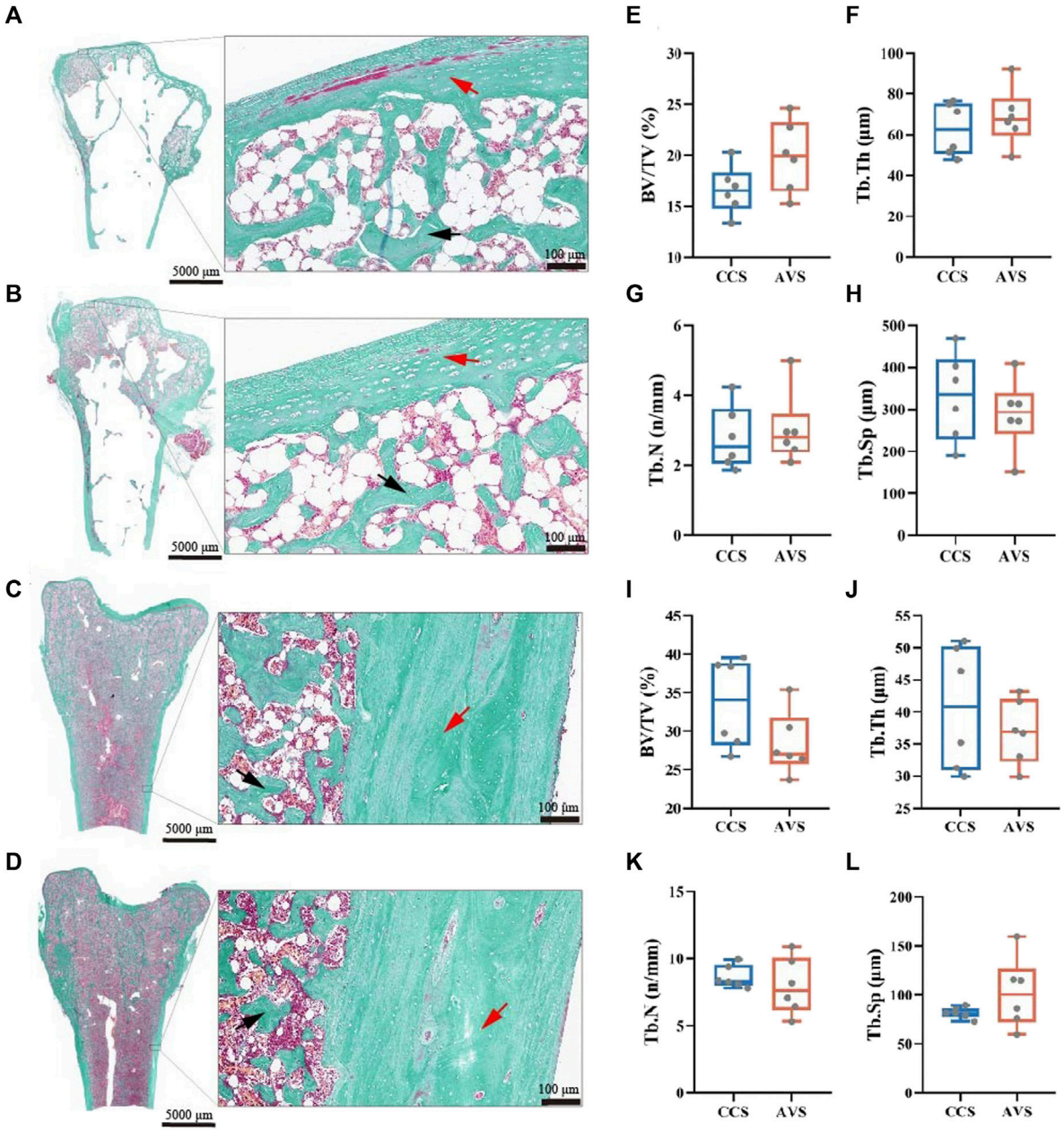

FIGURE 4
Effect of rearing systems on bone histomorphometry of aged laying hens (95 weeks of age) [humerus, **(A,B,E–H)**; femur, **(C,D,I-L)**]. Humeri and femurs were sectioned and stained with Goldner's trichrome [**(A,C)**, the CCS group; **(B,D)**, the AVS group; red arrow, cortical bone; black arrow, trabecular bone]. **(E,I)** Trabecular bone volume/tissue volume (BV/TV), **(F,J)** Trabecular thickness (Tb.Th), **(G,K)** Trabecular number (Tb.N), **(H,L)** Trabecular separation (Tb.Sp). BV/TV, Tb.Th, Tb.N and Tb.Sp were counted under blinded analysis (n = 6). CCS, conventional caging system; AVS, aviary system.

potential cation channel, subfamily V, member 6 (TRPV6) gene relative expression level in the mucosa of uterus compared to the CCS group ($p < 0.05$), while no significant effects were observed on the relative expression levels of CALB, Na^+/Ca^{2+} exchange (NCX) and Ca^{2+} ATPase (PMCA) ($p > 0.05$).

Discussion

Decreased eggshell quality in the late phase of laying poses a considerable threat to the economic benefit of poultry industry. Here, this study traced the eggshell quality of hens at the age of 55–95 weeks. In this stage, the egg size gradually increased and

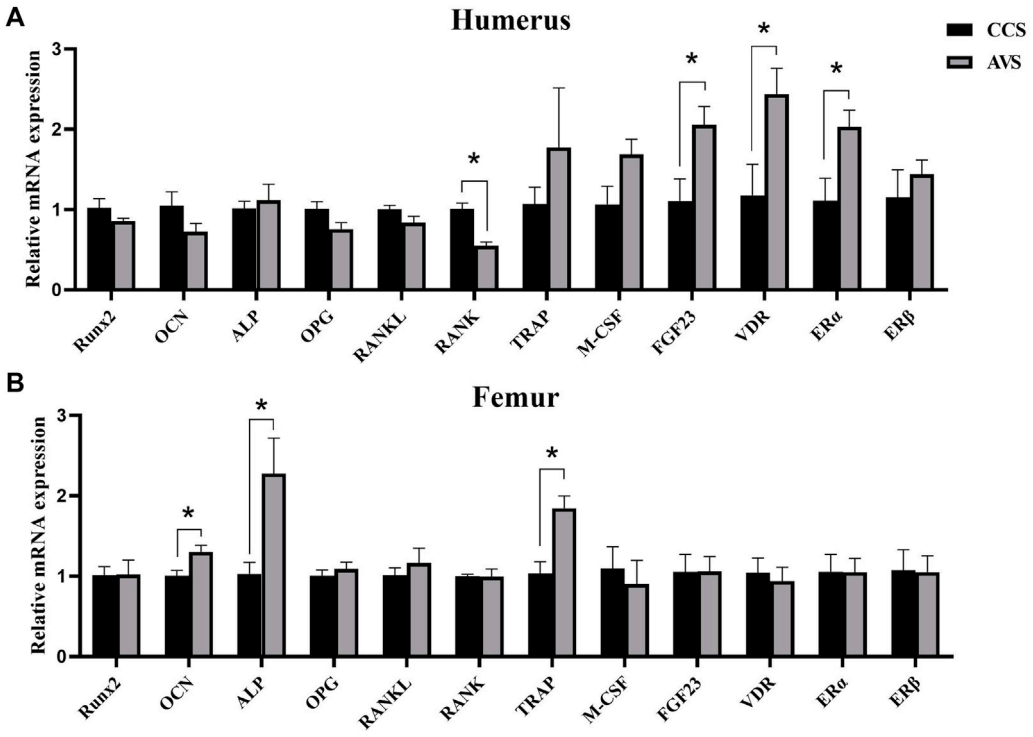

FIGURE 5
Effect of rearing systems on quantification of bone remodeling-related mRNA in bone of aged laying hens (95 weeks of age) (n = 6). **(A)** In the humerus, **(B)** in the femur. CCS, conventional caging system; AVS, aviary system. Runx2, runt-related transcription factor 2; OCN, osteocalcin; ALP, alkaline phosphatase; OPG, osteoprotegerin; RANKL, receptor activator of nuclear factor-kappa B ligand; RANK, receptor activator of nuclear factor-kappa B; TRAP, tartrate-resistant acid phosphatase; M-CSF, macrophage colony-stimulating factor; FGF23, fibroblast growth factor 23; VDR, vitamin D receptor; ERα, estrogen receptor alpha; ERβ, estrogen receptor beta. Data represent means with standard error. *$p < 0.05$.

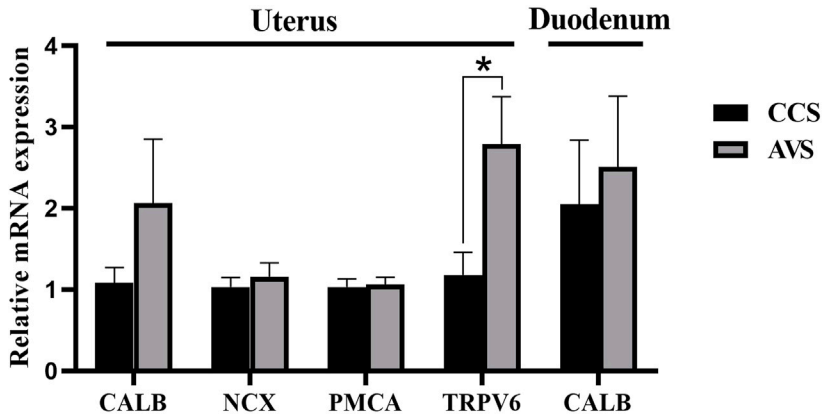

FIGURE 6
Effect of rearing systems on quantification of Ca transport-related mRNA in duodenum and uterus of aged laying hens (95 weeks of age) (n = 6). CCS, conventional caging system; AVS, aviary system. CALB, calbindin; NCX, Na^{+}/Ca^{2+} exchange; PMCA, Ca^{2+} ATPase; TRPV6, transient receptor potential cation channel, subfamily V, member 6. Data represent means with standard error. *$p < 0.05$.

elongated as the age advanced, while eggshell breaking strength, thickness, weight, weight ratio, stiffness and fracture toughness exhibited a gradually decreasing trend, which well agreed with previous studies (Sirri et al., 2018; Gu et al., 2021). Notably, the AVS group seemed to delay these changes. Compared to CCS group, the AVS group had higher eggshell breaking strength, stiffness and fracture toughness. Previous report demonstrated that the AVS had eggshell with thicker thickness than CCS (Leyendecker et al., 2005; Ahammed et al., 2014). Thus, the hens that housed in AVS could produce high-quality eggshells. Calcium carbonate makes up about 96% of the eggshell and is a predominant contributor to its mechanical properties (Hincke et al., 2012). We found that total Ca and P per egg of the AVS group higher than those of the CCS group. This demonstrated that Ca involved in eggshell formation was more in AVS group, and the increase of Ca supply may be a reason of the enhancement in eggshell mechanical properties (Fu et al., 2021a).

During bone remodeling, more bone formation and less bone loss increased bone strength and reduced the incidence of bone fracture (Whitehead, 2004). The AVS group exhibited higher weight, volume, length, midpoint perimeter, cortical index, fat-free dry weight, ash content, total Ca per bone and total P per bone in the humerus, indicating the AVS group had benefits in bone development and remodeling compared to the CCS group. The ultrastructure and mineral measurements of bones are the primary means of diagnosing OP (Brandi, 2009; Rachner et al., 2011). The average BMD of humerus and the distal BMD of femur were significantly increased in the AVS group compared to the CCS group. Similarly, there was a trend ($p = 0.085$) towards increased BV/TV in the humerus. Although no objective diagnostic parameters of OP existed in laying hens, the humerus of the CCS group tilted towards OP symptoms (Brandi, 2009) compared to that of the AVS group. The most severe consequence of OP is fracture, which is the leading cause of osteoporosis-related mortality. A three-point bending test was performed in our current study to simulate the process by which a bone was damaged by force. The strength, stiffness and work to fracture of the humerus were lower in the CCS group, indicating the hens held in this group may be susceptible to fracture in routine activities or accidental injuries. The increase of mechanical properties in the AVS group may be attributed to the enhancements of bone ultrastructure and bone mineral measurements, since the increase of trabecular bone connectivity and mineral deposition offered higher bone fracture resistance (Chen et al., 2020). Previous studies confirmed that exercise played roles in enhancing bone mineral density and ultrastructure (Zymbal et al., 2019), and preventing OP in elder people (Feskanich et al., 2002). These benefits were also confirmed in pullets housed in AVS, which were equipped with perches and platforms to increase opportunities for locomotion (Regmi et al., 2015; Casey-Trott et al., 2017). Our study demonstrated that such effects would carry over to the end of laying phase, but only in the humerus and not in the femur, since similar differences were not found in the femur. Similar results were also observed in a previous study, wherein hens housed in the CCS and AVS had no significant differences on the ash and Young's Modulus of the tibia (Regmi et al., 2016). The marrow cavity of the femur contains medullary bone, which is a source of Ca for eggshell formation (Nys and Le Roy, 2018). The AVS group with high-quality eggshells had a higher demand for Ca, and its bone resorption was more active, which may be susceptible to more bone loss (Dacke et al., 2015). We speculated that the AVS group was beneficial for both humerus and femur development compared to the CCS group, however, such differences may be weakened in the femur due to the differences of eggshell Ca supply.

Eggshell formation occurs primarily in the uterus. At least four Ca transporters (CALB, TRPV6, PMCA, NCX) have already been identified to be involved in the transcellular transport of Ca in the uterus (Bar, 2009). TRPV6 plays important roles in epithelial cellular entry for Ca, and there appeared to be a positive correlation between TRPV6 expression levels and Ca transport capacity (Yang et al., 2013). TRPV6 mRNA increased in the AVS group, which may indicate an enhanced Ca transport capacity, resulting in more Ca to enter the uterus. This could be an explanation for the increased content of eggshell Ca. The Ca transport in the intestinal tract primarily occurs in the anterior section of the small intestine and is considered to be dominated by transmembrane activities associated with CALB (Sugiyama et al., 2007). Herein, no differences were found at the mRNA expression level of CALB in the duodenum, hinting no significant differences in intestinal Ca absorption between the CCS and AVS groups.

Bone homeostasis requires the dynamic balance of bone formation and bone resorption (Feng and McDonald, 2011). Bone resorption could lead to bone mineral loss and damage to bone structure when bone homeostasis is out of the balance (Whitehead, 2004). However, this loss is required in some special physiological states, such as eggshell formation, whenever intestinal Ca absorption is insufficient. Bone resorption contributes 20%–40% of the eggshell Ca content and is one of the major means to supply eggshell Ca (Comar and Driggers, 1949; Clunies et al., 1993). TRAP has been recognized as a histochemical marker for osteoclasts more than several decades (Burstone, 1959). Although TRAP deletion did not affect osteoclast differentiation and resorption pits formation, it impaired the capacity of bone resorption (Hayman et al., 1996). The relative expression value of femur TRAP mRNA in the AVS group was significantly higher compared with the CCS group, which may indicate a higher bone resorption capacity for the femur in the AVS group. ALP and OCN are considered as markers for the early and late osteogenic stages, respectively (Farley et al., 1994; Xu et al., 2019). ALP plays a role in bone mineralization by promoting the hydroxyapatite growth (Nizet et al., 2020). OCN is involved in regulating the process of bone mineralization, and its upregulation promotes terminal

osteogenic differentiation (Xu et al., 2019). The relative expression levels of femur ALP and OCN in the AVS group were also higher than those in the CCS group, suggesting the bone formation of the AVS group might be increased compared to the CCS group. Therefore, the increased expressions of TRAP, ALP and OCN indicated a higher bone remodeling of the femur in the AVS group, which may affect the Ca supply of eggshells, since bone resorption contributes 20%–40% of the eggshell Ca content and is one of the major means to supply eggshell Ca (Comar and Driggers, 1949; Clunies et al., 1993).

The RANK/RANKL/OPG pathway plays a dominant role in osteoclastogenesis. RANK is expressed on the osteoclast precursors, and its binding to RANKL activates NF-κB signaling in osteoclast precursors and induces osteoclasts maturation (Khosla, 2001). However, the decoy receptor OPG released by osteoblasts competes with RANK for binding to RANKL to block this process (Boyce and Xing, 2007). The ratio of RANKL/OPG is considered as a critical factor for osteoclast maturation and activation (Khosla, 2001; Dacke et al., 2015). Although the relative expression level of RANK in the CCS group was higher than in the AVS group, no significant differences were observed in the relative expression levels and rate of RANKL and OPG. Thus, there might be no differences between the CCS and AVS on the bone resorption of the humerus.

However, the humerus in the CCS group showed less bone formation. Active vitamin D and estrogen are involved in osteogenesis and bone formation after binding with the target receptor (mainly VDR and ER, respectively) (Hayashi et al., 2019; Chen et al., 2021). The deficiency of either of them accelerated bone loss and led to an OP phenotype (Chokalingam et al., 2012; Yang et al., 2020). Both VDR and ERα in the AVS group were higher expressed compared to those in the CCS group. In the AVS group, the increased expression of VDR and ERα could prevent bone loss (Peacock et al., 2002; Lam et al., 2014). On the contrary, the CCS group exhibited lower osteogenic ability and bone mass and was more prone to OP, which was consistent with the mechanical and compositional results. Similarly, the relative expression of FGF23 was also higher in the AVS group, and this result may be related to the change of VDR, since FGF23 is a phosphate regulator and involves a negative feedback regulation of vitamin D (Masuyama et al., 2006). Furthermore, the increased expression value of FGF23 may also be related to the increased Ca supply of the uterus in the AVS group. It has been reported that the constant stimulation of parathyroid hormone (PTH) secretion induced by the daily eggshell formation in the uterus could cause a chronic overexpression of FGF23 (Gloux et al., 2020). In our current study, the regulation of rearing systems on bone formation of humerus may be mainly through hormone-dependent pathways. Ca is precisely transmitted among the organs (i.e., the intestine, the kidney, the uterus and bone) by a complex network mediated by endocrine hormones, which mainly involves 1,25-dihydroxyvitamin D, PTH, and estrogen (Dacke et al., 2015). A previous study demonstrated that the effect of in-cage facilities on bone formation in laying hens was independent of PTH-related pathways (Dale et al., 2015). We found that the effect of rearing systems on the humerus may be related to 1,25-dihydroxyvitamin D and estrogen. Further studies will be necessary to determine the regulatory mechanism of the rearing systems on the secretion of 1,25-dihydroxyvitamin D and estrogen. It is also worth investigating whether the regulations of 1,25-dihydroxyvitamin D and estrogen can increase bone formation of the layers housed in the CCS.

In conclusion, compared with the CCS, the AVS alleviated the deterioration of eggshell and bone qualities of aged laying hens. The AVS upregulated the expression of genes associated with bone formation in the femur (ALP, OCN) and humerus (VDR, ERα and FGF23), which may be partly responsible for the improvement in bone quality. The AVS increased the expression of TRAP gene in the femur, hinting a higher bone resorption in the AVS, which may partly account for the improvement of eggshell quality.

Data availability statement

All data can be found in the article. The raw data supporting the conclusion of this article is available from the corresponding author upon reasonable request.

Ethics statement

The animal study was reviewed and approved by the Animal Care and Use Committee of Institute of Feed Research, Chinese Academy of Agricultural Sciences (approval No. AEC-CAAS-20191027).

Author contributions

YF performed the experiment, analyzed data and drafted the manuscript. JW, GQ and BL conceived and designed the experiment. GQ, GC, MS, SW and HZ revised the manuscript. BL and GC contributed rearing systems and experimental animals. SW and HZ contributed reagents and laboratory. All authors have read and approved the manuscript.

Funding

This study was supported by China Agriculture Research System (CARS-40) and the Agricultural Science and Technology Innovation Program (ASTIP) of CAAS. Apart from providing funds, they were not involved in the experiment design, data analysis or writing of this manuscript.

Acknowledgments

The authors thank the other staffs of Nutritional Modulation Lab of Institute of Feed Research and the staffs of Shangzhuang Farm of China Agricultural University for their assistance in conducting the experiment. YF acknowledges support from the graduate student's international exchange grant of Chinese Academy of Agricultural Sciences.

Conflict of interest

The authors declare that the research was conducted in the absence of any commercial or financial relationships that could be construed as a potential conflict of interest.

Publisher's note

All claims expressed in this article are solely those of the authors and do not necessarily represent those of their affiliated organizations, or those of the publisher, the editors and the reviewers. Any product that may be evaluated in this article, or claim that may be made by its manufacturer, is not guaranteed or endorsed by the publisher.

Supplementary material

The Supplementary Material for this article can be found online at: https://www.frontiersin.org/articles/10.3389/fphys.2022.962330/full#supplementary-material

References

Ahammed, M., Chae, B. J., Lohakare, J., Keohavong, B., Lee, M. H., Lee, S. J., et al. (2014). Comparison of aviary, barn and conventional cage raising of chickens on laying performance and egg quality. *Asian-Australas. J. Anim. Sci.* 27, 1196–1203. doi:10.5713/ajas.2013.13394

Bar, A. (2009). Calcium transport in strongly calcifying laying birds: Mechanisms and regulation. *Comp. Biochem. Physiol. A Mol. Integr. Physiol.* 152, 447–469. doi:10.1016/j.cbpa.2008.11.020

Bessei, W. (2019). Impact of animal welfare on worldwide poultry production. *World's. Poult. Sci. J.* 74, 211–224. doi:10.1017/s0043933918000028

Boyce, B. F., and Xing, L. (2007). The RANKL/RANK/OPG pathway. *Curr. Osteoporos. Rep.* 5, 98–104. doi:10.1007/s11914-007-0024-y

Brandi, M. L. (2009). Microarchitecture, the key to bone quality. *Rheumatol. Oxf.* 48, iv3–8. doi:10.1093/rheumatology/kep273

Brzoska, M. M., Majewska, K., and Moniuszko-Jakoniuk, J. (2005). Mechanical properties of femoral diaphysis and femoral neck of female rats chronically exposed to various levels of cadmium. *Calcif. Tissue Int.* 76, 287–298. doi:10.1007/s00223-004-0089-x

Burstone, M. S. (1959). Histochemical demonstration of acid phosphatase activity in osteoclasts. *J. Histochem. Cytochem.* 7, 39–41. doi:10.1177/7.1.39

Campbell, D. L., Makagon, M. M., Swanson, J. C., and Siegford, J. M. (2016). Laying hen movement in a commercial aviary: Enclosure to floor and back again. *Poult. Sci.* 95, 176–187. doi:10.3382/ps/pev186

Casey-Trott, T. M., Korver, D. R., Guerin, M. T., Sandilands, V., Torrey, S., and Widowski, T. M. (2017). Opportunities for exercise during pullet rearing, Part I: Effect on the musculoskeletal characteristics of pullets. *Poult. Sci.* 96, 2509–2517. doi:10.3382/ps/pex059

Chen, C., Adhikari, R., White, D. L., and Kim, W. K. (2021). Role of 1, 25-dihydroxyvitamin D3 on osteogenic differentiation and mineralization of chicken mesenchymal stem cells. *Front. Physiol.* 12, 479596. doi:10.3389/fphys.2021.479596

Chen, C., Turner, B., Applegate, T. J., Litta, G., and Kim, W. K. (2020). Role of long-term supplementation of 25-hydroxyvitamin D3 on laying hen bone 3-dimensional structural development. *Poult. Sci.* 99, 5771–5782. doi:10.1016/j.psj.2020.06.080

Chokalingam, K., Roforth, M. M., Nicks, K. M., McGregor, U., Fraser, D., Khosla, S., et al. (2012). Examination of ERα signaling pathways in bone of mutant mouse models reveals the importance of ERE-dependent signaling. *Endocrinology* 153, 5325–5333. doi:10.1210/en.2012-1721

Clunies, M., Etches, R. J., Fair, C., and Leeson, S. (1993). Blood, intestinal and skeletal calcium dynamics during egg formation. *Can. J. Anim. Sci.* 73, 517–532. doi:10.4141/cjas93-056

Comar, C. L., and Driggers, J. C. (1949). Secretion of radioactive calcium in the hen's egg. *Science* 109, 282. doi:10.1126/science.109.2829.282

Cransberg, P. H., Parkinson, G. B., Wilson, S., and Thorp, B. H. (2001). Sequential studies of skeletal calcium reserves and structural bone volume in a commercial layer flock. *Br. Poult. Sci.* 42, 260–265. doi:10.1080/00071660120048528

Cui, Y. M., Wang, J., Zhang, H. J., Feng, J., Wu, S. G., and Qi, G. H. (2019). Effect of photoperiod on growth performance and quality characteristics of tibia and femur in layer ducks during the pullet phase. *Poult. Sci.* 98, 1190–1201. doi:10.3382/ps/pey496

Dacke, C. G., Arkle, S., Cook, D. J., Wormstone, I. M., Jones, S., Zaidi, M., et al. (1993). Medullary bone and avian calcium regulation. *J. Exp. Biol.* 184, 63–88. doi:10.1242/jeb.184.1.63

Dacke, C. G., Sugiyama, T., and Gay, C. V. (2015). "The role of hormones in the regulation of bone turnover and eggshell calcification," in *Sturkie's avian Physiology*, 549–575.

Dale, M. D., Mortimer, E. M., Kolli, S., Achramowicz, E., Borchert, G., Juliano, S. A., et al. (2015). Bone-remodeling transcript levels are independent of perching in end-of-lay white Leghorn chickens. *Int. J. Mol. Sci.* 16, 2663–2677. doi:10.3390/ijms16022663

Farley, J. R., Hall, S. L., Tanner, M. A., and Wergedal, J. E. (1994). Specific activity of skeletal alkaline phosphatase in human osteoblast-line cells regulated by phosphate, phosphate esters, and phosphate analogs and release of alkaline phosphatase activity inversely regulated by calcium. *J. Bone Min. Res.* 9, 497–508. doi:10.1002/jbmr.5650090409

Farr, J. N., Xu, M., Weivoda, M. M., Monroe, D. G., Fraser, D. G., Onken, J. L., et al. (2017). Targeting cellular senescence prevents age-related bone loss in mice. *Nat. Med.* 23, 1072–1079. doi:10.1038/nm.4385

Feng, X., and McDonald, J. M. (2011). Disorders of bone remodeling. *Annu. Rev. Pathol.* 6, 121–145. doi:10.1146/annurev-pathol-011110-130203

Feskanich, D., Willett, W., and Colditz, G. (2002). Walking and leisure-time activity and risk of hip fracture in postmenopausal women. *JAMA* 288, 2300–2306. doi:10.1001/jama.288.18.2300

Fossum, O., Jansson, D. S., Etterlin, P. E., and Vågsholm, I. (2009). Causes of mortality in laying hens in different housing systems in 2001 to 2004. *Acta Vet. Scand.* 51, 3. doi:10.1186/1751-0147-51-3

Fu, Y., Wang, J., Zhang, H. J., Wu, S. G., Zhou, J. M., and Qi, G. H. (2021a). The partial replacement of sodium chloride with sodium bicarbonate or sodium sulfate in laying hen diets improved laying performance, and eggshell quality and ultrastructure. *Poult. Sci.* 100, 101102. doi:10.1016/j.psj.2021.101102

Fu, Y., Zhang, H. J., Wu, S. G., Zhou, J. M., Qi, G. H., and Wang, J. (2021b). Dietary supplementation with sodium bicarbonate or sodium sulfate affects eggshell quality by altering ultrastructure and components in laying hens. *Animal* 15, 100163. doi:10.1016/j.animal.2020.100163

Gloux, A., Le Roy, N., Meme, N., Piketty, M. L., Prie, D., Benzoni, G., et al. (2020). Increased expression of fibroblast growth factor 23 is the signature of a deteriorated Ca/P balance in ageing laying hens. *Sci. Rep.* 10, 21124. doi:10.1038/s41598-020-78106-7

Gu, Y. F., Chen, Y. P., Jin, R., Wang, C., Wen, C., and Zhou, Y. M. (2021). A comparison of intestinal integrity, digestive function, and egg quality in laying hens with different ages. *Poult. Sci.* 100, 100949. doi:10.1016/j.psj.2020.12.046

Hayashi, M., Nakashima, T., Yoshimura, N., Okamoto, K., Tanaka, S., and Takayanagi, H. (2019). Autoregulation of osteocyte Sema3A orchestrates

estrogen action and counteracts bone aging. *Cell Metab.* 29, 627–637. doi:10.1016/j.cmet.2018.12.021

Hayman, A. R., Jones, S. J., Boyde, A., Foster, D., Colledge, W. H., Carlton, M. B., et al. (1996). Mice lacking tartrate-resistant acid phosphatase (Acp 5) have disrupted endochondral ossification and mild osteopetrosis. *Development* 122, 3151–3162. doi:10.1242/dev.122.10.3151

Hester, P. Y., Garner, J. P., Enneking, S. A., Cheng, H. W., and Einstein, M. E. (2014). The effect of perch availability during pullet rearing and egg laying on the behavior of caged White Leghorn hens. *Poult. Sci.* 93, 2423–2431. doi:10.3382/ps.2014-04038

Hester, P. Y. (2014). The effect of perches installed in cages on laying hens. *World's. Poult. Sci. J.* 70, 247–264. doi:10.1017/S0043933914000270

Hincke, M. T., Nys, Y., Gautron, J., Mann, K., Rodriguez-Navarro, A. B., and McKee, M. D. (2012). The eggshell: Structure, composition and mineralization. *Front. Biosci.* 17, 1266–1280. doi:10.2741/3985

Janczak, A. M., and Riber, A. B. (2015). Review of rearing-related factors affecting the welfare of laying hens. *Poult. Sci.* 94, 1454–1469. doi:10.3382/ps/pev123

Khosla, S. (2001). Minireview: The OPG/RANKL/RANK system. *Endocrinology* 142, 5050–5055. doi:10.1210/endo.142.12.8536

King, D. F. (1965). Effects of cage size on cage layer fatigue. *Poult. Sci.* 44, 898–900. doi:10.3382/ps.0440898

Kjaer, J. B. (2009). Feather pecking in domestic fowl is genetically related to locomotor activity levels: Implications for a hyperactivity disorder model of feather pecking. *Behav. Genet.* 39, 564–570. doi:10.1007/s10519-009-9280-1

Lam, N. N., Triliana, R., Sawyer, R. K., Atkins, G. J., Morris, H. A., O'Loughlin, P. D., et al. (2014). Vitamin D receptor overexpression in osteoblasts and osteocytes prevents bone loss during vitamin D-deficiency. *J. Steroid Biochem. Mol. Biol.* 144, 128–131. doi:10.1016/j.jsbmb.2014.01.002

Lei, T., Li, F., Liang, Z., Tang, C., Xie, K., Wang, P., et al. (2017). Effects of four kinds of electromagnetic fields (EMF) with different frequency spectrum bands on ovariectomized osteoporosis in mice. *Sci. Rep.* 7, 553. doi:10.1038/s41598-017-00668-w

Leyendecker, M., Hamann, H., Hartung, J., Kamphues, J., Neumann, U., Sürie, C., et al. (2005). Keeping laying hens in furnished cages and an aviary housing system enhances their bone stability. *Br. Poult. Sci.* 46, 536–544. doi:10.1080/00071660500273094

Livak, K. J., and Schmittgen, T. D. (2001). Analysis of relative gene expression data using real-time quantitative PCR and the 2(-Delta Delta C(T)) Method. *Methods* 25, 402–408. doi:10.1006/meth.2001.1262

Mabe, I., Rapp, C., Bain, M. M., and Nys, Y. (2003). Supplementation of a corn-soybean meal diet with manganese, copper, and zinc from organic or inorganic sources improves eggshell quality in aged laying hens. *Poult. Sci.* 82, 1903–1913. doi:10.1093/ps/82.12.1903

Masuyama, R., Stockmans, I., Torrekens, S., Van Looveren, R., Maes, C., Carmeliet, P., et al. (2006). Vitamin D receptor in chondrocytes promotes osteoclastogenesis and regulates FGF23 production in osteoblasts. *J. Clin. Invest.* 116, 3150–3159. doi:10.1172/JCI29463

Nizet, A., Cavalier, E., Stenvinkel, P., Haarhaus, M., and Magnusson, P. (2020). Bone alkaline phosphatase: An important biomarker in chronic kidney disease - mineral and bone disorder. *Clin. Chim. Acta.* 501, 198–206. doi:10.1016/j.cca.2019.11.012

Nys, Y., and Le Roy, N. (2018). *Calcium homeostasis and eggshell biomineralization in female chicken*, 361–382. in Vitamin D.

Peacock, M., Turner, C. H., Econs, M. J., and Foroud, T. (2002). Genetics of osteoporosis. *Endocr. Rev.* 23, 303–326. doi:10.1210/edrv.23.3.0464

Pottgüter, R. (2016). Feeding laying hens to 100 Weeks of age. *LOHMANN Inf.* 50, 18–21.

Rachner, T. D., Khosla, S., and Hofbauer, L. C. (2011). Osteoporosis: Now and the future. *Lancet* 377, 1276–1287. doi:10.1016/S0140-6736(10)62349-5

Regmi, P., Deland, T. S., Steibel, J. P., Robison, C. I., Haut, R. C., Orth, M. W., et al. (2015). Effect of rearing environment on bone growth of pullets. *Poult. Sci.* 94, 502–511. doi:10.3382/ps/peu041

Regmi, P., Smith, N., Nelson, N., Haut, R. C., Orth, M. W., and Karcher, D. M. (2016). Housing conditions alter properties of the tibia and humerus during the laying phase in Lohmann white Leghorn hens. *Poult. Sci.* 95, 198–206. doi:10.3382/ps/pev209

Sirri, F., Zampiga, M., Berardinelli, A., and Meluzzi, A. (2018). Variability and interaction of some egg physical and eggshell quality attributes during the entire laying hen cycle. *Poult. Sci.* 97, 1818–1823. doi:10.3382/ps/pex456

Sugiyama, T., Kikuchi, H., Hiyama, S., Nishizawa, K., and Kusuhara, S. (2007). Expression and localisation of calbindin D28k in all intestinal segments of the laying hen. *Br. Poult. Sci.* 48, 233–238. doi:10.1080/00071660701302270

Whitehead, C. C. (2004). Overview of bone biology in the egg-laying hen. *Poult. Sci.* 83, 193–199. doi:10.1093/ps/83.2.193

Wilson, S., and Thorp, B. H. (1998). Estrogen and cancellous bone loss in the fowl. *Calcif. Tissue Int.* 62, 506–511. doi:10.1007/s002239900470

Xu, Y., An, J. J., Tabys, D., Xie, Y. D., Zhao, T. Y., Ren, H. W., et al. (2019). Effect of lactoferrin on the expression profiles of long non-coding RNA during osteogenic differentiation of bone marrow mesenchymal stem cells. *Int. J. Mol. Sci.* 20, E4834. doi:10.3390/ijms20194834

Yang, J. H., Zhao, Z. H., Hou, J. F., Zhou, Z. L., Deng, Y. F., and Dai, J. J. (2013). Expression of TRPV6 and CaBP-D28k in the egg shell gland (uterus) during the oviposition cycle of the laying hen. *Br. Poult. Sci.* 54, 398–406. doi:10.1080/00071668.2013.791385

Yang, R., Chen, J., Zhang, J., Qin, R., Wang, R., Qiu, Y., et al. (2020). 1, 25-Dihydroxyvitamin D protects against age-related osteoporosis by a novel VDR-Ezh2-p16 signal axis. *Aging Cell* 19, e13095. doi:10.1111/acel.13095

Zymbal, V., Baptista, F., Letuchy, E. M., Janz, K. F., and Levy, S. M. (2019). Mediating effect of muscle on the relationship of physical activity and bone. *Med. Sci. Sports Exerc.* 51, 202–210. doi:10.1249/MSS.0000000000001759

frontiers | Frontiers in Physiology

TYPE Brief Research Report
PUBLISHED 04 January 2023
DOI 10.3389/fphys.2022.1085935

OPEN ACCESS

EDITED BY
Anthony Pokoo-Aikins,
Toxicology and Mycotoxin Research Unit, U.S. National Poultry Research Center, Agricultural Research Service (USDA), United States

REVIEWED BY
Gregoy Y Bedecarrats,
University of Guelph, Canada
Yulin Bai,
Xiamen University, China
Li Gao,
Baotou Teachers' College, China

*CORRESPONDENCE
Woo Kyun Kim,
wkkim@uga.edu
Kichoon Lee,
lee.2626@osu.edu

SPECIALTY SECTION
This article was submitted to Avian Physiology, a section of the journal Frontiers in Physiology

RECEIVED 31 October 2022
ACCEPTED 12 December 2022
PUBLISHED 04 January 2023

CITATION
Lee J, Tompkins Y, Kim D-H, Kim WK and Lee K (2023), Increased sizes and improved qualities of tibia bones by myostatin mutation in Japanese quail. *Front. Physiol.* 13:1085935. doi: 10.3389/fphys.2022.1085935

Increased sizes and improved qualities of tibia bones by myostatin mutation in Japanese quail

Joonbum Lee[1], Yuguo Tompkins[2], Dong-Hwan Kim[1], Woo Kyun Kim[2]* and Kichoon Lee[1]*

[1]Department of Animal Sciences, The Ohio State University, Columbus, OH, United States, [2]Department of Poultry Science, University of Georgia, Athens, GA, United States

Production of large amounts of meat within a short growth period from modern broilers provides a huge economic benefit to the poultry industry. However, poor bone qualities of broilers caused by rapid growth are considered as one of the problems in the modern broilers industry. After discovery and investigation of myostatin (MSTN) as an anti-myogenic factor to increase muscle mass by targeted knockout in various animal models, additional positive effects of MSTN mutation on bone qualities have been reported in MSTN knockout mice. Although the same beneficial effects on muscle gain by MSTN mutation have been confirmed in MSTN mutant quail and chickens, bone qualities of the MSTN mutant birds have not been investigated, yet. In this study, tibia bones were collected from MSTN mutant and wild-type (WT) quail at 4 months of age and analyzed by Micro-Computed Tomography scanning to compare size and strength of tibia bone and quality parameters in diaphysis and metaphysis regions. Length, width, cortical thickness, and bone breaking strength of tibia bones in the MSTN mutant group were significantly increased compared to those of the WT group, indicating positive effects of MSTN mutation on tibia bone sizes and strength. Furthermore, bone mineral contents and bone volume of whole diaphysis, diaphyseal cortical bone, whole metaphysis, and metaphyseal trabecular and cortical bones were significantly increased in the MSTN mutant group compared to the WT group, indicating increased mineralization in the overall tibia bone by MSTN mutation. Especially, higher bone mineral density (BMD) of whole diaphysis, higher total surface of whole metaphysis, and higher BMD, trabecular thickness, and total volume of metaphyseal trabecular bones in the MSTN mutant group compared to the WT group suggested improvements in bone qualities and structural soundness of both diaphysis and metaphysis regions with significant changes in trabecular bones by MSTN mutation. Taken together, MSTN can be considered as a potential target to not only increase meat yield, but also to improve bone qualities that can reduce the incidence of leg bone problems for the broiler industry.

KEYWORDS

myostatin, quail, tibia bone, micro-CT, long bone quality

Introduction

In the modern poultry industry, fast growing broilers provide a huge economic benefit by providing a large amount of meat within a short growth period. However, abnormal leg bone development has been considered as one of the major problems of the fast growing broilers (Julian, 2005; Tompkins et al., 2022b; 2022a). Especially, rapid growth of the body and bone during the early growth phase of a broiler is suggested as one of the main causes of poor bone quality in fast growing broilers (Williams et al., 2000, 2004; Tompkins et al., 2022a; 2022b). To minimize economic losses and concerns about animal welfare caused by the leg bone problems of broilers, genetic factors should also be considered and investigated in addition to other aspects including nutritional and environmental factors (Shim et al., 2011; Liu et al., 2015; Huang et al., 2017).

Myostatin (MSTN) is a major anti-regulator in muscle growth and has been investigated in various MSTN mutant animals and humans (Grobet et al., 1997; McPherron et al., 1997; McPherron and Lee, 1997; Schuelke et al., 2004; Mosher et al., 2007; Bi et al., 2016; Lv et al., 2016). Recently developed chickens and quail carrying a mutation in the *MSTN* gene showed increased body and muscle weights, confirming the anti-myogenic function of the MSTN in avian species (Kim et al., 2020; Lee et al., 2020). In addition, a decrease in fat deposition, another major phenotype of MSTN mutant animals (McPherron and Lee, 2002; Ren et al., 2020), was also reported in the MSTN mutant birds (Kim et al., 2020; Lee et al., 2020), indicating the conserved functions of MSTN between mammals and birds.

MSTN knockout mice showed higher bone mineral contents (BMC), bone mineral density (BMD), and bone volume (BV) compared to those of WT mice from Dual-energy X-ray absorptiometry analysis of the whole body at 10 weeks of age (Suh et al., 2020). Also, morphological changes caused by MSTN mutations, such as an extra rib bone and pelvic tilt in MSNT mutant pigs (Qian et al., 2015) and rabbits (Zhang et al., 2019), respectively, were reported. However, the phenotypic changes in bones of the MSTN mutant birds has not been reported, yet.

According to the positive effect of MSTN inactivation on bone qualities demonstrated in mice models (Suh et al., 2020), it is hypothesized that the bone quality of MSTN mutant birds may be improved compared to wild-type (WT) controls. To address this, tibia bones of 4 months old WT and MSTN mutant quail, generated in our previous study (Lee et al., 2020), were analyzed by Micro-Computed Tomography (micro-CT) scanning. Micro-CT is a precise evaluation approach that can provide a comprehensive overview of the architectural characteristics in poultry bones (Tompkins et al., 2022a; 2022b). The three-dimensional structural assessment can provide in-depth understanding behind genetic modulation and bone traits alteration. In addition, breaking strength tests were used to further confirm the quality measured by micro-CT scanning.

Materials and methods

Animal care and bone sampling

Animal care protocol and experimental procedures were approved by The Ohio State University Institutional Animal Care and Use Committee (IACUC; Protocol 2019A00000024-R1; Approved 21 January 2022). WT quail and quail carrying homozygous single amino acid deletion mutation in the *MSTN* gene were previously produced using CRISPR/Cas9-mediated genome editing (Lee et al., 2020) and used in this study as WT and MSTN mutant quail, respectively. All quail were maintained together at The Ohio State University Poultry Facility in Columbus, Ohio and fed *ad libitum*. Quail at 4 months of age were euthanized *via* CO_2 inhalation. After euthanasia, tibia bones of both legs were sampled from eight WT and eight MSTN mutant males. Bones were rolled with paper towels individually and stored in plastic tubes at −20°C freezer until further analysis.

Analysis of tibia bone

To evaluate bone morphologic changes and microarchitectural changes, the left tibia bones of eight quail of each group were collected, and muscles were removed before analyzing by micro-CT scanning. Bones scanned according to a standard protocol at 73kV, 136 μA, and a 0.5 mm aluminum filter, and analysis was performed with SkyScan 1172 (SkyScan, Kontich, Belgium). The pixel size was fixed at 25 μm and a 0.25° rotation angle was applied at each step. Images were transferred to CTAn software (CTAn, SkyScan) for 3-D structure construction and quantification. The metaphysis and diaphysis sections of tibia bones were manually selected in the CTAn. Cortical bone and trabecular bone parameters were analyzed, respectively. The following parameters were quantified: BMC, BMD, total tissue volume (TV), BV, bone volume per tissue volume or bone volume fraction (BV/ TV), trabecular thickness (Tb. Th), volume of total pores (Po.V (tot)), total porosity percentage (Po (tot)), tissue surface area (TS), bone surface area (BS), bone surface per total volume or bone surface density (BS/TV), bone surface per bone volume or specific bone surface (BS/BV) (Chen and Kim, 2020). All the bone traits are highly correlated with the health status and bone strength in many species (Chen et al., 2020; Tompkins et al., 2022a; b). Besides, the whole bone length and bone diaphyseal width were measured by using the CTAn ruler tool which measures straight line distance (Figures 1A,B). The large pore for blood vein and nerve fibers to run through (haversian canal) was used as the landmark to select the specific location on the long bone of where the diaphyseal width and the cortical bone thickness were measured using the CTAn software ruler tool (Figure 1A). The cortical bone thickness was calculated by an average thickness of four opposite directional measurements over cortical mid-shaft (Figure 1A).

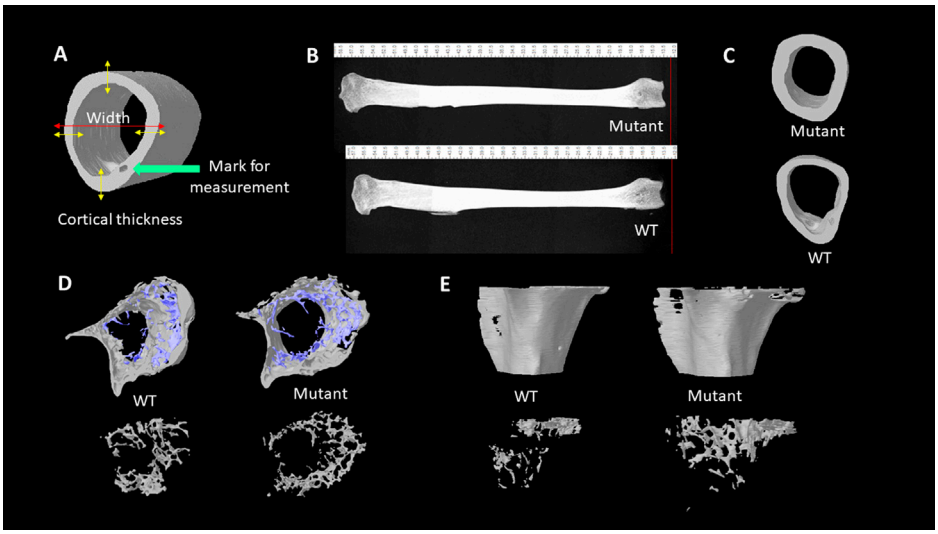

FIGURE 1
(A). Illustration of cortical thickness and wideness measurement. **(B).** Lateral views of 4 months old male quail tibia bones. The length of bones was measured with the CTAn ruler tool. **(C).** Transverse views of tibia diaphysis acquired from the micro-CT scanning. **(D).** Transverse views of tibia metaphysis with trabecular bones (blue) and cortical (grey) structures. Transverse views of tibia metaphysis trabecular bone structures (bottom). **(E).** Lateral views of the reconstructed metaphysis of tibia bones (top). Lateral views of trabecular bones at tibial metaphysis area (bottom).

Bone breaking strength

Right tibia bones were used to analyze the difference of bone breaking strength (BBS) between WT and MSTN mutant groups. Before measuring BBS, the bones were thawed for 3 h at room temperature and remaining soft tissues around the breaking point of the bones were cleaned. BBS was determined by a three-point bending test using a material testing machine (Stable Micro Systems TA. XT plus 100, Stable Micro System Corp., Surrey, UK) with a 100-kg loading cell and speed of 2 mm/s until the bones fractured.

Statistical analysis

Student's *t*-test was used to analyze measurements of left tibia bone sizes and parameters and right tibia bone BBS with the significance level set as $p < 0.05$.

Results

The effects of MSTN mutation on tibia bone sizes and strength

The whole tibia bone length was greater in the MSTN mutant group compared to the WT group (Table 1; Figure 1B). Diaphyseal bone width and diaphyseal cortical thickness in the MSTN group were significantly larger than those in the WT group (Table 1; Figure 1C). In addition, BBS of tibia bone was significantly increased in the MSTN group compared to the WT group (Table 1).

The effects of MSTN mutation on tibia bone diaphyseal material and structural properties

The diaphysis is a shaft region in the middle of the tibia bone and mainly formed by a compact outer bone layer, called a cortical bone, and medullary cavity inside (Figure 1C). Using micro-CT scanning, material and structural properties of the whole diaphysis and cortical bone were analyzed (Table 2). Whole diaphyseal structural assay showed higher BMC and BMD of tibia bone in the MSTN mutant group compared to those of the WT group (Table 2). Although the difference of TV was not significant between the two groups, BV of diaphysis in the MSTN mutant group were higher than those in the WT group (Table 2). In addition, BS/BV and BS/TV, but not BS itself, of diaphysis in the MSTN mutant group were significantly different from those in the WT group (Table 2).

As a main component of a diaphysis region, diaphyseal cortical bone in the MSTN mutant group showed higher

TABLE 1 Length, width, cortical bone thickness, and bone breaking strength of 4 months old WT and MSTN mutant quail tibia bone.

	Unit	WT	Mutant	Sem	*p*-value
Length	mm	43.104	44.783	0.337	0.007*
Width	mm	2.461	2.546	0.024	0.043*
Cortical thickness[a]	mm	0.287	0.360	0.014	0.006*
Bone breaking strength	KgF	3.633	4.318	0.206	0.005*

[a]Cortical thickness: a mean thickness of cortical mid-shaft. *means a significantly difference between groups by student's *t*-test, $p < 0.05$; N = 8 per group.

BMC, TV, and BV compared to those of the WT group (Table 2). However, BMD, Po.V (tot), and Po (tot) of the diaphyseal cortical bone were not significantly different between the two groups (Table 2).

The effects of MSTN mutation on tibia bone metaphyseal material and structural properties

Unlike diaphysis, trabecular bone is formed inside of the outer cortical bone within the metaphysis region (Figure 1D,E). Therefore, metaphyseal trabecular and cortical bones were separately analyzed along with whole metaphyseal structural assay (Table 3). Whole metaphysis of the tibia bone in the MSTN mutant group showed higher BMC, TV, BV, and TS compared to those of the WT group (Table 3). However, BMD of whole metaphysis was not significantly different between the two groups (Table 3).

In the metaphyseal trabecular bone, all the parameters, BMC, BMD, Tb.Th, and TV, were significantly increased in the MSTN mutant group compared to the WT group (Table 3). However, metaphysis cortical bone of the MSTN mutant tibia bone showed higher BMC and BV, but not BMD and TV, compared to those of the WT tibia bone (Table 3).

Discussion

Avian bones are fast growing, thin, and relatively denser than the mammals (Dumont, 2010). The MSTN mutant quail model has provided a new approach for examining MSTN function regarding to bone quality. As an anti-myogenic regulator, MSTN mutation resulted in increased body weight of quail in our previous study (Lee et al., 2020). In addition to the increased muscle mass, based on the current data, MSTN mutant quail have shown longer and wider tibia bones compared to WT quail, which is similar to MSTN knockout mice having longer femur bones with thicker cortical bones (Hamrick, 2003). Although the BMD remained unchanged in diaphyseal cortical bone between the groups, the cortical thickness and BBS were also increased in the MSTN mutant group compared to the WT group, suggesting that MSTN mutation had increased bone mass and improved bone quality in quail. The diaphysis is the midsection of a long bone that is mainly composed of dense cortical bone (compact bone), where radical growth is characterized at cortical bone over the diaphysis, and the diaphyseal cortical bone structure is essential for structural strength (Isojima and Sims, 2021). In general, cortical bone quality and thickness are highly correlated to BBS (Augat and Schorlemmer, 2006). Thus, the significantly increased BV by *MSTN* gene knockout can result in higher BBS, and the changes in bone mass was the main factor that attribute to better bone quality in the current study.

Like diaphysis results, significant increases in BMC and BV of metaphysis in the MSTN group compared to those in the WT group indicate more mineralization in metaphysis by MSTN mutation. Furthermore, increased TV of whole metaphysis in the MSTN mutant group compared to the WT group also indicates wider metaphysis in the MSTN mutant group. At metaphysis, a higher BMC, BMD, Tb.Th, and TV of the metaphyseal trabecular bone were observed in the MSTN mutant group compared to the WT group, suggesting improved trabecular bone quality by MSTN mutation. Trabecular bone is a dynamic structure compared to cortical bone. Trabecular bone quality is one of the major contributors of bone strength and quality (Garrison et al., 2011). The changed structure and decreased bone mineral content/density were reported in pathogenic challenge models in broilers (Raehtz et al., 2018; Tompkins et al., 2022b). Therefore, the improved trabecular bone quality can possibly increase bone integrity to confronting stressed condition. Interestingly, unlike higher BMD of whole diaphysis in the MSTN mutant group, BMD of whole metaphysis was similar between the two groups. This might be further supported by the finding that a 22% increase of BMC of the whole metaphysis bone results mainly from a similar increasing rate, 19%, of TV of whole metaphysis bone rather than changes in BMD in the MSTN mutant group.

Similar to the results from structural assay of tibia bones of MSTN mutant quail, diaphyseal cortical bone thickness and BV, without BMD improvement, were higher in tibia and humerus bones of MSTN mutant mice compared to those of WT mice (Suh et al., 2020). In addition, trabecular bone quality was improved in quail by MSTN mutation as shown in higher

TABLE 2 Diaphyseal properties of WT and MSTN mutant tibia bone.

		Unit	WT	Mutant	Sem	*p*-value
Whole Diaphysis	BMC	g	13.945	16.258	0.443	0.002*
	BMD	g/mm^3	0.837	0.922	0.018	0.006*
	TV	mm^3	16.693	17.659	0.416	0.124
	BV	mm^3	9.778	10.844	0.237	0.008*
	BS	mm^2	62.108	60.813	1.261	0.688
	BS/BV	mm^2/ mm^3	6.358	5.613	0.148	0.004*
	BS/TV	mm^2/ mm^3	3.722	3.450	0.056	0.005*
Diaphysis Cortical	BMC	g	11.006	13.168	0.353	<0.001*
	BMD	g/mm^3	1.641	1.638	0.030	0.517
	TV	mm^3	6.738	8.075	0.248	0.003*
	BV	mm^3	6.670	8.011	0.244	0.003*
	Po.V (tot)	mm^3	0.074	0.067	0.016	0.106
	Po (tot)	%	0.961	0.912	0.201	0.201

BMC, bone mineral content; BMD, bone mineral density; TV, total tissue volume; BV, bone volume (TV, minus bone marrow volume); BS, bone surface area; BS/TV, bone surface/ total volume; BS/BV, bone surface/ bone volume; Po.V (tot), total volume of pore space; Po. (tot), total pore percentage. *means a significantly difference between groups by student's *t*-test, $p < 0.05$; N = 8 per group.

trabecular BMC in the humerus bone (Hamrick et al., 2002) and trabecular BMD in fifth lumbar vertebra (Hamrick et al., 2003). These results indicate a similar function of the *MSTN* gene on regulation of bone development and quality, along with anti-myogenic function, between mammals and birds. In murine *in vitro* studies, a direct effect of the MSTN on bone remodeling status by promoting osteoclast differentiation (Dankbar et al., 2015) and inhibiting osteoblast differentiation (Qin et al., 2017) was reported. MSTN mutation can positively affect bone formation rate and reduce bone resorption, eventually resulting in a larger bone volume in MSTN knockout mice (Suh et al., 2020). Osteoblasts contribute to bone formation and mineral deposition, while osteoclasts resolve the bone and initiate the bone remodeling (Matsuo and Irie, 2008). The differentiation and activity of these two bone-related cells are critical in maintaining bone quality and integrity (Alliston, 2014). Studies using mice *in vitro* cell models indicated that MSTN interacts with regulators essential in bone homeostasis by regulating osteoblast and osteoclast activity (Ewendt et al., 2021). For example, studies using mice osteoblastic MC3T3 cells show that the increased level of MSTN promotes expression of bone growth inhibitor such as sclerostin (SOST), and also the osteoclastogenic stimulators such as RANKL (Qin et al., 2017). Besides, the increased MSTN also associated with a marked reduction of Runx2, which is one of the essential osteoblastogenic regulators, *via* the down-regulation of the WNT signaling (Qin et al., 2017). With the current research, it is likely that the activity of osteogenic differentiation or osteoclastogenic differentiation can be mediated by MSTN mutation, which can positively affect bone formation rate and remodeling status, eventually resulting in a larger bone volume in MSTN mutant quail. Moreover, in mice studies, the increased bone mass was associated with the change in the osteogenic differentiation of osteoblast, and MSNT was shown to inhibit adipogenesis. It is well-known that the WNT pathway is one of the most important signaling pathway to promote osteoblast differentiation, and the activation of this pathway showed an anti-adipogenesis and anti-chondrogenesis (but promotes chondrocyte hypertrophy) function during bone formation (Olivares-Navarrete et al., 2011; Lee et al., 2017; Riddle and Clemens, 2017). The activation of WNT pathway can block PPAR-gamma-induced adipogenesis and induce RUNX2 expression, which commit mesenchymal stem cells differentiated into the osteoblast phenotype (Santos et al., 2010). Thus, the regulation of WNT pathway, and the interaction between osteogenic differentiation and adipogenic differentiation can be critical in understanding MSTN in bone homeostasis in future studies.

Chicken muscle yield has been considered one of the most important traits in genetic breed selection (Bailey et al., 2020). However, the continuous selection for rapid growth and high muscle yield has shifted the broilers' center of gravity and altered the biomechanical structure (Huang et al., 2019). The unbalanced development between muscle and skeleton has been unexpectedly associated with the incidence of metabolic and skeletal disorders in modern broiler breeds. For broilers, most of skeleton disorders occur on the long bone (tibia and femur) (Cook, 2000; Akyüz and Onbaşılar, 2020). Thus, leg disorders are

TABLE 3 Metaphyseal properties of WT and MSTN mutant tibia bone.

		Unit	WT	Mutant	Sem	*p*-value
Whole metaphysis	BMC	g	15.567	19.034	0.758	0.007*
	BMD	g/mm^3	0.413	0.425	0.011	0.298
	TV	mm^3	37.81	44.86	1.574	0.007*
	BV	mm^3	15.543	18.526	0.734	0.017*
	TS	mm^2	83.531	93.990	2.080	0.005*
Metaphysis Trabecular	BMC	g	0.396	0.899	0.144	0.036*
	BMD	g/mm^3	0.862	0.898	0.008	0.018*
	Tb.Th	mm	0.079	0.095	0.003	0.023*
	TV	mm^3	0.450	0.997	0.157	0.037*
Metaphysis Cortical	BMC	g	6.942	8.022	0.204	0.002*
	BMD	g/mm^3	0.836	0.888	0.024	0.157
	TV	mm^3	8.370	9.128	0.291	0.104
	BV	mm^3	7.378	8.429	0.239	0.018*

TS, total bone surface area; Tb.Th, trabecular bone thickness. * means a significantly difference between groups by student's *t*-test, $p < 0.05$; N = 8 per group.

a significant cause of welfare issues in broilers. Compared to slow growing chickens, fast growing broilers is characterized with a relative lower mineral contents, higher porosity, and lower BBS (Williams et al., 2000). Significantly increased mineralization in the tibia bone by MSTN mutation as shown in higher BMC and BV in all diaphyseal and metaphyseal regions suggests MSTN as a potential genetic factor that can improve bone mineralization, bone strength, and structural integrity in fast growing broilers.

In summary, MSTN mutation resulted in longer, wider, thicker, and stronger tibia bone with significant improvements of bone quality parameters in both diaphysis and metaphysis regions of quail tibia bone. The current study provides scientific evidence for potential applications of MSTN to not only increase meat yield, but also improve bone quality in poultry.

Data availability statement

The original contributions presented in the study are included in the article/supplementary material, further inquiries can be directed to the corresponding authors.

Ethics statement

The animal study was reviewed and approved by Animal care protocol and experimental procedures were approved by The Ohio State University Institutional Animal Care and Use Committee (IACUC; Protocol 2019A00000024-R1; Approved 21 January 2022).

Author contributions

WK and KL contributed to the conception and design of the study. JL, YT, and DK performed experiments and organized the data. JL, YT, and WK performed the statistical analysis. JL, YT, WK, and KL wrote the first draft of the manuscript. All authors contributed to manuscript revision, read, and approved the submitted version.

Funding

This research was funded by the United States Department of Agriculture National Institute of Food and Agriculture Grant (Project No. 2020–67030–31338).

Acknowledgments

We thank Madeline C. Karolak and Benjamin M. Bohrer for their support in a bone breaking strength experiment, and Michelle Milligan for her invaluable assistance by proofreading this manuscript.

Conflict of interest

The authors declare that the research was conducted in the absence of any commercial or financial relationships that could be construed as a potential conflict of interest.

Publisher's note

References

Akyüz, H. Ç., and Onbaşılar, E. E. (2020). *Non-infectious skeletal disorders in broilers*. doi:10.1080/00439339.2020.1759388

Alliston, T. (2014). Biological regulation of bone quality. *Curr. Osteoporos. Rep.* 12, 366–375. doi:10.1007/s11914-014-0213-4

Augat, P., and Schorlemmer, S. (2006). The role of cortical bone and its microstructure in bone strength. *Age Ageing* 35 (2), ii27–ii31. doi:10.1093/ageing/afl081

Bailey, R. A., Souza, E., and Avendano, S. (2020). Characterising the influence of genetics on breast muscle myopathies in broiler chickens. *Front. Physiol.* 11, 1041. doi:10.3389/fphys.2020.01041

Bi, Y., Hua, Z., Liu, X., Hua, W., Ren, H., Xiao, H., et al. (2016). Isozygous and selectable marker-free MSTN knockout cloned pigs generated by the combined use of CRISPR/Cas9 and Cre/LoxP. *Sci. Rep.* 6, 31729. doi:10.1038/srep31729

Chen, C., and Kim, W. K. (2020). The application of micro-CT in egg-laying hen bone analysis: Introducing an automated bone separation algorithm. *Poult. Sci.* 99, 5175–5183. doi:10.1016/j.psj.2020.08.047

Chen, C., Turner, B., Applegate, T. J., Litta, G., and Kim, W. K. (2020). Role of long-term supplementation of 25-hydroxyvitamin D(3) on laying hen bone 3-dimensional structural development. *Poult. Sci.* 99, 5771–5782. doi:10.1016/j.psj.2020.06.080

Cook, M. E. (2000). Skeletal deformities and their causes: Introduction. *Poult. Sci.* 79, 982–984. doi:10.1093/ps/79.7.982

Dankbar, B., Fennen, M., Brunert, D., Hayer, S., Frank, S., Wehmeyer, C., et al. (2015). Myostatin is a direct regulator of osteoclast differentiation and its inhibition reduces inflammatory joint destruction in mice. *Nat. Med.* 21, 1085–1090. doi:10.1038/nm.3917

Dumont, E. R. (2010). Bone density and the lightweight skeletons of birds. *Proc. Biol. Sci.* 277, 2193–2198. doi:10.1098/rspb.2010.0117

Ewendt, F., Feger, M., and Föller, M. (2021). Myostatin regulates the production of fibroblast growth factor 23 (FGF23) in UMR106 osteoblast-like cells. *Pflugers Arch.* 473, 969–976. doi:10.1007/s00424-021-02561-y

Garrison, J. G., Gargac, J. A., and Niebur, G. L. (2011). Shear strength and toughness of trabecular bone are more sensitive to density than damage. *J. Biomech.* 44, 2747–2754. doi:10.1016/j.jbiomech.2011.09.002

Grobet, L., Jose, L., Martin, R., Poncelet, D., Pirottin, D., Brouwers, B., et al. (1997). A deletion in the bovine myostatin gene causes the double-muscled phenotype in cattle. *Nat. Genet.* 17, 71–74. doi:10.1038/ng0997-71

Hamrick, M. W. (2003). Increased bone mineral density in the femora of GDF8 knockout mice. *Anat. Rec. Part A, Discov. Mol. Cell. Evol. Biol.* 272, 388–391. doi:10.1002/ar.a.10044

Hamrick, M. W., McPherron, A. C., and Lovejoy, C. O. (2002). Bone mineral content and density in the humerus of adult myostatin-deficient mice. *Calcif. Tissue Int.* 71, 63–68. doi:10.1007/s00223-001-1109-8

Hamrick, M. W., Pennington, C., and Byron, C. D. (2003). Bone architecture and disc degeneration in the lumbar spine of mice lacking GDF-8 (myostatin). *J. Orthop. Res. Off. Publ. Orthop. Res. Soc.* 21, 1025–1032. doi:10.1016/S0736-0266(03)00105-0

Huang, S., Kong, A., Cao, Q., Tong, Z., and Wang, X. (2019). The role of blood vessels in broiler chickens with tibial dyschondroplasia. *Poult. Sci.* 98, 6527–6532. doi:10.3382/ps/pez497

Huang, S., Zhang, L., Rehman, M. U., Iqbal, M. K., Lan, Y., Mehmood, K., et al. (2017). High altitude hypoxia as a factor that promotes tibial growth plate development in broiler chickens. *PLoS One* 12, e0173698. doi:10.1371/journal.pone.0173698

Isojima, T., and Sims, N. A. (2021). Cortical bone development, maintenance and porosity: Genetic alterations in humans and mice influencing chondrocytes, osteoclasts, osteoblasts and osteocytes. *Cell. Mol. Life Sci.* 78, 5755–5773. doi:10.1007/s00018-021-03884-w

Julian, R. J. (2005). Production and growth related disorders and other metabolic diseases of poultry-a review. *Vet. J.* 169, 350–369. doi:10.1016/j.tvjl.2004.04.015

Kim, G. D., Lee, J. H., Song, S., Kim, S. W., Han, J. S., Shin, S. P., et al. (2020). Generation of myostatin-knockout chickens mediated by D10A-Cas9 nickase. *FASEB J.* 34, 5688–5696. doi:10.1096/fj.201903035R

Lee, J., Kim, D. H., and Lee, K. (2020). Muscle hyperplasia in Japanese quail by single amino acid deletion in MSTN propeptide. *Int. J. Mol. Sci.* 21, 1504. doi:10.3390/ijms21041504

Lee, W.-C., Guntur, A. R., Long, F., and Rosen, C. J. (2017). Energy metabolism of the osteoblast: Implications for osteoporosis. *Endocr. Rev.* 38, 255–266. doi:10.1210/er.2017-00064

Liu, R., Jin, C., Wang, Z., Wang, Z., Wang, J., and Wang, L. (2015). Effects of manganese deficiency on the microstructure of proximal tibia and OPG/RANKL gene expression in chicks. *Vet. Res. Commun.* 39, 31–37. doi:10.1007/s11259-015-9626-5

Lv, Q., Yuan, L., Deng, J., Chen, M., Wang, Y., Zeng, J., et al. (2016). Efficient generation of myostatin gene mutated rabbit by CRISPR/Cas9. *Sci. Rep.* 6, 25029. doi:10.1038/srep25029

Matsuo, K., and Irie, N. (2008). Osteoclast-osteoblast communication. *Arch. Biochem. Biophys.* 473, 201–209. doi:10.1016/j.abb.2008.03.027

McPherron, A. C., Lawler, A. M., and Lee, S. J. (1997). Regulation of skeletal muscle mass in mice by a new TGF-beta superfamily member. *Nature* 387, 83–90. doi:10.1038/387083a0

McPherron, A. C., and Lee, S.-J. (2002). Suppression of body fat accumulation in myostatin-deficient mice. *J. Clin. Invest.* 109, 595–601. doi:10.1172/JCI13562

McPherron, A. C., and Lee, S. J. (1997). Double muscling in cattle due to mutations in the myostatin gene. *Proc. Natl. Acad. Sci. U. S. A.* 94, 12457–12461. doi:10.1073/pnas.94.23.12457

Mosher, D. S., Quignon, P., Bustamante, C. D., Sutter, N. B., Mellersh, C. S., Parker, H. G., et al. (2007). A mutation in the myostatin gene increases muscle mass and enhances racing performance in heterozygote dogs. *PLoS Genet.* 3, 779–786. doi:10.1371/journal.pgen.0030079

Olivares-Navarrete, R., Hyzy, S. L., Hutton, D. L., Dunn, G. R., Appert, C., Boyan, B. D., et al. (2011). Role of non-canonical Wnt signaling in osteoblast maturation on microstructured titanium surfaces. *Acta Biomater.* 7, 2740–2750. doi:10.1016/j.actbio.2011.02.030

Qian, L., Tang, M., Yang, J., Wang, Q., Cai, C., Jiang, S., et al. (2015). Targeted mutations in myostatin by zinc-finger nucleases result in double-muscled phenotype in Meishan pigs. *Sci. Rep.* 5, 14435. doi:10.1038/srep14435

Qin, Y., Peng, Y., Zhao, W., Pan, J., Ksiezak-Reding, H., Cardozo, C., et al. (2017). Myostatin inhibits osteoblastic differentiation by suppressing osteocyte-derived exosomal microRNA-218: A novel mechanism in muscle-bone communication. *J. Biol. Chem.* 292, 11021–11033. doi:10.1074/jbc.M116.770941

Raehtz, S., Hargis, B. M., Kuttappan, V. A., Pamukcu, R., Bielke, L. R., and McCabe, L. R. (2018). High molecular weight polymer promotes bone health and prevents bone loss under Salmonella challenge in broiler chickens. *Front. Physiol.* 9, 384. doi:10.3389/fphys.2018.00384

Ren, H., Xiao, W., Qin, X., Cai, G., Chen, H., Hua, Z., et al. (2020). Myostatin regulates fatty acid desaturation and fat deposition through MEF2C/miR222/SCD5 cascade in pigs. *Commun. Biol.* 3, 612. doi:10.1038/s42003-020-01348-8

Riddle, R. C., and Clemens, T. L. (2017). Bone cell bioenergetics and skeletal energy homeostasis. *Physiol. Rev.* 97, 667–698. doi:10.1152/physrev.00022.2016

Santos, A., Bakker, A. D., de Blieck-Hogervorst, J. M. A., and Klein-Nulend, J. (2010). WNT5A induces osteogenic differentiation of human adipose stem cells via rho-associated kinase ROCK. *Cytotherapy* 12, 924–932. doi:10.3109/14653241003774011

Schuelke, M., Wagner, K. R., Stolz, L. E., Hübner, C., Riebel, T., Kömen, W., et al. (2004). Myostatin mutation associated with gross muscle hypertrophy in a child. *N. Engl. J. Med.* 350, 2682–2688. doi:10.1056/nejmoa040933

Shim, M. Y., Parr, C., and Pesti, G. M. (2011). The effects of dietary fluoride on growth and bone mineralization in broiler chicks. *Poult. Sci.* 90, 1967–1974. doi:10.3382/ps.2010-01240

Suh, J., Kim, N., Lee, S., Eom, J., Lee, Y., Park, J., et al. (2020). GDF11 promotes osteogenesis as opposed to MSTN, and follistatin, a MSTN/GDF11 inhibitor, increases muscle mass but weakens bone. *increases muscle mass but weakens bone* 117, 4910–4920. doi:10.1073/pnas.1916034117

Tompkins, Y. H., Chen, C., Sweeney, K. M., Kim, M., Voy, B. H., Wilson, J. L., et al. (2022a). The effects of maternal fish oil supplementation rich in n-3 PUFA on offspring-broiler growth performance, body composition and bone microstructure. *PLoS One* 17, e0273025. doi:10.1371/journal.pone.0273025

Tompkins, Y. H., Teng, P., Pazdro, R., and Kim, W. K. (2022b). Long bone mineral loss, bone microstructural changes and oxidative stress after eimeria challenge in broilers. *Front. Physiol.* 13, 945740. doi:10.3389/fphys.2022.945740

Williams, B., Solomon, S., Waddington, D., Thorp, B., and Farquharson, C. (2000). Skeletal development in the meat-type chicken. *Br. Poult. Sci.* 41, 141–149. doi:10.1080/713654918

Williams, B., Waddington, D., Murray, D. H., and Farquharson, C. (2004). Bone strength during growth: Influence of growth rate on cortical porosity and mineralization. *Calcif. Tissue Int.* 74, 236–245. doi:10.1007/s00223-002-2124-0

Zhang, T., Lu, Y., Song, S., Lu, R., Zhou, M., He, Z., et al. (2019). Double-muscling" and pelvic tilt phenomena in rabbits with the cystine-knot motif deficiency of myostatin on exon 3. *Biosci. Rep.* 39, BSR20190207. doi:10.1042/BSR20190207

frontiers | Frontiers in Physiology

TYPE Original Research
PUBLISHED 26 January 2023
DOI 10.3389/fphys.2023.1124355

OPEN ACCESS

EDITED BY
Anthony Pokoo-Aikins,
Toxicology and Mycotoxin Research Unit,
U.S. National Poultry Research Center,
Agricultural Research Service (USDA),
United States

REVIEWED BY
Frank Idan,
Kwame Nkrumah University of Science and Technology, Ghana
Xiao Lin,
Northwestern Polytechnical University, China

*CORRESPONDENCE
W. K. Kim,
wkkim@uga.edu

SPECIALTY SECTION
This article was submitted to Avian Physiology, a section of the journal Frontiers in Physiology

RECEIVED 15 December 2022
ACCEPTED 19 January 2023
PUBLISHED 26 January 2023

CITATION
Tompkins YH, Liu G and Kim WK (2023), Impact of exogenous hydrogen peroxide on osteogenic differentiation of broiler chicken compact bones derived mesenchymal stem cells.
Front. Physiol. 14:1124355.
doi: 10.3389/fphys.2023.1124355

Impact of exogenous hydrogen peroxide on osteogenic differentiation of broiler chicken compact bones derived mesenchymal stem cells

Y. H. Tompkins, G. Liu and W. K. Kim*

Department of Poultry Science, University of GA, Athens, GA, United States

The effects of hydrogen peroxide (H_2O_2) on the osteogenic differentiation of primary chicken mesenchymal stem cells (MSCs) were investigated. MSCs were subjected to an osteogenic program and exposed to various concentrations of H_2O_2 for 14 days. Results showed that high concentrations of H_2O_2 (200 and 400 nM) significantly increased pro-apoptotic marker *CASP8* expression and impaired osteogenic differentiation, as indicated by decreased mRNA expression levels of osteogenesis-related genes and reduced *in vitro* mineralization. In contrast, long-term H_2O_2 exposure promoted basal expression of adipogenic markers at the expense of osteogenesis in MSCs during osteogenic differentiation, and increased intracellular reactive oxygen species (ROS) production, as well as altered antioxidant enzyme gene expression. These findings suggest that long-term H_2O_2-induced ROS production impairs osteogenic differentiation in chicken MSCs under an osteogenic program.

KEYWORDS

bone health, oxidative stress, chicken MSCs, cellular ROS, cell differentiation

Introduction

Modern commercial poultry production is strictly operated based on balanced nutrition and optimized environmental conditions. However, oxidative stress is ubiquitous in broiler production systems. For example, unbalanced nutrition, pathogen infection, and poor environmental conditions including heat stress, ammonia exposure, and flock density, can induce oxidative stress in broilers (Mishra and Jha, 2019; Ali Hassan and Li, 2021; Chauhan et al., 2021). Oxidative stress has been reported as a negative factor in broiler performance, healthy growth, and production quality (Mishra and Jha, 2019; Surai et al., 2019), representing an unbalanced condition between the production of reactive oxygen species (ROS) and the antioxidant defense systems (Sies et al., 2017). In broiler production, in addition to management-associated physiological oxidative stress, infectious agents are key factors that can cause severe oxidative stress in broilers (Zorov et al., 2014; Forrester et al., 2018).

Bone growth depends on the activity of bone-related cells, where osteoblasts are important cells involved in bone formation (Hambli, 2014). Osteoblast originates from mesenchymal stem cells (Zomorodian and Baghaban Eslaminejad, 2012). There is an ongoing interest in using mesenchymal stem cells (MSCs) as a study model to understand cell physiology, and etiology of bone disease (Svoradova et al., 2021), and the effect of oxidative stress on mammal MSCs has been well noted (Denu and Hematti, 2016). Hydrogen peroxide (H_2O_2), a non-radical ROS, has been extensively studied for its effects (Sharma et al., 2012). It is one of the most common

endogenous byproducts of mitochondrial respiration that is present in the avian system (Ojano-Dirain et al., 2007). At a cellular level, ROS level is tightly regulated by the antioxidant defense system and is critical for MSCs multipotency (Atashi et al., 2015). A low basal level of ROS is a critical mediator in pathophysiological responses (Maraldi et al., 2015), while differentiated MSCs presented a higher intracellular ROS production which is essential for cell survival and early differentiation (Hu et al., 2018). However, the uncontrollable high levels of ROS not only impair the cell membrane fluidity and permeability but are also responsible for oxidation damage to DNA, RNA, protein, and lipid damage in mitochondria, leading to cellular senescence including cell dysfunction, cellular injury and cell apoptosis (Denu and Hematti, 2016). For cellular homeostasis, endogenous scavengers such as enzymatic proteins, including superoxide dismutase (SOD), glutathione peroxidase (GPx), and catalases (CAT), and non-enzymatic antioxidants, such as vitamins and trace minerals (Hu et al., 2018), are all work together for controlling intracellular ROS-related stress by removing and converting excessive ROS (Denu and Hematti, 2016).

Relatively high level of ROS can directly interact with critical signaling molecules in essential osteogenic pathways, negatively impacts bone homeostasis (Atashi et al., 2015). Oxidative stress induced by ROS over-production has been considered a pathogenic factor involved in human skeletal disorders (Sharma et al., 2015). Moreover, in response to oxidative stress, ROS can activate extracellular signal-regulated kinases that modulate nuclear factor kappa light chain enhancer of activated B-cell (NF-κB) and NF-E2 p45-related factor 2 (NRF2) signaling pathways, which are critical for regulating inflammation, cellular redox status, and bone homeostasis by regulating osteoblast or osteoclast differentiation and activity (Sun et al., 2015; Yuan et al., 2017). For example, in the mouse cell line, ROS induced MSCs commit to adipogenesis rather than osteogenesis at the transcriptional level (Lin et al., 2018). However, the response of chicken MSCs to high ROS levels and the effect of ROS production on avian osteoblastic differentiation are not well understood. Understanding the impact of ROS on MSC terminal fate and differentiation capacity is important for developing novel strategies for prevent, anticipate, or revert oxidative stress-induced leg problems in chicken production. Therefore, in the current study, H_2O_2 was used as a stimulator of oxidative stress in MSCs culture. This study aimed to investigate the effects of H_2O_2 on the osteogenic differentiation of chicken MSCs isolated from broiler compact bones.

Materials and methods

Animal use and ethics statement

The study was carried out in compliance with the ARRIVE guidelines. All experiment protocols and animal use were approved by the Institutional Animal Care and Use Committee at the University of Georgia, Athens, GA.

Isolation of broiler MSCs

MSCs were isolated using previously described methods (Adhikari et al., 2018). Briefly, legs from one-day old chicks were obtained after cervical dislocation. The leg tissue was soaked in alcohol for a minute and then dried with Kimwipes (Kimberly Clark, Irving, TX, United States). Muscle was removed, and long bones were harvested. The long bones were kept in high glucose Dulbecco's Modified Eagle's medium (DMEM; contains 4.5 g/L glucose, 25 mM HEPES, sodium pyruvate, and without L-glutamine; 15–018-cv, Corning, Corning, NY, United States) until muscle and cartilage tissues were completely removed using a scalpel and scissors in a bio-safety cabinet (NuAire, Plymouth, MN, United States). The bones were placed in washing buffer to cut off the metaphysis. Only tibia diaphysis and femur diaphysis were kept for cell isolation. Washing buffer contained 2% fetal bovine serum (FBS) (Hyclone Laboratories Inc., Logan, UT) in Dulbecco's phosphate-buffer saline (PBS) (Corning). The bones were cracked with a scalpel, bone marrow was flushed out with washing buffer, and bone marrow was discarded. The bones were chopped into small fragments and suspended in a 50 mL tube containing a 10 mL digestion medium consisting of 100 IU/mL penicillin, 100 ug/mL streptomycin, 0.25% collagenase (Sigma-Aldrich, St. Louis, MO, USA), 20% FBS, and high glucose DMEM. The tubes were placed in a 37°C incubated with an orbital shaker set at 180 rpm for 60 min (VWR, Radnor, PA, United States). The digested bone solution was filtered with a 40 μm cell strainer (Thermo Fisher Scientific, Waltham, MA, United States) set over a 50 ml tube to remove the bone fragments, and then the filtered medium was centrifuged at 1,200 rpm for 10 min. The supernatant was discarded and the cell pellet was resuspended in 20 ml growth medium consisting of DMEM with 10% FBS, 100 U/mL penicillin, 100 μg/mL streptomycin, and 0.292 mg/mL L-glutamine (Thermo Fisher Scientific), and 10 ml resuspend cells were plated in a 100 mm cell culture dishes (Corning). Cells were incubated at 37°C in a humidified incubator (NuAire) containing 5% CO_2. Half of the medium was replaced with fresh growth medium after 24 h of culture, and the culture medium was changed every two days thereafter. For cell passing, when the cells reached 80% confluency, they were washed twice with 5 mL pre-warmed PBS, dissociated with 1.5 mL 0.1% Trypsin-EDTA (Corning) for 2 min at 37°C, and subcultured with cell density of 25,000 cells/cm^2 in 100 mm cell culture dishes.

Viability of cultured chicken MSCs with H_2O_2 exposure

The viability of cells was determined using cellular 3-(4,5-dimethylthiazol-2-yl)-2,5-diphenyltetrazolium bromide (MTT) kits (Cayman Chemical, Ann Arbor, MI, USA). Cells were seeded at a concentration of 5×10^4 cells/100 μL in differentiation medium per well with 96-well black wall culture plates. The treatment of MSCs with various concentrations of H_2O_2 (50, 100, 200, 400, and 800 nM; H_2O_2, 30% (w/w) solution, Sigma-Aldrich) during culture was also examined. The H_2O_2 stock was diluted by PBS, and the same volume of diluted H_2O_2 solution was added to the culture medium. MSCs were cultured without H_2O_2 but PBS (osteogenic differentiation medium with 0 nM H_2O_2) as a control. Cells were incubated with different levels of H_2O_2 treatments for 6, 24, and 48 h in the dark. The MTT viability assay was not performed for longer periods of time because high cell density led to high absorbance readings that impaired the accuracy of detection. DMEM with 10% MTT was added and incubated for 4 h, after wich the culture medium was completely discarded. The formed formazan was dissolved with 100 μl dimethyl sulfoxide (DMSO; Sigma-Aldrich) to produce a purple color, and the

plates were then placed on an orbital shaker (VWR) set at low speed for 5 min. The absorbance was measured at 570 nm using a microplate reader (BioTek, Winooski, VT, United states).

Intracellular reactive oxygen species detection

The intracellular ROS levels were examined using the DCFDA/H_2DCFDA cellular ROS assay kits (Abcam Cambridge, MA, United states)) according to the manufacturer's instruction. Briefly, as per manufacturer's instructions, 3×10^4 cells were seeded in a black clear-flat-bottom 96-well microplate and allowed to adhere overnight. The cells were treated with or without H_2O_2 treatment for 2 h, 6 h, 24 h, and 48 h, but not for longer periods of time as the ROS detection required relatively low cell density for accurate results. After the corresponding treatments, the medium was removed, 100 µL/well of 1× washing buffer was added to remove any residual material, and then 100 µL/well of the diluted DCFDA solution was added to stain for 45 min at 37°C in the culture incubator. After removing the DCFDA solution, the cells were rinsed once with a washing buffer, 100 µL/well of washing buffer was then added for microplate measurement. The fluorescence density was measured with a microplate reader (Spectramax M5, Molecular Devices, San Jose, CA) at an excitation wavelength of 485 nm and an emission wavelength of 535 nm. Images were obtained using a fluorescence microscope (Keyence bz-X8000, Keyence Corp., Osaka, Japan) at ×10 magnification.

Osteogenic differentiation

MSC cells were expanded to passage 4 for osteogenic differentiation study. After selecting the proper concentration for H_2O_2 treatment based on the MTT assay, the cells were seeded at a density of 8×10^4 cells per well in 0.2% gelatin-coated (Alfa Aesar, Ward Hill, MA USA) 24-well cell culture plates (Corning), and cultured in growth medium at 37°C in the cell culture incubator (NuAire) until 100% confluency. The cells were then treated with osteogenic differentiation medium containing high glucose DMEM with 10^{-7} M dexamethasone (Sigma-Aldrich), 10 mM β-glycerophosphate (Sigma-Aldrich), 50 µg/mL ascorbate (Sigma-Aldrich), 5% FBS, and 100 U/mL penicillin, 100 µg/mL streptomycin, and 0.292 mg/mL L-glutamine (Thermo Fisher Scientific) to induce osteogenic differentiation. Cells cultured in growth medium served as the negative control. Culture medium was replaced with fresh pre-warmed differentiation medium daily. The cells underwent differentiation for 6 h, 24 h, 48 h, 72 h, 96 h, 5 days, 6 days, 10 days and 14 days.

Alizarin red S staining and mineral deposit quantification

The degree of mineralization of chicken MSCs was determined using Alizarin red S staining (Adhikari et al., 2018). Briefly, the cells were seeded at a density of 8×10^4 cells per well in 0.2% gelatin-coated (Alfa Aesar) 24-well cell culture plates (Corning), and cultured in a growth medium at 37°C in the cell culture incubator (NuAire) until 100% confluency. The cells were then exposed to H_2O_2 in osteogenic differentiation medium for 6, 10, and 14 days. On each day of staining, the cells were fixed with 10% neutral buffered formalin for 1 h and then stained with 0.2% Alizarin red S (Sigma-Aldrich, St. Louis, MO) in distilled water for 45 min at room temperature. After rinsing with distilled water, images of cell culture plates were captured in ×2 magnification using a microscope with a camera (Keyence bz-×8000, Keyence). Mineralized nodules were labeled as dark red spots. To quantify the mineral deposition, the stained cells were solubilized with 200 µl of 10% acetic acid per well and incubated for 30 min with low-speed shaking on an orbital shaker (VWR). After the monolayer was loosely attached, the cells were gently scraped from the plate and transferred to a 1.5 mL microcentrifuge tube. The microcentrifuge tubes containing the cells were then vortexed vigorously for 40 s and heated to 85 °C for 10 min. The tubes were transferred on ice to cool down for 5 min and then centrifuged at 20,000 g for 15 min. After that, 150 µl of the supernatant was aliquoted to a new 1.5 ml microcentrifuge tube and the pH was neutralized with 60 µl 10% ammonium hydroxide. After supernatant neutralization, 50 µl of each sample was loaded into an opaque-walled transparent bottom 96-well plate and read at OD 405 nm using a microplate reader (BioTek) for Alizarin red S staining quantification (Serguienko et al., 2018).

Von kossa staining and quantification

The degree of mineralization of chicken MSCs was determined using the von Kossa staining (Adhikari et al., 2018). Cells were seeded at a density of 8×10^4 cells per well in 0.2% gelatin-coated (Alfa Aesar) 24-well cell culture plates (Corning), and cultured in growth medium at 37°C until 100% confluency. Then the cells were exposed to H_2O_2 in osteogenic differentiation medium for 6, 10, and 14 days. At different time points, the cell culture plates were washed three times with PBS and then fixed with 0.1% glutaraldehyde (G5882, Sigma-Aldrich) in PBS (pH 7.0) for 15 min at room temperature. After discarding the fixation buffer, the cells were washed three times with distilled water and then incubated in 5% silver nitrate (Sigma-Aldrich) for 30 min. The silver nitrate solution was discarded, and the cells were washed with distilled water at least three times, air-dried, and exposed to bright light until black color developed in areas of calcification. Images of cell culture plates were captured at ×2 magnification using a microscope with a camera (Keyence bz-×8000, Keyence). Mineralized nodules were observed as dark brown to black spots. The stained plates were quantified using the area fractions method with the ImageJ program (National Institutes of Health, Bethesda, MD, USA). Three images from each well were analyzed, and the mean area fraction from each well was used for statistical analysis.

RNA isolation, cDNA synthesis, and real-time polymerase chain reaction (qRT-PCR) analysis

The cell culture process for RNA isolation was the same as the osteogenic differentiation. Briefly, MSC cells were expanded to passage 4 and seeded at a density of 8×10^4 cells per well in 0.2% gelatin-coated (Alfa Aesar) 24-well cell culture plates (Corning), and cultured in growth medium until they reached100% confluency. The cells were differentiated for 6 h, 24 h, 48 h, 72 h, 96 h, 5 days, 6 days, 10 days and 14 days, with or without H_2O_2 treatment. At each time point, total

10.3389/fphys.2023.1124355

TABLE 1 Nucleotide sequences of the primers used for quantitative real-time RT-PCR.

Gene1	Primer sequence (5′-3′	Product length (bp)	Annealing temperature (°C)	Accession #
18S rRNA	F-AGCCTGCGGCTTAATTTGAC	121	56.5	AF_173612.1
	R-CAACTAAGAACGGCCATGCA			
HMBS	F-GGCTGGGAGAATCGCATAGG	131	59	XM_004947916.3
	R-TCCTGCAGGGCAGATACCAT			
ACTB	F-CAACACAGTGCTGTCTGGTGGTA	205	61	NM_205518.1
	R-ATCGTACTCCTGCTTGCTGATCC			
C/EBPa	F-CCTACGGCTACAGAGAGGCT	206	60	NM_001031459.1
	R-GAAATCGAAATCCCCGGCCA			
PPARG	F-GAGCCCAAGTTTGAGTTTGC	131	58	XM_025154400.1
	R-TCTTCAATGGGCTTCACATTT			
FABP4	F-GCAGAAGTGGGATGGCAAAG	153	60	NM_204290.1
	R-GTTCGCCTTCGGATCAGTCC			
ALPL	F-CGACCACTCACACGTCTTCA	140	60	NM_205360.1
	R-CGATCTTATAGCCAGGGCCG			
RUNX2	F-ACTTTGACAATAACTGTCCT	192	60	XM_015285081.2
	R-GACCCCTACTCTCATACTGG			
BGLAP	F-GGATGCTCGCAGTGCTAAAG	142	57	NM_205387.3
	R-CTCACACACCTCTCGTTGGG			
SPP1	F-GCCCAACATCAGAGCGTAGA	204	57	NM_204535.4
	R-ACGGGTGACCTCGTTGTTTT			
BMP2	F-TCAGCTCAGGCCGTTGTTAG	163	57	XM_025148488.1
	R-GTCATTCCACCCCACGTCAT			
COL1A2	F- CTGGTGAAAGCGGTGCTGTT	222	60	NM_001079714.2
	R-CACCAGTGTCACCTCTCAGAC			
SOD2	F- GCCACCTACGTGAACAACCT	140	61	NM_204211.2
	R- AGTCACGTTTGATGGCTTCC			
SOD1	F-ATTACCGGCTTGTCTGATGG	173	58	NM_205064.1
	R-CCTCCCTTTGCAGTCACATT			
CAT	F-ACTGCAAGGCGAAAGTGTTT	222	60	NM_001031215.1
	R-GGCTATGGATGAAGGATGGA			
GSTa	F- GAGTCAATTCGGTGGCTGTT	157	59	XM_046913335.1
	R- TGCTCTGCACCATCTTCATC			
NOS2	F-CCTGTACTGAAGGTGGCTATTGG	66	58	NM_204961.2
	R-AGGCCTGTGAGAGTGTGCAA			
GPX1	F-AACCAATTCGGGCACCAG	122	60	NM_001277853.2
	R-CCGTTCACCTCGCACTTCTC			
NFR2	F- GAGCCCATGGCCTTTCCTAT	210	59	XM_046907885.1
	R- CACAGAGGCCCTGACTCAAA			
CASP3	F-TGGTATTGAAGCAGACAGTGGA	103	60	XM_015276122.2

(Continued on following page)

TABLE 1 (*Continued*) Nucleotide sequences of the primers used for quantitative real-time RT-PCR.

Gene1	Primer sequence (5′-3′	Product length (bp)	Annealing temperature (°C)	Accession #
	R-GGAGTAGTAGCCTGGAGCAGTAGA			
CASP8	F-ATTTGGCTGGCATCATCTGT	146	59	NM_204592.4
	R-ACTGCTTCCCTGGCTTTTG			
CASP6	F-AAACCTACACCAACCACCACA	196	60	NM_001396146.1
	R-TTCTGTCTGCCAAAGTCCCA			

[a]18S rRNA:18 S ribosomal RNA; HMBS: hydroxymethylbilane synthase; ACTB: actin beta; PPARG: peroxisome proliferator-activated receptor gamma; C/EBPα: CCAAT/enhancer-binding protein alpha; FABP4: fatty acid binding protein 4; SPP1: secreted phosphoprotein, osteopontin; BMP2: bone morphogenetic protein two; BGLAP: bone gamma-carboxyglutamic acid-containing protein (osteocalcin); RUNX2: runt-related transcription factor 2; ALPL: alkaline phosphatase, biomineralization associated; COL1A2: collagen type I alpha two chain; CAT: catalase; SOD1: superoxide dismutase one; SOD2: superoxide dismutase two; GPX1: glutathione peroxidase one; NOS2: nitric oxide synthase two; NFR2: GA, binding protein transcription factor alpha subunit (GABP2); GSTa: GSTA2, glutathione S-transferase alpha two; CASP3: caspase three; CASP6: caspase six; CASP8: caspase 8.

RNA was extracted from the cells using QIAzol lysis reagents (Qiagen 79,306, Germantown, MD, USA) according to the manufacturer's instructions. The Nano-Drop 1000 Spectrophotometer (ThermoFisher Scientific) was used to determine the quantity of extracted RNA. cDNA was synthesized from 2000 ng of total RNA using high-capacity cDNA reverse transcription kits (Thermo Fisher Scientific). Quantitative real-time reverse transcription polymerase chain reaction (qRT-PCR) was used to measure mRNA expression. Primers were designed using the Primer-BLAST program (https://www.ncbi.nlm.nih.gov/tools/primer-blast/). The specificity of primers was validated by PCR product sequencing; the details of primer sequences used for the experiment are presented in Table 1. Primer quality was verified through melting curve analysis and gel electrophoresis in this study. The qRT-PCR was performed on an Applied Biosystems StepOnePlus™ (Thermo Fisher Scientific) with iTaq™ universal SYBR Green Supermix (BioRad, Hercules, CA, United states) using the following conditions for all genes: 95°C for 10 min followed 40 cycles at 95°C for 15 s, annealing temperature (Table 1) for 20 s, and extending at 72°C for 1 min.

The geometric means of the cycle threshold (Ct) values of three housekeeping genes, including hydroxymethylbilane synthase (*HMBS*), 18 S ribosomal RNA (*18S rRNA*), and actin beta (*ACTB*) were used for normalization. The stability of the housekeeping genes was confirmed by their consistent Ct values among the treatments ($p > 0.1$) and also assessed by statistical algorithms by software program NormFinder (Version 0.953; https://moma.dk/normfinder-software) (Wan et al., 2011). Peroxisome proliferator-activated receptor gamma (*PPARG*), adipose tissue fatty acid binding protein 4 (*FABP4*), and CCAAT enhancer binding protein alpha (*CEBPA*) were used as early markers of adipogenic differentiation, and alkaline phosphatase-biomineralization associated (*ALPL*), bone gamma-carboxyglutamate protein (*BGLAP*), runt-related transcription factor 2 (*RUNX2*), secreted phosphoprotein 1 (*SPP1*), collagen type I alpha two chain (*COL1A2*), bone–specific alkaline phosphatase (*ALP*), and bone morphogenetic protein 2 (*BMP2*) were used as osteogenic marker genes in the bone marrow. Nuclear factor kappa B subunit 1 (*NFKB1*) and antioxidant enzyme protein coding genes including catalase (*CAT*), superoxide dismutase type 1 (*SOD1*), superoxide dismutase type 2 (*SOD2*), glutathione peroxidase 1 (*GPX1*), glutathione S-transferase alpha 2 (*GSTA2*), and nitric oxide synthase 2 (*NOS2*) were used to determine the antioxidant enzyme activity and oxidative stress status. Pro-apoptotic marker genes, such as Caspase 3 (*CASP3*), Caspase 8 (*CASP8*), and Caspase 6 (*CASP6*), were used to assess the cell apoptosis. Samples were run in triplicate, and relative gene expression data were analyzed using the $2^{-\Delta\Delta Ct}$ formula (Livak and Schmittgen, 2001). The expression levels of the other treatment groups were presented as fold changes relative to the average ΔCT value for each gene in the control group.

Statistical analysis

All experimental data were expressed as means with standard errors of the mean (SEM). The data were tested for homogeneity of variances and normality of studentized residuals. The differences between the treatment groups were analyzed using one-way ANOVA, and the means were statistically analyzed using Tukey's test using JMP Pro14 (SAS Institute, Cary, NC, USA). Statistical significance was set at $p \leq 0.05$, and values of $0.05 \leq p \leq 0.1$ were also presented to show a trend towards statistical significance (Serdar et al., 2021).

Results

Cell viability, cell apoptosis, and intracellular ROS production with exogenous H_2O_2 exposure

Cell viability was measured by MTT assay after H_2O_2 exposure (Figure 1). The viability of chicken MSCs exposed to H2O2 showed a different rate of decline among doses. Chicken MSCs were cultured with different concentrations (50–800 nM) of H_2O_2 in osteogenic differentiation medium for 6 h showed a non-cytotoxic effect ($p > 0.05$; Figure 1A). At 24 h of treatment, 800 nM of H_2O_2 significantly reduced cell viability ($p < 0.05$; Figure 1B) by approximately 70% compared to the untreated control. After 48 h, 800 nM of H_2O_2 reduced cell viability by approximately 90% compared to the untreated control ($p < 0.05$; Figure 1C). No statistically significant change in cell viability was observed with treatment concentrations lower than 800 nM. Treatment doses above 400 nM significantly reduced the number of cells to an extent that was not adequate to conduct the experiment. Therefore, doses below 400 nM were selected for further studies. The final treatment concentrations of 100, 200, and 400 nM of H_2O_2 were selected as the treatment doses for the following experiments.

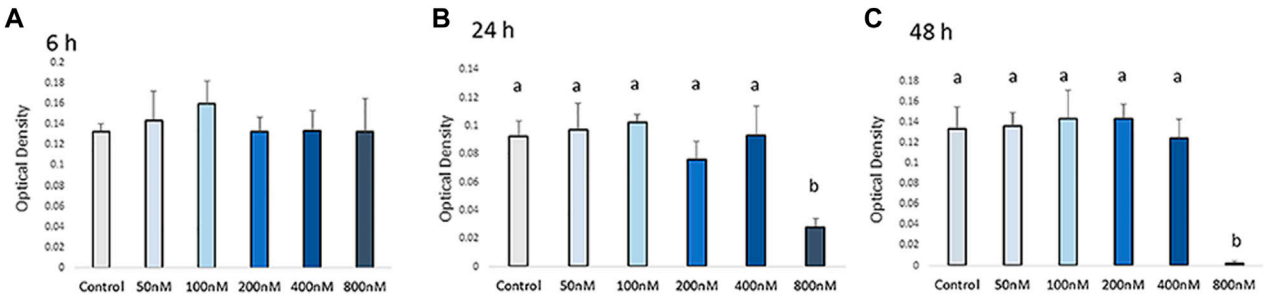

FIGURE 1
Effects of H_2O_2 on the cell viability. Cells were treated with the indicated concentrations of H_2O_2 for 6 h **(A)**, 24 h **(B)** and 48 h **(C)**. The graphs show changes in cellular growth as assessed by MTT assays. The MTT assay showed that exposure to concentrations higher than 400 nM of H_2O_2 can reduce cell viability. Therefore, the appropriate H_2O_2 concentration was screened out and final treatment concentrations of 100 nM, 200 nM and 400 nM of H_2O_2 were selected as the treatments dose for the following experiments. [a, b] Treatments with different letters indicate a significantly difference between treatments using Tukey's HSD test, $p < 0.05$; data are shown as mean ± SEM of four independent replicates ($n = 4$).

Intracellular ROS production in chicken MSCs after H_2O_2 exposure was monitored using a cellular DCFDA assay (Figures 2A,B). A significant increase in intracellular ROS production was detected in 100, 200, and 400 nM H_2O_2-treated chicken MSCs after 6 h compared to the control ($p < 0.05$; Figure 2B), with the highest upregulated ROS response observed at 100 nM of H_2O_2. After 12 h of H_2O_2 exposure, there was a significant difference in ROS production between 100 nM and 400 nM groups ($p < 0.05$; Figure 2B). However, intracellular ROS signal were not significantly affected by H_2O_2 treatment after 24 and 48 h of H_2O_2 exposure. Based on these data, the effective treatment duration is 12 h following exogenous H_2O_2 exposure. To minimized damage to the cell membrane and reduce variations in results due to cell death and reduced cell number caused by prolonged severe stress, the frequency of medium change was set to be every 24 h.

At low concentrations of H_2O_2 treatment, mRNA expression of pro-apoptotic markers, including *CASP-3*, *CASP-6* and *CASP-8* remained unchanged in chicken MSCs during the early differentiation stage from 6 h to day 5 ($p > 0.05$; Figure 3). This suggests that the effect of H_2O_2 on the osteogenic differentiation of MSCs was not due to a cytotoxic effect causing cell apoptosis at the early differentiation stage. However, 200 nM H_2O_2 significantly increased mRNA expression of *CASP-8* compared to the control on day 6 ($p < 0.05$; Figure 3), and 400 nM H_2O_2 numerically increased expression of *CASP-8* ($p < 0.05$; Figure 3). Neither of the higher treatment doses changed the expression of *CASP-3* or *CASP-6* on day 6. On day 10 and day 14, high cycle threshold (Ct > 38) value indicating the expression of *CASP-6* and *CASP-8* were not detected.

Altered gene expression of antioxidant enzyme in response to extracellular H_2O_2 exposure

There was no significant change in the expression of antioxidant enzyme mRNA after 6 h of differentiation, except for expression of *NOS2*, which showed a trend of decreasing with higher H_2O_2 treatment doses ($p = 0.087$; Figure 4). At 24 h of treatment, the mRNA expression of *SOD1* was decreased by the highest concentration of H_2O_2 (400 nM) ($p < 0.05$; Figure 4). At 48 h of treatment, 100 nM H_2O_2 augmented the expression of *CAT* compared to the control. After 5 days of treatment and differentiation, the mRNA expression of *GPX1* was upregulated by 400 nM H_2O_2 compared to the control ($p < 0.05$). 200 nM H_2O_2 significantly increased mRNA expression of *CAT* compared to the 400 nM H_2O_2 treatment group ($p < 0.05$). After 6 days of H_2O_2 treatment, 400 nM H_2O_2 significantly upregulated mRNA expression of *SOD2* compared to the 100 nM H_2O_2 group ($p < 0.05$). There was a trend of increasing expression of *NRF2* with 200 and 400 nM H_2O_2 treatments ($p = 0.077$). After 14 days of differentiation, a trend of increasing mRNA level of *CAT* ($p = 0.068$) was observed with 400 nM H_2O_2 treatment. However, expression of *SOD2*, *GSTa* and *NRF2* was not detected on day 10 and day 14 of differentiation. In conclusion, depending on the different treatment concentration of H_2O_2, the expression of antioxidant enzyme gene was altered at the later stage of differentiation.

Effect of H_2O_2 on osteogenesis in chicken MSCs

Chicken MSCs were treated with various concentrations of H_2O_2 in osteogenic differentiation medium for 14 days, the effects on osteogenic differentiation varied at different time points (Figure 5). At the beginning of differentiation, there was a significant decrease in *SPP1* ($p < 0.05$) and a numerically decreased mRNA expression of *BMP2* ($p = 0.053$) after 6 h of H_2O_2 treatment. In the following days, the mRNA expression of osteogenic marker genes was unchanged. After 96 h of treatment, cells exposure to 400 nM H_2O_2 showed significantly higher mRNA expression of *ALP* ($p < 0.05$), *BGLAP* ($p < 0.05$) and *SPP1* ($p < 0.05$), and 400 nM H_2O_2 tended to increase the expression of *BMP2* ($p = 0.092$) and *Col1A2* ($p = 0.060$). After 5 days of H_2O_2 exposure, mRNA expression of *BGLAP* ($p < 0.05$), *ALP* ($p < 0.05$) and *Col1A2* ($p < 0.05$) was suppressed by 200 nM H_2O_2 compared to the control. In contrast, mRNA expression of *BGLAP* was upregulated by 400 nM H_2O_2 compared to the other treatment groups ($p < 0.05$) and the expression of *ALP* was increased by 400 nM H_2O_2 ($p < 0.05$) compared to the low treatment doses of 100 and 200 nM H_2O_2. After 6 days of daily treatment, mRNA expression of *ALP* ($p < 0.05$), *BGLAP* ($p < 0.05$) and *Col1A2* ($p < 0.05$) was reduced by H_2O_2

10.3389/fphys.2023.1124355

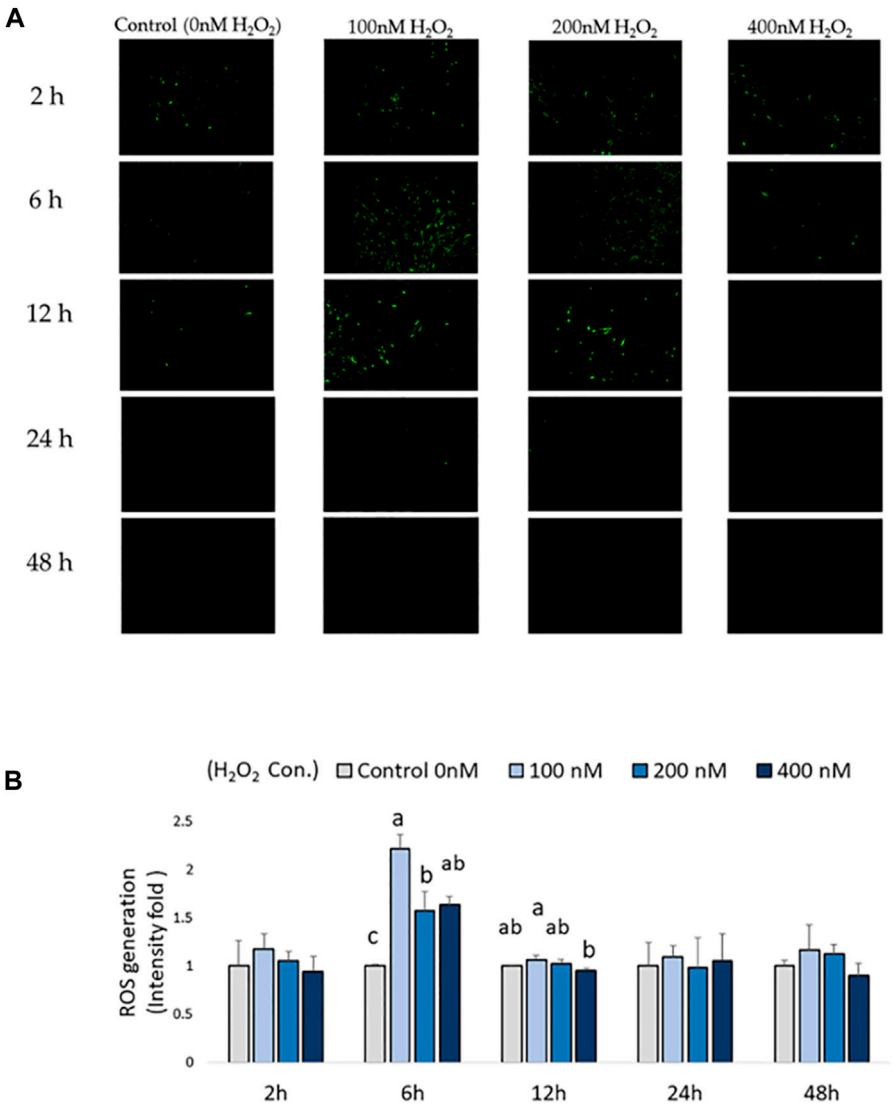

FIGURE 2
Effects of H_2O_2-induced reactive oxygen species (ROS) production in chicken MSCs. 3×10^4 cells were seeded in a black clear-flat-bottom 96-well microplate and allowed to adhere overnight. Cells were then treated with the indicated concentrations of H_2O_2 for 2 h, 6 h, 12 h, 24 h and 48 h. ROS levels in MSCs were measured using a DCFDA/H_2DCFDA cellular ROS assay kit. MSCs cultured without H_2O_2 but PBS (osteogenic differentiation medium with 0 nM H_2O_2) were used as the control. **(A)** Figures were selected as representative images from the DCFDA/H_2DCFDA cellular ROS assay at different time points. MSCs cultured without any treatments or DCFDA/H_2DCFDA was used to set the background adjustment. **(B)** Quantitative analysis was performed by measuring fluorescence intensity. Each value represents the mean ± SEM of three independent replicates (n = 3). MSCs cultured in osteogenic differentiation medium without H_2O_2 treatment (0 nM H_2O_2) were used as the control, and data were present as fold-change normalized to the fluorescence intensity level of the control. $^{a, ab, b, c}$ Treatments with different letters indicate a significantly difference between treatments using Tukey's HSD test, $p < 0.05$.

treatments, and there was a trend of decreasing in *SPP1* ($p = 0.066$) with H_2O_2 treatments. On day 10, the expression of *BMP2* was significantly reduced by H_2O_2 treatments compared to the control ($p < 0.05$), and there was a trend of decreasing in *RUNX2* ($p = 0.079$) with H_2O_2 treatments. On day 14, 100 nM H_2O_2 significantly reduced the expression of *BMP2* compared to the control ($p < 0.05$), and 400 nM H_2O_2 significantly reduced expression of *Col1A2* compared to the control ($p < 0.05$). There was also a trend of decreasing in *SPP1* ($p = 0.092$) with H_2O_2 treatments on day 14. However, *ALP* expression was not detected on day 10 and day 14 of differentiation.

In parallel with the mRNA expression mentioned above, the inhibition of osteogenic differentiation was characterized by a reduction in mineral accumulation after 6 days, 10 days and 14 days of differentiation. The effects of H_2O_2 on the mineralization were visualized using Alizarin red staining (Figure 6A). The optical density (O.D.) value result showed that 400 nM of H_2O_2 significantly reduced the O.D. value by 30% compared to the control after 6 days of H_2O_2 exposure ($p < 0.05$; Figure 6B). There were no statistically significant changes after 10 and 14 days of differentiation, but smaller mineralized crystals were observed with a higher dose of H_2O_2 treatment, and 400 nM H_2O_2 led a decrease in mineralization by 20% and 40%. The extracellular calcium (black crystals) content was quantified by von Kossa staining (Figure 7). After 6 days of differentiation, there were smaller and fewer extensive crystals and less mineralized matrix with higher doses of H_2O_2 treatment. The colorimetric analysis showed a significant

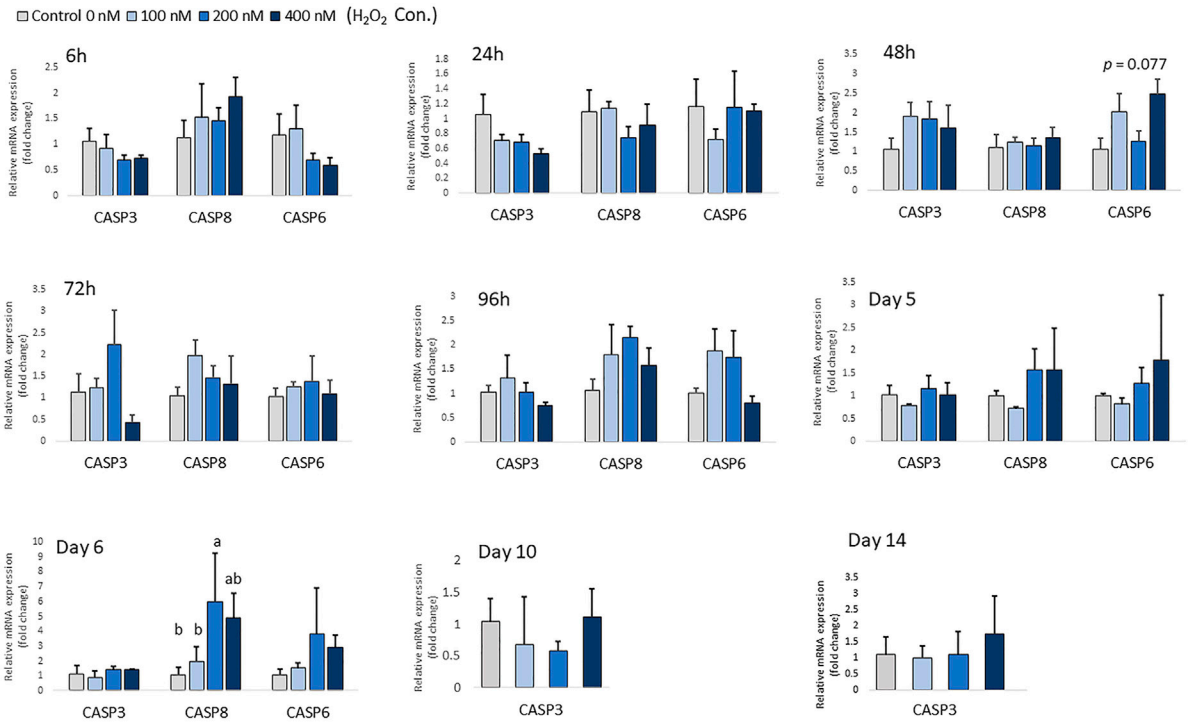

FIGURE 3
Effects of H_2O_2 on mRNA expression of apoptosis markers in chicken MSCs. Differentiation cells were treated with the indicated concentrations of H_2O_2 for 6 h, 24 h, 48 h, 72 h, 96 h, 5 days, 6 days, 10 days and 14 days. Each value represents the mean ± SEM of three independent experiments (n = 3). CASP3: caspase three; CASP6: caspase six; CASP8: caspase eight; [a, ab, b, c] Treatments with different letters indicate a significantly difference between treatments using Tukey's HSD test, $p < 0.05$.

decrease in O.D. with 400 nM H_2O_2 treatment ($p < 0.05$; Figure 7B). After 10 days of H_2O_2 treatment, a lower number of mineralized nodules and smaller size of crystals were observed with higher concentrations of H_2O_2 treatment; the O.D. showed that 200 and 400 nM H_2O_2 led to a significant decrease in mineralization, with the least mineral deposition observed in the 400 nM H_2O_2 group ($p < 0.05$; Figure 7B). After 14 days of differentiation, 400 nM H_2O_2 significantly suppressed mineralization compared to the other groups ($p < 0.05$; Figure 7B). In conclusion, the different doses of H_2O_2 treatment resulted in varying effects on osteogenic gene expression at different time points, while mineralization was significantly reduced by H_2O_2 treatment, with the greatest reduction observed in the high treatment concentration groups after 10 and 14 days of differentiation.

Meanwhile, under the condition of osteogenic induction differentiation, the expression of adipogenic-related genes was altered with H_2O_2 treatment. Decreases in *PPARG* expression with 200 nM and 400 nM H_2O_2 treatment doses were observed at 6 h ($p < 0.05$; Supplementary Figure). Afterward, H_2O_2 reduced the expression of *PPARG* ($p = 0.053$; Supplementary Figure), *CEBPA* ($p < 0.05$) and *FABP4* ($p < 0.05$) after 24 h of osteogenic differentiation. In contrast, with prolonged treatment periods, 400 nM H_2O_2 significantly elevated the expression of *PPARG* ($p < 0.05$) and *FABP4* ($p < 0.05$) after 96 h of treatment. A similar expression pattern was observed after 5 days of H_2O_2 treatment under osteogenic differentiation condition, where 400 nM H_2O_2 significantly increased the expression of *PPARG* ($p < 0.05$), *CEBPA* ($p < 0.05$) compared to the control; the expression level of *FABP4* was significantly elevated by 200nM and 400 nM H_2O_2 treatment ($p < 0.05$) compared to the control. After 6 days of H_2O_2 treatment, 200 and 400 nM H_2O_2 treatments increased the expression of *PPARG* ($p < 0.05$; Supplementary Figure) compared to the control; 400 nM H_2O_2 treatment drastically increased the expression of *FABP4* ($p < 0.05$; Supplementary Figure) compared to other groups. However, 100 nM H_2O_2 reduced expression of *CEBPA* ($p < 0.05$; Supplementary Figure) compared to the control. Adipogenic expression was not significantly changed by H_2O_2 treatment on day 10 and day 14.

Discussion

Cell fate with the presence of oxidative stress can vary depending on the cell types, treatment intensity, duration, dosage, and the cell differentiation status (Denu and Hematti, 2016). Moreover, several studies have pointed out that undifferentiated stem cells have superior antioxidant defense than differentiated cells; for example, undifferentiated MSCs are known to have relatively low levels of intracellular ROS and high levels of glutathione in the human cell line (Valle-Prieto and Conget, 2010). Studies have shown that mouse embryonic stem cells exhibit high antioxidant activity and stress-resistance, but several antioxidant and cellular resistance genes are downregulated during differentiation (Saretzki et al., 2004). Under normal circumstances during mineralization, MSCs differentiate and their expression of mineralization factors increases (Blair et al., 2017). The size of mineral crystals increases during bone mineralization, and the collagen fibers become more organized and condensed (Blair et al., 2017). Studies on other cell types have indicated that H_2O_2 solutions have a significant effect on collagen production (Nashchekina et al.,

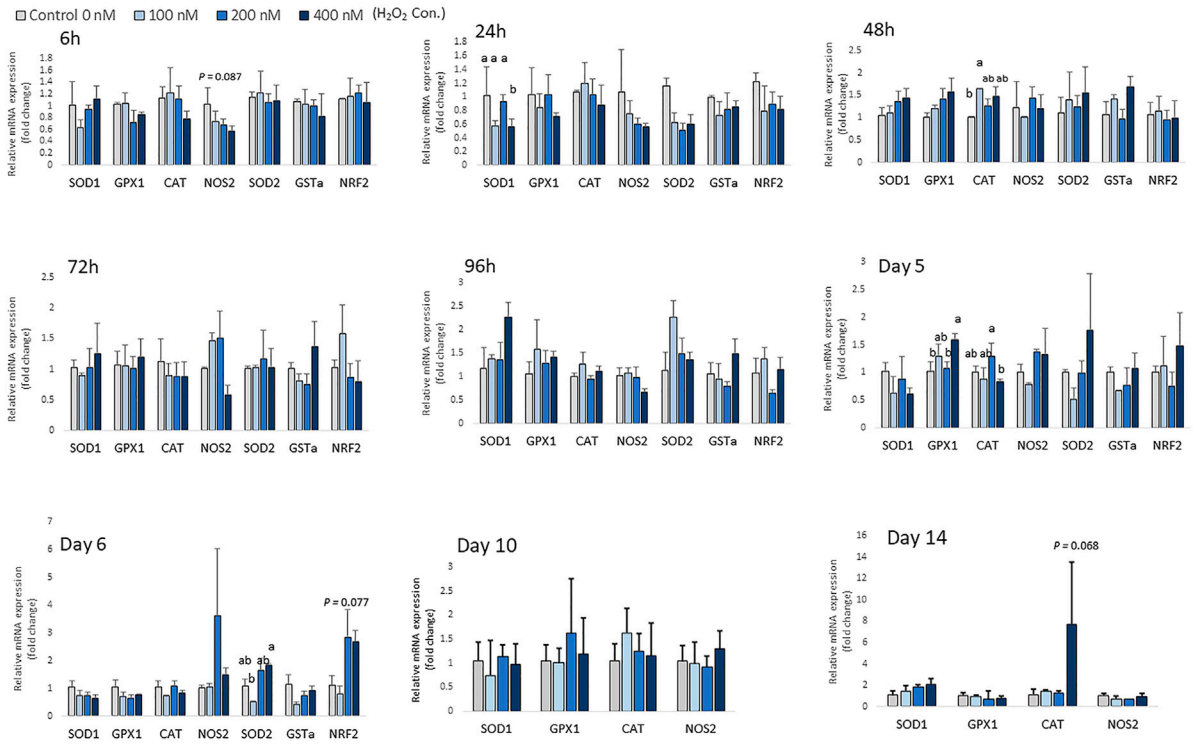

FIGURE 4
Effects of H_2O_2 on mRNA expression of antioxidant enzymes in chicken MSCs. Cells were treated with the indicated concentrations of H_2O_2 for 6 h, 24 h, 48 h, 72 h, 96 h, 5 days, 6 days, 10 days and 14 days. The expression of *SOD2*, *GSTa* and *NRF2* was not detected on day 10 and day 14 of differentiation. Each value represents the mean ± SEM of three independent experiments (n = 3). CAT: catalase; SOD1: superoxide dismutase one; SOD2: superoxide dismutase two; GPX1: glutathione peroxidase one; NOS2: nitric oxide synthase two; NFR2: GA binding protein transcription factor alpha subunit (GABP2); GSTa: glutathione S-transferase alpha two; [a, ab, b] Treatments with different letters indicate a significantly difference between treatments using Tukey's HSD test, $p < 0.05$.

2021), as previous studies have reported the increased activities of oxidative stress was linked to decreased collagen synthesis in fibroblasts (Siwik et al., 2001), human cartilage (Altindag et al., 2007), and chick embryo tissue culture (Ramp et al., 1987). Moreover, the chicken embryo tissue culture has also indicated that multiple exposures to H_2O_2 markedly inhibit collagen synthesis (Ramp et al., 1987). In this report, exogenous H_2O_2 (100–400 nM) suppressed the osteoblastic mineralization of chicken compact bone-derived MSCs, manifested by reduced osteogenic differentiation gene markers and less mineral deposition. The decreased expression of *Col1A2* after 6 days of H_2O_2 treatment supported the hypothesis that H_2O_2-induced oxidative stress can directly interrupt type 1 collagen production. Moreover, the concentration of H_2O_2 in the present study is much lower than the H_2O_2 doses used in human and mouse stem cell studies (Nouri et al., 2019), demonstrating that chicken compact bone-derived MSCs are relatively sensitive to oxidative stress compared to other cell types in chicken (chicken cardiomyocytes: 0.2 mM H_2O_2 (Jiang et al., 2005; Wan et al., 2016); chicken cardiac cells, 0.2–2.0 mM H_2O_2; and chicken epithelial cells, 300 μM H_2O_2 (Lin et al., 2016)). Interestingly, a previous study indicated that ROS production did not influence the aging process of avian fibroblast cells (Strecker et al., 2010). Comparing the blood redox state markers of 78 free-living avian species revealed that relatively long-lived bird species had high levels of antioxidants status (especially total antioxidant status and total glutathione) and low levels of ROS (Xia and Møller, 2018). With the rapid growth and relatively short lifespan of broilers, it is likely that high levels of ROS due to oxidative stress may occur in a great extent in broiler production. Chicken MSCs-differentiated osteoblasts are particularly susceptible to oxidative stress, making the negative impact of ROS production on bone homeostasis a potential factor in the development of skeletal abnormalities.

MSCs have the ability to differentiate into various cell phenotype types, which are controlled by transcription factors such as *PPARG*, *RUNX2* and *SOX9*, which regulate adipogenesis, osteogenesis and chondrogenesis, respectively (Robert et al., 2020). In particular, adipogenesis and osteogenesis have a reciprocal relationship (Takada et al., 2007; Robert et al., 2020). For example, in human and mouse primary MSCs, *PPARG2* insufficiency resulted in increased osteogenesis of osteoblast (Takada et al., 2007), while depletion of *RUNX2* promoted adipogenesis (Enomoto et al., 2004). ROS level in MSCs also plays a crucial role in determining their differentiation potential (Ho et al., 2013; Denu and Hematti, 2016). Previous studies have shown that mRNA expression of antioxidant enzymes such as *SOD, CAT,* and *GPX* is upregulated during adipogenesis in human MSCs (Ho et al., 2013). In this study, prolonged exposure to H_2O_2 increased cellular oxidative stress and increased the basal expression of adipogenic differentiation markers at the later stages of differentiation, which was accompanied by decreased mineralization. This is consistent with previous studies that have shown that H_2O_2 exposure altered the differentiation potential in human and mouse MSCs or cell lines (Ho et al., 2013; Lin et al., 2018). In addition, by

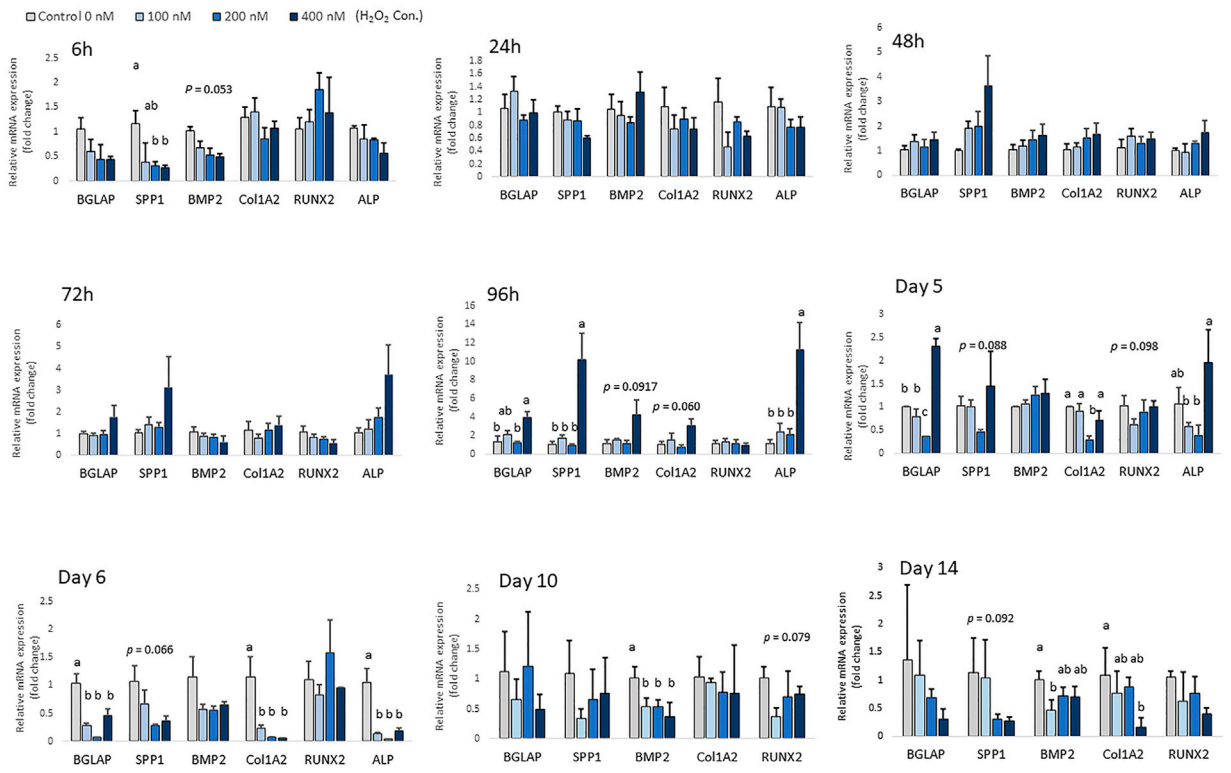

FIGURE 5
Effects of H_2O_2 on mRNA expression of osteogenic differentiation markers in chicken MSCs. Cells were treated with the indicated concentrations of H_2O_2 in differentiation medium for 6 h, 24 h, 48 h, 72 h, 96 h, 5 days, 6 days, 10 days and 14 days. Each value represents the mean ± SEM of three independent experiments (n = 3). SPP1: secreted phosphoprotein, osteopontin; BMP2: bone morphogenetic protein two; BGLAP: bone gamma-carboxyglutamic acid-containing protein (osteocalcin); RUNX2: runt-related transcription factor 2; ALP: alkaline phosphatase, biomineralization associated; Col1A2: collagen type I alpha two chain. [a, ab, b, c] Treatments with different letters indicate a significantly difference between treatments using Tukey's HSD test, $p < 0.05$.

analyzing genome-wide gene expression profiling, Menssen et al. (Menssen et al., 2011) reported an upregulated *CASP8* level during adipogenic differentiation in human bone marrow-derived MSCs. Therefore, the increased expression of *CASP8* on day 6 might have been due to adipogenic differentiation of chicken MSCs, rather than apoptosis directly caused by H_2O_2-induced oxidative stress. Moreover, the effect of H_2O_2 treatment on regulating cell differentiation has been observed in different types of cells, where sublethal doses of oxidative stress induce morphological alterations (Shadel and Horvath, 2015; Diebold and Chandel, 2016; Infante and Rodriguez, 2018). For example, prolonged H_2O_2 treatment activates NF-κB transcriptional activity while stimulating brown adipogenesis during myogenic differentiation in mice satellite cells (Morozzi et al., 2017). Therefore, at least in part, oxidative stress is a factor for the dysfunction of bone tissue, not only by causing cell death, but also by interrupting MSCs differentiation capacity and decreasing the osteogenic ability directly.

In the current study, several osteogenic differentiation markers were significantly upregulated with the highest H_2O_2 treatment dose after 4 and 5 days of treatment, and then drastically dropped after 6 days of treatment. We made several hypotheses to explain the upregulated and downregulated expression patterns. Firstly, studies pointed out that the cellular effects of ROS may differ depending on the cell differentiation stage due to the difference between progenitor cells and mature cells (Khalid et al., 2020). For example, during the initial differentiation process, MSCs commit to pre-osteoblasts while actively proliferating (Infante and Rodriguez, 2018). Over the later stage of differentiation, the pre-osteoblasts can further mature into non-proliferating osteoblasts that start matrix secretion, maturation, and mineralization (Infante and Rodriguez, 2018). Studies showed that H_2O_2 treatment significantly enhance bone marrow MSCs proliferation and migration ability (Pendergrass et al., 2013). Human and mouse studies revealed a low level of intracellular ROS and high levels of antioxidants in undifferentiated MSCs (Hu et al., 2018). In contrast, differentiated MSCs show a higher level of ROS and lower activity of antioxidative enzymes (Hu et al., 2018). Therefore, it is important to distinguish the multiple roles of ROS in pre-osteoblast differentiation and osteoblast maturation. Secondly, we hypothesize that ROS over-production mediated the cell cycle and caused cell prematurity. ROS is a fundamental signal in many signaling pathways metabolisms (Shadel and Horvath, 2015). The low level of ROS allowed reversible oxidative modifications until the ROS production overwhelm its antioxidant capacity, which leads to severe cellular damage (Diebold and Chandel, 2016). Redox status plays a vital role in the cell cycle, and accumulated intracellular ROS can force MSCs to undergo cellular senescence, substantially interrupt stem cells differentiation (Brandl et al., 2011). The expression of *GPX*, *CAT* and *SOD2* changed in current study, indicating an altered oxidation-reduction status. *SOD2*, which plays a vital role in regulating mitochondrial stress and osteoblastogenesis, was upregulated (Gao et al., 2018). This helped reduce mRNA over-expression of *PPARG and FABP-4* in diabetic mouse models (Sen et al., 2015). In the current study, the increased expression of *SOD2* suggested that cells were

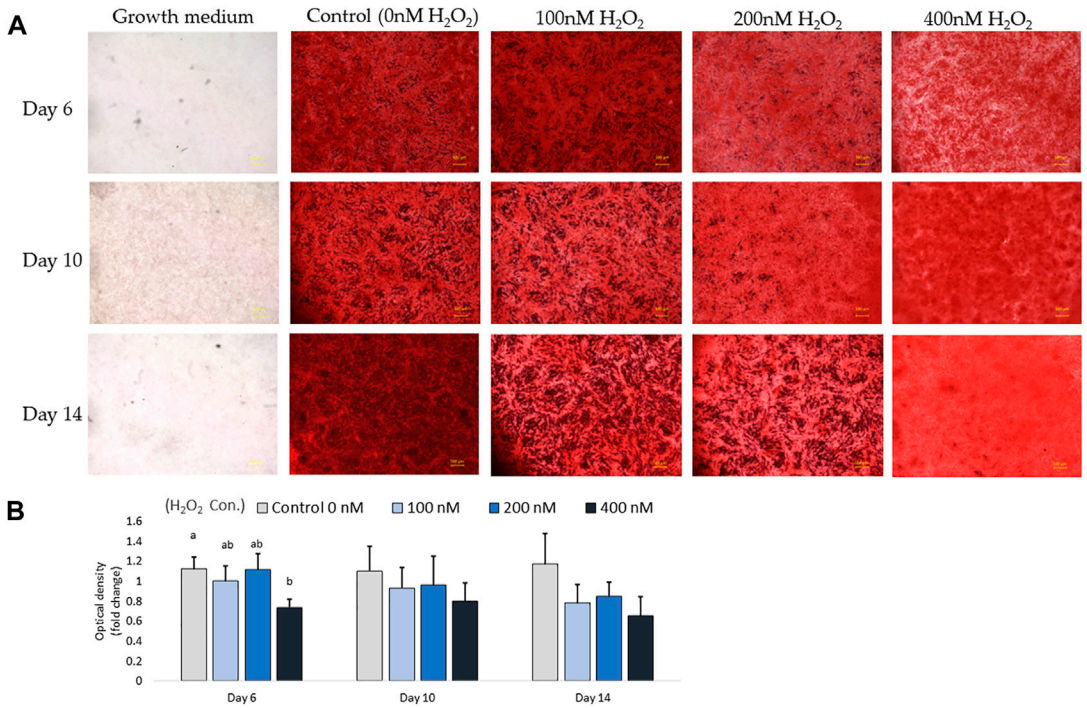

FIGURE 6
Alizarin red S staining for mineralization on day 6, day 10 and day 14. Images were randomly acquired at ×2 magnification. The calcified nodules appeared bright red in color. Mineral deposit quantification was conducted, with each value representing the mean ± SEM of three independent experiments (n = 3). [a, b] Treatments with different letters indicate a significantly difference between treatments using Tukey's HSD test at each time points, respectively, $p < 0.05$.

actively suppressing adipogenic differentiation under oxidative stress. However, we speculated that long-term exposure cells to higher levels of exogenous H_2O_2 stimulated intracellular ROS production and promoted pre-osteoblast commitment at the early differentiation stage, but also led to the accumulation of ROS, which resulted in cell prematurity and apoptosis, decreasing mineral accrual at the later stage. The molecular mechanisms by which ROS affects the avian cell cycle, however, are largely unexplored and require further investigation.

Another hypothesis is that exogenous H_2O_2 stimulated a regeneration response. H_2O_2 is well-known ROS signaling intermediate in response to tissue injury (Sanchez-de-Diego et al., 2019). ROS activates signaling that influences vital pathways, such as Wnt or TGF/BMP pathways, which are response to fracture healing and tissue repairment mechanism by regulating osteogenic differentiation of stem cells (Wang et al., 2017; Sheppard et al., 2022). MSCs can migrate to the sites of injury in response to various stimuli, including cytokines or growth factors, and differentiate into tissue-specific cell types to repair the damaged region (Merimi et al., 2021). Additionally, ROS can regulate the activation of BMPs and RUNX2 pathways in MSCs during the repair process by mediating the activity of NF-κB signaling (Mandal et al., 2011). Therefore, in the present study, the increased expression of bone formation marks *ALP*, *SPP1* and *BGLAP* after 5 days of differentiation may suggested that the high ROS level stimulated a cell repair-response, which recruited MSCs to differentiate into osteoblasts to maintain cell population and homeostasis. However, continuous oxidative stress cause MSCs to commit apoptosis, ultimately reducing mineralization.

Oxidative stress has been linked to many bone-related diseases in humans and mammals (Reis and Ramos, 2021). In broilers, at least 30% of birds showed poor locomotion during the fast growth period (Wideman, 2016; Zhang et al., 2020), which interfered chicken' accessibility to feed and water, predominantly reducing the growth and causing an economic loss in production. Generally, cultured cells have higher throughput and shorter turnaround times than *in vivo* study models (Dawson et al., 2014), and the response of avian stem cells to different stress stimuli has been widely studied in the context of growth and physiology (Ali Hassan and Li, 2021; Xu et al., 2022). Therefore, understanding oxidative stress in a cell model is essential for a better understanding of bone pathogenic process in chickens. Tibial dyschondroplasia (TD) and bacterial osteomyelitis (BCO) are two common skeletal abnormalities in the broiler production that cause bones deformation and lameness (Hartcher and Lum, 2019). Previous studies have indicated that BCO is initiated by mechanical micro-fracturing, followed by bacterial colonization and bone degradation, leading to necrosis (Wideman, 2016). Mitochondrial dysfunction and apoptosis are also involved in BCO in broilers (Ferver et al., 2021). Although there is no direct evidence linking oxidative stress and BCO pathogenesis, higher levels of oxidative stress in response to local infection have been reported in human patients with chronic osteomyelitis (Massaccesi et al., 2022). The pathology of osteomyelitis is characterized by localized inflammation, bone mineral loss, and structural damage, which share similarities with broiler BCO (Grbic et al., 2014). Furthermore, a recent study on femoral

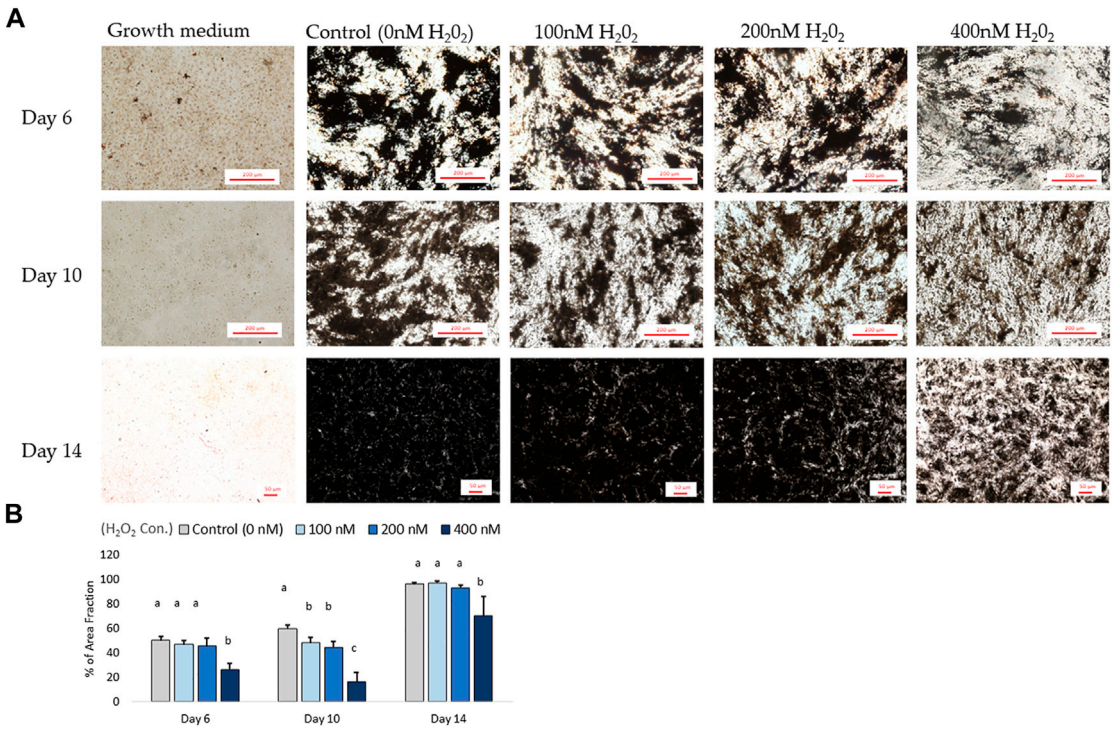

FIGURE 7
The von Kossa staining results for mineralization on day 6, day 10 and day 14. **(A)** Images were randomly acquired in ×4 magnification for day 6 and 10 images. On day 14, the figure was acquired at ×2 magnification due to mineralization interrupting autofocus using higher magnification lenses. Four images per well were analyzed. Black objects indicates phosphate and calcium deposition. ImageJ analysis quantified the percent area fraction for each treatment based on three independently sampled experiments of each species, with each value representing the mean ± SEM of three independent experiments (n = 3). [a, b] Treatments with different letters indicate a significantly difference between treatments using Tukey's HSD test at each time points, respectively; $p < 0.05$.

necrosis pathogenicity also reported an abnormal increased in lipid metabolism and decreases in bone formation in a chicken femoral head necrosis disease model (Fan et al., 2021). Therefore, by gathering all the evidence above, we proposed that oxidative stress could potentially be a co-factor involved in chicken bone necrosis. Moreover, tibial dyschondroplasia (TD) is another common bone abnormality in fast-growing broilers, characterized by tibial bone deformities with non-vascular, non-mineralized growth plates (Mehmood et al., 2017; Zhang et al., 2019). It is a chondrogenesis-related growth plate development disease that is highly associated with premature and apoptosis of cells (Mehmood, 2018). There is an known relationship between TD and oxidative stress induced by thiram, which reduces liver antioxidation capability and damages liver function (Li et al., 2007). Altered systemic antioxidant activity has also been reported in broilers with TD (Zhang et al., 2018; Huang et al., 2021). Although the function of osteoblast has not been fully illustrated in broiler TD model, osteoblasts are responsible for forming the type I collagen matrix surrounding vasculature buds, and osteoblast and osteocyte have direct association with chondrocyte maturation and hypotrophy (Zhang et al., 2020). Based on this information, we hypothesize that TD may be partially associated with systemic oxidative stress. Studies have shown that *mycoplasma* (M.) can produce H_2O_2 and superoxide radicals, which induce oxidative stress in the respiratory epithelium and directly affect bone metabolism (Shimizu, 2016). Clinical signs of *M. synoviae* infection include joint lesions in avian species (Osorio et al., 2007). These results provide evidence of the pathogenicity of mycoplasmas on bone integrity and support our current results showing that high level and long-term effects of H_2O_2 negatively regulate osteoblast cell activity.

Although many questions remain, ever-growing numbers of observations regarding chicken bone disorders and avian bone health rapidly shape our understanding of various topics, such as metabolic regulation and the pathogenesis of bone disorders in broilers (Porto et al., 2015). The knowledge of ROS generation and antioxidant defense systems has generated a great deal of interest due to its potential applications in animal production, but it remains to be profoundly explored in chicken stem cell models. In conclusion, the concentration of ROS is in a dynamic equilibrium and is modulated by cellular processes that produce and eliminate ROS. Cellular effects of ROS may vary depending on the differentiation stage of the cells. Treatment with H_2O_2 altered the expression of cellular antioxidant enzyme gene, and long-term treatment with H_2O_2 inhibited osteogenic biomineralization and decreased the expression of osteogenic differentiation markers in chicken MSCs. The impaired osteogenic differentiation potential was associated with an increased potential for adipogenesis in chicken MSCs under oxidative stress, highlighting that cellular oxidative stress caused by exogenous H_2O_2 accumulation modulates stem cell differentiation capacity.

Data availability statement

The raw data supporting the conclusions of this article will be made available by the authors, without undue reservation.

Ethics statement

The animal study was reviewed and approved by the Institutional Animal Care and Use Committee at the University of Georgia, Athens, GA.

Author contributions

All authors listed have made a substantial, direct and intellectual contribution to the work, and approved it for publication. YT and WK conceived and designed this study. YT and GL contributed to sample collection. YT contributed to data analyses. The paper was written through contribution and critical review of the manuscript by all authors (YT, GL, and WK).

Conflict of interest

The authors declare that the research was conducted in the absence of any commercial or financial relationships that could be construed as a potential conflict of interest.

Publisher's note

All claims expressed in this article are solely those of the authors and do not necessarily represent those of their affiliated organizations, or those of the publisher, the editors and the reviewers. Any product that may be evaluated in this article, or claim that may be made by its manufacturer, is not guaranteed or endorsed by the publisher.

Supplementary material

The Supplementary Material for this article can be found online at: https://www.frontiersin.org/articles/10.3389/fphys.2023.1124355/full#supplementary-material

References

Adhikari, R., Chen, C., Waters, E., West, F. D., and Kim, W. K. (2018). Isolation and differentiation of mesenchymal stem cells from broiler chicken compact bones. *Front. Physiol.* 9, 1892. doi:10.3389/fphys.2018.01892

Ali Hassan, N., and Li, Z. (2021). Oxidative stress in broiler chicken and its consequences on meat quality. *Int. J. Life Sci. Res. Archive* 1 (1), 045–054. doi:10.53771/ijlsra.2021.1.1.0054

Altindag, O., Erel, O., Aksoy, N., Selek, S., Celik, H., and Karaoglanoglu, M. (2007). Increased oxidative stress and its relation with collagen metabolism in knee osteoarthritis. *Rheumatol. Int.* 27 (4), 339–344. doi:10.1007/s00296-006-0247-8

Atashi, F., Modarressi, A., and Pepper, M. S. (2015). The role of reactive oxygen species in mesenchymal stem cell adipogenic and osteogenic differentiation: A review. *Stem Cells Dev.* 24 (10), 1150–1163. doi:10.1089/scd.2014.0484

Blair, H. C., Larrouture, Q. C., Li, Y., Lin, H., Beer-Stoltz, D., Liu, L., et al. (2017). Osteoblast differentiation and bone matrix formation *in vivo* and *in vitro*. *Tissue Eng. Part B Rev.* 23 (3), 268–280. doi:10.1089/ten.TEB.2016.0454

Brandl, A., Meyer, M., Bechmann, V., Nerlich, M., and Angele, P. (2011). Oxidative stress induces senescence in human mesenchymal stem cells. *Exp. Cell Res.* 317 (11), 1541–1547. doi:10.1016/j.yexcr.2011.02.015

Chauhan, S. S., Rashamol, V. P., Bagath, M., Sejian, V., and Dunshea, F. R. (2021). Impacts of heat stress on immune responses and oxidative stress in farm animals and nutritional strategies for amelioration. *Int. J. Biometeorol.* 65 (7), 1231–1244. doi:10.1007/s00484-021-02083-3

Dawson, J. I., Kanczler, J., Tare, R., Kassem, M., and Oreffo, R. O. (2014). Concise review: Bridging the gap: Bone regeneration using skeletal stem cell-based strategies - where are we now? *Stem Cells* 32 (1), 35–44. doi:10.1002/stem.1559

Denu, R. A., and Hematti, P. (2016). Effects of oxidative stress on mesenchymal stem cell biology. *Oxid. Med. Cell Longev.* 2016, 2989076. doi:10.1155/2016/2989076

Diebold, L., and Chandel, N. S. (2016). Mitochondrial ROS regulation of proliferating cells. *Free Radic. Biol. Med.* 100, 86–93. doi:10.1016/j.freeradbiomed.2016.04.198

Enomoto, H., Furuichi, T., Zanma, A., Yamana, K., Yoshida, C., Sumitani, S., et al. (2004). Runx2 deficiency in chondrocytes causes adipogenic changes *in vitro*. *J. Cell Sci.* 117 (3), 417–425. doi:10.1242/jcs.00866

Fan, R., Liu, K., and Zhou, Z. (2021). Abnormal lipid profile in fast-growing broilers with spontaneous femoral head necrosis. *Front. Physiol.* 12, 685968. doi:10.3389/fphys.2021.685968

Ferver, A., Greene, E., Wideman, R., and Dridi, S. (2021). Evidence of mitochondrial dysfunction in bacterial chondronecrosis with osteomyelitis-affected broilers. *Front. Vet. Sci.* 8, 640901. doi:10.3389/fvets.2021.640901

Forrester, S. J., Kikuchi, D. S., Hernandes, M. S., Xu, Q., and Griendling, K. K. (2018). Reactive oxygen species in metabolic and inflammatory signaling. *Circ. Res.* 122 (6), 877–902. doi:10.1161/CIRCRESAHA.117.311401

Gao, J., Feng, Z., Wang, X., Zeng, M., Liu, J., Han, S., et al. (2018). SIRT3/SOD2 maintains osteoblast differentiation and bone formation by regulating mitochondrial stress. *Cell Death Differ.* 25 (2), 229–240. doi:10.1038/cdd.2017.144

Grbic, R., Miric, D. J., Kisic, B., Popovic, L., Nestorovic, V., and Vasic, A. (2014). Sequential analysis of oxidative stress markers and vitamin C status in acute bacterial osteomyelitis. *Mediat. Inflamm.* 2014, 975061. doi:10.1155/2014/975061

Hambli, R. (2014). Connecting mechanics and bone cell activities in the bone remodeling process: An integrated finite element modeling. *Front. Bioeng. Biotechnol.* 2, 6. doi:10.3389/fbioe.2014.00006

Hartcher, K. M., and Lum, H. K. (2019). Genetic selection of broilers and welfare consequences: A review. *World's Poult. Sci. J.* 76 (1), 154–167. doi:10.1080/00439339.2019.1680025

Ho, P. J., Yen, M. L., Tang, B. C., Chen, C. T., and Yen, B. L. (2013). H2O2 accumulation mediates differentiation capacity alteration, but not proliferative decline, in senescent human fetal mesenchymal stem cells. *Antioxid. Redox Signal* 18 (15), 1895–1905. doi:10.1089/ars.2012.4692

Hu, C., Zhao, L., Peng, C., and Li, L. (2018). Regulation of the mitochondrial reactive oxygen species: Strategies to control mesenchymal stem cell fates *ex vivo* and *in vivo*. *J. Cell Mol. Med.* 22 (11), 5196–5207. doi:10.1111/jcmm.13835

Huang, S. C., Cao, Q. Q., Cao, Y. B., Yang, Y. R., Xu, T. T., Yue, K., et al. (2021). Morinda officinalis polysaccharides improve meat quality by reducing oxidative damage in chickens suffering from tibial dyschondroplasia. *Food Chem.* 344, 128688. doi:10.1016/j.foodchem.2020.128688

Infante, A., and Rodriguez, C. I. (2018). Osteogenesis and aging: Lessons from mesenchymal stem cells. *Stem Cell Res. Ther.* 9 (1), 244. doi:10.1186/s13287-018-0995-x

Jiang, B., Xiao, W., Shi, Y., Liu, M., and Xiao, X. (2005). Heat shock pretreatment inhibited the release of Smac/DIABLO from mitochondria and apoptosis induced by hydrogen peroxide in cardiomyocytes and C2C12 myogenic cells. *Cell Stress Chaperones* 10 (3), 252–262. doi:10.1379/csc-124r.1

Khalid, S., Yamazaki, H., Socorro, M., Monier, D., Beniash, E., and Napierala, D. (2020). Reactive oxygen species (ROS) generation as an underlying mechanism of inorganic phosphate (Pi)-induced mineralization of osteogenic cells. *Free Radic. Biol. Med.* 153, 103–111. doi:10.1016/j.freeradbiomed.2020.04.008

Li, J., Bi, D., Pan, S., and Zhang, Y. (2007). Effect of diet with thiram on liver antioxidant capacity and tibial dyschondroplasia in broilers. *Br. Poult. Sci.* 48 (6), 724–728. doi:10.1080/00071660701665858

Lin, C. H., Li, N. T., Cheng, H. S., and Yen, M. L. (2018). Oxidative stress induces imbalance of adipogenic/osteoblastic lineage commitment in mesenchymal stem cells through decreasing SIRT1 functions. *J. Cell Mol. Med.* 22 (2), 786–796. doi:10.1111/jcmm.13356

Lin, X., Jiang, S., Jiang, Z., Zheng, C., and Gou, Z. (2016). Effects of equol on H2O2-induced oxidative stress in primary chicken intestinal epithelial cells. *Poult. Sci.* 95 (6), 1380–1386. doi:10.3382/ps/pew034

Livak, K. J., and Schmittgen, T. D. (2001). Analysis of relative gene expression data using real-time quantitative PCR and the 2(-Delta Delta C(T)) Method. *Methods* 25 (4), 402–408. doi:10.1006/meth.2001.1262

Mandal, C. C., Ganapathy, S., Gorin, Y., Mahadev, K., Block, K., Abboud, H. E., et al. (2011). Reactive oxygen species derived from Nox4 mediate BMP2 gene transcription and osteoblast differentiation. *Biochem. J.* 433 (2), 393–402. doi:10.1042/BJ20100357

Maraldi, T., Angeloni, C., Giannoni, E., and Sell, C. (2015). Reactive oxygen species in stem cells. *Oxid. Med. Cell Longev.* 2015, 159080. doi:10.1155/2015/159080

Massaccesi, L., Galliera, E., Pellegrini, A., Banfi, G., and Corsi Romanelli, M. M. (2022). Osteomyelitis, oxidative stress and related biomarkers. *Antioxidants (Basel)* 11 (6), 1061. doi:10.3390/antiox11061061

Mehmood, K. (2018). Tetramethylpyrazine mitigates toxicity and liver oxidative stress in tibial dyschondroplasia chickens. *Pak. Veterinary J.* 38 (01), 76–80. doi:10.29261/pakvetj/2018.015

Mehmood, K., Zhang, H., Iqbal, M. K., Rehman, M. U., Shahzad, M., Li, K., et al. (2017). *In vitro* effect of apigenin and danshen in tibial dyschondroplasia through inhibition of heat-shock protein 90 and vascular endothelial growth factor expressions in avian growth plate cells. *Avian Dis.* 61 (3), 372–377. doi:10.1637/11641-032817-RegR

Menssen, A., Haupl, T., Sittinger, M., Delorme, B., Charbord, P., and Ringe, J. (2011). Differential gene expression profiling of human bone marrow-derived mesenchymal stem cells during adipogenic development. *BMC Genomics* 12, 461. doi:10.1186/1471-2164-12-461

Merimi, M., El-Majzoub, R., Lagneaux, L., Moussa Agha, D., Bouhtit, F., Meuleman, N., et al. (2021). The therapeutic potential of mesenchymal stromal cells for regenerative medicine: Current knowledge and future understandings. *Front. Cell Dev. Biol.* 9, 661532. doi:10.3389/fcell.2021.661532

Mishra, B., and Jha, R. (2019). Oxidative stress in the poultry gut: Potential challenges and interventions. *Front. Vet. Sci.* 6, 60. doi:10.3389/fvets.2019.00060

Morozzi, G., Beccafico, S., Bianchi, R., Riuzzi, F., Bellezza, I., Giambanco, I., et al. (2017). Oxidative stress-induced S100B accumulation converts myoblasts into Brown adipocytes via an NF-κB/YY1/miR-133 axis and NF-κB/YY1/BMP-7 axis. *Cell Death Differ.* 24 (12), 2077–2088. doi:10.1038/cdd.2017.132

Nashchekina, Y., Nikonov, P., Mikhailova, N., and Nashchekin, A. (2021). Collagen scaffolds treated by hydrogen peroxide for cell cultivation. *Polym. (Basel)* 13 (23), 4134. doi:10.3390/polym13234134

Nouri, F., Nematollahi-Mahani, S. N., and Shari fi, A. M. (2019). Preconditioning of mesenchymal stem cells with non-toxic concentration of hydrogen peroxide against oxidative stress induced cell death: The role of hypoxia-inducible factor-1. *Adv. Pharm. Bull.* 9 (1), 76–83. doi:10.15171/apb.2019.010

Ojano-Dirain, C., Tinsley, N. B., Wing, T., Cooper, M., and Bottje, W. G. (2007). Membrane potential and H2O2 production in duodenal mitochondria from broiler chickens (Gallus gallus domesticus) with low and high feed efficiency. *Comp. Biochem. Physiol. A Mol. Integr. Physiol.* 147 (4), 934–941. doi:10.1016/j.cbpa.2007.02.029

Osorio, C., Fletcher, O. J., Abdul-Aziz, T., Gonder, E., Tilley, B., and Ley, D. H. (2007). Pneumonia of Turkey breeder hens associated with mycoplasma synoviae. *Avian Dis.* 51 (3), 791–796. doi:10.1637/0005-2086(2007)51[791:POTBHA]2.0.CO;2

Pendergrass, K. D., Boopathy, A. V., Seshadri, G., Maiellaro-Rafferty, K., Che, P. L., Brown, M. E., et al. (2013). Acute preconditioning of cardiac progenitor cells with hydrogen peroxide enhances angiogenic pathways following ischemia-reperfusion injury. *Stem Cells Dev.* 22 (17), 2414–2424. doi:10.1089/scd.2012.0673

Porto, M. L., Rodrigues, B. P., Menezes, T. N., Ceschim, S. L., Casarini, D. E., Gava, A. L., et al. (2015). Reactive oxygen species contribute to dysfunction of bone marrow hematopoietic stem cells in aged C57BL/6 J mice. *J. Biomed. Sci.* 22, 97. doi:10.1186/s12929-015-0201-8

Ramp, W. K., Arnold, R. R., Russell, J. E., and Yancey, J. M. (1987). Hydrogen peroxide inhibits glucose metabolism and collagen synthesis in bone. *J. Periodontol.* 58 (5), 340–344. doi:10.1902/jop.1987.58.5.340

Reis, J., and Ramos, A. (2021). In sickness and in health: The oxygen reactive species and the bone. *Front. Bioeng. Biotechnol.* 9, 745911. doi:10.3389/fbioe.2021.745911

Robert, A. W., Marcon, B. H., Dallagiovanna, B., and Shigunov, P. (2020). Adipogenesis, osteogenesis, and chondrogenesis of human mesenchymal stem/stromal cells: A comparative transcriptome approach. *Front. Cell Dev. Biol.* 8, 561. doi:10.3389/fcell.2020.00561

Sanchez-de-Diego, C., Valer, J. A., Pimenta-Lopes, C., Rosa, J. L., and Ventura, F. (2019). Interplay between BMPs and reactive oxygen species in cell signaling and pathology. *Biomolecules* 9 (10), 534. doi:10.3390/biom9100534

Saretzki, G., Armstrong, L., Leake, A., Lako, M., and von Zglinicki, T. (2004). Stress defense in murine embryonic stem cells is superior to that of various differentiated murine cells. *Stem Cells* 22 (6), 962–971. doi:10.1634/stemcells.22-6-962

Sen, S., Domingues, C. C., Rouphael, C., Chou, C., Kim, C., and Yadava, N. (2015). Genetic modification of human mesenchymal stem cells helps to reduce adiposity and improve glucose tolerance in an obese diabetic mouse model. *Stem Cell Res. Ther.* 6, 242. doi:10.1186/s13287-015-0224-9

Serdar, C. C., Cihan, M., Yucel, D., and Serdar, M. A. (2021). Sample size, power and effect size revisited: Simplified and practical approaches in pre-clinical, clinical and laboratory studies. *Biochem. Med. Zagreb.* 31 (1), 010502. doi:10.11613/BM.2021.010502

Serguienko, A., Wang, M. Y., and Myklebost, O. (2018). Real-time vital mineralization detection and quantification during *in vitro* osteoblast differentiation. *Biol. Proced. Online* 20, 14. doi:10.1186/s12575-018-0079-4

Shadel, G. S., and Horvath, T. L. (2015). Mitochondrial ROS signaling in organismal homeostasis. *Cell* 163 (3), 560–569. doi:10.1016/j.cell.2015.10.001

Sharma, P., Jha, A. B., Dubey, R. S., and Pessarakli, M. (2012). Reactive oxygen species, oxidative damage, and antioxidative defense mechanism in plants under stressful conditions. *J. Bot.* 2012, 1–26. doi:10.1155/2012/217037

Sharma, T., Islam, N., Ahmad, J., Akhtar, N., and Beg, M. (2015). Correlation between bone mineral density and oxidative stress in postmenopausal women. *Indian J. Endocrinol. Metab.* 19 (4), 491–497. doi:10.4103/2230-8210.159053

Sheppard, A. J., Barfield, A. M., Barton, S., and Dong, Y. (2022). Understanding reactive oxygen species in bone regeneration: A glance at potential therapeutics and bioengineering applications. *Front. Bioeng. Biotechnol.* 10, 836764. doi:10.3389/fbioe.2022.836764

Shimizu, T. (2016). Inflammation-inducing factors of mycoplasma pneumoniae. *Front. Microbiol.* 7, 414. doi:10.3389/fmicb.2016.00414

Sies, H., Berndt, C., and Jones, D. P. (2017). Oxidative stress. *Annu. Rev. Biochem.* 86, 715–748. doi:10.1146/annurev-biochem-061516-045037

Siwik, D. A., Pagano, P. J., and Colucci, W. S. (2001). Oxidative stress regulates collagen synthesis and matrix metalloproteinase activity in cardiac fibroblasts. *Am. J. Physiol. Cell Physiol.* 280 (1), C53–C60. doi:10.1152/ajpcell.2001.280.1.C53

Strecker, V., Mai, S., Muster, B., Beneke, S., Burkle, A., Bereiter-Hahn, J., et al. (2010). Aging of different avian cultured cells: Lack of ROS-induced damage and quality control mechanisms. *Mech. Ageing Dev.* 131 (1), 48–59. doi:10.1016/j.mad.2009.11.005

Sun, Y. X., Xu, A. H., Yang, Y., and Li, J. (2015). Role of Nrf2 in bone metabolism. *J. Biomed. Sci.* 22, 101. doi:10.1186/s12929-015-0212-5

Surai, P. F., KochishII, Fisinin, V. I., and Kidd, M. T. (2019). Antioxidant defence systems and oxidative stress in poultry biology: An update. *Antioxidants (Basel)* 8 (7), 235. doi:10.3390/antiox8070235

Svoradova, A., Zmrhal, V., Venusova, E., and Slama, P. (2021). Chicken mesenchymal stem cells and their applications: A mini review. *Anim. (Basel)* 11 (7), 1883. doi:10.3390/ani11071883

Takada, I., Suzawa, M., Matsumoto, K., and Kato, S. (2007). Suppression of PPAR transactivation switches cell fate of bone marrow stem cells from adipocytes into osteoblasts. *Ann. N. Y. Acad. Sci.* 1116, 182–195. doi:10.1196/annals.1402.034

Valle-Prieto, A., and Conget, P. A. (2010). Human mesenchymal stem cells efficiently manage oxidative stress. *Stem Cells Dev.* 19 (12), 1885–1893. doi:10.1089/scd.2010.0093

Wan, C., Xiang, J., Li, Y., and Guo, D. (2016). Differential gene expression patterns in chicken cardiomyocytes during hydrogen peroxide-induced apoptosis. *PLoS One* 11 (1), e0147950. doi:10.1371/journal.pone.0147950

Wan, H., Yuan, W., Ruan, M., Ye, Q., Wang, R., Li, Z., et al. (2011). Identification of reference genes for reverse transcription quantitative real-time PCR normalization in pepper (Capsicum annuum L.). *Biochem. Biophys. Res. Commun.* 416 (1-2), 24–30. doi:10.1016/j.bbrc.2011.10.105

Wang, T., Zhang, X., and Bikle, D. D. (2017). Osteogenic differentiation of periosteal cells during fracture healing. *J. Cell Physiol.* 232 (5), 913–921. doi:10.1002/jcp.25641

Wideman, R. F., Jr. (2016). Bacterial chondronecrosis with osteomyelitis and lameness in broilers: A review. *Poult. Sci.* 95 (2), 325–344. doi:10.3382/ps/pev320

Xia, C., and Møller, A. P. (2018). Long-lived birds suffer less from oxidative stress. *Avian Res.* 9 (1), 41. doi:10.1186/s40657-018-0133-6

Xu, J., Strasburg, G. M., Reed, K. M., and Velleman, S. G. (2022). Thermal stress and selection for growth affect myogenic satellite cell lipid accumulation and adipogenic gene expression through mechanistic target of rapamycin pathway. *J. Anim. Sci.* 100 (8), skac001. doi:10.1093/jas/skac001

Yuan, Z., Zhang, J., Huang, Y., Zhang, Y., Liu, W., Wang, G., et al. (2017). NRF2 overexpression in mesenchymal stem cells induces stem-cell marker expression and enhances osteoblastic differentiation. *Biochem. Biophys. Res. Commun.* 491 (1), 228–235. doi:10.1016/j.bbrc.2017.07.083

Zhang, H., Mehmood, K., Jiang, X., Li, Z., Yao, W., Zhang, J., et al. (2019). Identification of differentially expressed MiRNAs profile in a thiram-induced tibial dyschondroplasia. *Ecotoxicol. Environ. Saf.* 175, 83–89. doi:10.1016/j.ecoenv.2019.03.043

Zhang, H., Mehmood, K., Li, K., Rehman, M. U., Jiang, X., Huang, S., et al. (2018). Icariin ameliorate thiram-induced tibial dyschondroplasia via regulation of WNT4 and VEGF expression in broiler chickens. *Front. Pharmacol.* 9, 123. doi:10.3389/fphar.2018.00123

Zhang, H., Wang, Y., Mehmood, K., Chang, Y. F., Tang, Z., and Li, Y. (2020). Treatment of tibial dyschondroplasia with traditional Chinese medicines: "Lesson and future directions. *Poult. Sci.* 99 (12), 6422–6433. doi:10.1016/j.psj.2020.08.055

Zomorodian, E., and Baghaban Eslaminejad, M. (2012). Mesenchymal stem cells as a potent cell source for bone regeneration. *Stem Cells Int.* 2012, 980353. doi:10.1155/2012/980353

Zorov, D. B., Juhaszova, M., and Sollott, S. J. (2014). Mitochondrial reactive oxygen species (ROS) and ROS-induced ROS release. *Physiol. Rev.* 94 (3), 909–950. doi:10.1152/physrev.00026.2013

frontiers | Frontiers in Physiology

TYPE Mini Review
PUBLISHED 07 February 2023
DOI 10.3389/fphys.2023.1112499

OPEN ACCESS

EDITED BY
Anthony Pokoo-Aikins,
Agricultural Research Service (USDA), United States

REVIEWED BY
Wu Shugeng,
Feed Research Institute, Chinese Academy of Agricultural Sciences, China
Michel Duclos,
UMR BOA INRAE University of Tours, France
Catarina Stefanello,
Federal University of Santa Maria, Brazil
Matthew F. Warren,
University of Wisconsin-Madison, United States
Yves Nys,
INRAE centre de Tours, France

*CORRESPONDENCE
Laura E. Ellestad,
lellestad@uga.edu

SPECIALTY SECTION
This article was submitted to Avian Physiology, a section of the journal Frontiers in Physiology

RECEIVED 30 November 2022
ACCEPTED 27 January 2023
PUBLISHED 07 February 2023

CITATION
Sinclair-Black M, Garcia RA and Ellestad LE (2023), Physiological regulation of calcium and phosphorus utilization in laying hens. *Front. Physiol.* 14:1112499. doi: 10.3389/fphys.2023.1112499

Physiological regulation of calcium and phosphorus utilization in laying hens

Micaela Sinclair-Black, R. Alejandra Garcia and Laura E. Ellestad*

Department of Poultry Science, University of Georgia, Athens, GA, United States

Commercial laying hens can produce one egg approximately every 24 h. During this process, regulatory systems that control vitamin D_3 metabolism, calcium and phosphorus homeostasis, and intestinal uptake of these minerals work in concert to deliver components required for eggshell calcification and bone mineralization. Commercial production cycles have been extended in recent years to last through 100 weeks of age, and older hens often exhibit an increased prevalence of skeletal fractures and poor eggshell quality. Issues such as these arise, in part, through imbalances that occur in calcium and phosphorus utilization as hens age. As a result, an in-depth understanding of the mechanisms that drive calcium and phosphorus uptake and utilization is required to develop solutions to these welfare and economic challenges. This paper reviews factors that influence calcium and phosphorus homeostasis in laying hens, including eggshell formation and development and roles of cortical and medullary bone. Metabolism and actions of vitamin D_3 and physiological regulation of calcium and phosphorus homeostasis in key tissues are also discussed. Areas that require further research in avian species, such as the role of fibroblast growth factor 23 in these processes and the metabolism and action of bioactive vitamin D_3, are highlighted and the importance of using emerging technologies and establishing *in vitro* systems to perform functional and mechanistic studies is emphasized.

KEYWORDS

laying hen, calcium, phosphorus, vitamin D_3, skeletal health, egg formation

1 Introduction

As the global population grows, there is increased demand for affordable, high-quality, and sustainable protein sources like table eggs. Commercial laying hens have been selected to increase eggs produced per hen lifetime, with production cycles now lasting past 100 weeks of age. Economic and sustainability benefits of extended lay persistency include decreased cost and environmental impact on a per-egg basis (Bain et al., 2016), but there are challenges associated with egg quality and bird welfare as hens age.

Older hens often produce larger, weak-shelled eggs (Al-Batshan et al., 1994) and exhibit compromised skeletal structure. Efficiency of intestinal calcium absorption decreases with age (Diana et al., 2021), leading to increased reliance on bone-derived calcium contributing to fractures (Gregory and Wilkins, 1989). Elucidating physiological mechanisms responsible for the uptake and utilization of calcium and phosphorus throughout the hen's productive lifecycle will provide insights that can be used to develop strategies limiting economic losses to producers and improving animal welfare.

2 Egg formation

Commercial laying hens produce an egg approximately every 24 h (Nys and Guyot, 2011) and must efficiently regulate calcium and phosphorus utilization for eggshell calcification and cuticle formation, respectively (Cusack et al., 2003). Ovulation occurs 15–75 min after oviposition, or egg-laying (Sturkie and Mueller, 1976), and the follicle resides in the infundibulum for under 30 min (Sah and Mishra, 2018). It continues into the magnum where albumen is added over the next 3.25–3.5 h (Nys and Guyot, 2011) and enters the isthmus where inner and outer shell membranes are deposited around the albumen (Warren and Scott, 1935). Organic eggshell matrix proteins (e.g. ovalbumins, osteopontins, ovocleidins, ovocalyxins) and calcium carbonate are deposited onto the outer shell membrane (Hincke et al., 2010) in the shell gland, and the eggshell forms over the final 19–20 h (Nys and Guyot, 2011; Gautron et al., 2021).

As previously described (Nys and Guyot, 2011; Gautron et al., 2021), the eggshell develops as distinct mamillary, palisade, and cuticle layers deposited from interior to exterior. During mineralization of the mammillary and palisade layers, deposition of amorphous calcium carbonate is followed by its transformation into calcite crystals (Rodriguez-Navarro et al., 2015). Initially, the mamillary layer forms at nucleation sites laid on the outer shell membrane between 5–6 h post-oviposition (HPOP) and the mamillary core develops between 7–10 HPOP. Large calcite crystal units form the columnar palisade layer between 10–22 HPOP, and the cuticle forms an organic film preventing bacterial penetration of the egg about 2 h before oviposition. A calcium and phosphorus-rich hydroxyapatite [$Ca_{10}(PO_4)_6(OH)_2$] crystal layer lies just internal to the cuticle (Wedral et al., 1974; Cusack et al., 2003). Since phosphorus is a potent inhibitor of calcite formation (Bachra et al., 1963; Simkiss, 1964), some authors speculate that these crystals (Dennis et al., 1996) or the secretion of phosphate-containing organic eggshell constituents towards the end of shell formation (Nys et al., 1991) may be involved in terminating calcification.

3 Bone development and remodeling

Since most eggshell calcification takes place in the dark when dietary calcium is largely unavailable, hens mobilize approximately 20%–40% of calcium required for eggshell formation from bone (Comar and Driggers, 1949). Structural cortical and trabecular bone with highly organized hydroxyapatite crystals is formed during embryonic and juvenile development. After structural bone deposition subsides (Hudson et al., 1993), increased circulating estrogen at the onset of sexual maturity around 18 weeks of age leads to development of medullary bone in pneumatic and long bones (Whitehead, 2004). Medullary bone is highly vascularized with randomly orientated hydroxyapatite crystals (Dacke et al., 1993), allowing for rapid anabolism and catabolism of hydroxyapatite during egg formation. Since hydroxyapatite is composed of calcium and phosphorus, bone resorption releases both minerals into circulation as ionized calcium (iCa^{2+}) and inorganic phosphate [PO_4^{3-} (P_i)] that must be utilized for shell formation or excreted.

Medullary bone undergoes remineralization when eggshell calcification is not occurring (Wilson and Duff, 1990; Kerschnitzki et al., 2014) and is resorbed during eggshell calcification (Van de Velde et al., 1984b) through increased osteoclast activity driven by parathyroid hormone (PTH) and the bioactive form of vitamin D_3, 1,25-dihydroxycholecalciferol [$1,25(OH)_2D_3$] (Taylor and Belanger, 1969). When PTH binds PTH receptor 1 (PTH1R) on osteocytes (Silve et al., 1982; Zhao et al., 2002), receptor activator of nuclear factor-kappa B ligand (RANKL) is secreted and interacts with receptor activator of nuclear factor-kappa B (RANK) on osteoclasts, stimulating bone resorption. Additionally, PTH increases osteoclast vacuolar-type adenosine triphosphatase (V-ATPase) activity, causing intracellular acidification required for bone breakdown (Liu et al., 2016). Osteoclast activity increases nine-fold during shell calcification (Van de Velde et al., 1984b), and osteoporosis can develop when osteoclasts resorb structural bone once medullary bone is depleted. Dysregulation of medullary bone remodeling may contribute to development of osteoporosis in aged hens, which exhibit increased medullary bone expression of the resorption marker carbonic anhydrase 2 (*CA2*) and vitamin D_3 receptor (*VDR*), as well as reduced expression of accretion proteins like collagen type 1 alpha 1 (*COL1A1*), relative to younger hens (Gloux et al., 2020b).

4 Vitamin D_3 metabolism and mechanism of action

Skeletal integrity and eggshell quality depend on $1,25(OH)_2D_3$ because of its role in regulating calcium and phosphorus homeostasis. Dietary vitamin D_3 is constitutively hydroxylated in the liver by a 25-hydroxylase enzyme encoded by the *CYP2R1* gene (Watanabe et al., 2013), with >90% converted into $25(OH)D_3$ (Heaney et al., 2008; San Martin Diaz, 2018). A second, more tightly regulated hydroxylation occurs in the kidney at the 1α-carbon to form $1,25(OH)_2D_3$ (Jones et al., 1998). In mammals and fish, this is carried out by an enzyme encoded by *CYP27B1* (Monkawa et al., 1997; Shinki et al., 1997; Chun et al., 2014); however, this gene has not been identified in chickens and the enzyme responsible is currently unknown despite recent publications that have reported measuring expression of *CYP27B1* mRNA or an equivalent (Shanmugasundaram and Selvaraj, 2012; Gloux et al., 2020a; Gloux et al., 2020b; Yan et al., 2022). Investigation into transcripts amplified reveals these are an enzyme involved in retinoic acid metabolism (*CYP27C1*) or one identified as vitamin D_3 hydroxylase-associated protein (Ettinger et al., 1994; Ettinger and DeLuca, 1995), neither of which have demonstrable 1α-hydroxylase activity. PTH stimulates 1α-hydroxylation of vitamin D_3 when circulating iCa^{2+} and $1,25(OH)_2D_3$ are low; however, the efficiency of this may decrease with age (Abe et al., 1982; Gloux et al., 2020b). During periods of elevated circulating $1,25(OH)_2D_3$, 1α-hydroxylase is inhibited and 24-hydroxylase, encoded for by *CYP24A1*, is upregulated. The 24-hydroxylase enzyme inactivates $25(OH)D_3$ by producing biologically inert $24,25(OH)_2D_3$ or $1,24,25(OH)_3D_3$ (Holick et al., 1973; Omdahl et al., 2002), thereby preventing excessive bone resorption and intestinal calcium absorption. Hydroxylation of $25(OH)D_3$ into either active or inactive metabolites provides an additional level of control by fine-tuning the availability of this hormone.

Vitamin D_3 affects calcium and phosphorus homeostasis through its influence on expression and activity of transport and chaperone molecules for these minerals. When bound by $1,25(OH)_2D_3$, VDR acts as a ligand-activated transcription factor that enters the nucleus to form a heterodimeric complex with retinoid-X-receptor alpha

(RXRA) or gamma (RXRG) and binds vitamin D_3 response elements (VDRE) in regulatory regions of vitamin D_3-responsive genes (Bikle, 2014). Not all tissues respond to $1,25(OH)_2D_3$ in the same way. For example, shell gland calbindin D-28k (*CALB1*) expression does not appear to be influenced by $1,25(OH)_2D_3$ (Bar et al., 1977), unlike that in the kidney and small intestine (Taylor and Wasserman, 1972). It may be under the control of estrogen (Nys et al., 1992; Corradino et al., 1993), driven by half-palindromic estrogen response elements in the *CALB1* promoter as has been shown in mice (Gill and Christakos, 1995), and intracellular calcium levels (Corradino, 1993). Since CALB1 in shell gland, intestine, and kidney share the same electrophoretic mobility, amino acid composition, and immunoreactivity, it is likely the same protein (Fullmer et al., 1976); however, estrogen receptor rather than VDR could be a key regulatory protein driving its expression in the shell gland.

5 Calcium homeostasis and transport

Regulation of calcium homeostasis is required to maintain the daily flux of this mineral in laying hens. The highest demand occurs when the eggshell is actively calcifying during the nocturnal fast, and hens must rely on reduced intestinal pH to solubilize coarse limestone retained in the gizzard (Scanes et al., 1987). This occurs through stimulation of H^+/K^+-ATPase activity in the proventriculus (Guinotte et al., 1995) and subsequent secretion of hydrochloric acid (Guinotte et al., 1993).

During eggshell calcification, decreased circulating iCa^{2+} due to high demand by the shell gland (Parsons and Combs, 1980) is detected by calcium-sensing receptor (CASR) (Hofer and Brown, 2003) and leads to PTH secretion from the parathyroid gland (Van de Velde et al., 1984a; Singh et al., 1986). PTH rectifies circulating iCa^{2+} back to its homeostatic range by stimulating bone resorption (Taylor and Belanger, 1969) and increasing $1,25(OH)D_3$ production in the kidney (Brenza and DeLuca, 2000); $1,25(OH)D_3$ works to increase calcium absorption from the small intestine (Spencer et al., 1978; Chandra et al., 1990) and reabsorption in the kidney (Jande et al., 1981).

Calcitonin (CALC), produced within ultimobranchial bodies near the thyroid gland (Copp et al., 1967; Kraintz and Intscher, 1969), may reduce iCa^{2+} in chickens (Luck et al., 1979), and expression of CALC receptor (*CALCR*) in shell gland, kidney, and bone of laying hens (Yasuoka et al., 1998; Ieda et al., 2001) suggests it could play a role in regulating calcium homeostasis. However, unlike in mammals, CALC does not influence avian osteoclast activity under normal physiological conditions (Nicholson et al., 1987; Eliam et al., 1988), nor does it appear to affect renal cyclic adenosine monophosphate formation in chickens or pigeons (Dousa, 1974). This implies that avian CALCR could use alternative intracellular signaling pathways or that CALC does not have the same effect on bone as it does in mammals. At present, there is limited evidence that CALC strongly influences calcium homeostasis in birds, suggesting it may not be an important regulator of calcium availability for egg production.

Calcium absorption from the small intestine appears to fluctuate throughout the daily egg formation cycle (Hurwitz and Bar, 1969; Hurwitz et al., 1973) and is thought to occur primarily in the duodenum and jejunum, with smaller amounts absorbed in the ileum (Hurwitz and Bar, 1965; Hurwitz and Bar, 1968). Intestinal calcium uptake occurs through active transcellular and passive paracellular pathways. Active transcellular absorption accounts for most calcium uptake and involves ATPase plasma membrane calcium transporting 1 (ATP2B1), 2 (ATP2B2), and 4 (ATP2B4), sodium-calcium exchanger 1 (NCX1), transient receptor potential cation channel subfamilies C member 1 (TRPC1), M member 7 (TRPM7), and V member 2 (TRPV2), and CALB1 (Bar, 2009; Gloux et al., 2019). Passive paracellular calcium absorption likely takes place *via* tight junction proteins 1 (TJP1), 2 (TJP2), and 3 (TJP3), claudin 2 (CLDN2) and 12 (CLDN12), and occludin (OCLN) (Gloux et al., 2019; Gloux et al., 2020b). Findings suggest that intestinal capacity for calcium absorption could change with age, as expression of some transcellular (*ATP2B4*, *TRPV2*) and paracellular (*TJP3*, *CLDN2*, *OCLN*) transporters decreased in older hens (Gloux et al., 2020b). Calcium transport in the shell gland (Brionne et al., 2014) and kidney occurs through many of these same proteins, with the addition of transient receptor potential cation channel subfamily V member 6 (TRPV6) in the kidney (Proszkowiec-Weglarz and Angel, 2013; Gautron et al., 2021; Wang et al., 2022). This has been shown to decrease with age in hens (Gloux et al., 2020b), indicating that the calcium-handling capacity of the kidney is perturbed in older layers. In addition to the above-listed transporters, recent findings suggest vesicular transport systems may export calcium into the shell gland lumen (Stapane et al., 2020).

6 Phosphorus homeostasis and transport

Approximately 80% of phosphorus is stored in the skeleton as hydroxyapatite. It is released when bone is resorbed during eggshell calcification, and this excess P_i (Nys et al., 1986; Frost and Roland, 1990) must be excreted to negate toxic effects. Maintenance of circulating P_i occurs in the kidney, small intestine, and bone (Michigami et al., 2018) and is primarily regulated by fibroblast growth factor 23 (FGF23); however, PTH and $1,25(OH)_2D_3$ also influence it through their actions on calcium homeostasis (Ren et al., 2020).

In mice (Perwad et al., 2005) and laying hens (Ren et al., 2017; Wang et al., 2018; Gloux et al., 2020a; Ren et al., 2020), hyperphosphatemia increases FGF23 production in bone. It has been shown to bind to one of four FGF receptors (FGFR1-4) along with the co-receptor klotho (KL) in mammals (Razzaque, 2009), and this complex induces expression of P_i transport proteins that mediate FGF23's phosphaturic effects. Laying hens express *FGF23* mRNA in both medullary and structural bone (Hadley et al., 2016; Wang et al., 2018), and increases in its expression occur as they age (Gloux et al., 2020b). Furthermore, hens exhibit *FGFR1-4* and *KL* mRNA expression in the kidney, intestine, and bones (Ren et al., 2020). Immunoneutralization of FGF23 in laying hens led to increased plasma P_i and bone ash under phosphorus-deficient conditions (Bobeck et al., 2012; Ren et al., 2017), and limiting dietary P_i in laying hens reduced circulating P_i, suppressed bone *FGF23* mRNA, circulating FGF23, and renal sodium-dependent P_i transporter IIa (*NaP_iIIa*) expression, and induced duodenal sodium-dependent P_i transporter IIb (*NaP_iIIb*) expression (Ren et al., 2020). These changes corresponded with reduced phosphorus excretion and increased calcium excretion. Studies conducted in mammals have found that FGF23 directly inhibited PTH secretion (Ben-Dov et al., 2007), decreased renal P_i transporter 2 (*P_iT-2*) expression (Tomoe et al., 2009), and limited $1,25(OH)_2D_3$ production in the kidney, in part

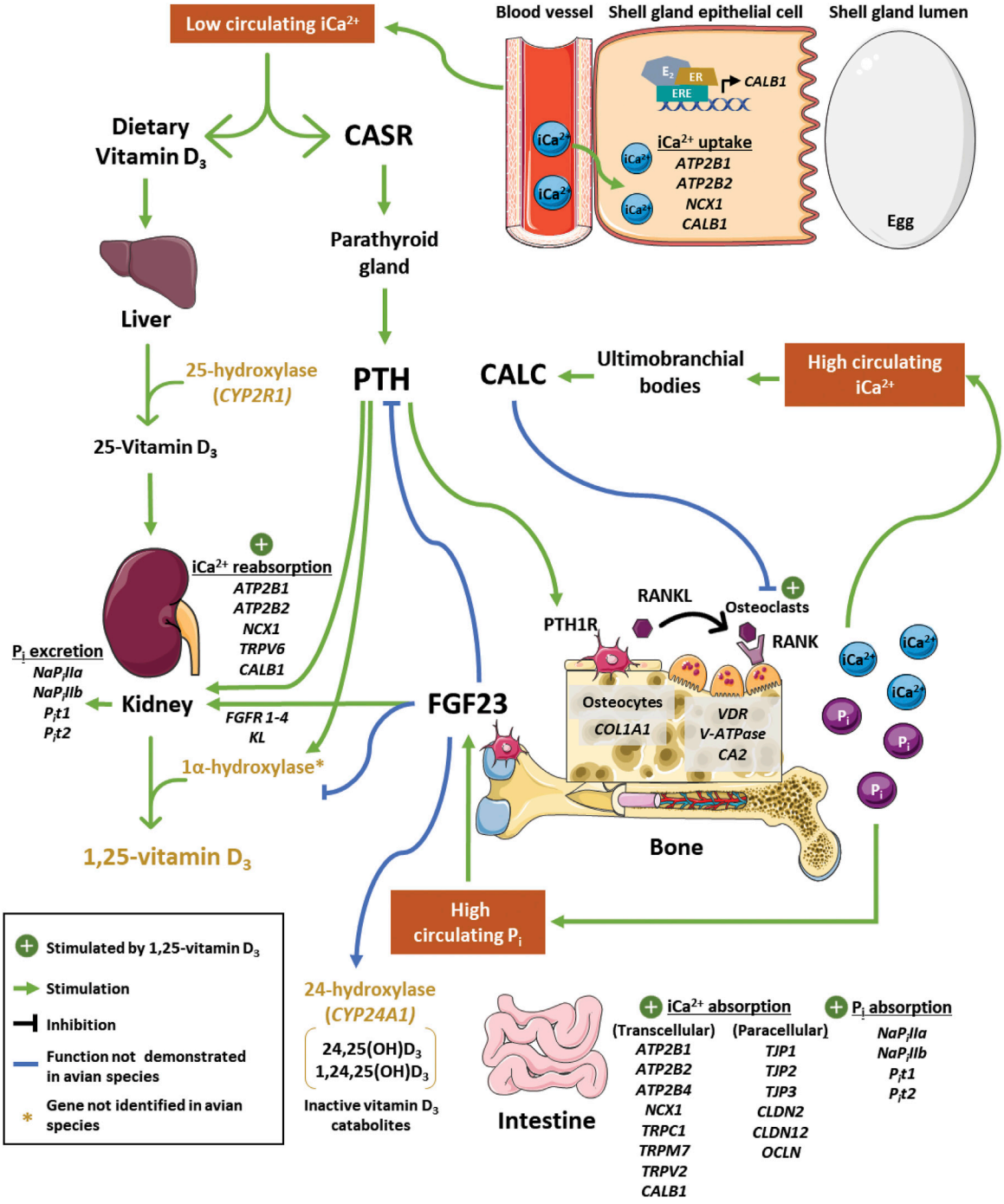

FIGURE 1
Regulation of calcium and phosphorus homeostasis during eggshell mineralization in laying hens. During eggshell calcification, high demand for calcium decreases circulating ionized calcium (iCa^{2+}). Low iCa^{2+} is detected by calcium-sensing receptor (CASR), which stimulates parathyroid hormone (PTH) secretion from the parathyroid gland. Secreted PTH binds to PTH receptor 1 (PTH1R) on osteocytes to promote interaction between receptor activator of nuclear factor-kappa B (RANK) and RANK ligand (RANKL) on the osteoclast surface. This induces vacuolar-type adenosine triphosphatase (V-ATPase) production to facilitate bone resorption alongside carbonic anhydrase 2 (CA2). In contrast, bone accretion is facilitated by deposition of matrix proteins such as collagen type 1 alpha 1 (COL1A1). In the kidney, PTH stimulates inorganic phosphate (P_i) excretion and upregulates production of $1,25(OH)_2D_3$. Bioactive $1,25(OH)_2D_3$, which binds to vitamin D_3 receptor (VDR), stimulates osteoclast activity, calcium transport in the kidney, and calcium and phosphorus uptake in the intestine. Impacts of $1,25(OH)_2D_3$ in the shell gland and on paracellular intestinal calcium uptake still need to be elucidated. Transcellular transport of calcium in these tissues is thought to occur through ATPase plasma membrane calcium transporting 1, 2, and 4 (ATP2B1, ATB2B2, ATP2B4; intestine only), sodium-calcium exchanger 1 (NCX1), calbindin-28K (CALB1), transient receptor potential cation channels subfamily C member 1 (TRPC1; intestine only), transient receptor potential cation channels subfamily M member 7 (TRPM7; intestine only), and transient receptor potential cation channel subfamily V member two and six (TRPV2, intestine only; TRPV6, kidney only). Paracellular transport in the intestine is achieved by tight junction proteins 1, 2, and 3 (TJP1, TJP2, TJP3), claudin 2 and 12 (CLDN2, CLDN12) and occludin (OCLN). Transport of phosphorus in these tissues is thought to occur by sodium-dependent phosphorus transporters IIa and IIb (NaPiIIa and NaPiIIb) and sodium-dependent inorganic phosphorus transporters 1 and 2 (PiT1 and PiT2). Shell gland calcium transport by CALB1 may be under the control of estradiol (E_2) through estrogen receptor (ER) interaction with estrogen-response elements (EREs) in its promoter region. Bone breakdown releases P_i into circulation, which induces production of fibroblast growth factor 23 (FGF23). In chickens and mammals,
(*Continued*)

FIGURE 1 (Continued)
this peptide stimulates renal phosphorus excretion, which has been shown to be mediated through its binding to FGF23 receptors (FGFR1, FGFR2, FGFR3, FGFR4) and co-receptor klotho (KL) in mammals. In mice, FGF23 has also been shown to exhibit negative feedback on PTH and 1α-hydroxylase activity, as well as stimulate 24-hydroxylase activity. During periods of elevated iCa^{2+}, calcitonin (CALC) is secreted from cells in ultimobranchial bodies to inhibit osteoclast activity in mammals, but its effects in birds are unclear. Further investigation into several of these processes and how transporters function in a tissue-specific manner is required to determine their role in calcium and phosphorus homeostasis in chickens. Parts of the figure were drawn by using pictures from servier medical art, licensed under a creative commons attribution 3.0 unported license (https://creativecommons.org/licenses/by/3.0/).

through upregulation of 24-hydroxylase (Perwad et al., 2007). In hens, similarities exist whereby elevated medullary *FGF23* mRNA during eggshell calcification was followed by increased renal mRNA for *CYP24A1* after oviposition, which may have led to observed reductions in $1,25(OH)_2D_3$ (Gloux et al., 2020a).

In birds, $1,25(OH)_2D_3$ appears to directly stimulate renal P_i reabsorption in the short-term and inhibit it in the long-term (Liang et al., 1982; Liang et al., 1984). Renal P_i reabsorption was decreased, and therefore P_i excretion increased, by PTH (Wideman and Braun, 1981). The capacity of the kidney to regulate P_i balance could change with age, as expression of *NaP$_i$IIa* and P_i transporter 1 (*P$_i$T-1*) in kidney decreased in older hens (Gloux et al., 2020b). Since PTH stimulates production of $1,25(OH)_2D_3$, it indirectly increases P_i absorption from the intestine (Liao et al., 2017). Intestinal P_i uptake in chickens is thought to be mediated by P_iT-1, P_iT-2, NaP_iIIa, and NaP_iIIb (Yan et al., 2007; Huber et al., 2015; Li et al., 2018), with NaP_iIIb as the primary transporter in the duodenum and jejunum and P_iT-1 as the primary transporter in the ileum (Gloux et al., 2019).

7 Discussion

This review investigates physiological mechanisms influencing calcium and phosphorus utilization in laying hens during egg production (Figure 1). Age-dependent changes in levels of FGF23, $1,25(OH)_2D_3$, and several calcium and phosphorus transporters in the intestine and kidney suggest that the ability of hens to maintain adequate mineral balance for optimal shell strength and bone health is compromised during extended lay. This leads to deterioration of structural bone when the rate of medullary bone resorption required for eggshell calcification exceeds that of remineralization during periods outside eggshell development, predisposing hens to fractures that negatively impact their welfare and reduce egg production in an age-dependent fashion (Rufener et al., 2019). To maintain healthy, high-producing hens throughout extended production, skeletal development should be prioritized during rearing to ensure adequate deposition of structural bone prior to initiation of medullary bone accretion.

Improvements in laying hen skeletal health require an in-depth understanding of regulatory systems driving calcium and phosphorus utilization and how they change with age. Further research on how FGF23 influences PTH secretion, vitamin D_3 metabolism, and other aspects of calcium and phosphorus homeostasis in birds is necessary. Though a role for FGF23 in regulating P_i homeostasis in layers has been supported by the findings described above, functional and mechanistic studies demonstrating its direct involvement are limited. As there are differences in medullary bone expression of *FGF23* mRNA with age (Gloux et al., 2020b), and FGF23 appears to influence phosphorus and calcium balance (Bobeck et al., 2012; Ren et al., 2017; Ren et al., 2020), understanding effects of FGF23 on mineral homeostasis and how to manage changes across the production cycle is crucial for maintaining skeletal health and egg production throughout extended lay.

A second area needing further elucidation is the metabolism and action of vitamin D_3. The gene encoding 1-α hydroxylase has not been identified in avian species, hindering mechanistic studies of its activity. Characterization of *CYP27B1* or a functional equivalent would provide valuable insights into ways that vitamin D_3 metabolism could be harnessed to improve eggshell integrity and skeletal welfare in layers, including using selection strategies for hens that exhibit stronger bones and eggshells. Furthermore, the influence of $1,25(OH)_2D_3$ on shell gland calcium transport has been questioned due to unresponsiveness of typical $1,25(OH)_2D_3$-dependent proteins (Bar et al., 1977; Bar, 2008); additional studies are needed to confirm if this applies to other aspects of shell gland calcium transport. This is especially important, as regulation of ionic calcium transfer into the shell gland lumen is poorly understood (Nys et al., 2022) despite it being a limiting factor in calcium supply to the eggshell (Cohen et al., 1978), so alterations in this process with age likely contribute to decreased shell quality in older hens.

Though a better picture of laying hen calcium, phosphorus, and vitamin D_3 metabolism has emerged in recent years, critical knowledge gaps exist and much of our understanding of these homeostatic mechanisms is derived from mammalian research. However, hens undergo additional biological processes such as development and maintenance of medullary bone and eggshell calcification, so direct inferences from mammals to birds may be flawed. Availability of the chicken genome in conjunction with "omics" approaches should help identify relevant gene networks across tissues that are involved in these processes, allowing development of testable hypotheses that can be used to discern functionality where it is lacking. Establishment of reliable *in vitro* models for bone, kidney, and shell gland and validated assays for functional proteins would greatly facilitate fundamental, mechanistic studies on these systems. This is essential for generating successful nutritional and genetic management strategies that prioritize skeletal welfare throughout the productive lifecycle of the hen.

Author contributions

MS-B drafted the manuscript; RG assisted with drafting the manuscript and prepared Figure 1; LE conceptualized the review, edited the manuscript and Figure 1, and obtained funding. All

authors have read and approved the submitted version of the manuscript.

Funding

Graduate student support for MS-B and RG was provided to LE by H&N International (Cuxhaven, Germany) and Iluma Alliance (Durham, NC, United States).

Acknowledgments

The authors thank Brett Marshall, Lauren Vaccaro, Charles Meeks, Colin Barcelo, and Shailes Bhattrai for initial editing of this review.

Conflict of interest

The authors declare that the research was conducted in the absence of any commercial or financial relationships that could be construed as a potential conflict of interest.

Publisher's note

All claims expressed in this article are solely those of the authors and do not necessarily represent those of their affiliated organizations, or those of the publisher, the editors and the reviewers. Any product that may be evaluated in this article, or claim that may be made by its manufacturer, is not guaranteed or endorsed by the publisher.

References

Abe, E., Horikawa, H., Masumura, T., Sugahara, M., Kubota, M., and Suda, T. (1982). Disorders of cholecalciferol metabolism in old egg-laying hens. *J. Nutr.* 112 (3), 436–446. doi:10.1093/jn/112.3.436

Al-Batshan, H. A., Scheideler, S. E., Black, B. L., Garlich, J. D., and Anderson, K. E. (1994). Duodenal calcium uptake, femur ash, and eggshell quality decline with age and increase following molt. *Poult. Sci.* 73 (10), 1590–1596. doi:10.3382/ps.0731590

Bachra, B. N., Trautz, O. R., and Lawrence Simon, S. (1963). Precipitation of calcium carbonates and phosphates. I. Spontaneous precipitation of calcium carbonates and phosphates under physiological conditions. *Biochem. Bioph.* 103, 124–138. doi:10.1016/0003-9861(63)90018-3

Bain, M. M., Nys, Y., and Dunn, I. C. (2016). Increasing persistency in lay and stabilizing egg quality in longer laying cycles. What are the challenges? *Br. Poul. Sci.* 57 (3), 330–338. doi:10.1080/00071668.2016.1161727

Bar, A. (2008). Calcium homeostasis and vitamin D metabolism and expression in strongly calcifying laying birds. *Comp. Biochem. Physiol.* 151 (4), 477–490. doi:10.1016/j.cbpa.2008.07.006

Bar, A. (2009). Calcium transport in strongly calcifying laying birds: Mechanisms and regulation. *Comp. Biochem. Physiol.* 152 (4), 447–469. doi:10.1016/j.cbpa.2008.11.020

Bar, A., Cohen, A., Eisner, U., Riesenfeld, G., and Hurwitz, S. (1977). Differential response of calcium transport systems in laying hens to exogenous and endogenous changes in vitamin D status. *J. Nutr.* 108 (8), 1322–1328. doi:10.1093/jn/108.8.1322

Ben-Dov, I. Z., Galitzer, H., Lavi-Moshayoff, V., Goetz, R., Kuro-o, M., Mohammadi, M., et al. (2007). The parathyroid is a target organ for FGF23 in rats. *J. Clin. Invest.* 117 (12), 4003–4008. doi:10.1172/Jci32409

Bikle, D. D. (2014). Vitamin D metabolism, mechanism of action and clinical applications. *Chem. Biol.* 21 (3), 319–329. doi:10.1016/j.chembiol.2013.12.016

Bobeck, E. A., Burgess, K. S., Jarmes, T. R., Piccione, M. L., and Cook, M. E. (2012). Maternally-derived antibody to fibroblast growth factor-23 reduced dietary phosphate requirements in growing chicks. *Biochem. Bioph. Res. Co.* 420 (3), 666–670. doi:10.1016/j.bbrc.2012.03.063

Brenza, H. L., and DeLuca, H. F. (2000). Regulation of 25-Hydroxyvitamin D_3 1α-hydroxylase gene expression by parathyroid hormone and 1,25-dihydroxyvitamin D_3. *Biochem. Bioph.* 381 (1), 143–152. doi:10.1006/abbi.2000.1970

Brionne, A., Nys, Y., Hennequet-Antier, C., and Gautron, J. (2014). Hen uterine gene expression profiling during eggshell formation reveals putative proteins involved in the supply of minerals or in the shell mineralization process. *BMC Genomics* 15 (220), 220–317. doi:10.1186/1471-2164-15-220

Chandra, S., Fullmer, C. S., Smith, C. A., Wasserman, R. H., and Morrison, G. H. (1990). Ion microscopic imaging of calcium transport in the intestinal tissue of vitamin D deficient and vitamin D replete chickens: A ^{44}Ca stable isotope study. *P. Natl. Acad. Sci. U. S. A.* 87 (15), 5715–5719. doi:10.1073/pnas.87.15.5715

Chun, R. F., Blatter, E., Elliott, S., Fitz-Gibbon, S., Rieger, S., Sagasti, A., et al. (2014). Cloning of a functional 25-hydroxyvitamin D-1α-hydroxylase in zebrafish (*Danio rerio*). *Cell biochem. Funct.* 32 (8), 675–682. doi:10.1002/cbf.3071

Cohen, A., Bar, A., Eisner, U., and Hurwitz, S. (1978). Calcium absorption, calcium binding protein, and eggshell quality in laying hens fed hydroxylated vitamin D derivatives. *Poult. Sci.* 57 (6), 1646–1651. doi:10.3382/ps.0571646

Comar, C. L., and Driggers, J. C. (1949). Secretion of radioactive calcium in the hen's egg. *Science* 109 (2829), 282. doi:10.1126/science.109.2829.282

Copp, D. H., Cockcroft, D. W., and Kueh, Y. (1967). Calcitonin from ultimobranchial glands of dogfish and chickens. *Science* 158 (3803), 924–925. doi:10.1126/science.158.3803.924

Corradino, R. A. (1993). Calbindin D_{28k} regulation in precociously matured chick egg shell gland *in vitro*. *Gen. Comp. Endocr.* 91 (2), 158–166. doi:10.1006/gcen.1993.1115

Corradino, R. A., Smith, C. A., Krook, L. P., and Fullmer, C. S. (1993). Tissue-specific regulation of shell gland calbindin D28K biosynthesis by estradiol in precociously matured, vitamin D-depleted chicks. *Endocrinology* 132 (1), 193–198. doi:10.1210/endo.132.1.8419123

Cusack, M., Fraser, A. C., and Stachel, T. (2003). Magnesium and phosphorus distribution in the avian eggshell. *Comp. Biochem. Physiol.* 134 (1), 63–69. doi:10.1016/s1096-4959(02)00185-9

Dacke, C. G., Arkle, S., Cook, D. J., Wormstone, I. M., Jones, S., Zaidi, M., et al. (1993). Medullary bone and avian calcium regulation. *J. Exp. Biol.* 184, 63–88. doi:10.1242/jeb.184.1.63

Dennis, J. E., Xiao, S., Agarwal, M., Fink, D., Heuer, A. H., and Caplan, A. (1996). Microstructure of matrix and mineral components of eggshells from White Leghorn chickens (*Gallus gallus*). *J. Morph.* 228 (3), 287–306. doi:10.1002/(SICI)1097-4687(199606)228:3<287::AID-JMOR2>3.0.CO;2-%23

Diana, T. F., Calderano, A. A., Tavernari, F. d. C., Rostagno, H. S., Teixeira, A. d. O., and Albino, L. F. T. (2021). Age and calcium sources in laying hen feed affect calcium digestibility. *J. Anim. Sci.* 11, 501–513. doi:10.4236/ojas.2021.113034

Dousa, T. P. (1974). Effects of hormones on cyclic AMP formation in kidneys of nonmammalian vertebrates. *Am. J. Physiol.* 226 (5), 1193–1197. doi:10.1152/ajplegacy.1974.226.5.1193

Eliam, M. C., Basle, M., Bouizar, Z., Bielakoff, J., Moukhtar, M., and De Vernejoul, M. C. (1988). Influence of blood calcium on calcitonin receptors in isolated chick osteoclasts. *J. Endocrinol.* 199 (2), 243–248. doi:10.1677/joe.0.1190243

Ettinger, R. A., and DeLuca, H. F. (1995). The vitamin D_3 hydroxylase-associated protein is a propionamide-metabolizing amidase enzyme. *Arch. Biochem. Biophys.* 316 (1), 14–19. doi:10.1006/abbi.1995.1003

Ettinger, R. A., Ismail, R., and DeLuca, H. F. (1994). cDNA cloning and characterization of a vitamin D_3 hydroxylase-associated protein. *J. Biol. Chem.* 269 (1), 176–182. doi:10.1016/S0021-9258(17)42331-3

Frost, T. J., and Roland, D. A. (1990). The effects of various dietary phosphorus levels on the circadian patterns of plasma 1,25-dihydroxycholecalciferol, total calcium, ionized calcium and phosphorus in laying hens. *Poult. Sci.* 70, 1564–1570. doi:10.3382/ps.0701564

Fullmer, C. S., Brindak, M. E., Wasserman, R. H., and Bar, A. (1976). The purification of calcium-binding protein from the uterus of the laying hen. *P. Soc. Exp. Biol. Med.* 152 (2), 237–241. doi:10.3181/00379727-152-39369

Gautron, J., Le Roy, N., Nys, Y., Rodriguez-Navarro, A. B., and Hincke, M. T. (2021). Avian eggshell biomineralization: An update on its structure, mineralogy, and protein tool kit. *BMC Mol. Biol.* 22 (11), 11–17. doi:10.1186/s12860-021-00350-0

Gill, R. K., and Christakos, S. (1995). Regulation by estrogen through the 5' flanking region of the mouse calbindin-D28K gene. *Mol. Endocrinol.* 9 (3), 319–326. doi:10.1210/mend.9.3.7776978

Gloux, A., Le Roy, N., Brionne, A., Bonin, E., Juanchich, A., Benzoni, G., et al. (2019). Candidate genes of the transcellular and paracellular calcium absorption pathways in the small intestine of laying hens. *Poult. Sci.* 98 (11), 6005–6018. doi:10.3382/ps/pez407

Gloux, A., Le Roy, N., Ezagal, J., Meme, N., Hennequet-Antier, C., Piketty, M. L., et al. (2020a). Possible roles of parathyroid hormone, $1,25(OH)_2D_3$, and fibroblast growth factor 23 on genes controlling calcium metabolism across different tissues of the laying hen. *Dom. Anim. Endocrinol.* 72 (72), 106407–106412. doi:10.1016/j.domaniend.2019.106407

Gloux, A., Le Roy, N., Meme, N., Piketty, M. L., Prie, D., Benzoni, G., et al. (2020b). Increased expression of fibroblast growth factor 23 is the signature of a deteriorated Ca/P balance in ageing laying hens. *Sci. Rep.* 10 (1), 21124. doi:10.1038/s41598-020-78106-7

Gregory, N. G., and Wilkins, L. J. (1989). Broken bones in domestic fowl: Handling and processing damage in end-of-lay battery hens. *Br. Poul. Sci.* 30 (3), 555–562. doi:10.1080/00071668908417179

Guinotte, F., Gautron, J., Nys, Y., and Soumarmon, A. (1995). Calcium solubilization and retention in the gastrointestinal tract in chicks (*Gallus domesticus*) as a function of gastric acid secretion inhibition and of calcium carbonate particle size. *Brit. J. Nut.* 73 (1), 125–139. doi:10.1079/Bjn19950014

Guinotte, F., Gautron, J., Soumarmon, A., Robert, J. C., Peranzi, G., and Nys, Y. (1993). Gastric acid secretion in the chicken: Effect of histamine H_2 antagonists and H^+/K^+-ATPase inhibitors on gastro-intestinal pH and of sexual maturity calcium carbonate level and particle size on proventricular H^+/K^+-ATPase activity. *Comp. Biochem. Physiol.* 106, 319–327. doi:10.1016/0300-9629(93)90520-E

Hadley, J. A., Horvat-Gordon, M., Kim, W. K., Praul, C. A., Burns, D., and Leach, R. M., Jr (2016). Bone sialoprotein keratan sulfate proteoglycan (BSP-KSPG) and FGF-23 are important physiological components of medullary bone. *Comp. Biochem. Physiol.* 194, 1–7. doi:10.1016/j.cbpa.2015.12.009

Heaney, R. P., Armas, L. A., Shary, J. R., Bell, N. H., Binkley, N., and Hollis, B. W. (2008). 25-Hydroxylation of vitamin D_3: Relation to circulating vitamin D_3 under various input conditions. *Am. J. Clin. Nutr.* 87 (6), 1738–1742. doi:10.1093/ajcn/87.6.1738

Hincke, M. T., Nys, Y., and Gautron, J. (2010). The role of matrix proteins in eggshell formation. *J. Poult. Sci.* 47 (3), 208–219. doi:10.2141/jpsa.009122

Hofer, A. M., and Brown, E. M. (2003). Extracellular calcium sensing and signalling. *Nat. Rev. Mol. Cell Bio.* 4, 530–538. doi:10.1038/nrm1154

Holick, M. F., Kleiner-Bossallier, A., Schnoes, H. K., Kasten, P. M., Boyle, I. T., DeLuca, H. F., et al. (1973). 1,24,25-Trihydroxyvitamin D_3. *J. Biol. Chem.* 248 (19), 6691–6696. doi:10.1016/S0021-9258(19)43408-X

Huber, K., Zeller, E., and Rodehutscord, M. (2015). Modulation of small intestinal phosphate transporter by dietary supplements of mineral phosphorus and phytase in broilers. *Poult. Sci.* 94, 1009–1017. doi:10.3382/ps/pev065

Hudson, H. A., Britton, W. M., Rowland, G. N., and Buhr, R. J. (1993). Histomorphometric bone properties of sexually immature and mature white leghorn hens with evaluation of fluorochrome injection on egg production traits. *Poult. Sci.* 72 (8), 1537–1547. doi:10.3382/ps.0721537

Hurwitz, S., and Bar, A. (1965). Absorption of calcium and phosphorus along the gastrointestinal tract of the laying fowl as influenced by dietary calcium and eggshell formation. *J. Nutr.* 86, 433–438. doi:10.1093/jn/86.4.433

Hurwitz, S., and Bar, A. (1968). Activity, concentration, and lumen-blood electrochemical protential difference of calcium in the intestine of the laying hen. *J. Nutr.* 95, 647–654. doi:10.1093/jn/95.4.647

Hurwitz, S., Bar, A., and Cohen, I. (1973). Regulation of calcium absorption by fowl intestine. *Am. J. Physiol.* 225 (1), 150–154. doi:10.1152/ajplegacy.1973.225.1.150

Hurwitz, S., and Bar, A. (1969). Intestinal calcium absorption in the laying fowl and its importance in calcium homeostasis. *Am. J. Clin. Nutr.* 22 (4), 391–395. doi:10.1093/ajcn/22.4.391

Ieda, T., Takahasi, T., Saito, N., Yasuoka, T., Kawashima, M., Izumi, T., et al. (2001). Changes in calcitonin receptor bonding in the shell gland of laying hens (*Gallus domesticus*) during the oviposition cycle. *Poult. Sci.* 38, 203–212. doi:10.2141/jpsa.38.203

Jande, S. S., Tolnai, S., and Lawson, D. E. M. (1981). Immunohistochemical localization of vitamin D-dependent calcium binding protein in duodenum, kidney, uterus, and cerebellum of chickens. *Histochemistry* 71, 99–116. doi:10.1007/BF00592574

Jones, G., Strungnell, S. A., and DeLuca, H. F. (1998). Current understanding of the molecular actions of vitamin D. *Phys. Rev.* 78 (4), 1193–1231. doi:10.1152/physrev.1998.78.4.1193

Kerschnitzki, M., Zander, T., Zaslansky, P., Fratzl, P., Shahar, R., and Wagermaier, W. (2014). Rapid alterations of avian medullary bone material during the daily egg-laying cycle. *Bone* 69, 109–117. doi:10.1016/j.bone.2014.08.019

Kraintz, L., and Intscher, K. (1969). Effect of calcitonin on the domestic fowl. *Can. J. Physiol. Pharm.* 47 (3), 313–315. doi:10.1139/y69-057

Li, P., Wang, R. M., Jiao, H. C., Wang, X. J., Zhao, J. P., and Lin, H. (2018). Effects of dietary phosphorus level on the expression of calcium and phosphorus transporters in laying hens. *Front. Physiol.* 9, 627–712. doi:10.3389/fphys.2018.00627

Liang, C. T., Balakir, R., Barnes, J., and Sacktor, B. (1984). Responses of chick renal cell to parathyroid hormone: Effect of vitamin D. *Am. J. Physiol.* 246 (5), 401–406. doi:10.1152/ajpcell.1984.246.5.C401

Liang, C. T., Barnes, J., Cheng, L., Balakir, R., and Sacktor, B. (1982). Effects of 1,25-$(OH)_2D_3$ administered *in vivo* on phosphate uptake by isolated chick renal cells. *Am. J. Physiol.* 242 (5), 312–318. doi:10.1152/ajpcell.1982.242.5.C312

Liao, X. D., Suo, H. Q., Lu, L., Hu, Y. X., Zhang, L. Y., and Luo, X. G. (2017). Effects of sodium, 1,25-dihydroxyvitamin D_3 and parathyroid hormone fragment on inorganic P absorption and Type IIb sodium-phosphate cotransporter expression in ligated duodenal loops of broilers. *Poult. Sci.* 96 (7), 2344–2350. doi:10.3382/ps/pex033

Liu, S., Zhu, W., Ma, J., Zhang, H., Li, Z., Zhang, L., et al. (2016). Bovine parathyroid hormone enhances osteoclast bone resorption by modulating V-ATPase through PTH1R. *Int. J. Mol. Med.* 37 (2), 284–292. doi:10.3892/ijmm.2015.2423

Luck, M. R., Sommerville, B. A., and Scanes, C. G. (1979). The effect of egg-shell calcification on the response of plasma calcium activity to parathyroid hormone and calcitonin in the domestic fowl (*Gallus domesticus*). *Comp. Biochem. Physiol.* 65, 151–154. doi:10.1016/0300-9629(80)90397-7

Michigami, T., Kawai, M., Yamazaki, M., and Ozono, K. (2018). Phosphate as a signaling molecule and its sensing mechanism. *Am. J. Physiol.* 98 (4), 2317–2348. doi:10.1152/physrev.00022.2017

Monkawa, T., Yoshida, T., Wakino, S., Shinki, T., Anazawa, H., DeLuca, H. F., et al. (1997). Molecular cloning of cDNA and genomic DNA for human 25-hydroxyvitamin D_3 1α-hydroxylase. *Biochem. Bioph. Res. Co.* 239 (2), 527–533. doi:10.1006/bbrc.1997.7508

Nicholson, G. C., Moseley, J. M., Sexton, P. M., and Martin, T. J. (1987). Chicken osteoclasts do not possess calcitonin receptors. *J. Bone Min. Res.* 2 (1), 53–59. doi:10.1002/jbmr.5650020109

Nys, Y., Baker, K., and Lawson, D. E. M. (1992). Estrogen and a calcium flux dependent factor modulate the calbindin gene expression in the uterus of laying hens. *Gen. Comp. Endocr.* 87 (1), 87–94. doi:10.1016/0016-6480(92)90153-b

Nys, Y., Gautron, J., Rodriguez-Navarro, A. B., and Hincke, M. T. (2022). "Mechanisms and hormonal regulation of shell formation: Supply of ionic and organic precursors, shell mineralization," in *Sturkie's avian Physiology*. Editors C. G. Scanes and S. Dridi 7 ed (Academic Press), 833–879.

Nys, Y., and Guyot, N. (2011). "Egg formation and chemistry," in *Improving the safety and quality of eggs and egg products* (SawstonCambridge: Woodhead Publishing), 83–132.

Nys, Y., N'Guyen, T. M., Williams, J., and Etches, J. R. (1986). Blood levels of ionized calcium, inorganic phosphorus, 1,25-dihydroxycholecalciferol and gonadal hormones in hens laying hard-shelled or shell-less eggs. *J. Endocrinol.* 111 (1), 151–157. doi:10.1677/joe.0.1110151

Nys, Y., Zawadzki, J., Gautron, J., and Mills, A. D. (1991). Whitening of Brown-shelled eggs: Mineral composition of uterine fluid and rate of protoporphyrin deposition. *Poult. Sci.* 70 (5), 1236–1245. doi:10.3382/ps.0701236

Omdahl, J. L., Morris, H. A., and May, B. K. (2002). Hydroxylase enzymes of the vitamin D pathway: Expression, function, and regulation. *Annu. Rev. Nutr.* 22, 139–166. doi:10.1146/annurev.nutr.22.120501.150216

Parsons, A. H., and Combs, G. F., Jr. (1980). Blood ionized calcium cycles in the chicken. *Poult. Sci.* 60, 1520–1524. doi:10.3382/ps.0601520

Perwad, F., Azam, N., Zhang, M. Y. H., Yamashita, T., Tenenhouse, H. S., and Portale, A. A. (2005). Dietary and serum phosphorus regulate fibroblast growth factor 23 expression and 1,25-dihydroxyvitamin D metabolism in mice. *Endocrinology* 146 (12), 5358–5364. doi:10.1210/en.2005-0777

Perwad, F., Zhang, M. Y. H., Tenenhouse, H. S., and Portale, A. A. (2007). Fibroblast growth factor 23 impairs phosphorus and vitamin D metabolism *in vivo* and suppresses 25-hydroxyvitamin D-1alpha-hydroxylase expression *in vitro*. *Am. J. Physiol.* 293 (5), 1577–1583. doi:10.1152/ajprenal.00463.2006

Proszkowiec-Weglarz, M., and Angel, R. (2013). Calcium and phosphorus metabolism in broilers: Effect of homeostatic mechanism on calcium and phosphorus digestibility. *J. Appl. Poult. Res.* 22 (3), 609–627. doi:10.3382/japr.2012-00743

Razzaque, M. S. (2009). The FGF23-klotho axis: Endocrine regulation of phosphate homeostasis. *Nat. Rev. Endocrinol.* 5 (11), 611–619. doi:10.1038/nrendo.2009.196

Ren, Z., Ebrahimi, M., Butz, D. E., Sand, J. M., Zhang, K., and Cook, M. E. (2017). Antibody to fibroblast growth factor 23-peptide reduces excreta phosphorus of laying hens. *Poult. Sci.* 96 (1), 127–134. doi:10.3382/ps/pew189

Ren, Z., Yan, J., Hu, Q., Liu, X., Pan, C., Liu, Y., et al. (2020). Phosphorus restriction changes the expression of fibroblast growth factor 23 and its receptors in laying hens. *Front. Physiol.* 11, 85–12. doi:10.3389/fphys.2020.00085

Rodriguez-Navarro, A. B., Marie, P., Nys, Y., Hincke, M. T., and Gautron, J. (2015). Amorphous calcium carbonate controls avian eggshell mineralization: A new paradigm for understanding rapid eggshell calcification. *J. Struct. Biol.* 190 (3), 291–303. doi:10.1016/j.jsb.2015.04.014

Rufener, C., Baur, S., Stratmann, A., and Toscano, M. J. (2019). Keel bone fractures affect egg laying performance but not egg quality in laying hens housed in a commercial aviary system. *Poult. Sci.* 98 (4), 1589–1600. doi:10.3382/ps/pey544

Sah, N., and Mishra, B. (2018). Regulation of egg formation in the oviduct of laying hen. *World Poult. Sci. J.* 74 (3), 509–522. doi:10.1017/S0043933918000442

San Martin Diaz, V. E. (2018). *Effects of 1α-hydroxycholecalciferol and other vitamin D analogues on liver performance, bone development, meat yield and quality, and mineral digestibility in broilers*. Master of Science. Raleigh, NC: North Carolina State University.

Scanes, C. G., Campbell, R., and Griminger, P. (1987). Control of energy balance during egg production in the laying hen. *J. Nutr.* 117 (3), 605–611. doi:10.1093/jn/117.3.605

Shanmugasundaram, R., and Selvaraj, R. K. (2012). Vitamin D-1α-hydroxylase and vitamin D-24-hydroxylase mRNA studies in chickens. *Poult. Sci.* 91 (8), 1819–1824. doi:10.3382/ps.2011-02129

Shinki, T., Shimada, H., Wakino, S., Anazawa, H., Hayashi, M., Saruta, T., et al. (1997). Cloning and expression of rat 25-hydroxyvitamin D_3-1a-hydroxylase cDNA. *P. Natl. Acad. Sci. U. S. A.* 94, 12920–12925. doi:10.1073/pnas.94.24.12920

Silve, C. M., Hradek, G. T., Jones, A. L., and Arnaud, C. D. (1982). Parathyroid hormone receptor in intact embryonic chicken bone: Characterization and cellular localization. *J. Cell. Biol.* 94 (2), 379–386. doi:10.1083/jcb.94.2.379

Simkiss, K. (1964). Phosphates as crystal poisons of calcification. *Biol. Rev.* 39 (4), 487–505. doi:10.1111/j.1469-185X.1964.tb01166.x

Singh, R., Joyner, C. J., Peddie, M. J., and Geoffrey Taylor, T. (1986). Changes in the concentrations of parathyroid hormone and ionic calcium in the plasma of laying hens during the egg cycle in relation to dietary deficiencies of calcium and vitamin D. *Gen. Comp. Endocr.* 61 (1), 20–28. doi:10.1016/0016-6480(86)90245-5

Spencer, R., Charman, M., Wilson, P. W., and Lawson, E. M. (1978). The relationship between vitamin D stimulated calcium transport and intestinal calcium binding protein in the chicken. *Biochemistry* 170, 93–101. doi:10.1042/bj1700093

Stapane, L., Le Roy, N., Ezagal, J., Rodriguez-Navarro, A. B., Labas, V., Combes-Soia, L., et al. (2020). Avian eggshell formation reveals a new paradigm for vertebrate mineralization via vesicular amorphous calcium carbonate. *J. Biol. Chem.* 295 (47), 15853–15869. doi:10.1074/jbc.RA120.014542

Sturkie, P. D., and Mueller, w. J. (1976). "Reproduction in the female and egg production," in *Avian Physiology*. Editor C. G. Scanes (Berlin, Heidelberg: Springer Springer Advanced Texts in Life Sciences), 302–330.

Taylor, T. G., and Belanger, L. F. (1969). The mechanism of bone resorption in laying hens. *Calc. Tiss. Res.* 4 (2), 162–173. doi:10.1007/BF02279117

Taylor, T. G., and Wasserman, R. H. (1972). Vitamin D-induced calcium-binding protein: Comparative aspects in kidney and intestine. *Am. J. Physiol.* 223, 110–114. doi:10.1152/ajplegacy.1972.223.1.110

Tomoe, Y., Segawa, H., Shiozawa, K., Kaneko, I., Tominaga, R., Hanabusa, E., et al. (2009). Phosphaturic action of fibroblast growth factor 23 in Npt2 null mice. *Am. J. Physiol. Ren. Physiol.* 298 (6), 1341–1350. doi:10.1152/ajprenal.00375.2009

Van de Velde, J. P., Loveridge, N., and Vermieden, J. P. W. (1984a). Parathyroid hormone responses to calcium stress during eggshell calcification. *Endocrinology* 115 (5), 1901–1904. doi:10.1210/endo-115-5-1901

Van de Velde, J. P., Vermieden, J. P. W., Touw, J. J. A., and Veldhuizen, J. P. (1984b). Changes in activity of chicken medullary bone cell populations in relation to the egg laying cycle. *Metab. Bone Dis. Relat.* 5 (4), 191–193. doi:10.1016/0221-8747(84)90029-8

Wang, R. M., Zhao, J. P., Wang, X. J., Jiao, H. C., Wu, J. M., and Lin, H. (2018). Fibroblast growth factor 23 mRNA expression profile in chickens and its response to dietary phosphorus. *Poult. Sci.* 97 (7), 2258–2266. doi:10.3382/ps/pey092

Wang, X. J., Li, P., Zhao, J. P., Jiao, H. C., and Lin, H. (2022). The temporal gene expression profiles of calcium and phosphorus transporters in Hy-Line Brown layers. *Poult. Sci.* 101 (4), 101736–101811. doi:10.1016/j.psj.2022.101736

Warren, D. C., and Scott, H. M. (1935). Physiological factors influencing the rate of egg formation in the domestic hen. *J. Agric. Res.* 51 (6), 565–572.

Watanabe, K. P., Kawai, Y. K., Ikenaka, Y., Kawata, M., Ikushiro, S., Sakaki, T., et al. (2013). Avian cytochrome P450 (CYP) 1-3 family genes: Isoforms, evolutionary relationships, and mRNA expression in chicken liver. *PLoS One* 8 (9), 756899–e75711. doi:10.1371/journal.pone.0075689

Wedral, E. M., Vadehra, D. V., and Baker, R. C. (1974). Chemical composition of the cuticle, and the inner and outer shell membranes from eggs of *gallus gallus*. *Comp. Biochem. Physiol.* 47 (3), 631–640. doi:10.1016/0305-0491(74)90011-x

Whitehead, C. C. (2004). Overview of bone biology in the egg-laying hen. *Poult. Sci.* 83 (2), 193–199. doi:10.1093/ps/83.2.193

Wideman, R. F., Jr., and Braun, E. J. (1981). Stimulation of avian renal phosphate secretion by parathyroid hormone. *Am. J. Physiol.* 241 (3), 263–272. doi:10.1152/ajprenal.1981.241.3.F263

Wilson, S., and Duff, S. R. (1990). Morphology of medullary bone during the egg formation cycle. *Vet. Sci.* 48 (2), 216–220. doi:10.1016/s0034-5288(18)30993-7

Yan, F., Angel, R., and Ashwell, C. M. (2007). Characterization of the chicken small intestine type IIb sodium phosphate cotransporter. *Poult. Sci.* 86, 67–76. doi:10.1093/ps/86.1.67

Yan, J., Pan, C., Liu, Y., Liao, X., Chen, J., Zhu, Y., et al. (2022). Dietary vitamin D_3 deprivation suppresses fibroblast growth factor 23 signals by reducing serum phosphorus levels in laying hens. *Anim. Nutr.* 9, 23–30. doi:10.1016/j.aninu.2021.07.010

Yasuoka, T., Kawashima, M., Takahasi, T., and Tanaka, K. (1998). Calcitonin receptor binding properties in bone and kidney of the chicken during the oviposition cycle. *J. Bone Min. Res.* 13 (9), 1412–1419. doi:10.1359/jbmr.1998.13.9.1412

Zhao, Q., Brauer, P. R., Xiao, L., McGuire, M. H., and Yee, J. A. (2002). Expression of parathyroid hormone-related peptide (PTHrP) and its receptor (PTH1R) during the histogenesis of cartilage and bone in the chicken mandibular process. *J. Anat.* 201 (2), 137–151. doi:10.1046/j.1469-7580.2002.00078.x

frontiers | Frontiers in Physiology

TYPE Original Research
PUBLISHED 24 April 2023
DOI 10.3389/fphys.2023.1056481

OPEN ACCESS

EDITED BY
Colin Guy Scanes,
University of Wisconsin–Milwaukee,
United States

REVIEWED BY
Katarzyna B. Miska,
Agricultural Research Service (USDA),
United States
Kyung-Woo Lee,
Konkuk University, Republic of Korea

*CORRESPONDENCE
Woo Kyun Kim,
wkkim@uga.edu

SPECIALTY SECTION
This article was submitted
to Avian Physiology,
a section of the journal
Frontiers in Physiology

RECEIVED 28 September 2022
ACCEPTED 30 March 2023
PUBLISHED 24 April 2023

CITATION
White D, Chen C and Kim WK (2023),
Effect of the combination of 25-
hydroxyvitamin D3 and higher level of
calcium and phosphorus in the diets on
bone 3D structural development
in pullets.
Front. Physiol. 14:1056481.
doi: 10.3389/fphys.2023.1056481

Effect of the combination of 25-hydroxyvitamin D3 and higher level of calcium and phosphorus in the diets on bone 3D structural development in pullets

Dima White, Chongxiao Chen and Woo Kyun Kim*

Department of Poultry Science, University of Georgia, Athens, GA, United States

Bone issues such as osteoporosis are major concerns for the laying hen industry. A study was conducted to improve bone-health in pullets. A total of 448 one-day-old Hyline W36 pullets were randomly assigned to four treatments (8 rep; 14 birds/rep) until 17 weeks (wks). Dietary treatments were: 1) vitamin D_3 at (2,760 IU/kg) (D), 2) vitamin D_3 (2,760 IU/kg)+62.5 mg 25-(OH)D_3/ton (H25D), 3) vitamin D_3 (2,760 IU/kg) + 62.5 mg 25-(OH)D_3/ton + high Ca&P (H25D + Ca/P), and 4) vitamin D_3 (2,760 IU/kg) + high Ca&P (D + Ca/P). The high calcium (Ca) and phosphorus (P) diet was modified by increasing both high calcium and phosphorus by 30% (2:1) for the first 12 wks and then only increasing P for 12–17 wks to reduce the Ca to P ratio. At 17 wk, growth performance was measured, whole body composition was measured by dual energy x-ray absorptiometry (DEXA), and femur bones were scanned using Micro-computed tomography (Micro-CT) for bone 3D structure analyses. The data were subjected to a one-way ANOVA using the GLM procedure, with means deemed significant at $p < 0.05$. There was no significant outcome for growth performance or dual energy x-ray absorptiometry parameters. Micro-computed tomography results indicated that the H25D + Ca/P treatment had lower open pore volume space, open porosity, total volume of pore space, and total porosity in the cortical bone compared to the D + Ca/P. It also showed that a higher cortical bone volume/tissue volume (BV/TV) in the H25D + Ca/P than in the D + Ca/P. Furthermore, the H25D + Ca/P treatment had the lowest trabecular pattern factor and structure model index compared to the other treatments, which indicates its beneficial effects on trabecular structural development. Moreover, the H25D + Ca/P had a higher trabecular percentage compared to the D and 25D, which suggests the additional high calcium and phosphorus supplementation on top of 25D increased trabecular content in the cavity. In conclusion, the combination of 25D with higher levels of high calcium and phosphorus could improve cortical bone quality in pullets and showed a beneficial effect on trabecular bone 3D structural development. Thus, combination of a higher bio-active form of vitamin D_3 and higher levels of high calcium and phosphorus could become a potential feeding strategy to improve bone structural integrity and health in pullets.

KEYWORDS

25-hydroxyvitamin D 3, bone 3D structure, pullets, micro-CT (μCT) scanning technology, bone health

Introduction

The ever-increasing improvement in laying hen nutrition and genetics has resulted in vastly more efficient hens capable of laying more than 340 eggs by 72 weeks of age (Lohmann, 2016; Preisinger, 2018). With advancements challenges, come with increased susceptibility to bone problems as demonstrated by osteoporosis and bone fractures in laying hens (Lohmann, 2016). Therefore, a better understanding of bone modeling; restoration before or during egg laying periods would be crucial to address bone development and health issues. One of the physiological changes in laying hens is that the structural bone development ceases at sexual maturity, meaning that the elongation, widening, and mineralization of structural bones (cortical and trabecular) discontinue when laying starts (Whitehead, 2004; Kim et al., 2012; Chen et al., 2020a). Hens lay eggs continuously without molting, suggesting no opportunity for the possibility of cortical bone regeneration once laying starts (Whitehead, 2004). Hence, rearing is a vital period for establishing optimal bone mineralization and structural development with implications on eggshell quality and bone health during laying (Regmi et al., 2015; Chen et al., 2020a; Chen et al., 2020b).

Osteoporosis is described as a progressive decrease in the amount of mineralized structural bone and leads to bone fragility and susceptibility to fracture (Kim et al., 2012; Toscano, 2018). These anomalies can also diminish skeletal calcium reserves and contribute to the seriousness of osteoporosis. However, even in the lack of caged layer paralysis, osteoporosis is prevalent in laying flocks (Whitehead and Fleming, 2000) and is a foremost contributory factor in the high incidence (approx. 30%) of hens experiencing fractures (Gregory and Wilkins, 1989; Clark et al., 2008; Kim et al., 2012). Nutritional deficiencies of calcium, phosphorus, or cholecalciferol have been shown to result in bone loss attributable to osteomalacia (Wilson and Duff, 1991) and are likely to lead to greater severity of osteoporosis (Clark et al., 2008; Kim et al., 2012).

Numerous pullet studies have addressed the importance of early bone development, and its prolonged effects on bone health during laying periods (Casey-Trott et al., 2017; Chen et al., 2020a; Chen et al., 2020b; Hester et al., 2013; Kim et al., 2012; Regmi et al., 2015). However, prior nutritional studies seldom focused on the pullet period because osteoporosis was observed during the laying period; it was not successful to reverse it by using nutritional approaches targeting the laying period (Rennie et al., 1997; Kim et al., 2012; Chen et al., 2020a). Thus, exploring early intervention for resolving late issues of osteoporosis in laying hens is recommended.

25-Hydroxyvitamin D_3 (H25D) is an intermediate form of vitamin D_3 and is now readily available for commercial use in the poultry industry since 2006 (Adhikari et al., 2020). H25D has been numerously studied in broiler research for enhancing bone health and Ca and P absorption (Kim et al., 2011; Wideman et al., 2015; Han et al., 2016; Świątkiewicz et al., 2017; Chen et al., 2020a; Chen et al., 2020b). However, only few studies on laying hens and especially pullets for developing the healthy bone structures for performance and maintenance during the laying period (Käppeli et al., 2011; Nascimento et al., 2014; Silva, 2017; Adhikari et al., 2020; Chen et al., 2020a; Chen et al., 2020b). The exploration of nutrients simply during a laying phase is too late for finding ways to fix or improve concerns with bone issues that should have been prevented in the rearing period to avoid the ultimate outcome of osteoporosis. Even human clinical trials demonstrated that there was little to no effect of supplementation of vitamin D or calcium on fracture occurrences in elder populations (Zhao et al., 2017).

Previous research has found that an additional 25-$(OH)D_3$ in the pullet diet stimulated bone growth, increased bone size, and created more pores in the cortical bone during a pullet period, which allowed more mineral deposition in the bones during a laying period (Chen et al., 2020a), maintaining better bone structural integrity and health in the later laying period. Due to the larger structure size, the bone mineral density (BMD) was decreased in 25-$(OH)D_3$ treatment during the pullet period, and this was possibly attributed to the calcium (Ca) and available phosphorous (P) level and ratio in the diets which were not ideal to provide sufficient Ca and P to induce proper mineral deposition in increased bone size by H25D (Chen et al., 2020a). Thus, increasing minerals, such as calcium and phosphorus in addition to H25D supplementation in rearing diets, can ultimately develop structurally sound bones and in the long run can possibly improve laying hen performances while maintaining bone health. Therefore, a study was conducted to explore the effect of dietary 25-Hydroxyvitamin D_3combined with modified Ca and P level and ratio on bone development and mineralization in pullets. The objective was to evaluate the effect of H25D combined with modified Ca and P level and ratio in the diets on growth performance, body composition, and bone 3D structural development in pullets.

Materials and methods

Animal and housing

The study was conducted at the research facility of the Department of Poultry Science at the University of Georgia. The trial was conducted in accordance with the Institutional Animal Care and Use Committee at the University of Georgia. A total of 448 one-day-old Hyline W36 chicks were randomly assigned to 4 dietary treatments (8 replicates and14 birds/replicate) and raised until 17 wks. Chicks were obtained from at Hy-line North America hatchery (Mansfield, GA). Birds were housed in colony cages for 17 wks [(90 cm (L) × 46 cm (W) × 38 cm (H)]. Water and experimental diets were offered *ad libitum* from 0 to 17 wks. There were two nipples per cage. The pullets received an intermittent lighting program during the first 7 days with 4 h of light followed by 2 h of dark circles. The lighting management was customized by Hy-line North America lighting program throughout 2–17 wks (http://sales.hyline.com/NALighting/WebLighting.aspx).

Experimental diets

The diets were designed based on the Hy-Line W36 guide (2020). The formulation of corn-soybean based diet is shown in Table 1. Treatments consisted of: 1) control diet; vitamin D_3 at (2,760 IU/kg)IU/kg (D), 2) vitamin D_3 (2,760 IU/kg) + 62.5 mg 25-$(OH)D_3$/ton (H25D), 3) vitamin D_3 (2,760 IU/kg) + 62.5 mg 25-$(OH)D_3$/ton + high Ca and P (H25D + Ca/P), and 4) vitamin D_3 (2,760 IU/kg) + high Ca and P (D + Ca/P). The high Ca and P diet

10.3389/fphys.2023.1056481

TABLE 1 Ingredients and diet composition for treatments D and H25D of the control diets fed to pullets at different stages for 17 weeks.

Ingredients	Starter 1	Starter 2	Grower	Developer	Prelay
Unit %	1–3 weeks	4–6 weeks	7–12 weeks	13–15 weeks	16–17 weeks
Corn	66.63	64.62	70.00	69.43	66.00
Soybean Meal –48%	28.40	25.00	21.62	20.00	21.50
Soybean Oil	1.00	2.66	1.38	2.57	2.34
Limestone	0.68	0.71	0.81	1.95	4.69
Defluor. Phos	2.03	2.03	1.93	1.85	2.01
Common Salt	0.30	0.30	0.30	0.30	0.30
L-Lysine HCl	0.18	0.22	0.71	0.08	0.12
DL-Methionine	0.20	0.25	0.20	0.14	0.21
Threonine	0.10	0.12	0.09	0.05	0.05
Vitamin Premix (T)	0.05	0.05	0.05	0.05	0.05
Mineral Premix	0.06	0.06	0.06	0.06	0.06
Coccidiostat (Ampro)	0.05	0.05	0.05	0.05	0.05
Sand	0.31	3.93	2.79	3.47	2.62
ME (kcal/kg)	3,030	3,030	3,030	3,050	2,960
CP (%)	20.00	18.25	17.50	16.00	16.50
Ca (%)	1.00	1.00	1.00	1.40	2.50
Avail Phos (%)	0.50	0.49	0.47	0.45	0.48
Met (%)	0.51	0.53	0.47	0.40	0.47
Met + Cys (%)	0.83	0.83	0.75	0.67	0.74
Lys (%)	1.15	1.07	1.35	0.83	0.89
Thr (%)	0.82	0.77	0.70	0.62	0.64

[a]D = vitamin D3 (2,760 IU/kg); H25D = vitamin D3 (2,760 IU/kg) + 62.5 mg HyD/ton (full dose).

[b]Control diet contains 3,000 IU, of vitamin D3/kg of feed.

[c]Vitamin premix supplied per kilogram of complete feed: vitamin A, 8,250 IU; vitamin E, 30 IU; vitamin B_{12}, 0.013 mg; vitamin K_3, 2.0 mg; niacin, 23.6 mg; choline chloride, 1,081 mg; folic acid, 4.0 mg; biotin, 0.25 mg; pyridoxine, 4.0 mg; thiamine, 4.0 mg; vitamin D_3, 3,000 IU.

[d]Mineral premix supplied per kg of complete feed: manganese oxide, 70 mg; zinc oxide 80 mg, ferrous sulfate, 80 mg, copper sulfate, 10 mg; sodium selenium, 0.3 mg; calcium iodate premix, 0.5 mg.

[e]Starter 1 = fed from 1 to 3 wks, starter 2 = fed from 4 to 6 wks, grower = fed from 7 to 12 wks, developer = fed from 13 to 15 wks, prelay = fed from 16–17 wks.

was modified by increasing 30% of both Ca and P (2:1) for the first 12 wks, and then only increasing P for 12–17 wks to reduce the Ca to P ratio (Table 2). The experimental diets were fed for 17 wks. The diets were freshly mixed every 3 weeks to minimize degradation of supplemented vitamin D_3 or 25-(OH)D_3 in the diets.

Serum 25-(OH)D_3 content analysis

Blood samples (8 birds/treatment) were collected from the wing vein at 17 wks. After the blood was clotted, the blood samples were centrifuged at 1,500 g in a refrigerated centrifuge (Eppendorf Centrifuge 5430R; Eppendorf, Hamburg, Germany) for 12 min. The serum was collected and transferred into a clean polypropylene tube. The samples were maintained at −80°C until analysis. The serum 25-(OH)D_3 level was determined using a mass spectrometry procedure (Heartland Assays, Ames, IA).

Growth performance measurement

Body weight (BW), body weight gain (BWG), and feed intake (FI) were recorded at 0, 3, 6, 12, 15, and 17 wks. The phase periods for recording are 0–3 wks (Starter 1 period), 4–6 wks (Starter 2 period), 7–12 wks (Grower period), 13–15 wks (Developer period), and 16–17 wks (Peak period). However, growth performance was reported for 0–17 wks.

Bone quality measurements

At 17 wks, two birds per cage (2 birds × 8 replicates = 16 birds per treatment) were euthanized by cervical dislocation. Dual energy x-ray absorptiometry (DEXA; pDEXA®, Bone Densitometer, General Electric Company, 41 Farnsworth Street, Boston, MA 02210, United States) was used for whole bird body composition

10.3389/fphys.2023.1056481

TABLE 2 Ingredients and diet composition for treatments H25D + Ca/P and D + Ca/P diets with higher levels of Ca&P fed to pullets at different stages for 17 weeks.

Ingredients	Starter 1	Starter 2	Grower	Developer	Prelay
Unit %	0–3 weeks	3–6 weeks	6–12 weeks	12–15 weeks	15–17 weeks
Corn	65.38	64.62	70.00	69.43	66.00
Soybean Meal –48%	28.64	25.00	21.62	20.00	21.50
Soybean Oil	1.41	2.66	1.38	2.57	2.34
Limestone	0.77	0.80	0.94	0.78	2.59
Defluor. Phos	2.87	2.86	2.71	3.24	4.51
Common Salt	0.30	0.30	0.30	0.30	0.30
L-Lysine HCl	0.18	0.22	0.71	0.08	0.12
DL-Methionine	0.20	0.25	0.20	0.14	0.21
Threonine	0.10	0.12	0.09	0.05	0.05
Vitamin Premix (T)	0.05	0.05	0.05	0.05	0.05
Mineral Premix	0.06	0.06	0.06	0.06	0.06
Coccidiostat (Ampro)	0.05	0.05	0.05	0.05	0.05
Sand	0.00	3.01	1.88	3.25	2.22
Calculated value					
ME (kcal/kg)	3,030	3,030	3,030	3,050	2,960
CP (%)	20.00	18.25	17.50	16.00	16.50
Ca (%) (+30%)	1.30	1.30	1.30	1.40	2.50
Avail Phos (%) (+30%)	0.65	0.64	0.61	0.70	0.93
Met (%)	0.51	0.53	0.47	0.40	0.47
Met + Cys (%)	0.83	0.83	0.75	0.67	0.74
Lys (%)	1.15	1.07	1.35	0.83	0.89
Thr (%)	0.82	0.77	0.70	0.62	0.64
Analyzed value					
HPLC/D (mcg/g)	139.4	146.2	134.3 mcg/g	134.3	139.4
HPLC/H25D (mcg/g)	<6.3	77.3	159.7 mcg/g	159.7	<6.3
Analysis Calcium (%)	1.33	1.34	1.35	1.42	2.55
Analysis Total Phos (%)	0.86	0.84	0.90	1.00	1.17
Analysis Avail Phos (%)	0.66	0.64	0.70	0.80	0.97

[a]H25D + Ca/P = vitamin D3 (2,760 IU/kg) + 62.5 mg HyD/ton (full dose) + 10%–30% higher Ca&P levels; D + Ca/P = vitamin D3 (2,760 IU/kg) + 10%–30% higher Ca&P levels.
[b]Control diet contains 3,000 IU, of vitamin D3/kg of feed.
[c]Vitamin premix supplied per kilogram of complete feed: vitamin A, 8,250 IU; vitamin E, 30 IU; vitamin B_{12}, 0.013 mg; vitamin K_3, 2.0 mg; niacin, 23.6 mg; choline chloride, 1,081 mg; folic acid, 4.0 mg; biotin, 0.25 mg; pyridoxine, 4.0 mg; thiamine, 4.0 mg; vitamin D_3, 3,000 IU.
[d]Mineral premix supplied per kg of complete feed: manganese oxide, 70 mg; zinc oxide 80 mg, ferrous sulfate, 80 mg, copper sulfate, 10 mg; sodium selenium, 0.3 mg; calcium iodate premix, 0.5 mg.
[e]HPLC, High-performance liquid chromatography.
[f]Starter 1 = fed from 1 to 3 wks, starter 2 = fed from 4 to 6 wks, grower = fed from 7 to 12 wks, developer = fed from 13 to 15 wks, prelay = fed from 16–17 wks.

analyses, and the whole bird was defined as a region of interest (Kim et al., 2004; Chen et al., 2020a; Adhikari et al., 2020). Whole body region scans were conducted to measure bone mineral density (g/cm^2) (BMD), bone mineral content (g) (BMC), bone area (cm^2), fat weight (kg), fat percent (%), muscle weight (kg), muscle percentage (%), and total body weight (kg). Each sample bird was placed chest up on the scanner at the same position and orientation during the measurement. All scans were obtained at a scan speed of 2.5 mm/s, with a voxel resolution of 0.07 mm × 0.07 mm × 0.50 mm.

The left femur bone was taken from one bird per pen (8 bones/treatment) at 17 wks of age. After the soft tissue was removed completely, the samples were wrapped with PBS-soaked

TABLE 3 Micro-CT scanning settings and definitions/explanations.

Voltage	Current	Exposure time	Rotation	Average frame	Pixel size
(kv)	(mA)	(ms)	(degrees)	(Slides)	(Um/pixel)
80	125	55	0.4	6	25
Parameters	Definition/explanation				
Tissue volume	The volume of the volume-of-interest (VOI)				
Bone volume	The volume of binarized objects (mineralized bones) with in the VOI				
Pore number	The total number of closed pores within VOI				
Pore volume	The total volume of pores				
Closed pore	Closed pores in a 3D; is a connected assembly of space, surrounded on all slides in 3D by solid voxels. The measurement includes volume, surface and number				
Opened pore	Defined as any space located within a solid object or between solid objects, which has any connections in 3D to the space outside the object or objects. The measurement includes volume, surface, and number				
Porosity	The volume of pores as a percentage of total VOI volume				
Trabecular connectivity	A 3D calculation based on 2D scale. In simple, higher number means better connected trabecular structure				
Trabecular connectivity density	Connectivity/VOI				
Trabecular pattern Factor	This is an inverse index of connectivity. To simplify, lower number means better connectivity and trabecular structure				
Trabecular thickness	The diameter of the largest sphere which fulfils two conditions: the sphere encloses the point, and the sphere is entirely bound within the solid surfaces. This is mean value of the trabecular thickness in 3D space				
Structure model index	Widely used to measure rods and plates in trabecular bone. It exploits the change in surface curvature that occurs as a structure varies from spherical, to cylindrical to planar. To simplify, lower number indicates better connectivity and trabecular structure				
Degree of anisotropy	Isotropy is a measure of 3D symmetry or the presence or absence of preferential alignment of structures along a particular directional axis. Consider a region or volume containing two phases (solid and space), both having complex architecture, such as a region of trabecular bone. We can study this volume to determine isotropy. Values for DA calculated in this way vary from 1 (fully isotropic) to infinity (fully anisotropic). Higher number indicates positive connectivity which will also correspond with lower TPF and SMI				

TABLE 4 Growth performance at 17th week.

Treatment	BW/Bird (kg)	BWG/Bird (kg)	FI/Bird (kg)
D	1.239	1.202	5.268
H25D	1.229	1.192	5.298
H25D + Ca/P	1.246	1.209	5.266
D + Ca/P	1.248	1.211	5.215
SEM	0.025	0.024	0.027
p-value	0.998	0.992	0.302

[a]BW, Body weight; BWG, body weight gain; FI, Feed intake.
[b]D = vitamin D3 (2,760 IU/kg); H25D = vitamin D3 (2,760 IU/kg) + 62.5 mg HyD/ton (full dose); H25D + Ca/P = vitamin D3 (2,760 IU/kg) + 62.5 mg HyD/ton (full dose) + 10%–30% higher Ca&P levels; D + Ca/P = vitamin D3 (2,760 IU/kg) + 10%–30% higher Ca&P levels.

cheesecloth to keep the bones moist. The femur bones were scanned with micro-computed tomography (Micro-CT; Skyscan 1275; Bruker micro-CT, Kartuizersweg 3B Kontich, Belgium) which was used for 3- dimensional image acquisition (Chen and Kim, 2020; Yamada et al., 2021). The femur bone was held in a low-density 50 ml tube; extra cheesecloth was used for holding the sample in a vertical orientation and firmly inside the container. The container was then mounted on the scanning stage. Scan settings and definitions/explanations of measurements are shown in Table 3. Before the scanning, the alignment test and flat field correction were performed for calibration according to the Bruker Micro-CT manual (Bruker micro-CT, Kartuizersweg 3B Kontich, Belgium). Random movement and 180-degree scanning were applied along with a 0.5 mm aluminum filter used to reduce beam hardening. The x-ray source was set at 80 kV and 125 μA. The pixel size was fixed at 25 μm, the rotation angle of 0.40 was applied at each step, and four images per rotation were captured. A series of 2-D images

TABLE 5 DEXA results for week 17.

Treatment	BMD (g/cm^2)	BMC (g)	Bone area (cm^2)	Fat percent (%)	Fat wt (kg)	Muscle percent (%)	Muscle wt (kg)	Total weight (kg)
D	0.219	33.086	151.571	25.278	0.300	74.656	0.823	1.188
H25D	0.211	30.743	145.286	25.483	0.300	74.511	0.877	1.177
H25D + Ca/P	0.217	32.225	148.625	25.175	0.295	74.820	0.878	1.173
D + Ca/P	0.216	31.943	147.286	24.506	0.280	75.494	0.864	1.144
SEM	0.011	1.311	3.584	1.447	0.097	3.523	0.119	0.102
p-value	0.956	0.388	0.378	0.883	0.741	0.874	0.801	0.448

[a]BMD, Bone mineral density; BMC, Bone mineral content.
[b]D = vitamin D3 (2,760 IU/kg); H25D = vitamin D3 (2,760 IU/kg) + 62.5 mg HyD/ton (full dose); H25D + Ca/P = vitamin D3 (2,760 IU/kg) + 62.5 mg HyD/ton (full dose) + 10%–30% higher Ca&P levels; D + Ca/P = vitamin D3 (2,760 IU/kg) + 10%–30% higher Ca&P levels.

TABLE 6 Micro-CT results for bone tissue volume.

Treatment	Total	Trabecular	Cortical
	%	%	%
D	29.963	3.769[b]	95.729[a]
H25D	30.243	3.912[b]	94.794[ab]
H25D + Ca/P	32.032	5.120[a]	95.774[a]
D + Ca/P	31.566	4.435[ab]	93.525[b]
SEM	0.6985	0.5231	0.6324
p-value	0.3241	0.0492	0.0384

[a]D = vitamin D3 (2,760 IU/kg); H25D = vitamin D3 (2,760 IU/kg) + 62.5 mg HyD/ton (full dose); H25D + Ca/P = vitamin D3 (2,760 IU/kg) + 62.5 mg HyD/ton (full dose) + 10%–30% higher Ca&P levels; D + Ca/P = vitamin D3 (2,760 IU/kg) + 10%–30% higher Ca&P levels.
[b]Please refer to Table 3 for definitions of parameters.
a,b means within a column with different superscripts are significantly different ($p < 0.05$).

TABLE 7 Micro-CT results for cortical bone porosity analysis.

Treatment	Volume of closed pores	Closed porosity (percent)	Volume of open pore space	Open porosity (percent)	Total volume of pore space	Total porosity (percent)
Unit	mm^3	%	mm^3	%	mm^3	%
D	0.754	0.887	2.906[b]	3.414[b]	3.660[b]	4.271[b]
H25D	0.760	0.905	3.838[ab]	4.341[ab]	4.598[ab]	5.206[ab]
H25D + Ca/P	0.811	0.933	2.999[b]	3.325[b]	3.811[b]	4.226[b]
D + Ca/P	0.801	0.923	5.168[a]	5.606[a]	5.969[a]	6.475[a]
SEM	0.1285	0.1324	0.4025	0.4012	0.50124	0.4852
p-value	0.9956	0.9325	0.0398	0.0358	0.0497	0.0487

[a]D = vitamin D3 (2,760 IU/kg); H25D = vitamin D3 (2,760 IU/kg) + 62.5 mg HyD/ton (full dose); H25D + Ca/P = vitamin D3 (2,760 IU/kg) + 62.5 mg HyD/ton (full dose) + 10%–30% higher Ca&P levels; D + Ca/P = vitamin D3 (2,760 IU/kg) + 10%–30% higher Ca&P levels.
[b]Please refer to Table 3 for definitions of parameters.
a,b means within a column with different superscripts are significantly different ($p < 0.05$).

were capturedand later used to reconstruct a 3-D image using N-Recon (Bruker Micro-CT, Billerica, MA). After scanning, the pictures were carefully screened, and the appropriate alignment and mathematical method correction were used (beam-hardening correction: 35%; smoothing: NA; ring artifact reduction: NA). The 3-D model was then repositioned using

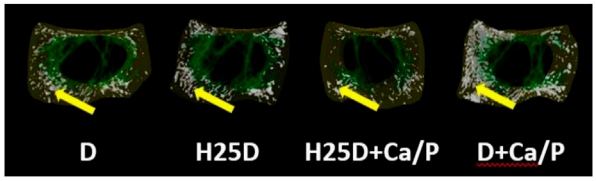

FIGURE 1
Total porosity within the cortical bone region. 1) Arrow indicating the open pores within the cortical region of the bone. 2) D = vitamin D3 (2,760 IU/kg); H25D = vitamin D3 (2,760 IU/kg) + 62.5 mg HyD/ton (full dose); H25D + Ca/P = vitamin D3 (2,760 IU/kg) + 62.5 mg HyD/ton (full dose) + 10%–30% higher Ca&P levels; D + Ca/P = vitamin D3 (2,760 IU/kg) + 10%–30% higher Ca&P levels. 3) Please refer to Table 3 for definitions of parameters.

Data Viewer software (Bruker Micro-CT, Billerica, MA) to ensure the consistency of selecting the region of interests for the following analysis. The volume of interest was selected using CTAn software (Bruker Micro-CT, Billerica, MA). The volume of interest was defined as the section of the bone from which morphometry and density measurements were analyzed. The bone section chosen was a distal supracondylar region from which a total of 300 slides/frames were analyzed. This 300 slide/frame section is the epiphyseal plate region of the long bone. Two phantoms (8 mm diameter) of known density (0.25 and 0.75 g/cm3) for calcium hydroxyapatite [(Ca5(PO4)3(OH)] were scanned to allow for calibration of bone mineral density (Sharma et al., 2021). The different parts of bones were separated according to the methods described by Chen and Kim (2020).

Statistical analysis

Data were subjected to statistical analyses using the general linear model procedure (GLM) of SAS (SAS Institute Inc., Cary, NC). One-way ANOVA was used with model $_{Yij} = \mu + \alpha_i + \varepsilon_{ij}$. Significant differences among the treatments were determined using GLM procedures. Data were considered significantly different at $p \leq 0.05$, and trends ($0.05 \leq p \leq 0.1$) were also presented (Choi et al., 2021).

Results

In the current study, the supplementation of different isoforms of vitamin D (D or H25D) along with higher Ca and P levels did not have an impact on growth performance parameters ($p > 0.05$) (Table 4) or whole bird body composition parameters (Table 5).

However, changes in mineral deposition and 3D structural changes were observed in the femurs. For cortical bone analyses by Micro-CT, the H25D + Ca/P had significantly higher cortical bone volume/tissue volume (BV/TV) compared to the D + Ca/P (Table 6). 25-(OH)D_3 with higher Ca and P levels (H25D + Ca/P) had significantly lower open pore volume space, open porosity (% cortical tissue volume), total volume of pore space, and total porosity (% cortical tissue volume) in the cortical bone compared to vitamin D_3 with higher Ca and P levels (D + Ca/P) ($p < 0.05$) (Table 7; Figure 1).

The H25D + Ca/P treatment had the lowest trabecular pattern factor (TPF) ($p = 0.009$) and structure model index (SMI) ($p = 0.031$) among the treatments (Table 8; Figure 2). Moreover, H25D + Ca/P had a higher trabecular percentage (trabecular bone/cavity volume %) compared to D and H25D ($p < 0.05$).

The 25-(OH)D_3 level in the serum was measured in the present study. The treatments with H25D always had the highest 25-(OH)D_3 level in the serum compared to the other treatments ($p < 0.0001$) (Table 9).

Discussion

Bone mineral acquisition is organized by a range of factors ranging from genetic determinants and nutritional influences on the hormonal balance, including traditional regulation of mineral homeostasis by vitamin D_3 (Dusso et al., 2005; Bouillon et al., 2008). Vitamin D_3 is obtained from dietary sources and is synthesized in the skin by photo-conversion of 7-dehydrocholesterol to vitamin D3, which afterwards undergoes

TABLE 8 Micro-CT results for trabecular bone structural analysis.

Treatment	Trabecular thickness	Trabecular pattern factor	Degree of anisotropy	Connectivity	Connectivity density	Trabecular SMI
	mm	mm^{-1}	None	None	mm^{-3}	None
D	0.152	5.751[a]	2.189	246.500	1.174	1.632[a]
H25D	0.156	5.834[a]	2.423	271.000	1.298	1.664[a]
H25D + Ca/P	0.159	4.555[b]	2.493	302.571	1.471	1.431[b]
D + Ca/P	0.153	5.323[a]	2.314	390.750	1.830	1.571[ab]
SEM	0.0095	0.2445	0.0986	48.3651	0.2982	0.07426
p-value	0.9026	0.02145	0.0721	0.1368	0.2512	0.0452

[a]D = vitamin D3 (2,760 IU/kg); H25D = vitamin D3 (2,760 IU/kg) + 62.5 mg HyD/ton (full dose); H25D + Ca/P = vitamin D3 (2,760 IU/kg) + 62.5 mg HyD/ton (full dose) + 10%–30% higher Ca&P levels; D + Ca/P = vitamin D3 (2,760 IU/kg) + 10%–30% higher Ca&P levels.
[b]Please refer to Table 3 for definitions of parameters.
a,b means within a column with different superscripts are significantly different ($p < 0.05$).

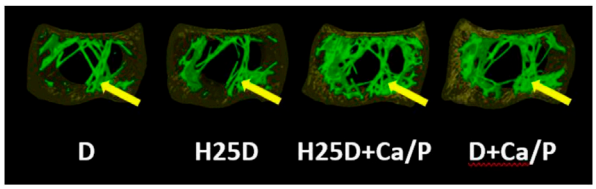

FIGURE 2
Total pattern factor, matrix, and thickness within the trabecular bone region. 1) Arrow indicating the pattern factor, matrix, and thickness within the trabecular region of the bone. 2) D = vitamin D3 (2,760 IU/kg); H25D = vitamin D3 (2,760 IU/kg) + 62.5 mg HyD/ton (full dose); H25D + Ca/P = vitamin D3 (2,760 IU/kg) + 62.5 mg HyD/ton (full dose) + 10%–30% higher Ca&P levels; D + Ca/P = vitamin D3 (2,760 IU/kg) + 10%–30% higher Ca&P levels. 3) Please refer to Table 3 for definitions of parameters.

two main modifications (Chen et al., 2020a). Firstly, it is metabolized in the liver to produce the circulating form 25-hydroxyvitamin D_3 (H25D, calcidiol), which is later converted in the kidney and other tissues including bone by 1α-hydroxylase to generate the active form 1,25-hydroxyvitamin D_3 ($1,25(OH)_2D_3$, calcitriol) (Chen et al., 2020a). $1,25(OH)_2D_3$ is the primary hormonal form of vitamin D3 which binds to vitamin D receptor (VDR), inducing a broad range of biological responses (Dusso et al., 2005; Bouillon et al., 2008).

The advantage of H25D during the rearing period is observed more commonly through the bone parameters of pullets such as the cortical and trabecular regions of the bone (Chen et al., 2020a). In the current study, the rearing growth parameters were not affected by H25D. This result agrees with studies reporting that different concentrations and forms of vitamin D_3 did not affect the growth parameters of pullets (Wen et al., 2019; Chen et al., 2020a; Li et al., 2021). Moreover, the dual-energy X-ray absorptiometry scanning did not detect beneficial changes by vitamin D_3 and Ca and P in the current study for the rearing period. Similar results were observed in the previous study (Chen et al., 2020a) where at 17 wk, there was no difference in whole-body BMD and BMC while feeding birds with 25D.

With 3D scanning and automatic bone separation process by Micro-CT, the effects of dietary H25D + Ca/P supplementation on pullet bone 3-dimensional structural changes were observed in the present study. In a previous study by Chen et al. (2020a), the H25D increased cortical bone size and porosity significantly but reduced cortical bone density compared to the D treatment alone, suggesting that mineral supplementation or utilization may not be adequate to fill in the larger cortical bone size. For the current study, the primary function of H25D in early bone development was to increase the bone structural size, and to fill the "larger" bone structure with the increased Ca and P in order to close the open pores within the cortical region. This may contribute to bone fracture resistance, as the cortical bone represents 70%–80% of the total bone mass, which is found on the outer surface of bones and its primary function is to support rigidity to the bone, with its relative ratio depending on the function and mechanical load of the respective bone (Digirolamo et al., 2013). It is distinguished by a volumetric fraction (bone mass volume/total volume ratio), which explains its common name of compact bone (Digirolamo et al., 2013). In previous research, the expansion of the cortical bone size with the same amount of BMC resulted in a low-density bone (Chen et al., 2020a). A low BMD is commonly associated with an elevated risk of bone fracture (Ammann and Rizzoli, 2003). A larger cortical region does not necessarily correlate to stronger or more structurally sound bones without having the proper mineral deposition (Estefania et al., 2019).

Inside the cortical cortex, the coupling between osteoblast and osteoclast activities is carried out in the matrix of cortical pores which provide a conduit for the movement of neurovascular structures (Rique et al., 2019). Cortical porosity is considered to be correlated with mechanical properties of cortical bone, manipulating bone strength and risk of fracture (Li et al., 2021). Because larger cavities indicate increased osteoclast recruitment and activity, there is a conjecture that higher bone resorption, either alone or in combination with inhibited osteoblast function, accounts for higher porosity. There is evidence that cortical diameter of pores increases with increased porosity, which can potentially result in decreased overall bone density (Rique et al., 2019). However,

TABLE 9 $25\text{-}(OH)D_3$ level in the serum.

Treatment	$25\text{-}(OH)D_3$
	ng/ml
D	28.21[b]
H25D	53.26[a]
H25D + Ca/P	54.31[a]
D + Ca/P	30.18[b]
SEM	2.214
p-value	<.0001

[a]D = vitamin D3 (2,760 IU/kg); H25D = vitamin D3 (2,760 IU/kg) + 62.5 mg HyD/ton (full dose); H25D + Ca/P = vitamin D3 (2,760 IU/kg) + 62.5 mg HyD/ton (full dose) + 10%–30% higher Ca&P levels; D + Ca/P = vitamin D3 (2,760 IU/kg) + 10%–30% higher Ca&P levels.
[b]MS/LC, mass spectrometry/liquid chromatography.
a,b means within a column with different superscripts are significantly different ($p < 0.05$).

decreased porosity and cortical diameter of pores can potentially lead to better overall bone density. In addition, a recent concept of two individual osteoblast types positioned in the cortical bone (Shapiro, 2008), creates another likelihood, that is $1,25(OH)_2D_3$ selectively suppresses the intracortical osteoblasts coating primary osteons, but without altering surface mesenchymal osteoblasts lining the periosteum. The current study observed a larger cortical bone size with increased pores, which were filled in with elevated levels of calcium (from 30% early on to 10% at later stages) and phosphorus (30% throughout) provided in the diet. This was further observed by the trending volume of closed pores and closed porosity for the H25D + Ca/P treatment, which complements the findings with the lower open pore space. Therefore, the nutritional strategy with H25D + Ca/P during rearing periods have potential to create a more compact and structurally sound bone.

In the present study, higher content of trabecular bone in the H25D treatment was found during the rearing period. The trabecular bone corresponds to 20%–30% of the bone mass, which is in the internal section of the bone (Digirolamo et al., 2013). It has a porous reticular structure with variable and rather low density that provides flexibility and strength to the whole bone structure. It is also distinguished by a relatively low volumetric fraction, offsetting with a surface area nearly twice as large as the compact bone (Digirolamo et al., 2013). Poultry bones were largely based on bone ash, breaking strength, or DEXA (Hester et al., 2004; Castro et al., 2019; Adhikari et al., 2020). These approaches are based on the results of planar morphology or bone mass. Although bone quantity and density are important factors for bone strength (Hester et al., 2004), these parameters do not consider the trabecular architectural changes that are independently related to bone strength (Siffert et al., 1996; Webber et al., 1998). An avian model study determined that over 10% loss of trabecular bone could impact bone strength (Reich and Gefen, 2006), indicating that the integrity of trabecular bone is essential for bone resistance to force. The increase of trabecular bone content within the cavity in the H25D treatment suggested the higher fracture resistance elevated by dietary supplementation. The current findings of a significant decrease in TPF and SMI by the H25D + Ca/P vs. the control D, which was complemented by higher trabecular thickness, number and bone mineral density along with lower separation for the H25D treatment is in agreement with a study (Idelevich et al., 2011). The study observed that inclusion of H25D increased trabecular number and thickness, while having a corresponding decrease in trabecular separation in rats. The study also revealed an increase in overall trabecular bone content with the inclusion of H25D. The correspondence of the SMI, which is an index evaluating whether trabecular bone is rod-like or plate-like, and a smaller value means a more plate-like structure (Hildebrand & Rüegsegger, 1997) and TPF, which is an index evaluating rod-like, plate-like, or honeycomb-like structure, and a small value means a more plate-like to honeycomb-like structure (Hahn et al., 1992), resembles a positive outcome when both parameters are lower as observed in this current study. This correlation of having both SMI and TPF lower also results in increasing overall trabecular structure by increasing connectivity (Chiba et al., 2010; Yokota et al., 2020). Furthermore, for both SMI and TPF, the smaller values indicate the positive plate-like or honeycomb-like structure also results in less osteoporosis cases vs. the rod-like structure increases osteoporosis incidences (Felder et al., 2020).

This study suggests that early supplementation of the combination of H25D with higher level of Ca and P could improve the cortical bone microstructure and have beneficial effects on trabecular bone 3D structural development in pullets. The combination of a higher bio-active forms of vitamin D_3 and higher levels of Ca and P during rearing periods may become a promising feeding strategy to enhance pullet bone quality.

Data availability statement

The raw data supporting the conclusion of this article will be made available by the authors, without undue reservation.

Ethics statement

The animal study was reviewed and approved by the Institutional Animal Care and Use Committee at the University of Georgia.

Author contributions

DW, CC, and WK conceived and designed this study. DW and CC contributed to pullet husbandry and sample collection, DW and CC contributed to Micro-CT assay. DW contributed to the data analyses. The paper was written through contribution and critical review of the manuscript by all authors (DW, CC, and WK). All authors listed have made a substantial, direct and intellectual contribution to the work, and approved it for publication.

Conflict of interest

The authors declare that the research was conducted in the absence of any commercial or financial relationships that could be construed as a potential conflict of interest.

Publisher's note

References

Adhikari, R., White, D., House, J. D., and Kim, W. K. (2020). Effects of additional dosage of vitamin D3, vitamin D2, and 25-hydroxyvitamin D3 on calcium and phosphorus utilization, egg quality and bone mineralization in laying hens. *Poult. Sci.* 99 (1), 364–373. doi:10.3382/ps/pez502

Ammann, P., and Rizzoli, R. (2003). Bone strength and its determinants. *Osteoporos. Int.* 14, 13–18. doi:10.1007/s00198-002-1345-4

Bikle, D. D. (2017). Vitamin D: Production, metabolism and mechanisms of action. [Updated 2021 Dec 31]. In: K. R. Feingold, B. Anawalt, A. Boyce, et al. editors. *Endotext [internet]*. South Dartmouth (MA): MDText.com, Inc.; Available from: https://www.ncbi.nlm.nih.gov/books/NBK278935/.

Bouillon, R., Carmeliet, G., Verlinden, L., Van Etten, E., Verstuyf, A., Luderer, H. F., et al. (2008). Vitamin D and human health: Lessons from vitamin D receptor null mice. *Endocr. Rev.* 29 (6), 726–776. doi:10.1210/er.2008-0004

Casey-Trott, T. M., Korver, D. R., Guerin, M. T., Sandilands, V., Torrey, S., and Widowski, T. M. (2017). Opportunities for exercise during pullet rearing, Part I: Effect on the musculoskeletal characteristics of pullets. *Poult. Sci.* 96, 2509–2517. doi:10.3382/ps/pex059

Castro, F. L. S., Su, S., Choi, H., Koo, E., and Kim, W. K. (2019). L-Arginine supplementation enhances growth performance, lean muscle, and bone density but not fat in broiler chickens. *Poult. Sci.* 98, 1716–1722. doi:10.3382/ps/pey504

Chen, C., and Kim, W. K. (2020). The application of micro-CT in egg-laying hen bone analysis: Introducing an automated bone separation algorithm. *Poult. Sci.* 99, 5175–5183. doi:10.1016/j.psj.2020.08.047

Chen, C., Turner, B., Applegate, T. J., Litta, G., and Kim, G. (2020a). Role of long-term supplementation of 25-hydroxyvitamin D3 on laying hen bone 3-dimensional structural development. *Poult. Sci.* 99, 5771–5782. doi:10.1016/j.psj.2020.06.080

Chen, C., Turner, B., Applegate, T. J., Litta, G., and Kim, W. K. (2020b). Role of long-term supplementation of 25-hydroxyvitamin D_3 on egg production and egg quality of laying hen. *Poult. Sci.* 99, 6899–6906. doi:10.1016/j.psj.2020.09.020

Chen, C., Adhikari, R., White, D., and Kim, W. K. (2021a). Role of 1, 25-dihydroxyvitamin D3 on osteogenic differentiation and mineralization of chicken mesenchymal stem cells. *Front. Physiol.* 12, 479596. doi:10.3389/fphys.2021.479596

Chen, C., White, D., Marshall, B., and Kim, W. K. (2021b). Role of 25-hydroxyvitamin D3 and 1,25-dihydroxyvitamin D3 in chicken embryo osteogenesis, adipogenesis, myogenesis, and vitamin D3 metabolism. *Front. Physiol.* 12, 631629. doi:10.3389/fphys.2021.637629

Chiba, K., Ito, M., Osaki, M., Uetani, M., and Shindo, H. (2010). *In vivo* structural analysis of subchondral trabecular bone in osteoarthritis of the hip using multi-detector row CT. *Osteoarthr. Cartil.* 19, 180–185. doi:10.1016/j.joca.2010.11.002

Choi, J., Ko, H., Tompkins, Y. H., Teng, P. Y., Lourenco, J. M., Callaway, T. R., et al. (2021). Effects of eimeria tenella infection on key parameters for feed efficiency in broiler chickens. *Animals* 11, 3428. doi:10.3390/ani11123428

Clark, W. D., Cox, W. R., and Silversides, F. G. (2008). Bone fracture incidence in end-of-lay high-producing, noncommercial laying hens identified using radiographs. *Poult. Sci.* 87 (10), 1964–1970. doi:10.3382/ps.2008-00115

Digirolamo, D. J., Kiel, D. P., and Esser, K. A. (2013). Bone and skeletal muscle: Neighbors with close ties. *J. Bone Min. Res.* 28, 1509–1518. doi:10.1002/jbmr.1969

Dusso, A., González, E. A., and Martin, K. J. (2005). Vitamin D in chronic kidney disease. *Best Pract. Res. Clin. Endocrinol. metabolism* 25 (4), 647–655. doi:10.1016/j.beem.2011.05.005

Estefania, S. R., Reyes, C. B., Torres, C., Gasca, N. D., Ruiz, A. I. G., Lopez, S. G., et al. (2019). Changes with age (from 0 to 37 D) in tibiae bone mineralization, chemical composition and structural organization in broiler chickens. *Poult. Sci.* 98, 5215–5225. doi:10.3382/ps/pez363

Felder, A. A., Monzem, S., De Souza, R., Javaheri, B., Mills, D., Boyde, A., et al. (2020). The plate-to-rod transition in trabecular bone loss is elusive. *R. Soc. Open Sci.* 14, 081042. doi:10.1101/2020.05.14.081042

Gregory, N. G., and Wilkins, L. J. (1989). Broken bones in domestic fowl: Handling and processing damage in end-of-lay battery hens. *Br. Poult. Sci.* 30, 555–562. doi:10.1080/00071668908417179

Hahn, P. Y., Stroebel, J. J., and Hahn, F. J. (1992). Verification of lumbosacral segments on MR images; identification of transitional vertebrae. *Radiology* 182, 580–581. doi:10.1148/radiology.182.2.1732988

Han, J. C., Chen, G. H., Wang, J. G., Zhang, J. L., Qu, H. X., Zhang, C. M., et al. (2016). Evaluation of relative bioavailability of 25- hydroxycholecalciferol to cholecalciferol for broiler chickens. *Asian-Australas J. Anim. Sci.* 29, 1145–1151. doi:10.5713/ajas.15.0553

Hester, P., Schreiweis, M., Orban, J., Mazzuco, H., Kopka, M., Ledur, M., et al. (2004). Assessing bone mineral density *in vivo*: Dual energy X-ray absorptiometry. *Poult. Sci.* 83, 215–221. doi:10.1093/ps/83.2.215

Hester, P. Y., Enneking, S. A., Haley, B. K., Cheng, H. W., Einstein, M. E., and Rubin, D. A. (2013). The effect of perch availability during pullet rearing and egg laying on musculoskeletal health of caged White Leghorn hens. *Poult. Sci.* 92, 1972–1980. doi:10.3382/ps.2013-03008

Hildebrand, T., and Rüegsegger, P. (1997). Quantification of bone microarchitecture with the structure model index. *Comput. Methods Biomech. Biomed. Engin* 1 (1), 15–23. doi:10.1080/01495739708936692

Holick, M. F. (2007). Vitamin D deficiency. *N. Engl. J. Med.* 357 (3), 266–281. doi:10.1056/NEJMra070553

Hy-Line (2020). *Hy-line variety W-36 commercial management guide 2020*. West Des Moines (IA): Hy-Line International.

Idelevich, A., Kerschnitzki, M., Shahar, R., and Monsonego-Ornan, E. (2011). 1,25(OH)2D3 alters growth plate maturation and bone architecture in young rats with normal renal function. *PLoS ONE* 6(6): e20772. doi:10.1371/journal.pone.0020772

Jendral, M. J., Korver, D. R., Church, J. S., and Feddes, J. J. (2008). Bone mineral density and breaking strength of White Leghorns housed in conventional, modified, and commercially available colony battery cages. *Poult. Sci.* 87, 828–837. doi:10.3382/ps.2007-00192

Käppeli, S., Fröhlich, E., Gebhardt-Henrich, S. G., Pfulg, A., Schäublin, H., Zweifel, R., et al. (2011). Effects of dietary supplementation with synthetic vitamin D3 and 25-hydroxycholecalciferol on blood calcium and phosphate levels and performance in laying hens. *Arch. Geflugelkd* 75, 179–184.

Kim, W. K., Ford, B. C., Mitchell, A. D., Elkin, R. G., and Leach, R. M., Jr. (2004). Comparative assessment of bone among wild-type, restricted ovulator and out-of-production hens. *Br. Poult. Sci.* 45, 463–470. doi:10.1080/00071660412331286172

Kim, W. K., Donalson, L. M., Michell, A. D., Kubena, L. F., Nisbet, D. J., and Ricke, S. C. (2006). Effects of alfalfa and fructooligosaccharide on molting parameters and bone qualities using dual energy x-ray absorptiometry and conventional bone assays. *Poult. Sci.* 85, 15–20. doi:10.1093/ps/85.1.15

Kim, W. K., Donalson, L. M., Bloomfield, S. A., Hogan, H. A., Kubena, L. F., Nisbet, D. J., et al. (2007). Molt performance and bone density of cortical, medullary, and cancellous bone in laying hens during feed restriction or alfalfa-based feed molt. *Poult. Sci.* 86, 1821–1830. doi:10.1093/ps/86.9.1821

Kim, W. K., Bloomfield, S. A., and Ricke, S. C. (2011). Effects of age, vitamin D3, and fructooligosaccharides on bone growth and skeletal integrity of broiler chicks. *Poult. Sci.* 90, 2425–2432. doi:10.3382/ps.2011-01475

Kim, W. K., Bloomfield, S. A., Sugiyama, T., and Ricke, S. C. (2012). Concepts and methods for understanding bone metabolism in laying hens. *World's Poult. Sci. J.* 68, 71–82. doi:10.1017/s0043933912000086

Landis, E., and Keane, D. T. (2010). X-ray microtomography. *Mater. Charc* 61 (12), 1305–1316. doi:10.1016/j.matchar.2010.09.012

Li, D., Zhang, K., Bai, S., Wang, J., Zeng, Q., Peng, H., et al. (2021). Effect of 25-hydroxycholecalciferol with different vitamin D3 levels in the hens diet in the rearing period on growth performance, bone quality, egg production, and eggshell quality. *Bone Qual. Egg Prod. Eggshell Qual. Agri.* 11, 698. doi:10.3390/agriculture11080698

Lohmann (2016). *Lohmann Brown and LSL-lite commercial management guide*. Available on: http://www.ltz.de/en/downloads/management-guides.php#anchor_0955c6a8_Accordion1-Cage (Accessed on October 29th, 2021).

Nakano, H., Matsunawa, M., Yasui, A., Adachi, R., Kawana, K., Shimomura, L., et al. (2005). Enhancement of ligand-dependent Vitamin D receptor transactivation by the cardiotonic steroid bufalin. *Biochem. Pharm.* 70, 1479–1486. doi:10.1016/j.bcp.2005.08.012

Nascimento, G. R. d., Murakami, A. E., Guerra, A., Ospinas-Rojas, I. C., Ferreira, M. F. Z., and Fanhani, J. C. (2014). Effect of different vitamin D sources and calcium levels in the diet of layers in the second laying cycle. *Rev. Bras. Cienc. Avic.* 16, 37–42. doi:10.1590/1516-635x160237-42

Preisinger, R. (2018). Innovative layer genetics to handle global challenges in egg production. *Br. Poult. Sci.* 59, 1–6. doi:10.1080/00071668.2018.1401828

Regmi, P., Deland, T. S., Steibel, J. P., Robison, C. I., Haut, R. C., Orth, M. W., et al. (2015). Effect of rearing environment on bone growth of pullets. *Poult. Sci.* 94, 502–511. doi:10.3382/ps/peu041

Regmi, P., Smith, N., Nelson, N., Haut, R. C., Orth, M. W., and Karcher, D. M. (2016a). Housing conditions alter properties of the tibia and humerus during the laying phase in Lohmann white Leghorn hens. *Poult. Sci.* 95, 198–206. doi:10.3382/ps/pev209

Regmi, P., Nelson, N., Steibel, J. P., Anderson, K. E., and Karcher, D. M. (2016b). Comparisons of bone properties and keel deformities between strains and housing systems in end-of-lay hens. *Poult. Sci.* 95, 2225–2234. doi:10.3382/ps/pew199

Reich, T., and Gefen, A. (2006). Effect of trabecular bone loss on cortical strain rate during impact in an *in vitro* model of avian femur. *Biomed. Eng. Online* 5, 45. doi:10.1186/1475-925X5-45

Rennie, J. S., Fleming, R. H., Mccormack, H. A., Mccorquodale, C. C., and Whitehead, C. C. (1997). Studies on effects of nutritional factors on bone structure

and osteoporosis in laying hens. *Br. Poult. Sci.* 38, 417–424. doi:10.1080/00071669708418012

Rique, A. M., Madeira, M., Luis, L., Mlde, F., Fleius Mlde, F., Paranhos, N. F., et al. (2019). Evaluating cortical bone porosity using Hr-Pqct. *Arch. Clin. Exp. Orthop.* 3, 008–013. doi:10.29328/journal.aceo.1001006

Shapiro, F. (2008). Bone development and its relation to fracture repair. The role of mesenchymal osteoblasts and surface osteoblasts. *Eur. Cell. Mater* 15, 53–76. doi:10.22203/ecm.v015a05

Sharma, M. K., White, D., Kim, W. K., and Adhikari, P. (2021). Effects of the housing environment and laying hen strain on tibia and femur bone properties of different laying phases of Hy-Line hens. *Poult. Sci.* 100 (3), 100933. doi:10.1016/j.psj.2020.12.030

Siffert, R., Luo, G., Cowin, S., and Kaufman, J. (1996). Dynamic relationships of trabecular bone density, architecture, and strength in a computational model of osteopenia. *Bone* 18, 197–206. doi:10.1016/8756-3282(95)00446-7

Silva, F. A. (2017). *Effects of dietary 25-hydroxycholecalciferol on growth, production performance, eggshell quality and bone traits of brown egg layers housed under commercial conditions*. University of Alberta, Edmonton.

ŚwiĄTkiewicz, S., Arczewska-Włosek, A., Bederska-Lojewska, D., and Józefiak, D. (2017). Efficacy of dietary vitamin D and its metabolites in poultry - review and implications of the recent studies. *Poult. Sci. J.* 73, 57–68. doi:10.1017/s0043933916001057

Tactacan, G. B., Guenter, W., Lewis, N. J., Rodriguez-Lecompte, J. C., and House, J. D. (2009). Performance and welfare of laying hens in conventional and enriched cages. *Poult. Sci.* 88, 698–707. doi:10.3382/ps.2008-00369

Toscano, M. (2018). in *Skeletal problems in contemporary commercial laying hens*. Editor J. A. Mench 1st ed (Elsevier Ltd).

Webber, C. E., Gordon, C. L., and Nicholson, P. S. (1998). Relation between image-based assessment of distal radius trabecular structure and compressive strength. *Can. Assoc. Radiol. J.* 49, 390–397.

Wen, J., Livingston, K. A., and Persia, M. E. (2019). Effect of high concentrations of dietary vitamin D3 on pullet and laying hen performance, skeleton health, eggshell quality, and yolk vitamin D3 content when fed to W36 laying hens from day of hatch until 68 wk of age. *Poult. Sci.* 98, 6713–6720. doi:10.3382/ps/pez386

Whitehead, C. C., and Fleming, R. H. (2000). Osteoporosis in cage layers. *Poult. Sci.* 79 (7), 1033–1041. doi:10.1093/ps/79.7.1033

Whitehead, C. C. (2004). Overview of bone biology in the egg-laying hen. *Poult. Sci.* 83, 193–199. doi:10.1093/ps/83.2.193

Wideman, R., Jr, Blankenship, J., Pevzner, I., and Turner, B. (2015). Efficacy of 25-OH Vitamin D3 prophylactic administration for reducing lameness in broilers grown on wire flooring. *Poult. Sci.* 94, 1821–1827. doi:10.3382/ps/pev160

Wilson, S., and Duff, S. R. I. (1991). Effects of vitamin or mineral deficiency on the morphology of medullary bone in laying hens. *Res. Vet. Sci.* 50, 216–221. doi:10.1016/0034-5288(91)90110-a

Yamada, M., Chen, C., Sugiyama, T., and Kim, W. K. (2021). Effect of age on bone structure parameters in laying hens. *Animals* 11, 570. doi:10.3390/ani11020570

Yokota, K., Chiba, K., Okazaki, N., Kondo, C., Doi, M., Yamada, S., et al. (2020). Deterioration of bone microstructure by aging and menopause in Japanese healthy women: Analysis by HR-pQCT. *J. Bone Min. Metab.* 38, 826–838. doi:10.1007/s00774-020-01115-z

Zhao, J. G., Zeng, X. T., Wang, J., and Liu, L. (2017). Association between calcium or vitamin D supplementation and fracture incidence in community-dwelling older adults: A systematic review and meta-analysis. *JAMA* 318, 2466–2482. doi:10.1001/jama.2017.19344

Frontiers in Physiology

Understanding how an organism's components work together to maintain a healthy state

The second most-cited physiology journal, promoting a multidisciplinary approach to the physiology of living systems - from the subcellular and molecular domains to the intact organism and its interaction with the environment.

Discover the latest Research Topics

See more →

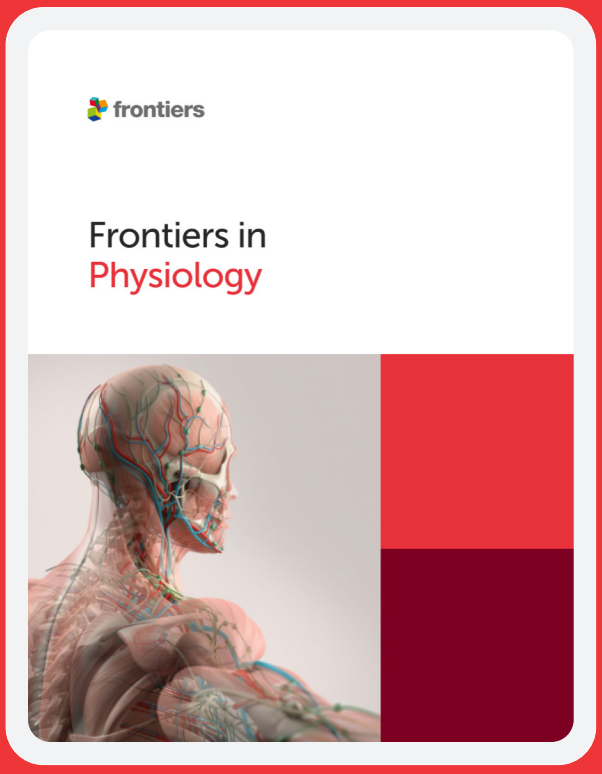

Frontiers

Avenue du Tribunal-Fédéral 34
1005 Lausanne, Switzerland
frontiersin.org

Contact us

+41 (0)21 510 17 00
frontiersin.org/about/contact